Instytut Geografii i Przestrzennego Zagospodarowania
Polska Akademia Nauk

Rozprawa doktorska

Krytyczne przejścia w degradacji wieloletniej zmarzliny – w świetle badań paleoekologicznych osadów torfowiskowych Północno-Zachodniej Syberii

Critical transitions in the degradation of permafrost – in the light of palaeoecological studies of peatland deposits from Northwestern Siberia

mgr Agnieszka Jolanta Halaś

napisana pod kierunkiem:
Prof. dr. hab. Michała Słowińskiego

Warszawa, 2026

„Największą przeszkodą w zdobywaniu wiedzy nie jest ignorancja,
lecz złudzenie jej posiadania.”

Daniel J. Boorstin

Niniejszą pracę dedykuję Mamie i Tacie

Podziękowania

Niniejsza praca nie powstałaby bez ogromnego wsparcia mojego promotora prof. dr. hab. **Michała Słowińskiego**. Chciałabym serdecznie podziękować za wprowadzenie mnie w niezwykły świat torfowisk, możliwość udziału w wielu ciekawych projektach badawczych oraz badaniach terenowych prowadzonych na różnych szerokościach geograficznych. Za dzielenie się wiedzą i doświadczeniem, inspirujące rozmowy oraz stworzenie warunków sprzyjających samodzielnemu rozwojowi naukowemu. Szczególnie dziękuję za zaufanie i wiarę w moje możliwości, które miały kluczowe znaczenie na każdym etapie realizacji tej rozprawy.

Serdecznie dziękuję również współautorom artykułów wchodzących w skład niniejszej rozprawy doktorskiej: prof. dr. hab. **Mariuszowi Lamentowiczowi,** dr **Dominice Łuców** oraz dr **Milenie Obremskiej** za dzielenie się wieloletnim doświadczeniem, cenne wskazówki i inspirujące dyskusje naukowe. Dziękuję za krytyczne spojrzenie, merytoryczne uwagi oraz wsparcie na kolejnych etapach realizacji badań i przygotowywania publikacji.

Szczególne podziękowania kieruję do pracowników Instytutu Geografii i Przestrzennego Zagospodarowania PAN w Warszawie, z którymi mam przyjemność pracować od 2019 roku. W szczególności dziękuję **Zakładowi Dynamiki Krajobrazów Minionych** za przyjazną atmosferę pracy, otwartość na współpracę oraz codzienne wsparcie w prowadzeniu badań.

Ogromne podziękowania należą się moim rodzicom **Jolancie** i **Krzysztofowi**, za rozbudzenie we mnie ciekawości świata oraz za wsparcie i zaufanie, które pozwoliły mi podążać własną drogą. Dziękuję również moim babciom **Cecylii** i **Janinie** oraz dziadkom **Władysławowi** i **Stanisławowi** za motywację, troskę i wiarę we mnie na każdym etapie mojej edukacyjnej drogi. Przyjaciołom dziękuję za obecność, wyrozumiałość i otuchę towarzyszącą mi podczas powstawania tej pracy.

Na koniec chciałabym podziękować mojemu chłopakowi, **Harremu**, za cierpliwość, nieustanne dodawanie mi sił i przekonanie, że mogę osiągnąć więcej, niż sama czasem przypuszczałam, a także psu **Tadziowi**, który zawsze z zainteresowaniem wysłuchiwał opowieści o torfowiskach Niziny Zachodniosyberyjskiej.

Informacje o finansowaniu

Badania przedstawione w niniejszej rozprawie doktorskiej zostały przeprowadzone w ramach projektu Preludium BIS 1 pt. „*Procesy topnienia wieloletniej zmarzliny, występowania pożarów i dekompozycji zarejestrowane w osadach torfowisk borealnych NW Syberii – PathThaw*” (nr 2019/35/O/ST10/02903), finansowanego przez Narodowe Centrum Nauki i realizowanego w Instytucie Geografii i Przestrzennego Zagospodarowania PAN pod kierownictwem prof. dr. hab. Michała Słowińskiego.

Realizacja rozprawy została również wsparta poprzez odbycie 4-miesięcznego zagranicznego stażu doktorskiego w Montrealu (Kanada), na Université du Québec à Montréal (UQAM), pod opieką prof. Michelle Garneau, finansowanego w ramach programu Preludium BIS NAWA (nr PPN/STA/2021/1/00038/PR/00001).

Spis treści

Wykaz publikacji wchodzących w skład rozprawy doktorskiej

Wyniki badań będących podstawą niniejszej rozprawy doktorskiej przedstawiono w cyklu trzech artykułów opublikowanych w międzynarodowych czasopismach naukowych posiadających współczynnik Impact Factor (IF).

Rozprawa składa się z następujących publikacji (w dalszej części pracy poszczególne artykuły będą przywoływane zgodnie z poniższą numeracją):

I. **Halaś, A.**, Lamentowicz, M., Łuców, D., & Słowiński, M. (2023). *Developing a new testate amoeba hydrological transfer function for permafrost peatlands of NW Siberia*. Quaternary Science Reviews, 308, 108067. https://doi.org/10.1016/j.quascirev.2023.108067
IF: 3,3; Punktacja MNiSW: 140 pkt

II. **Halaś, A.**, Lamentowicz, M., Obremska, M., Łuców, D., & Słowiński, M. (2025). *Peatland development reconstruction and complex biological responses to permafrost thawing in Western Siberia*. Biogeosciences, 22(18), 4797–4822. https://doi.org/10.5194/bg-22-4797-2025
IF: 3,9; Punktacja MNiSW: 140 pkt.

III. **Halaś, A.** & Słowiński, M. (2026). *Peat core research in the Western Siberian Lowland: applications of palaeoecological proxies, regions studied, and future prospects*. Earth System Science Data 18(6), 3853–3888. https://doi.org/10.5194/essd-18-3853-2026
IF: 11,6; Punktacja MNiSW: 200 pkt

Streszczenie

Torfowiska stanowią jeden z kluczowych komponentów globalnego systemu klimatycznego, odgrywając istotną rolę w regulacji obiegu węgla, magazynowaniu materii organicznej w długich skalach czasowych oraz retencji słodkiej wody w krajobrazie. Szczególne znaczenie mają torfowiska wysokich szerokości geograficznych na półkuli północnej (>45°N) związane z występowaniem wieloletniej zmarzliny, które magazynują ogromne ilości węgla organicznego i są szczególnie wrażliwe na współczesną zmianę klimatu. Jednym z największych i najważniejszych obszarów ich występowania jest Nizina Zachodniosyberyjska. Współczesne ocieplenie klimatu prowadzi jednak do postępującej degradacji wieloletniej zmarzliny w tym regionie, powodując zmiany hydrologiczne i ekologiczne mogące wpływać na funkcjonowanie torfowisk oraz stabilność zgromadzonych w nich zasobów węgla. Pomimo rosnącej liczby badań, konsekwencje tych procesów pozostają nadal słabo poznane, szczególnie w odniesieniu do reakcji poszczególnych mikrosiedlisk torfowiskowych.

Celem niniejszej rozprawy było **rozpoznanie oraz wyjaśnienie mechanizmów funkcjonowania oraz długoterminowych zmian hydrologicznych i ekologicznych torfowisk Niziny Zachodniosyberyjskiej położonych w strefie nieciągłej wieloletniej zmarzliny.** Szczególną uwagę poświęcono określeniu reakcji biotycznych wskaźników paleoekologicznych na procesy degradacji zmarzliny oraz ocenie ich przydatności w rekonstrukcjach paleohydrologicznych. Badania przeprowadzono na przykładzie kompleksu torfowiskowego Khanymei i oparto na analizie współczesnych relacji między zbiorowiskami ameb skorupkowych a warunkami środowiskowymi, opracowaniu lokalnej funkcji transferu do rekonstrukcji paleohydrologicznych, wielowskaźnikowej analizie paleoekologicznej oraz syntezie dotychczasowych badań z wykorzystaniem rdzeni torfowych prowadzonych na Nizinie Zachodniosyberyjskiej.

Wyniki wykazały, że poziom wód gruntowych stanowi główny czynnik kształtujący zbiorowiska ameb skorupkowych, przy czym zależność ta jest modyfikowana przez obecność wieloletniej zmarzliny, typ mikrosiedliska oraz skład roślinności. Opracowana lokalna funkcja transferu umożliwiła bardziej precyzyjne rekonstrukcje zmian hydrologicznych niż modele oparte na zbiorach kontynentalnych, poprzez uwzględnienie lokalnej specyfiki torfowisk w tym regionie. Rekonstrukcje

paleoekologiczne potwierdziły, że degradacja wieloletniej zmarzliny prowadzi do zróżnicowanych przestrzennie zmian hydrologicznych i ekologicznych, a odpowiedź poszczególnych mikrosiedlisk torfowiskowych na współczesne ocieplenie klimatu jest niejednorodna. Przeprowadzona synteza badań wykazała ponadto istotne luki przestrzenne i metodologiczne w dotychczasowych badaniach torfowisk Niziny Zachodniosyberyjskiej.

Uzyskane wyniki dostarczyły nowych informacji na temat funkcjonowania torfowisk strefy nieciągłej wieloletniej zmarzliny w warunkach postępującej jej degradacji, a także zaowocowały opracowaniem nowych narzędzi wspierających badania paleoekologiczne w tym regionie. Należą do nich lokalna funkcja transferu oraz baza metadanych rdzeni torfowych *Western Siberian Peat Core Database* (WSPC). Funkcja transferu umożliwia dokładniejsze rekonstrukcje paleohydrologiczne na torfowiskach strefy nieciągłej wieloletniej zmarzliny, natomiast baza WSPC wspiera planowanie przyszłych badań, porównywanie istniejących zapisów oraz identyfikację kluczowych luk badawczych. **Rozprawa wnosi tym samym wkład w rozwój paleoekologii torfowisk położonych w strefie wieloletniej zmarzliny oraz w lepsze zrozumienie ich reakcji na współczesną, a także prognozowaną zmianę klimatu.**

Słowa kluczowe: torfowiska, wskaźniki paleoekologiczne, ameby skorupkowe, hydrologiczna funkcja transferu, wieloletnia zmarzlina, Syberia

Abstract

Peatlands constitute one of the key components of the global climate system, playing a crucial role in regulating the carbon cycle, storing organic matter over long timescales, and retaining freshwater in the landscape. Of particular importance are high-latitude peatlands in the Northern Hemisphere (>45°N) associated with permafrost, which store vast amounts of organic carbon and are especially vulnerable to modern climate change. One of the largest and most important regions where these ecosystems occur is the Western Siberian Lowland. Contemporary climate warming is driving progressive permafrost degradation across this region, resulting in hydrological and ecological changes that may affect peatland functioning and the stability of their carbon pools. Despite a growing number of studies, the consequences of these processes remain poorly understood, particularly regarding the response of individual peatland microhabitats.

The aim of this dissertation was to **investigate and explain the mechanisms controlling the functioning and long-term hydrological and ecological dynamics of peatlands in the discontinuous permafrost zone of the Western Siberian Lowland.** Particular attention was paid to determining how biotic paleoecological indicators respond to permafrost degradation processes, as well as to evaluating their suitability for paleohydrological reconstructions. The study was conducted using the Khanymei peatland complex as a case study, and was based on analyses of modern relationships between testate amoeba communities and environmental conditions, the development of a local transfer function for palaeohydrological reconstructions, multi-proxy paleoecological analyses, and a synthesis of previous paleoecological studies conducted across the Western Siberian Lowland.

The results demonstrate that depth to water table is the primary factor shaping testate amoeba communities, although this relationship is modified by the presence of permafrost, microhabitat type, and vegetation composition. The locally developed transfer function enabled more accurate hydrological reconstructions than models based on continental-scale training sets by accounting for specific environmental characteristics of peatlands in the study area. Paleoecological reconstructions confirmed permafrost degradation leads to spatially heterogeneous hydrological and ecological changes, yet the response of individual peatland microhabitats to contemporary climate warming is not uniform. In addition, the synthesis revealed significant spatial and methodological gaps in existing peatland research across the Western Siberian Lowland.

The obtained results provide new insight into peatland functioning in the discontinuous permafrost zone under conditions of ongoing permafrost degradation, and have led to the development of new tools supporting paleoecological research in the region. These include a local transfer function and the *Western Siberian Peat Core Database* (WSPC), a peat-core metadata repository. The transfer function enables precise paleohydrological reconstructions of peatlands in the discontinuous permafrost zone, whilst the WSPC supports the planning of future research, comparing existing records, and identifying key knowledge gaps. **The dissertation thereby contributes to the development of the paleoecology of permafrost peatlands and to a better understanding of their response to contemporary as well as projected climate change.**

Keywords: peatlands, palaeoecological proxies, testate amoebae, hydrological transfer function, permafrost, Siberia

Wstęp

Torfowiska stanowią jeden z kluczowych komponentów globalnego systemu klimatycznego, odgrywając istotną rolę w regulacji obiegu węgla. Choć zajmują jedynie około 3% powierzchni lądów, magazynują blisko jedną trzecią światowych zasobów tego pierwiastka zgromadzonego w glebie (Scharlemann i in., 2014; Xu i in., 2018). Szacuje się, że od maksimum ostatniego zlodowacenia (ang. *Last Glacial Maximum*, LGM) torfowiska funkcjonowały jako trwały pochłaniacz dwutlenku węgla z atmosfery i zakumulowały od 500 do 700 petagramów (Pg) węgla (Yu i in., 2010). Mimo, iż ekosystemy te występują w różnych strefach klimatycznych, około 80% ich światowych zasobów znajduje się na obszarach wysokich szerokości geograficznych półkuli północnej, powyżej 45°N (Ryc. 1) (Frolking i in., 2011). W tych torfowiskach zgromadzone jest również blisko 90% całkowitych zasobów węgla obecnych w tych ekosystemach (Hugelius i in., 2020). Torfowiska zawdzięczają swoją zdolność magazynowania tak dużych ilości węgla organicznego specyficznym warunkom środowiskowym, w których dochodzi do powstawania i akumulacji torfu. Stałe uwodnienie oraz ograniczony dostęp tlenu hamują rozkład materii organicznej, umożliwiając jej stopniowe odkładanie się (nawet przez tysiące lat), a w strefie borealnej i subarktycznej proces ten jest dodatkowo spowalniany przez niską temperaturę powietrza (Rydin i in., 2013; Page i Baird, 2016).

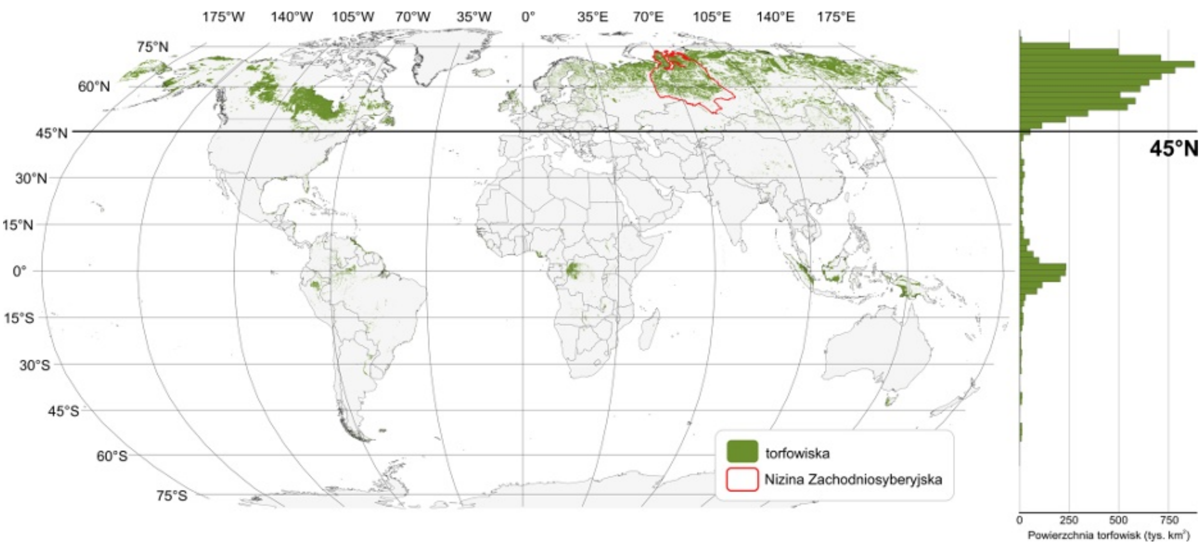

Ryc. 1 Zasięg występowania torfowisk na świecie z zaznaczonym obszarem Niziny Zachodniosyberyjskiej oraz równoleżnikiem 45°N, uznawanym za południową granicę występowania tzw. torfowisk wysokich szerokości geograficznych na półkuli północnej.
Źródło: opracowanie własne na podstawie Global Peatland Map 2.0 (Greifswald Mire Centre, 2022).

Torf jest materiałem organicznym powstającym *in situ* (w miejscu), ze szczątków różnorodnych roślin torfotwórczych, m.in. mszaków (zwłaszcza torfowców z rodzaju *Sphagnum*), turzyc, traw, liści, kłączy, korzeni oraz zdrewniałych fragmentów roślin (Rydin i in., 2013). Poza magazynowaniem węgla, torfowiska pełnią również szereg innych istotnych funkcji środowiskowych. Uczestniczą w regulacji obiegu wody oraz ograniczają ryzyko powodzi oraz suszy dzięki zdolności do retencjonowania i stopniowego uwalniania wody (Tobolski, 2000; Rydin i in., 2013). Torfowiska wpływają również na poprawę jakości wód poprzez ich naturalną filtrację i oczyszczanie (Nieminen i in., 2026). Ponadto specyficzne warunki hydrologiczne, troficzne i biogeochemiczne torfowisk sprzyjają występowaniu wyspecjalizowanych gatunków roślin i zwierząt o wąskiej amplitudzie ekologicznej, odgrywając istotną rolę w utrzymaniu różnorodności biologicznej (Minayeva i Sirin, 2012). Specyficzne warunki akumulacji torfu sprawiają również, że torfowiska stanowią jedne z najcenniejszych naturalnych archiwów zmian środowiskowych i klimatycznych (Chambers i Charman, 2004).

Jednym z największych i najważniejszych obszarów torfowiskowych na świecie jest Nizina Zachodniosyberyjska (Ryc. 1). Specyficzne cechy fizycznogeograficzne tego regionu, a przede wszystkim niezwykle płaska rzeźba terenu oraz obecność słabo przepuszczalnych osadów w podłożu, sprzyjają stagnacji wody i rozwojowi rozległych ekosystemów wodno-błotnych (Kirpotin i in., 2009). W efekcie około 50% powierzchni niziny zajmują obszary podmokłe, z czego niemal połowę stanowią torfowiska (Sheng i in., 2004). Istotnym elementem krajobrazu Niziny Zachodniosyberyjskiej, mającym wyraźny wpływ na znajdujące się tam torfowiska, jest wieloletnia zmarzlina (ang. *permafrost*).

W sprzyjających warunkach, wieloletnia zmarzlina i torfowiska tworzą na Nizinie Zachodniosyberyjskiej ściśle sprzężony system wzajemnego wzmocnienia. Wieloletnia zmarzlina odgrywa kluczową rolę w regulacji stosunków wodnych. Zmniejsza przepuszczalność osadów, skutecznie hamując ruch wody między systemem powierzchniowym a gruntowym oraz silnie ogranicza dostęp tlenu i spowalnia procesy rozkładu materii organicznej (Walvoord i Kurylyk, 2016; Jones i in., 2022; Treat i in., 2022). Warunki te sprzyjają długotrwałej akumulacji torfu oraz ograniczają uwalnianie węgla do atmosfery. Torf natomiast działa jak warstwa termoizolacyjna, ułatwiając agradację (rozrost) i utrzymywanie zmarzliny (Kujala i in., 2008). W regionach o ciągłej zmarzlinie, jej agradacja i akumulacja torfu często zachodzą równolegle (ang. *syngenetic permafrost*), prowadząc do powstawania słabo rozłożonych profili torfowych z charakterystycznymi strukturami lodowymi (Kanevskiy i in., 2014). Natomiast w południowej części zasięgu wieloletniej zmarzliny, gdzie występuje ona głównie w formie nieciągłej, dominuje zmarzlina epigenetyczna, rozwijająca się wtórnie w uprzednio zakumulowanych osadach torfowych (Treat i Jones, 2018a).

Agradacja zmarzliny wpływa również na rzeźbę terenu, powodując wynoszenie powierzchni torfowiska wskutek tworzenia soczewek lodowych, prowadząc do rozwoju charakterystycznych form peryglacjalnych, takich jak pagórki palsa (pagórki torfowe z rdzeniem lodowym), czy płaskowyże torfowe (ang. *peat plateau*) (Pissart i in., 1998). Proces ten prowadzi jednocześnie do osuszenia powierzchni wyniesionych fragmentów torfowisk i rozwoju zbiorowisk charakterystycznych dla suchszych siedlisk, zdominowanych przez mchy, porosty i krzewinki (Olefeldt i in., 2021). W strefie występowania nieciągłej zmarzliny, płaskowyże torfowe mogą pokrywać od 30 do 70% powierzchni torfowisk, podczas gdy pozostałe obszary (tam, gdzie obecnie zmarzlina nie występuje) zajmują torfowiska niskie i wysokie oraz zbiorniki wodne związane z procesami termokrasowymi (Kremenetski i in., 2003). Układ przestrzenny tych form jest silnie kontrolowany przez interakcje pomiędzy zmarzliną a hydrologią. Wyniesione płaskowyże torfowe sprzyjają odpływowi wód do otoczenia, ale jednocześnie mogą blokować odpływ wody z zagłębień termokrasowych, prowadząc do tworzenia torfowisk (Quinton i in., 2009). Rozwój dużych płaskowyżów torfowych może inicjować degradację zmarzliny wskutek gromadzenia się wód podpowierzchniowych, co zwiększa przewodnictwo cieplne i prowadzi do zapadania się ich powierzchni (Olefeldt i in., 2021). W początkowej fazie wiąże się to z zalaniem powierzchni torfowiska oraz gwałtowną zmianą roślinności, ze zbiorowisk suchych na higrofilne mchy *Sphagnum* i turzyce. W kolejnych etapach sukcesji następuje akumulacja torfu i stopniowe wynoszenie powierzchni ponad poziom wód gruntowych, co w skali kilkudziesięciu–kilkuset lat może skutkować ponowną agradacją zmarzliny i odtworzeniem płaskowyżu torfowego.

Współczesna zmiana klimatu może jednak zaburzać ten cykl poprzez nasiloną degradację wieloletniej zmarzliny. Najnowsze badania wskazują, że od 1979 r. Arktyka ociepla się niemal czterokrotnie szybciej niż obszary położone na niższych szerokościach geograficznych, co określane jest mianem arktycznego wzmocnienia (ang. *Arctic amplification*) (Ryc. 2) (Hantemirov i in., 2022; Rantanen i in., 2022; IPCC, 2023). Postępujący wzrost temperatury powietrza przekłada się bezpośrednio na ocieplenie gruntu i stopniową degradację zmarzliny (Biskaborn i in., 2019). Na obszarze Niziny Zachodniosyberyjskiej proces ten przejawia się m.in. zwiększaniem miąższości warstwy aktywnej (czynnej), rozwojem talików, procesów termokrasowych oraz drenażem torfowisk (Streletskiy i in., 2015; Vasiliev i in., 2020; Spiller i in., 2024). Szacuje się, że w latach 1999-2019 średnia grubość warstwy aktywnej na tym obszarze wzrosła nawet o 0,4 m (Smith i in., 2022). Degradacja zmarzliny wywiera wieloaspektowy wpływ na funkcjonowanie ekosystemów torfowiskowych. Postępujące rozmarzanie prowadzi do głębokich zmian ich morfologii, stosunków hydrologicznych oraz procesów biogeochemicznych (Olefeldt i in., 2021). Zmiany te wpływają również na skład zbiorowisk roślinnych, tempo akumulacji torfu, emisję metanu oraz częstość pożarów (Swindles i in., 2015; van der Kolk i in., 2016; Serikova i in., 2019; Masyagina i Menyailo, 2020).

Kluczowym, lecz wciąż nierozstrzygniętym pytaniem pozostaje kierunek i skala odpowiedzi torfowisk na postępującą degradację zmarzliny. Rozważane są dwie zasadniczo odmienne trajektorie zmian. Z jednej strony, rozmarzanie może prowadzić do nasilenia rozkładu materii organicznej i zwiększonego uwalniania gazów cieplarnianych, przede wszystkim dwutlenku węgla (CO_2) i metanu (CH_4), wskutek zapadania się części torfowisk i ich ponownego uwodnienia (Jeong i in., 2018; Karlsson i in., 2021). Przykładem tego jest zapadanie się obszarów brzegowych pagórków palsa i płaskowyżów torfowych, obserwowane obecnie m.in. na Syberii i w Norwegii (Ryc. 3). Z drugiej strony, część tych emisji może być kompensowana przez wzmożoną sekwestrację węgla wynikającą ze zwiększonej produktywności roślinnej (Loisel i Yu, 2013; Ogden i in., 2023). Ostateczny bilans wymiany CO_2 i CH_4 między torfowiskami a atmosferą pozostaje zatem trudny do przewidzenia i może stanowić istotne sprzężenie zwrotne w globalnym systemie klimatycznym (Frolking i Roulet, 2007; Schuur i in., 2015).

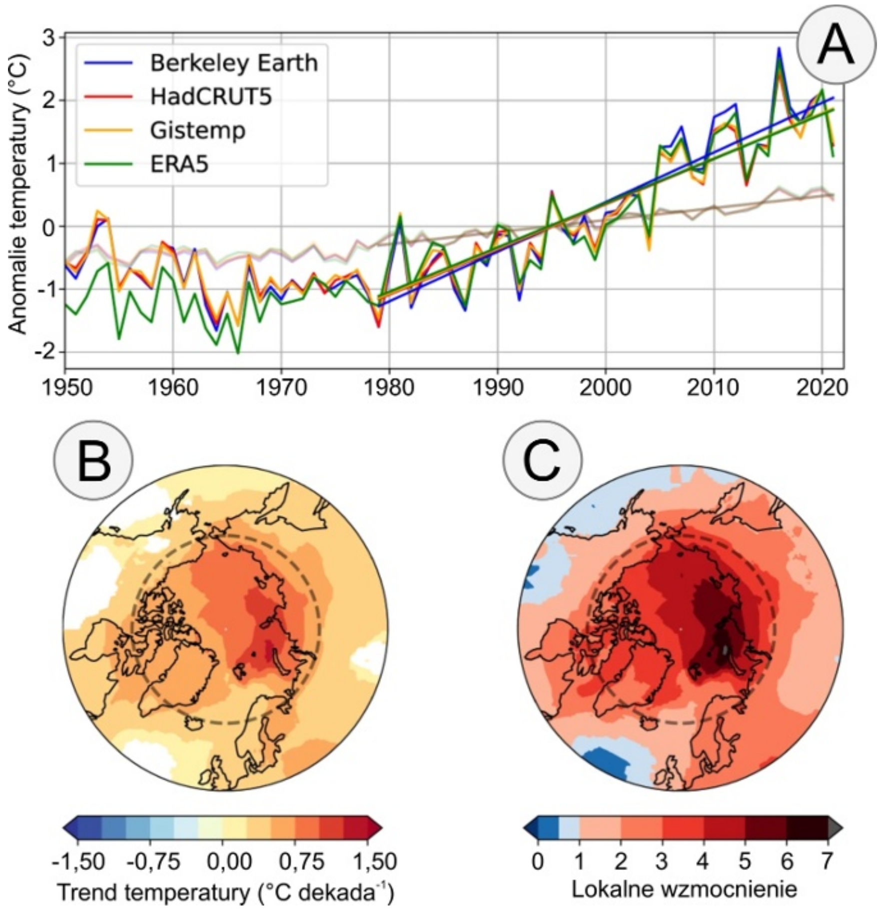

Ryc. 2 Zmiany średniej rocznej temperatury powietrza w Arktyce. **(A)** Anomalie średniej rocznej temperatury powietrza w Arktyce (66,5°–90°N) (ciemne kolory) oraz w skali globalnej (jasne kolory) w latach 1950–2021, wyznaczone na podstawie różnych zbiorów danych obserwacyjnych. Anomalie temperatury powietrza obliczono względem okresu referencyjnego 1981–2010. Przedstawiono również linie trendu temperatury powietrza dla okresu 1979–2021. **(B)** Roczne trendy średniej temperatury powietrza w okresie 1979–2021, wyznaczone jako średnia z danych obserwacyjnych. Obszary bez statystycznie istotnych zmian zostały zamaskowane. **(C)** Lokalny wskaźnik wzmocnienia obliczony dla okresu 1979–2021 na podstawie średniej z danych obserwacyjnych. Linia przerywana na panelach (B) i (C) oznacza koło podbiegunowe północne (66,5°N).
Źródło: Rantanen i in. (2022), tłumaczenie własne

Należy jednak podkreślić, że degradacja zmarzliny jest rezultatem współdziałania zarówno czynników klimatycznych, jak i lokalnych uwarunkowań środowiskowych. O ile coraz więcej badań koncentruje się na regionalnych i globalnych zmianach funkcjonowania torfowisk wskutek rozmarzania zmarzliny, m.in. z wykorzystaniem danych satelitarnych (m.in. Miles i Esau, 2016; Crichton i in., 2025), to procesy zachodzące w skali lokalnej (mikrosiedlisk) nadal pozostają słabo rozpoznane. Reakcja torfowisk na ocieplenie klimatu może bowiem znacznie różnić się nawet w obrębie jednego systemu torfowiskowego (Ryc. 4). Szczególne znaczenie ma tutaj mozaikowa struktura torfowisk, obejmująca występowanie suchszych wyniesionych form (takich jak płaskowyże torfowe), oraz wilgotnych dolinek i obniżeń termokrasowych.

Poszczególne mikrosiedliska różnią się istotnie warunkami termicznymi i wilgotnościowymi, co wpływa na kierunek oraz tempo przemian zachodzących podczas degradacji zmarzliny.

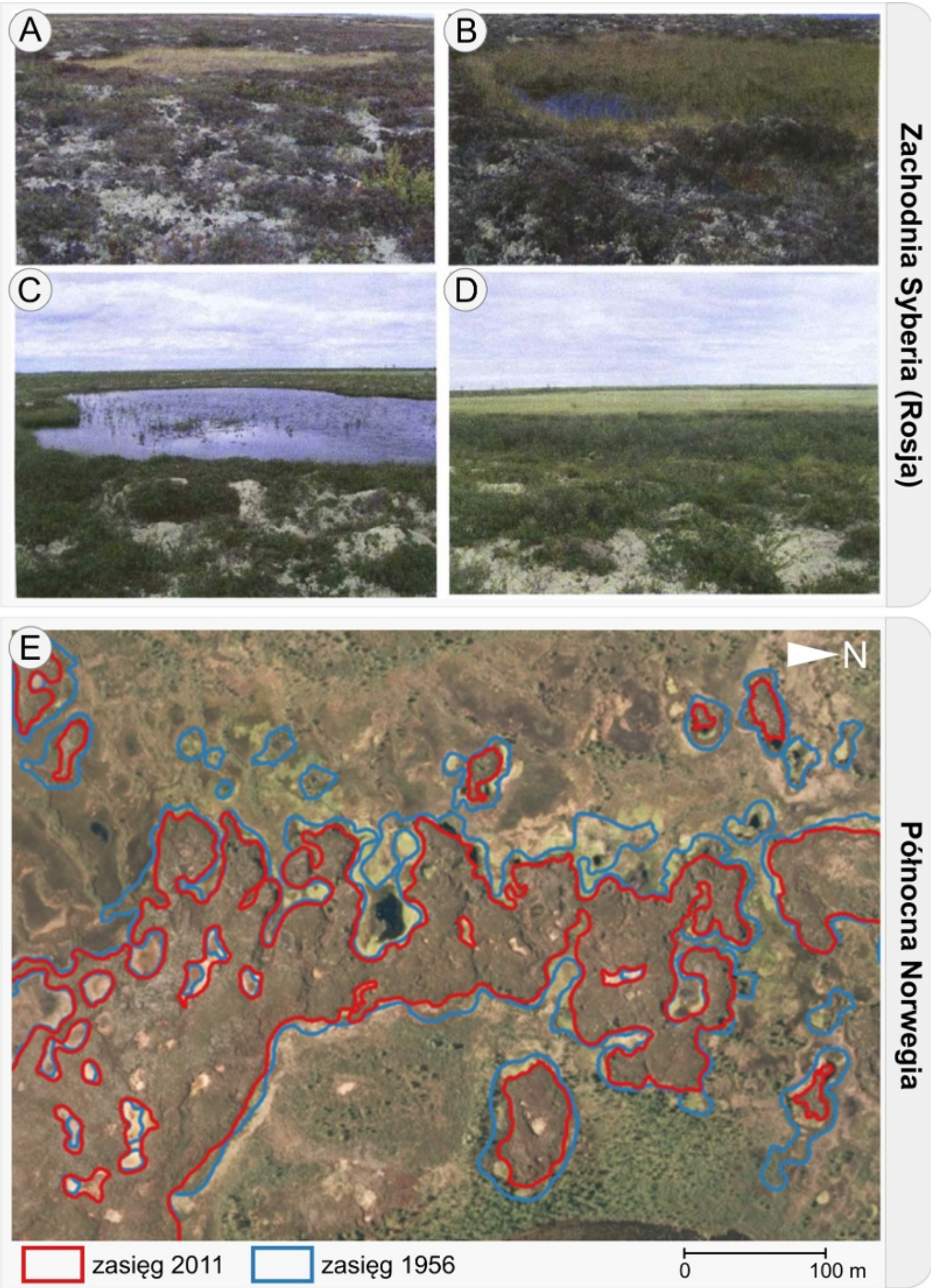

Ryc. 3 Przykłady transformacji torfowisk wieloletniej zmarzliny w Rosji i Norwegii. **(A–D)** Etapy cyklicznej sukcesji na torfowiskach typu palsa w zlewni Nadym-Pur (Nizina Zachodniosyberyjska): A – osiadanie termokrasowe; B – początkowe jezioro termokrasowe; C – młode jezioro termokrasowe; D – osuszona niecka po jeziorze termokrasowym „khasyrei", na podstawie Kirpotin i in. (2011). **(E)** Zasięg pagórków palsa oraz płaskowyży torfowych w okolicach Suossjavri (Norwegia) w 1956 i 2011 roku na podstawie: Borge i in. (2017).

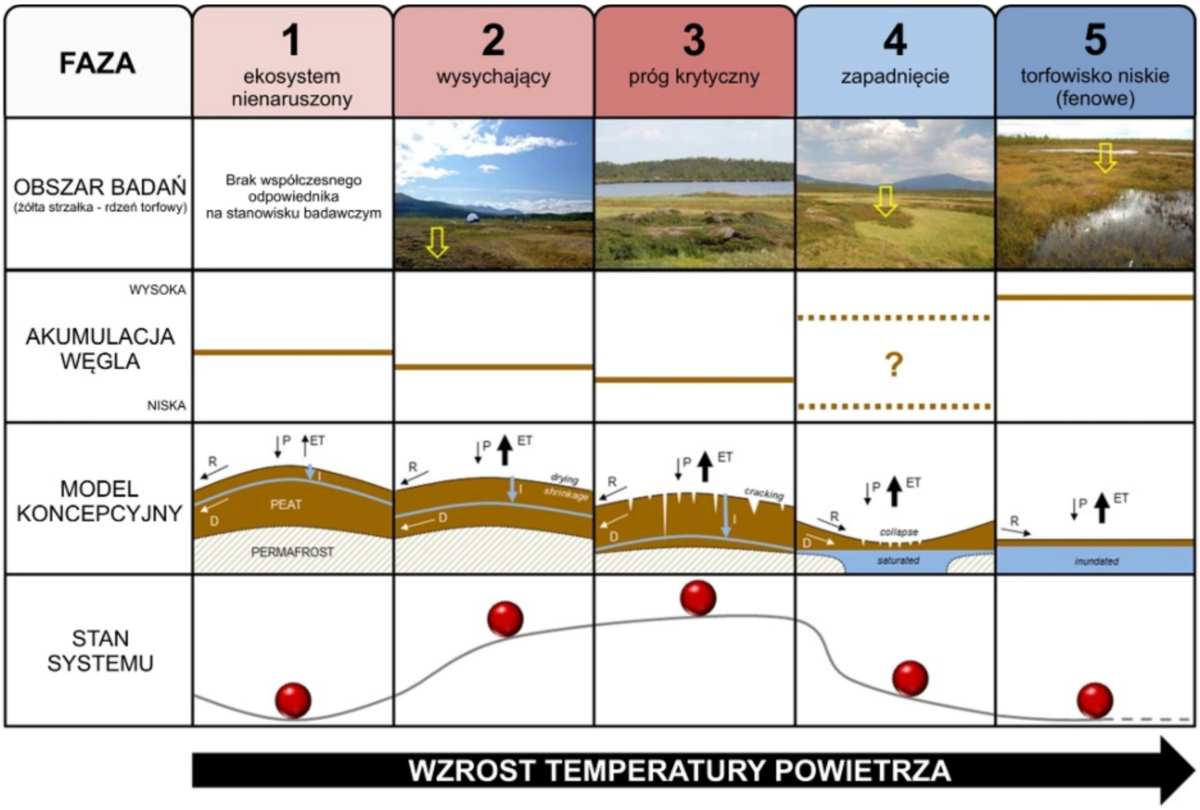

Ryc. 4 Pięciofazowy model degradacji torfowisk wieloletniej zmarzliny w odpowiedzi na wzrost temperatury powietrza na przykładzie torfowisk w regionie Abisko (Szwecja). Każda kolumna odpowiada jednej z pięciu odrębnych faz. Dolny rząd ilustruje stabilność ekohydrologiczną systemu z wykorzystaniem analogii „kuli i misy” (Scheffer i in., 2001). Pierwsza faza („nienaruszona”) reprezentuje jedyny stabilny stan równowagi przed zmianą wymuszoną klimatycznie, która przekształca stan systemu.

Objaśnienia: R = spływ powierzchniowy; D = odpływ podpowierzchniowy; P = opad atmosferyczny; ET = ewapotranspiracja; I = infiltracja.

Źródło: Swindles i in. (2015), tłumaczenie własne

Odpowiedź na pytanie o przyszły kierunek przemian torfowisk wymaga zatem lepszego zrozumienia ich reakcji na zmianę klimatu oraz procesy degradacji i agradacji wieloletniej zmarzliny zachodzące w przeszłości. Tymczasem bezpośredni monitoring torfowisk Syberii pozostaje ograniczony ze względu na ogromną powierzchnię regionu, trudną dostępność terenową oraz niedostatecznie rozwiniętą sieć pomiarową. Co więcej, obecna sytuacja geopolityczna, a zwłaszcza agresja Rosji na Ukrainę, doprowadziła do załamania dotychczasowej współpracy międzynarodowej z rosyjskimi instytucjami naukowymi. W konsekwencji ograniczony został dostęp zagranicznych naukowców do terenów badawczych i danych pomiarowych, a dotychczasowa współpraca naukowa realizowana w ramach międzynarodowych projektów badawczych na obszarze Syberii i rosyjskiej Arktyki uległa znacznemu osłabieniu. Utrudnia to prowadzenie długoterminowych obserwacji środowiskowych, w tym badań nad funkcjonowaniem torfowisk, obiegiem węgla, emisją gazów cieplarnianych oraz skutkami degradacji wieloletniej zmarzliny (Witze, 2022; López-Blanco i in., 2024; Schuur i in., 2024). Istotną lukę badawczą może wypełnić paleoekologia, umożliwiająca rekonstrukcję długoterminowej dynamiki zmian torfowisk na podstawie zapisu zachowanego w profilach torfowych.

Podejście paleoekologiczne opiera się na analizie biologicznych, chemicznych i fizycznych wskaźników (ang. *proxy*) zachowanych w osadach torfowych, które umożliwiają rekonstrukcję dawnych warunków środowiskowych i klimatycznych (Birks i in., 2010). Szczególne znaczenie mają badania wielowskaźnikowe (ang. *multi-proxy*), wykorzystujące równocześnie różne grupy wskaźników paleoekologicznych, co pozwala na bardziej wiarygodną i szczegółową rekonstrukcję oraz ogranicza ryzyko nadinterpretacji wyników bazujących na pojedynczym wskaźniku (Lamentowicz i in., 2025).

Podstawą rekonstrukcji wykorzystujących wskaźniki biologiczne jest założenie, że zależności pomiędzy organizmami a warunkami środowiskowymi obserwowane obecnie, funkcjonowały również w przeszłości, co umożliwia wykorzystanie współczesnych zależności ekologicznych do ilościowego odtwarzania dawnych parametrów środowiskowych (Birks, 1995). W ostatnich dekadach, wraz z rozwojem metod badawczych, nastąpił znaczący postęp w możliwościach rekonstrukcji minionych warunków klimatycznych i środowiskowych na podstawie zapisu biologicznego zachowanego w osadach. Do najczęściej stosowanych grup wskaźników biologicznych należą mikroorganizmy i mikroskamieniałości, takie jak okrzemki, ochotkowate (Chironomidae), wioślarki (Cladocera) oraz ameby skorupkowe (testate amoebae) (m.in. Płóciennik i in., 2011; Swindles i in., 2015; Słowiński i in., 2016; Leppänen i in., 2019; Carballeira i Pontevedra-Pombal, 2020). W rekonstrukcjach zmian hydrologicznych torfowisk szczególnie szerokie zastosowanie znajdują ameby skorupkowe, które dzięki dużej czułości na zmiany wilgotności stanowią jedne z najważniejszych bioindykatorów w badaniach paleoekologicznych (Lamentowicz i Mitchell, 2005).

Ameby skorupkowe są małymi (zazwyczaj 20-200 μm), jednokomórkowymi organizmami wytwarzającymi charakterystyczną skorupkę, odporną na rozkład i dobrze zachowującą się w osadach torfowych (Charman, 2001; Lamentowicz, 2007). Występują powszechnie w środowiskach bogatych w wilgoć, szczególnie w żywych częściach mchów (*Sphagnum*), glebie czy powierzchniowej warstwie osadów jeziornych (Ryc. 5). Można je spotkać na wszystkich kontynentach, a część z nich uznawana jest za gatunki kosmopolityczne. Analiza współczesnych zbiorowisk ameb skorupkowych w różnych mikrosiedliskach wykorzystywana jest do tworzenia tzw. zbiorów testowych (ang. *training sets*), które stanowią podstawę do ilościowych rekonstrukcji poziomu wód gruntowych (ang. *depth to water table*, DWT) (Lamentowicz, 2007; Mitchell, 2025).

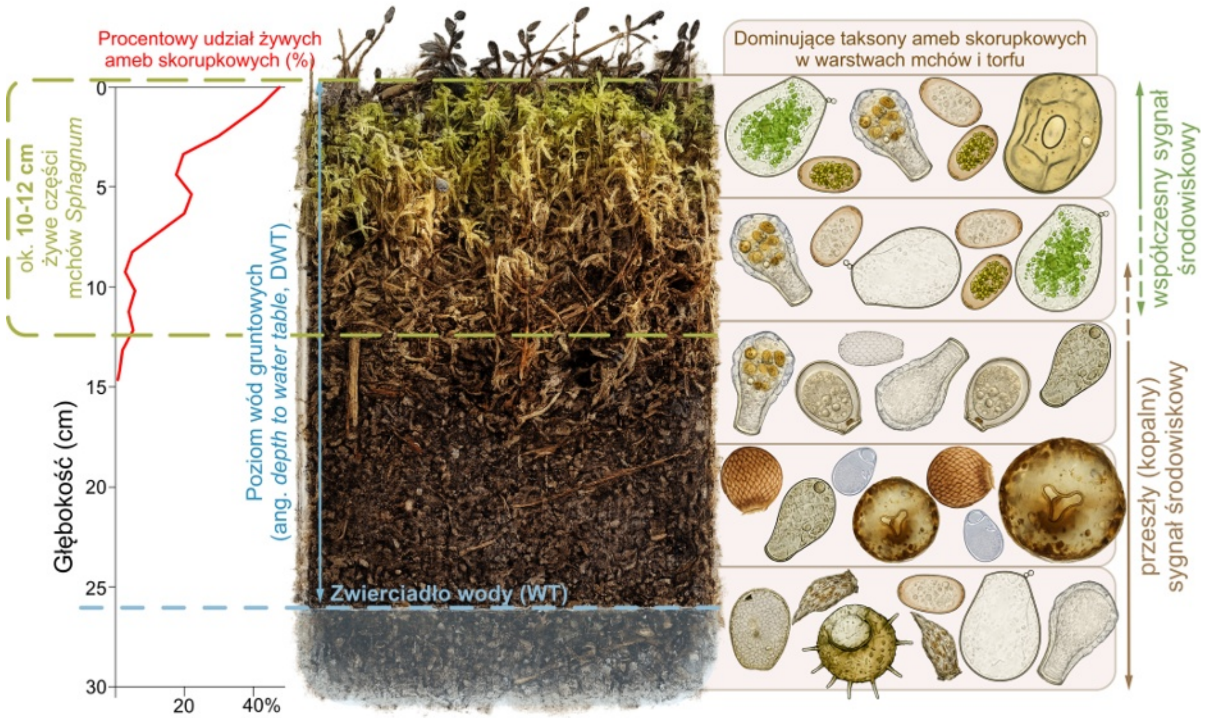

Ryc. 5 Koncepcyjny schemat rozkładu ameb skorupkowych w profilu torfowym wraz z dominującymi taksonami w poszczególnych warstwach oraz zmianami udziału żywych osobników w całkowitej liczbie zliczonych skorupek wraz z głębokością.
Źródło: opracowanie własne; krzywa procentowego udziału żywych ameb skorupkowych przedstawia przykładowy profil z torfowiska we wschodniej Kanadzie zaadaptowany na podstawie Roe i in.(2017). Przebieg tej krzywej może się znacząco różnić w zależności od lokalnych warunków środowiskowych.

Głównym narzędziem wykorzystywanym w tym celu są funkcje transferu, czyli modele matematyczne opisujące zależności między zbiorowiskami gatunków a parametrami środowiskowymi (Sachs i in., 1977; Woodland i in., 1998; Charman, 2001). Funkcje transferu mogą być tworzone zarówno na podstawie lokalnych zbiorów testowych, obejmujących próby pobrane z jednego regionu lub typu torfowiska (Lamentowicz i in., 2008; Lamarre i in., 2013), jak i szerokich zbiorów kontynentalnych, integrujących dane z wielu obszarów geograficznych (Amesbury i in., 2016, 2018; Qin i in., 2021). Lokalne funkcje transferu często pozwalają na dokładniejsze odwzorowanie specyficznych warunków środowiskowych badanego obszaru, natomiast modele kontynentalne umożliwiają analizę zmian hydrologicznych w szerszej skali przestrzennej oraz na obszarach, dla których lokalne funkcje transferu są niedostępne.

W przypadku Niziny Zachodniosyberyjskiej nadal brakuje regionalnego modelu uwzględniającego obecność wieloletniej zmarzliny oraz jej wpływ na hydrologię torfowisk, a tym samym na zbiorowiska ameb skorupkowych. Obecnie dostępne są jedynie funkcja kontynentalna (azjatycka) (Qin i in., 2021) lub modele lokalne opracowane dla pojedynczych stanowisk (Lamentowicz i in., 2015). Ogranicza to możliwość dokładnej rekonstrukcji warunków hydrologicznych torfowisk Niziny Zachodniosyberyjskiej w oparciu o dostępne narzędzia paleoekologiczne.

Pomimo rosnącego zainteresowania torfowiskami strefy borealnej i subarktycznej oraz dynamicznego rozwoju badań nad degradacją wieloletniej zmarzliny, wiele kluczowych mechanizmów odpowiedzialnych za funkcjonowanie tych ekosystemów nadal pozostaje słabo poznanych. Sam termin „degradacja zmarzliny" obejmuje bowiem szereg złożonych procesów fizycznych, hydrologicznych i biologicznych, zachodzących w różnych skalach przestrzennych i czasowych. Od lokalnych zmian mikrosiedliskowych, związanych ze zmianami uwilgotnienia, po regionalne przekształcenia krajobrazu wpływające na bilans węgla i funkcjonowanie całych ekosystemów torfowiskowych (Schuur i in., 2015; Hugelius i in., 2020). Procesy te prowadzą do głębokich zmian ekologicznych, obejmujących m.in. reorganizację zbiorowisk roślinnych i mikroorganizmów, zmiany tempa akumulacji torfu oraz modyfikację emisji gazów cieplarnianych (Swindles i in., 2015; van der Kolk i in., 2016; Jones i in., 2017; Ogden i in., 2023).

Mimo iż znaczenie torfowisk w systemie klimatycznym zostało wyraźnie dostrzeżone, a liczba badań poświęconych tym ekosystemom systematycznie wzrasta, wciąż istnieje wiele fundamentalnych pytań dotyczących ich reakcji na postępujące ocieplenie klimatu (Treat i in., 2022; Zhang i in., 2022). Znajduje to odzwierciedlenie również w najnowszych kierunkach światowych badań nad torfowiskami. Milner i in. (2026) wskazali 50 kluczowych pytań badawczych dotyczących współczesnej nauki o torfowiskach, a jedno z nich brzmiało:

„W jaki sposób torfowiska występujące w różnych strefach klimatycznych, na różnych wysokościach nad poziomem morza oraz w odmiennych warunkach hydrologicznych (w tym torfowiska związane z wieloletnią zmarzliną) będą

reagować na postępującą zmianę klimatu oraz jaki wpływ będzie miała ta zmiana na ich zasięg, procesy ekologiczne oraz ogólne funkcjonowanie?"

Dlatego szczególnie istotne jest lepsze zrozumienie dynamiki zmian hydrologicznych oraz towarzyszących im przemian środowiskowych zachodzących w torfowiskach związanych z wieloletnią zmarzliną. Kluczowe znaczenie ma również rozpoznanie mechanizmów odpowiedzialnych za zróżnicowaną reakcję poszczególnych mikrosiedlisk na procesy rozmarzania. Istotnym wyzwaniem pozostaje ponadto określenie, w jaki sposób biologiczne wskaźniki paleoekologiczne reagują na te przemiany oraz w jakim stopniu mogą być wykorzystywane do rekonstrukcji przeszłych zmian hydrologicznych i środowiskowych.

Odpowiedź na te pytania wymaga nie tylko dalszego monitoringu współczesnych zmian zachodzących na torfowiskach, lecz także rozwoju narzędzi umożliwiających rekonstrukcję ich długoterminowej dynamiki. Szczególnie ważne jest doskonalenie metod paleoekologicznych oraz pogłębianie wiedzy na temat współczesnych preferencji ekologicznych organizmów wykorzystywanych jako bioindykatory, takich jak ameby skorupkowe. Rozwój lokalnych funkcji transferu i badań wielowskaźnikowych może znacząco zwiększyć możliwości rekonstrukcji dawnych zmian hydrologicznych i środowiskowych, a tym samym przyczynić się do lepszego zrozumienia mechanizmów kształtujących reakcję torfowisk wysokich szerokości geograficznych na postępującą zmianę klimatu.

Cel badań

Głównym celem niniejszej rozprawy doktorskiej jest rozpoznanie mechanizmów funkcjonowania i długoterminowych zmian hydrologicznych wybranych torfowisk Niziny Zachodniosyberyjskiej położonych w strefie nieciągłej wieloletniej zmarzliny, ze szczególnym uwzględnieniem reakcji biotycznych wskaźników paleoekologicznych na procesy jej degradacji. Realizacja celu głównego opiera się na analizie zbiorowisk ameb skorupkowych (testate amoebae, TA) oraz podejściu wielowskaźnikowym (ang. *multi-proxy*), a także na syntetycznym ujęciu dotychczasowych badań paleoekologicznych prowadzonych na torfowiskach Niziny Zachodniosyberyjskiej.

W ramach celu głównego sformułowano następujące **cele szczegółowe**:

- Określenie zależności pomiędzy zbiorowiskami TA a warunkami środowiskowymi kompleksu torfowiskowego Khanymei, ze szczególnym uwzględnieniem poziomu wód gruntowych (ang. *depth to water table*, DWT), typu mikrosiedliska oraz składu roślinności.
- Opracowanie oraz ocena skuteczności lokalnej hydrologicznej funkcji transferu opartej na TA, obejmująca walidację statystyczną modelu oraz ocenę możliwości jego wykorzystania do rekonstrukcji paleohydrologicznych torfowisk strefy nieciągłej wieloletniej zmarzliny.
- Ocena wpływu uwzględnienia w zbiorze testowym zbiorowisk TA z prób powierzchniowych zdominowanych przez porosty rodzaju *Cladonia* na dokładność i parametry funkcji transferu.
- Rekonstrukcja zmian hydrologicznych i ekologicznych kompleksu torfowiskowego Khanymei w ciągu ostatnich ~200 lat, na podstawie analizy dwóch rdzeni torfowych, z wykorzystaniem podejścia wielowskaźnikowego.
- Ocena reakcji różnych mikrosiedlisk torfowiskowych (płaskowyżu torfowego i strefy brzegowej jeziora termokrasowego) na procesy degradacji wieloletniej zmarzliny oraz identyfikacja związanych z nimi zmian hydrologicznych i ekologicznych.
- Identyfikacja sygnałów degradacji wieloletniej zmarzliny zapisanych w archiwach torfowych oraz ocena ich znaczenia dla funkcjonowania torfowisk strefy nieciągłej zmarzliny.

- Scharakteryzowanie przestrzennego i metodologicznego zróżnicowania badań paleoekologicznych prowadzonych na torfowiskach Niziny Zachodniosyberyjskiej na podstawie opracowanej bazy metadanych obejmującej lokalizacje rdzeni oraz zastosowane wskaźniki paleoekologiczne.
- Wskazanie luk badawczych oraz priorytetowych kierunków przyszłych badań nad funkcjonowaniem torfowisk Niziny Zachodniosyberyjskiej.

Hipoteza badawcza testowana w niniejszej rozprawie zakłada, że postępująca zmiana klimatu prowadzi do degradacji wieloletniej zmarzliny na Nizinie Zachodniosyberyjskiej, a w konsekwencji do modyfikacji warunków hydrologicznych torfowisk. Zmiany te uruchamiają kaskadę przekształceń obejmującą reorganizację mikrosiedlisk i mikrostruktur torfowiskowych, przebudowę składu roślinności oraz zmiany dynamiki akumulacji torfu i węgla, co w ostatecznym rozrachunku znajduje bezpośrednie odzwierciedlenie w strukturze zbiorowisk TA.

Hipotezy szczegółowe:

H1. Struktura zbiorowisk TA na torfowiskach strefy nieciągłej wieloletniej zmarzliny Niziny Zachodniosyberyjskiej jest przede wszystkim kontrolowana przez DWT, przy czym typ mikrosiedliska oraz skład roślinności modyfikują siłę zależności pomiędzy DWT a strukturą tych zbiorowisk.

H2. Funkcja transferu skonstruowana na podstawie lokalnego zbioru testowego umożliwia bardziej precyzyjne rekonstrukcje zmian DWT niż modele oparte na kontynentalnych zbiorach danych.

H3. Zapis paleoekologiczny torfowisk strefy nieciągłej wieloletniej zmarzliny zawiera czytelny sygnał zmian związanych z procesami degradacji zmarzliny, możliwy do identyfikacji przy użyciu podejścia wielowskaźnikowego, przy czym reakcje środowiskowe poszczególnych mikrosiedlisk na te procesy są zróżnicowane.

H4. Dotychczasowe badania paleoekologiczne torfowisk Niziny Zachodniosyberyjskiej cechują się nierównomiernym rozmieszczeniem przestrzennym oraz nierówną reprezentacją poszczególnych podejść metodologicznych, co ogranicza możliwość regionalnych uogólnień dotyczących dynamiki ekosystemów torfowiskowych w tym regionie.

Obszar badań

Obiektem niniejszych badań są torfowiska Niziny Zachodniosyberyjskiej, analizowane zarówno w szerokim ujęciu regionalnym, jak i w szczegółowym kontekście lokalnym. Ze względu na zróżnicowaną skalę obszarów badawczych uwzględnionych w poszczególnych artykułach wchodzących w skład niniejszej rozprawy, opis obszaru badań został podzielony na dwie komplementarne części. Pierwszą, opisującą Nizinę Zachodniosyberyjską jako jednostkę fizycznogeograficzną (artykuł **III**) oraz drugą, szczegółowo charakteryzują kompleks torfowiskowy w okolicy miasta Khanymei (artykuł **I** i **II**).

Nizina Zachodniosyberyjska

Nizina Zachodniosyberyjska jest wielką równiną, zajmującą powierzchnię ok. 2,6 mln km^2 między 60–93°E a 52–73°N. Jej naturalne granice wyznaczają góry Ural na zachodzie, rzeka Jenisej na wschodzie, góry Ałtaj i stepy kazachskie na południu oraz Morze Karskie na północy (Ryc. 6). Jest to jedna z najbardziej płaskich i najniżej położonych dużych jednostek fizjograficznych Rosji – wysokości bezwzględne wynoszą 0-300 m n.p.m., a nachylenie terenu w kierunku północnym jest bardzo łagodne (Solomeshch, 2005).

Podłoże geologiczne stanowi młoda płyta tektoniczna przykryta grubą (3–11 km) sekwencją osadów mezozoiczno-kenozoicznych, a wierzchnią warstwę budują osady czwartorzędowe o miąższości 200-250 m (głównie gliny, piaski i iły) (Kremenetski i in., 2003; Kurakova, 2024). Płaski teren i słabo przepuszczalne osady sprzyjają wysokiemu zabagnieniu obszaru – ok. 50% powierzchni niziny pokrywają ekosystemy bagienne, a torfowiska (przy progu głębokości ≥ 50 cm) zajmują 592 440 km^2 (20% obszaru), tworząc jeden z największych kompleksów torfowiskowych na świecie (Sheng i in., 2004). W przeważającej części Niziny Zachodniosyberyjskiej dominuje klimat subarktyczny (Dfc w klasyfikacji Köppena-Geigera) z wyraźnym gradientem równoleżnikowym (Beck i in., 2018). Średnia roczna temperatura powietrza wynosi od –11,5°C na północy (Półwysep Gydański) do 1°C na południu, a suma rocznych opadów atmosferycznych wynosi 390–600 mm (Trofimova i Balybina, 2014). Region ten jest obecnie jednym z najszybciej ocieplających się obszarów na świecie, a modele klimatyczne wskazują na utrzymanie się tego trendu w przyszłości (Groisman i in., 2013; Hantemirov i in., 2022). W ostatnich dekadach nastąpił znaczący wzrost częstości dni z ekstremalnie wysoką temperaturą powietrza oraz zmniejszenie częstości dni z bardzo niskimi wartościami (Seneviratne i in., 2021). Jednocześnie nastąpiły istotne zmiany w reżimie opadów atmosferycznych – intensyfikacja opadów nawalnych w sezonie ciepłym oraz ogólny wzrost sum opadów i ekwiwalentu wodnego śniegu w sezonie zimowym (Bulygina i in., 2011; Groisman i in., 2013).

Ryc. 6 Obszar badań: mapa hipsometryczna wraz z ważniejszymi jednostkami geomorfologicznymi oraz zasięgiem torfowisk w granicach Niziny Zachodniosyberyjskiej. Źródło: opracowanie własne na podstawie: TanDEM-X © DLR e.V. 2010–2014; © Airbus DS GmbH 2014–2018 (program COPERNICUS, UE i ESA); torfowiska i granica niziny – Sheng i in. (2004). Rycina przetłumaczona i zaadaptowana z artykułu **III**.

Wieloletnia zmarzlina stanowi istotny element krajobrazu Niziny Zachodniosyberyjskiej. Jej zasięg obejmuje strefę ciągłą na północy, sięgającą do ok. 67°N, gdzie osiąga miąższość rzędu 100-500 m, a następnie przechodzi ku południu w strefy zmarzliny nieciągłej, sporadycznej i izolowanej, całkowicie zanikając w pobliżu 60°N (Ryc. 7) (Brown i in., 2002; Solomeshch, 2005). Główna faza rozwoju zmarzliny na Nizinie Zachodniosyberyjskiej przypada na późny plejstocen (18–27 tys. lat BP), kiedy jej południowa granica sięgała 48–49°N (Duchkov, 2006). Ocieplenie okresu atlantyckiego (ok. 6–5,5 tys. lat BP, optimum holoceńskie w tym regionie) doprowadziło do przesunięcia granicy zmarzliny ku północy, natomiast w okresie ochłodzenia subatlantyckiego (ok. 2–1,3 tys. lat BP) rozpoczęła się epigenetyczna agradacja zmarzliny, obejmująca przede wszystkim torfy nagromadzone po deglacjacji (Kondratjeva i in., 1993; Blyakharchuk, 2009). Dobre właściwości izolacyjne mchów torfowców sprzyjały utrzymywaniu się zmarzliny w cieplejszych porach roku i jej penetracji w głąb osadów mineralnych, co prowadziło do powstawania trwale zamarzniętych torfowisk oraz form peryglacjalnych takich jak pagórki palsa czy płaskowyże torfowe w wyniku kriogenicznego wyniesienia powierzchni torfowiska (Martini i in., 2007; Treat i Jones, 2018b).

Ryc. 7 Obszar badań: rozmieszczenie stref wieloletniej zmarzliny i głównych stref roślinności oraz zasięg torfowisk w granicach Niziny Zachodniosyberyjskiej.
Źródło: opracowanie własne na podstawie: roślinność – Olson i in. (2001); wieloletnia zmarzlina – Brown i in. (2002); torfowiska i granica niziny – Sheng i in. (2004).

Proces torfotwórczy na Nizinie Zachodniosyberyjskiej rozpoczął się we wczesnym holocenie, między 11 a 10 tys. lat BP, w odpowiedzi na postglacjalne ocieplenie północnej Syberii (Kremenetski i in., 2003). Choć najnowsze symulacje wskazują, że obszar ten nie był pokryty lądolodem podczas ostatniego zlodowacenia (Abe-Ouchi i in., 2015), warunki panujące w plejstocenie były niekorzystne dla akumulacji torfu. Ograniczony dopływ wilgoci znad Atlantyku, związany z ekspansją lodu na Oceanie Arktycznym oraz dominacją Wyżu Syberyjskiego, sprzyjał rozwojowi środowisk peryglacjalnych, charakteryzujących się suchymi latami i deficytem wilgoci (Velichko i in., 2011). Zaburzenie bilansu wodnego uznawane jest zatem za kluczowy czynnik blokujący rozwój torfowisk zdominowanych przez mchy *Sphagnum* na tym obszarze w okresie glacjalnym (Alexandrov i in., 2016).

Roślinność Niziny Zachodniosyberyjskiej odzwierciedla układ równoleżnikowy, przechodząc od arktycznej tundry na północy, przez rozległą strefę lasów borealnych (tajgi), do wąskiego pasa lasów liściastych i mieszanych, a ostatecznie do stepów i zarośli umiarkowanych na dalekim południu (Ryc. 7) (Olson i in., 2001). Krajobraz regionu charakteryzuje się także wyjątkowo dużą liczbą jezior, głównie płytkich (2–5 m), o powierzchni mniejszej niż 1 km^2, powstałych przede wszystkim w wyniku procesów termokrasowych związanych z degradacją zmarzliny (Kirpotin i in., 2009; Polishchuk i in., 2017). W strefie leśno-bagiennej jeziora mogą zajmować nawet 40–50% powierzchni zlewni, podczas gdy ich zagęszczenie maleje ku południowemu wschodowi, gdzie dominującą rolę w regulacji stosunków wodnych przejmują rozległe systemy bagienne (Kurakova, 2024).

Pomimo ogromnej powierzchni, Nizina Zachodniosyberyjska charakteryzuje się niską gęstością zaludnienia, szczególnie w części północnej, gdzie rozległe kompleksy torfowiskowe pozostają w dużej mierze słabo przekształcone. Od połowy lat 60. XX wieku region ten stał się jednak obszarem intensywnej eksploatacji ropy naftowej i gazu ziemnego, zwłaszcza w środkowym i dolnym biegu Obu. W konsekwencji działalność przemysłowa oraz zmiany użytkowania terenu wywierają coraz większą presję na ekosystemy torfowiskowe, prowadząc do modyfikacji ich struktury, hydrologii oraz funkcjonowania ekologicznego (Solomeshch, 2005).

"Kompleks torfowiskowy Khanymei"

Szczegółowy obszar badań obejmował kompleks torfowisk związanych z wieloletnią zmarzliną, położony w pobliżu miasta oraz stacji badawczej Khanymei (63°43′N, 75°57′E, ok. 70 m n.p.m.), w południowo-wschodniej części Jamalsko-Nienieckiego Okręgu Autonomicznego. Ze względu na brak oficjalnej nazwy badanego obszaru, w niniejszej pracy przyjęto nazwę „*kompleks torfowiskowy Khanymei*".

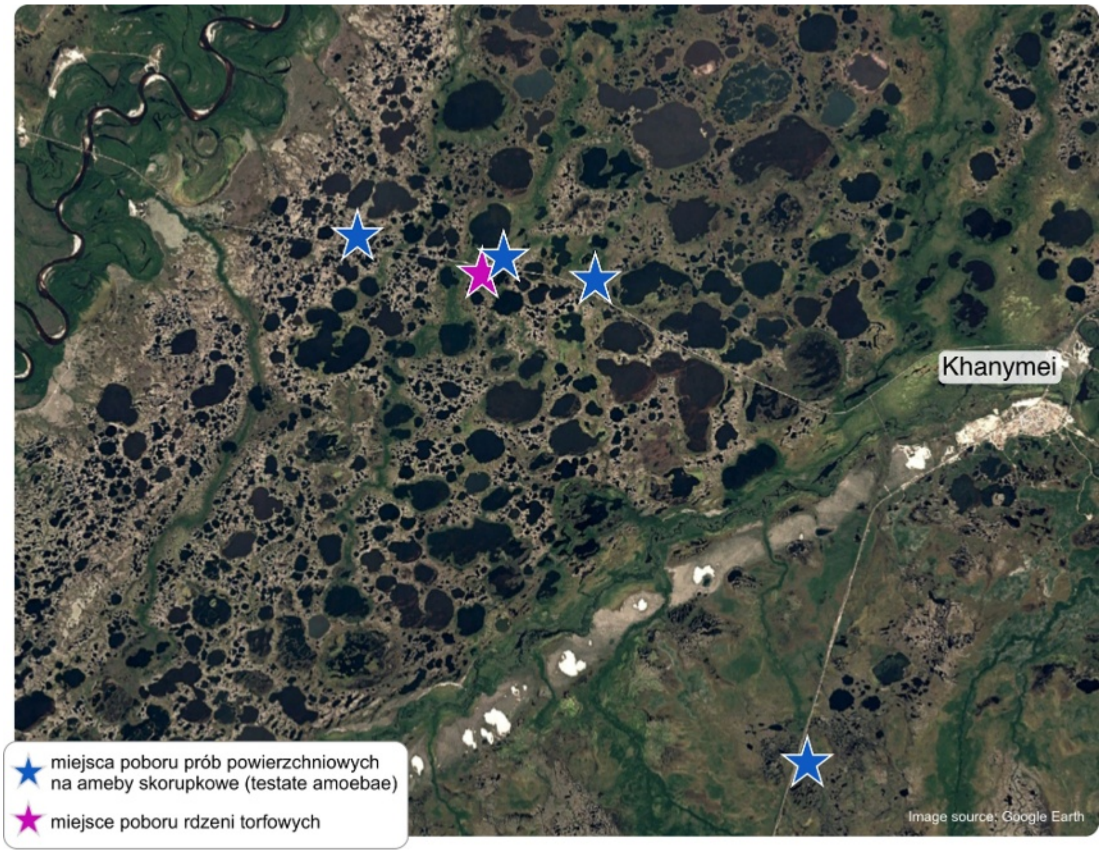

Ryc. 8 Obszar badań: zdjęcie satelitarne obszaru badań w okolicy miasta Khanymei z zaznaczonymi stanowiskami poboru prób powierzchniowych oraz rdzeni torfowych.
Źródło: Google Earth (data dostępu: 14.05.2025)

Obszar ten zlokalizowany jest w strefie nieciągłej wieloletniej zmarzliny i lasów borealnych (tajgi) (Ryc. 7). Klimat regionu ma charakter subarktyczny, z długimi i mroźnymi zimami oraz krótkimi, chłodnymi latami. Średnia roczna temperatura powietrza wynosi od –3,5 do –6°C, średnia temperatura powietrza stycznia od –22 do –24°C, natomiast lipca od 15,5 do 17°C (Trofimova i Balybina, 2014). Roczna suma opadów atmosferycznych wynosi około 436 mm (Kluge i in., 2021). Krajobraz badanego obszaru charakteryzuje się mozaiką kopulastych pagórków palsa oraz płaskowyżów torfowych o wysokości 2–6 m, zawierających rdzenie zmarzlinowe, otoczonych jeziorami termokrasowymi oraz otwartymi lasami iglastymi (Ryc. 8, 9A-C).

Dominują zbiorowiska sosnowo-modrzewiowe, tworzone głównie przez *Pinus siberica*, *Pinus sylvestris* oraz *Larix sibirica*, typowe dla tej części tajgi (Safronova i Yurkovsksya, 2019).

Powierzchnie płaskowyżów torfowych porasta mozaika zbiorowisk mchowo-porostowych z gęstym udziałem krzewinek, takich jak *Betula nana* oraz *Rhododendron tomentosum* (syn. *Ledum palustre*) (Ryc. 9D, 9F). Roślinność torfowisk wyniesionych jest dobrze rozwinięta i zdominowana przez torfowce, głównie *Sphagnum fuscum* oraz *Sphagnum medium/divinum*, przy jednoczesnym istotnym udziale porostów. Porosty, przede wszystkim z rodzajów *Cladonia* i *Cetraria*, zajmują około 70–80% powierzchni torfowisk i stanowią charakterystyczny element pokrywy roślinnej regionu Khanymei (Ryc. 9D) (Volkova i in., 2019). W odróżnieniu od bardziej południowych obszarów Niziny Zachodniosyberyjskiej, porosty w tym regionie uczestniczą w tworzeniu unikatowego typu torfu porostowego, często występującego w postaci wyraźnych warstw w profilu torfowym (Ryc. 9E) (Volkova i in., 2019). Miąższość złóż torfowych w tym regionie wynosi zazwyczaj od 0,1 do 1,4 m (Raudina i in., 2017).

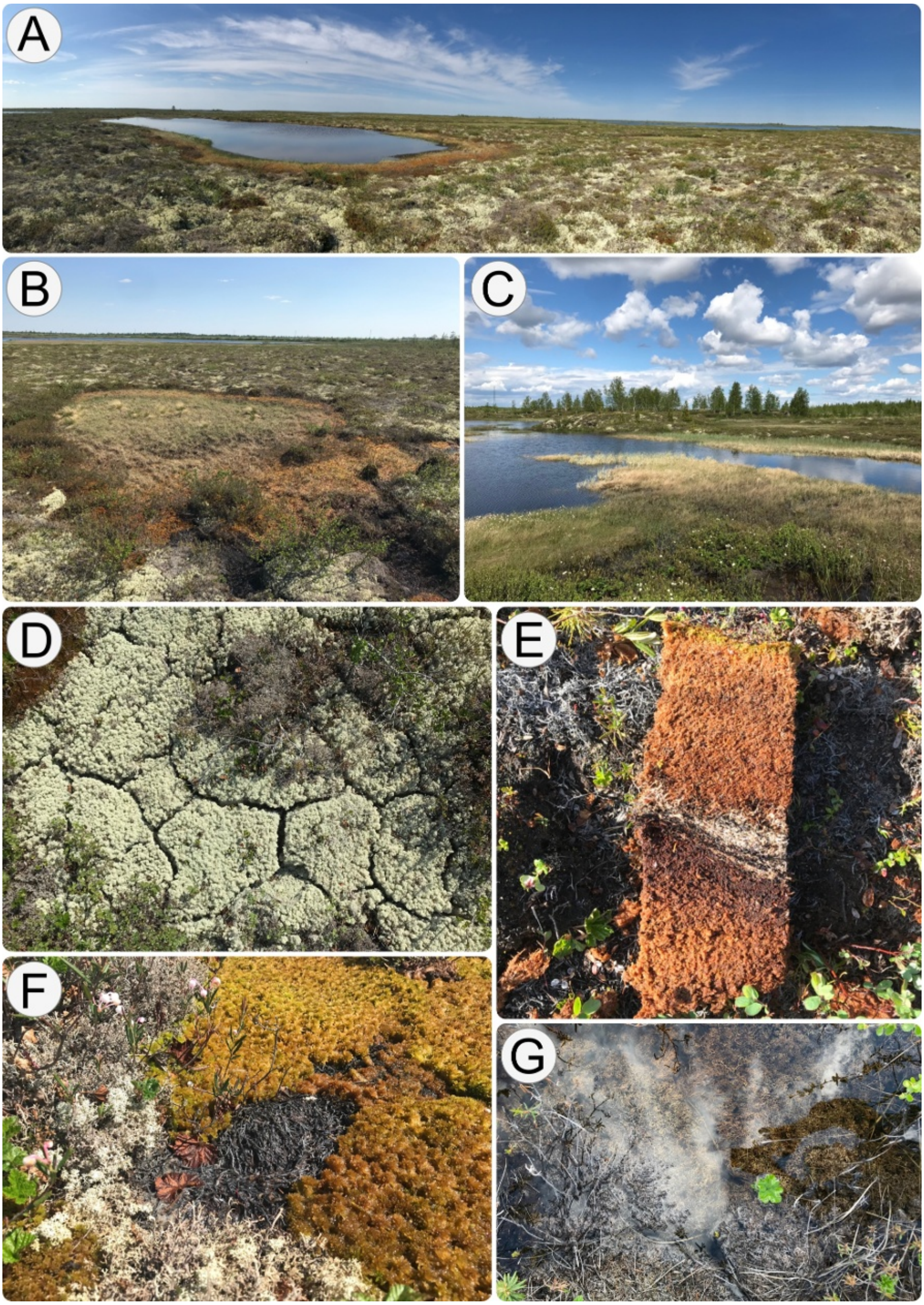

Ryc. 9 Kompleks torfowiskowy Khanymei: **(A-C)** formy typu palsa i płaskowyże torfowe (ang. *peat plateau*) oraz jeziora termokrasowe; **(D)** porosty oraz krzewinki; **(E)** przykład rdzenia torfowego z warstwą torfu porostowego; **(F)** mozaika zbiorowisk mchowo-porostowo-krzewinkowych; **(G)** porosty zatopione w wyniku rozmarzania zmarzliny oraz osiadania terenu.

Fot. Michał Słowiński, 2019

Metodyka badań

Metodyka niniejszej rozprawy doktorskiej łączy podejście kalibracyjno-rekonstrukcyjne (oparte na wykorzystaniu ameb skorupkowych (testate amoebae, TA) jako bioindykatorów warunków hydroekologicznych) z przeglądem i syntezą dostępnych danych paleoekologicznych z torfowisk Niziny Zachodniosyberyjskiej. Całość opiera się na trzech komplementarnych filarach: (1) kalibracji współczesnych zależności ekologicznych, (2) rekonstrukcji zmian paleoekologicznych oraz (3) integracji metadanych rdzeni torfowych z tego obszaru. Komponenty te zostały zrealizowane w ramach trzech powiązanych artykułów.

W artykule **I** przeprowadzono analizę współczesnych relacji pomiędzy zbiorowiskami TA a warunkami środowiskowymi na podstawie prób powierzchniowych pobranych z kompleksu torfowiskowego Khanymei. Analiza ta umożliwiła opracowanie lokalnej funkcji transferu, dostosowanej do specyfiki hydroklimatycznej badanego obszaru. W artykule **II** zastosowano podejście wielowskaźnikowe (ang. *multi-proxy*), w którym wykorzystano opracowaną funkcję transferu oraz szereg innych wskaźników do rekonstrukcji zmian paleoekologicznych w dwóch profilach torfowych. W artykule **III** dokonano syntezy danych paleoekologicznych z obszaru Niziny Zachodniosyberyjskiej tworząc bazę metadanych rdzeni torfowych *Western Siberian Peat Core Database* (WSPC), umożliwiającą analizę przestrzenną oraz ocenę reprezentatywności zapisów torfowych w ujęciu regionalnym.

Badania terenowe i pobór materiału

Badania terenowe przeprowadzono na kompleksie torfowiskowym w okolicy miasta Khanymei na przełomie czerwca i lipca 2019 roku (Ryc. 10). Celem kampanii było pozyskanie materiału do określenia współczesnych relacji TA–środowisko na badanym kompleksie torfowiskowym oraz pobór rdzeni torfowych do analiz paleoekologicznych.

Pobór prób powierzchniowych

W celu opracowania lokalnej funkcji transferu pobrano łącznie 76[1] prób powierzchniowych na czterech stanowiskach M1–M4 (Ryc. 10A, 10C). Próby zbierano

[1] Jedna próba powierzchniowa została wykluczona z dalszych analiz we względu na bardzo niską koncentrację skorupek TA

w transektach biegnących ku brzegom jezior termokrasowych, obejmujących gradient mikrotopograficzny: kępy (*hummocks*/*mounds*), dolinki (*lawns*), dywany mszarne (*carpets*) oraz jeziorka (*ponds*) (Ryc. 11) (Rydin i Jeglum, 2013). Głębokość poziomu wód gruntowych lub powierzchni zmarzliny (zamarzniętego torfu) mierzono bezpośrednio w terenie z dokładnością do 1 cm, przyjmując kulminację mchów i porostów lub poziom wody jako punkt odniesienia (0 cm). W celu możliwie najpełniejszej reprezentacji warunków środowiskowych w zbiorze testowym, pobierano zarówno mchy, jak i porosty, natomiast szczegółowy skład roślinności określono laboratoryjnie na podstawie analizy makroszczątków roślinnych. Do analizy TA pobierano próbki roślinności z powierzchni 10 cm², obejmujące górne 0–3 cm warstwy mszysto-porostowej.

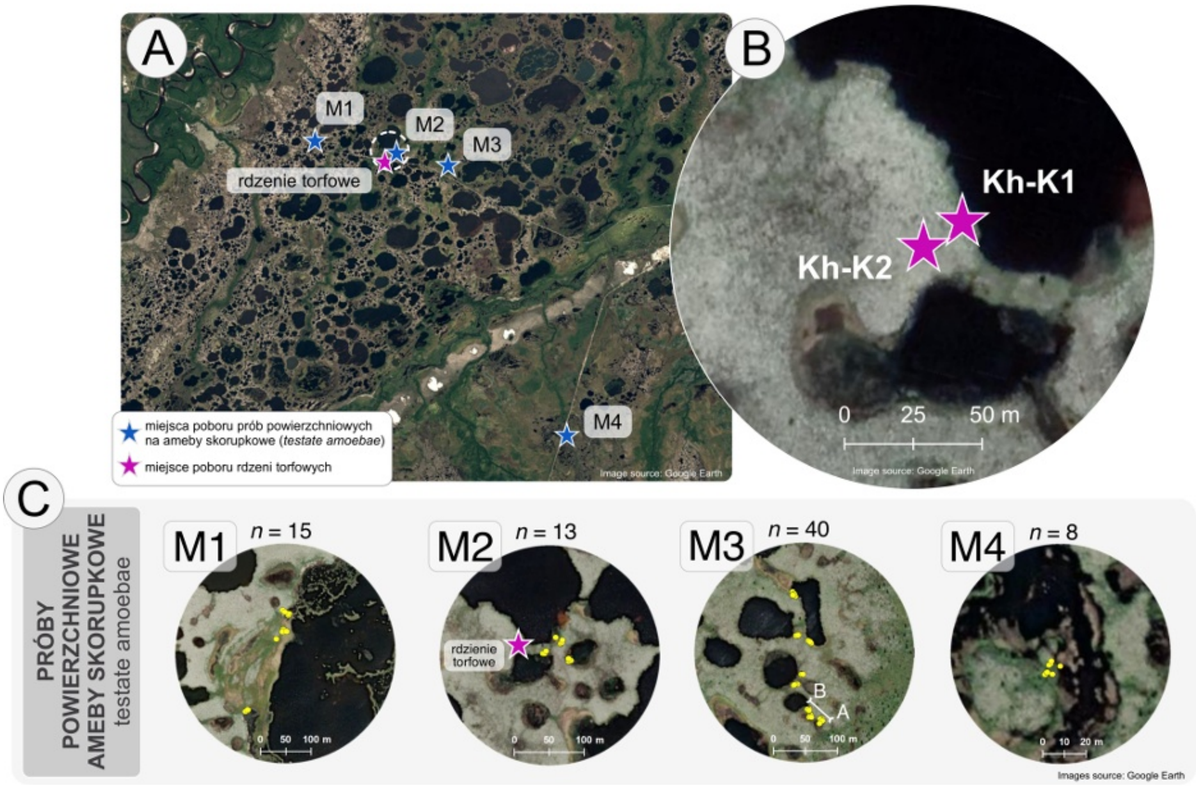

Ryc. 10 Obszar badań: **(A)** lokalizacja poboru prób powierzchniowych oraz rdzeni torfowych na kompleksie torfowiskowym Khanymei; **(B)** miejsca poboru rdzeni torfowych Kh-K1 i Kh-K2; **(C)** lokalizacja poboru prób powierzchniowych na czterech stanowiskach (M1-M4) wraz z przebiegiem transektu A-B przedstawionego na ryc. 15A.
Źródło: Google Earth (data dostępu: 14.05.2025). Panel B został zaadaptowany z artykułu **II**, natomiast panel C został przetłumaczony i zaadaptowany z artykułu **I**.

Pobór rdzeni torfowych

Dwa monolity torfowe (Kh-K1 i Kh-K2) o przekroju 10 × 10 cm pobrano z kompleksu płaskowyż torfowy–jezioro, w odległości około 5 m od siebie (Ryc. 10B). Rdzeń Kh-K1 (długość 34 cm) został pobrany ze strefy brzegowej jeziora termokrasowego, natomiast rdzeń Kh-K2 (27 cm) z powierzchni płaskowyżu torfowego i został pobrany do poziomu zamarzniętego torfu. Rdzenie podzielono z rozdzielczością 1 cm (z wyjątkiem warstwy 0–2 cm w rdzeniu Kh-K2) do analiz paleoekologicznych.

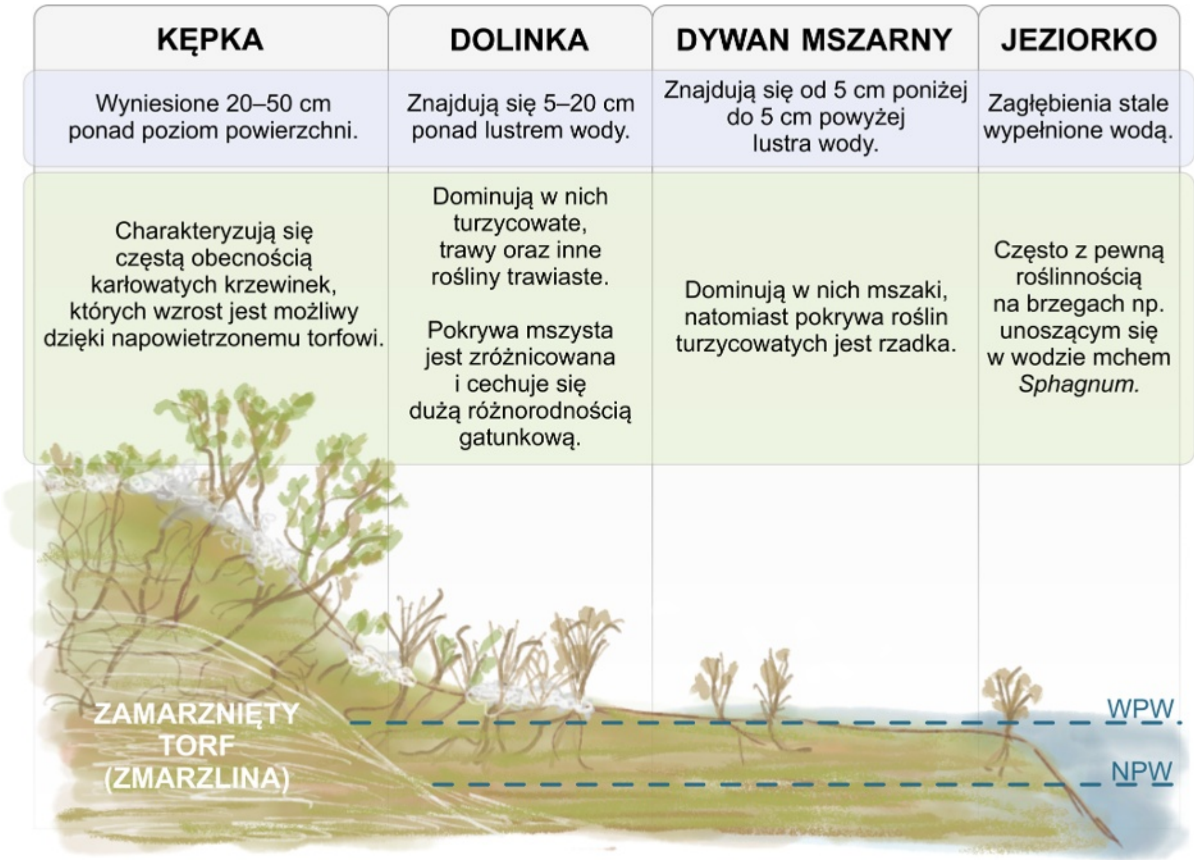

Ryc. 11 Schematyczne przedstawienie gradientu mikrotopograficznego torfowiska wysokiego z zaznaczonymi przybliżonymi poziomami wysokiej (WPW) i niskiej wody (NPW).
Źródło: opracowanie własne na podstawie Rydin i Jeglum (2013) oraz obserwacji terenowych.

Hydrologiczna funkcja transferu

Przygotowanie zbioru testowego – analiza ameb skorupkowych

Analizę TA w próbach powierzchniowych przeprowadzono zgodnie ze standardową procedurą (Hendon i Charman, 1997; Booth i in., 2010). Z każdej próby pobierano około 3 cm^3 materiału, zalewano wodą destylowaną, przesiewano przez sito 300 µm i badano pod mikroskopem świetlnym (200× i 400×). Liczono co najmniej 150 skorupek TA na próbę. Taksony identyfikowano na podstawie dostępnych kluczy taksonomicznych (m.in. Charman i in., 2000; Mazei i Tsyganov, 2006; Siemensma, 2022), a niektóre z nich łączono w grupy zgodnie z harmonizacją Amesbury i in. (2016) w celu minimalizacji błędów identyfikacji. Do przetestowania funkcji transferu wykorzystano materiał subfosylny z rdzenia Kh-K2, analizowany zgodnie z tą samą procedurą, w rozdzielczości 1 cm (oprócz odcinka 0-2 cm) (Ryc. 12).

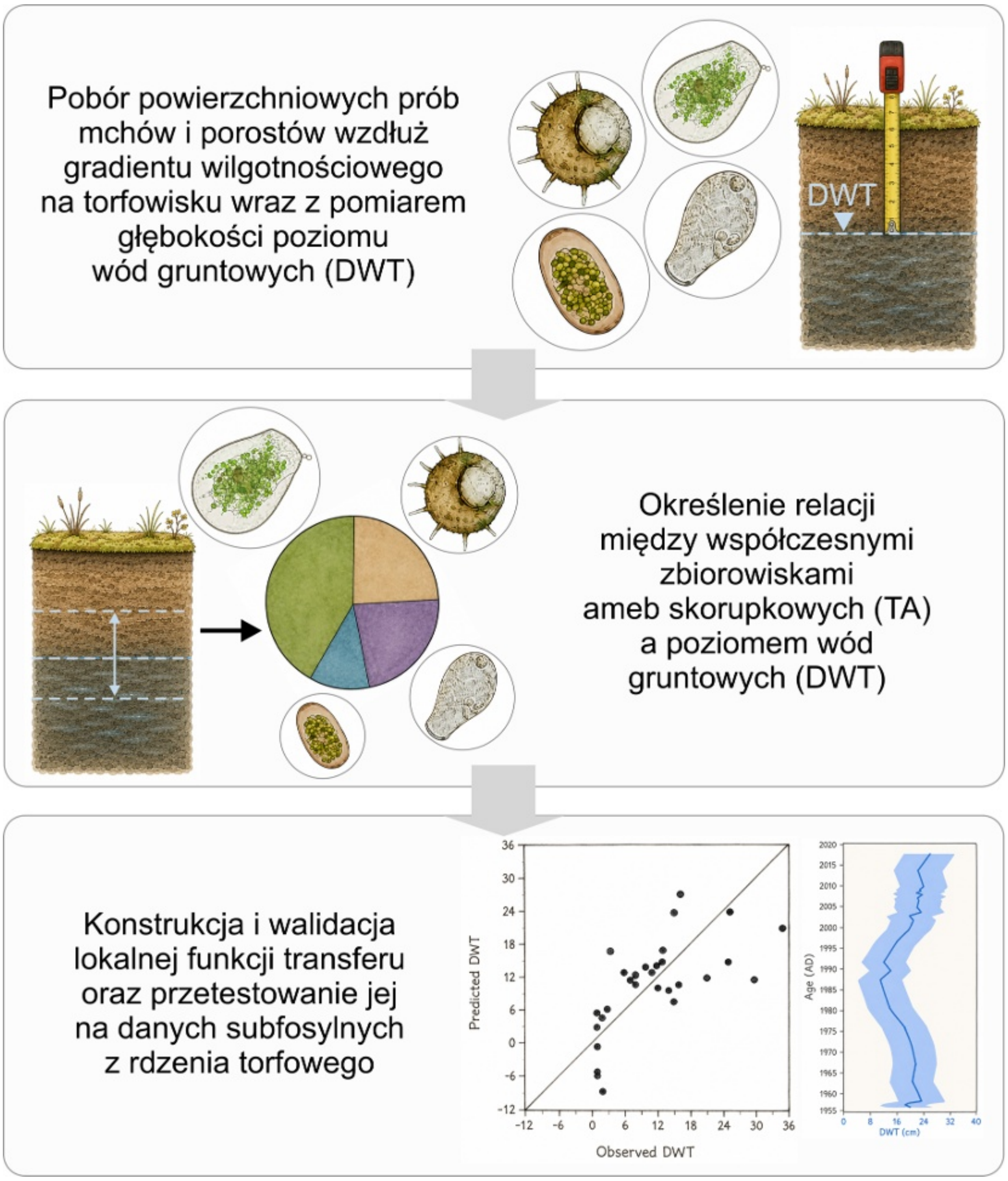

Ryc. 12 Schemat metodyki badań wykorzystany w artykule **I**.
Źródło: opracowanie własne; elementy graficzne ujednolicono stylistycznie przy użyciu ChatGPT (OpenAI).

Charakterystyka zbiorowisk ameb skorupkowych

Zarówno dla współczesnych jak i subfosylnych zbiorowisk TA określono różnorodność biologiczną zbiorowisk za pomocą wskaźnika Shannona (Daly i in., 2018). Podobieństwo zbiorowisk TA w próbach powierzchniowych oceniono metodą NMDS (Niemetryczne Skalowanie Wielowymiarowe, ang. *Non-metric Multidimensional Scaling*), standaryzując zbiór danych tak, aby zmniejszyć wpływ taksonów rzadkich i pospolitych. W celu oceny siły i istotności wpływu warunków wilgotnościowych, wektor zmiennej środowiskowej (DWT) został dopasowany do przestrzeni ordynacyjnej za pomocą funkcji *envfit*. Skalowanie wykonano dla pełnego zbioru danych (*n* = 75), zbioru bez prób porostowych (*n* = 55) oraz wyłącznie dla prób porostowych (*n* = 20). Obliczenia wykonano w programie R przy użyciu pakietu *vegan* (Oksanen i in., 2022; R Core Team, 2022).

Opracowanie i weryfikacja funkcji transferu

Hydrologiczną funkcję transferu opracowano w programie C2 (Juggins, 2007) dla pełnego zbioru danych (*n* = 75) oraz zbioru bez prób porostowych (*n* = 55), z zastosowaniem następujących modeli statystycznych:

- Weighted Averaging (WA) – średnia ważona,
- Weighted Averaging Partial Least Squares (WA-PLS) – średnia ważona z częściowymi najmniejszymi kwadratami,
- Modern Analogue Technique (MAT) – technika współczesnych analogów,
- Maximum Likelihood (ML) – metoda największej wiarygodności,
- Partial Least Squares (PLS) – częściowe najmniejsze kwadraty.

W celu oceny jakości modeli wykonano walidację krzyżową metodą *leave-one-out* oraz *bootstrapping* (1000 cykli). Modele oceniano pod kątem współczynnika determinacji (R^2), pierwiastka błędu średniokwadratowego prognozy (RMSEP) oraz średniego i maksymalnego błędu systematycznego (ang. *bias*). W celu oceny wpływu rozdzielczości taksonomicznej na jakość funkcji transferu zastosowano kilka konfiguracji agregacji taksonomicznej, obejmujących zarówno pełne uwzględnienie wszystkich zidentyfikowanych taksonów, jak i ich agregację w grupy o różnym stopniu uogólnienia (Charman i in., 2000; Amesbury i in., 2016). Trudne do oznaczenia taksony (*Cyclopyxis arcelloides* type, *Difflugia lucida* type, *Difflugia pulex* type) grupowano według podobieństwa morfologicznego (Mitchell i in., 2014), natomiast taksony kluczowe dla zbiorowisk TA pozostawiono rozdzielone, aby nie utracić informacji ekologicznej (np. *Corythion dubium*, *Trinema lineare*). Dodatkowo dla wszystkich zidentyfikowanych taksonów obliczono optima i zakresy tolerancji DWT przy pomocy modelu WA w programie C2, zarówno dla pełnego zbioru danych, jak i dla zbioru bez prób porostowych, aby ocenić wpływ tych specyficznych stanowisk na preferencje poszczególnych taksonów oraz funkcję transferu.

Najlepsze modele funkcji transferu zostały zastosowane do rekonstrukcji DWT na danych subfosylnych z rdzenia Kh-K2, w celu oceny ich zdolności rekonstrukcyjnej. Otrzymane wyniki porównano z wynikami rekonstrukcji opartych na wcześniej opublikowanych kontynentalnych funkcjach transferu: paneuropejskiej (Amesbury i in., 2016) oraz azjatyckiej (Qin i in., 2021).

Analizy paleoekologiczne

Każdy rdzeń torfowy został podzielony z rozdzielczością 1 cm (z wyjątkiem odcinka 0–2 cm w rdzeniu Kh-K2) w celu przeprowadzenia analiz: ameb skorupkowych (objętość próbki: 3 cm^3), pyłku roślin i mikrowęgli drzewnych (1 cm^2), makrowęgli drzewnych (2 cm^2), makroszczątków roślinnych (4 cm^3) oraz strat masy przy prażeniu (ang. *loss on ignition*, LOI; 1 cm^3) (Ryc. 13).

Datowanie radiowęglowe

Do datowania radiowęglowego wybrano osiem prób makroszczątków roślinnych z rdzenia Kh-K1 oraz pięć z rdzenia Kh-K2 (artykuł **II** – Tab. 1). Datowania wykonano metodą AMS ^{14}C, a uzyskane daty skalibrowano z wykorzystaniem krzywych IntCal20 (Reimer i in., 2020) oraz NH1 post-bomb (Hua i in., 2013). Modele wiek–głębokość obliczono w programie OxCal v4.4.4 (Ramsey, 2001).

Ameby skorupkowe

Analizę subfosylnych TA przeprowadzono zgodnie z metodyką przyjętą dla materiału współczesnego, którą opisano w podrozdziale *Przygotowanie zbioru testowego – analiza ameb skorupkowych*. Wyniki analizy wykorzystano do ilościowych rekonstrukcji DWT oraz pH dla rdzeni Kh-K1 i Kh-K2. Podział profili na poziomy stratygraficzne wykonano metodą hierarchicznej analizy skupień z zachowaniem chronologii (CONISS) z wykorzystaniem pakietu *rioja* w programie R (Juggins, 2020).

Dla każdej próby obliczono wskaźnik różnorodności Shannona. W celu oceny reakcji zbiorowisk TA na przeszłe zaburzenia na torfowisku przeanalizowano cechy funkcjonalne TA (ang. *functional traits*), obejmujące: status troficzny (miksotrofię), wielkość i pozycję apertury, objętość skorupki oraz stopień jej spłaszczenia. W celu określenia cech funkcjonalny całych zbiorowisk obliczono średnią ważoną cech dla całej społeczności (ang. *Community-Weighted Means*, CWM) wykorzystując pakiet *FD* w programie R (Laliberté i in., 2014; Fournier i in., 2015). Dodatkowo taksony sklasyfikowano według typu skorupki (Mitchell i in., 2008).

Zmiany struktury zbiorowisk TA w czasie analizowano metodą NMDS, zastosowaną dla rdzenia Kh-K1, w którym zapisane zostały najbardziej dynamiczne zmiany paleohydrologiczne. Rekonstrukcje zmian DWT przeprowadzono z wykorzystaniem lokalnej funkcji transferu opublikowanej w artykule **I**, natomiast zmiany pH zrekonstruowano za pomocą azjatyckiej funkcji transferu (Qin i in., 2021). Obliczenia wykonano w programie C2 (Juggins, 2007).

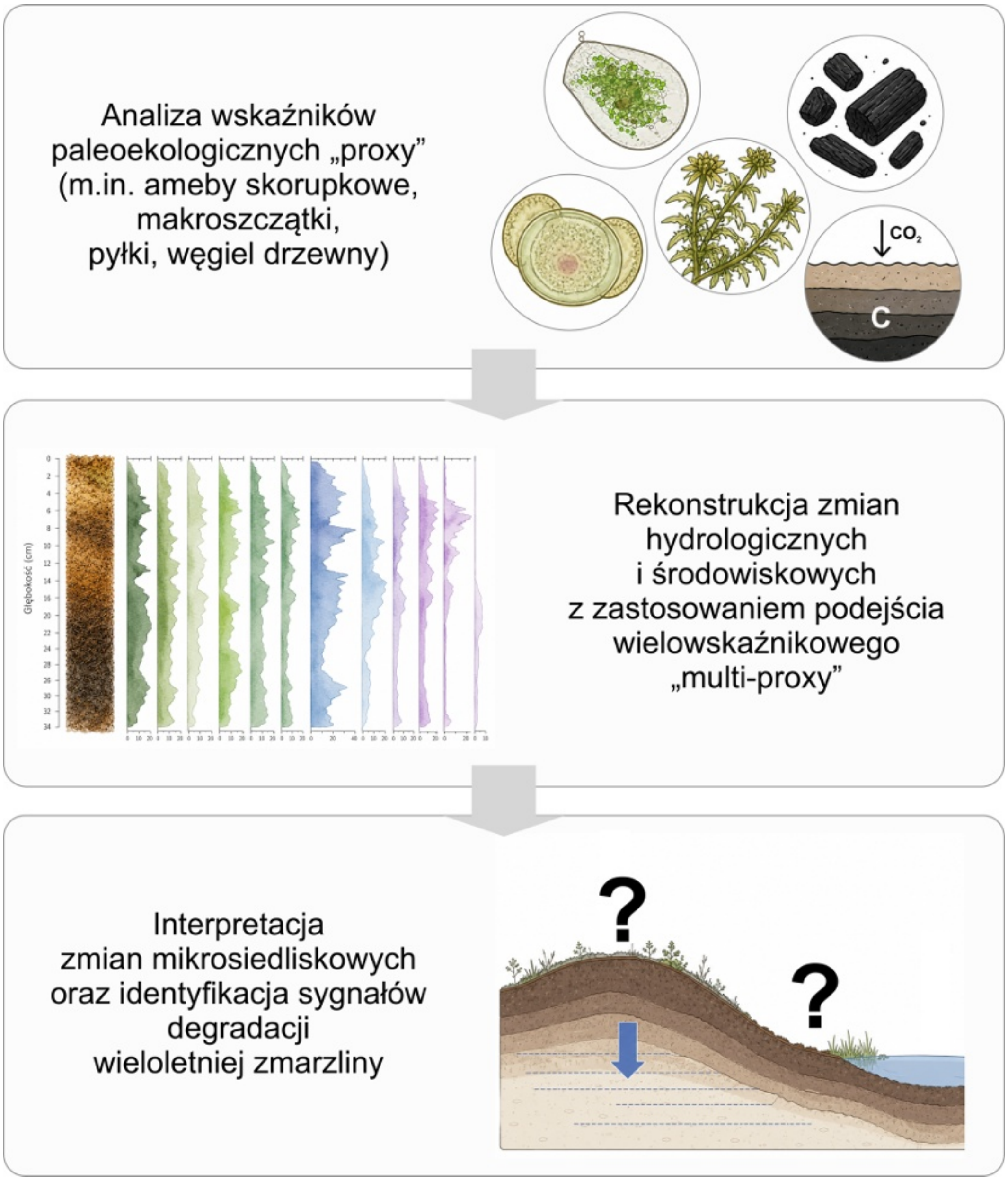

Ryc. 13 Schemat metodyki badań wykorzystany w artykule **II**.
Źródło: opracowanie własne; elementy graficzne ujednolicono stylistycznie przy użyciu ChatGPT (OpenAI).

Pyłek roślinny i palinomorfy niepyłkowe (NPPs)

Analizę pyłkową przeprowadzono według standardowej procedury (Berglund i Ralska-Jasiewiczowa, 1986) z zastosowaniem znaczników Lycopodium do wyznaczenia koncentracji palinomorfów (Stockmarr, 1971). W każdej próbie zliczano 300–500 ziaren pyłku roślin lądowych. Identyfikację taksonomiczną przeprowadzono na podstawie kluczy pyłkowych (m.in. Faegri i in., 1989; Moore i in., 1994) oraz fotografii referencyjnych, a palinomorfy niepyłkowe (NPPs) identyfikowano zgodnie z Van Geel (2001) i Shumilovskikh i in. (2015).

Makroszczątki roślinne

Materiał do analizy makroszczątków roślinnych był płukany wodą destylowaną i przesiewany przez sito 125 µm. Skład roślinności oceniano pod mikroskopem stereoskopowym, określając procentowy udział mszaków i roślin naczyniowych. Identyfikację makroszczątków roślinnych przeprowadzono na podstawie dostępnych kluczy i atlasów (Katz i in., 1977; Tobolski, 2000; Mauquoy i Geel, 2007).

Węgle drzewne

Węgle drzewne analizowano w trzech frakcjach wielkości: 10–100 µm (mikrowęgle), 100–500 µm i >500 µm (makrowęgle). Cząstki mikrowęgli drzewnych liczono podczas analizy palinologicznej na tych samych szkiełkach, natomiast makrowęgli drzewnych pod mikroskopem stereoskopowym po wybielaniu prób przez 24 h i przesiewaniu przez sita 100 i 500 µm (Mooney i Radford, 2001). Makrowęgle dzielono na dwie frakcje (100–500 µm i >500 µm), aby lepiej ocenić odległość źródła pożaru (Conedera i in., 2009).

Napływ mikrowęgli i makrowęgli drzewnych (MIC i MAC influx, cząstki· cm^{-2}· rok^{-1}) obliczono jako stosunek koncentracji cząsteczek węgla drzewnego do tempa akumulacji torfu, co pozwoliło ocenić zarówno regionalną, jak i lokalną aktywność pożarową.

Fizyczne i chemiczne właściwości torfu

Tempo akumulacji torfu (PAR, mm) obliczono jako stosunek grubości próbki do różnicy wieku między jej górną i dolną granicą. Zawartość materii organicznej (OM, %) określono metodą strat masy przy prażeniu (LOI) zgodnie ze standardowym protokołem (Heiri i in., 2001). Próby suszono w temperaturze 105°C przez 12 godzin, a następnie prażono w temperaturze 550°C przez 3 godziny. Gęstość objętościową suchej masy (BD, g · cm^{-3}) obliczono jako stosunek masy próby po wysuszeniu do jej objętości. Zawartość węgla przeliczono z OM, przyjmując, że stanowi on około 50% masy materii organicznej (Chambers i in., 2011; Treat i in., 2016). Na podstawie tych parametrów określono tempo akumulacji węgla (CAR, g C · m^{-2} · yr^{-1}).

Metody syntezy danych i analiz przestrzennych

Przegląd literatury

Przegląd literatury w artykule **III** zrealizowano w oparciu o bazy Google Scholar oraz Scopus, stosując zestaw słów kluczowych: „*Western Siberia*", „*reconstruction*" oraz „*peatland*". Wybór literatury ograniczono do pozycji w języku angielskim i rosyjskim opisujących rdzenie stratygraficzne lub przekroje torfowiskowe zlokalizowane w obrębie Niziny Zachodniosyberyjskiej, zgodnie z delimitacją zaproponowaną przez Sheng i in. (2004) (Ryc. 14). Analiza objęła wyłącznie prace zawierające oryginalne dane paleoekologiczne lub meta-analizy oparte na określonym zestawie rdzeni, przy czym każdy z nich musiał zawierać co najmniej jeden wskaźnik paleoekologiczny.

Ekstrakcja danych i tworzenie bazy metadanych

Na podstawie danych z wybranych publikacji stworzono *Western Siberian Peat Core Database* (WSPC). W bazie gromadzono dane dotyczące lokalizacji, nazwy rdzenia, zastosowanych wskaźników paleoekologicznych oraz (w przypadku ich dostępności) rodzaju datowania, liczby datowanych poziomów, zakresu czasowego oraz rozdzielczości próbkowania. Dane dotyczące tych samych rdzeni, opisywanych w różnych publikacjach, zostały połączone w pojedyncze rekordy. Dla rdzeni bez skalibrowanych dat przeprowadzono kalibrację w programie R przy użyciu pakietu *bchron* i krzywej IntCal20 (Haslett i Parnell, 2008). Każdemu rdzeniowi nadano unikalny identyfikator Core ID, zachowując jednocześnie oryginalne nazwy dla ułatwienia identyfikacji. Wszystkie obiekty zgeoreferencjonowano i skompilowano wraz z atrybutami do jednolitej warstwy *shapefile* w programie QGIS 3.16.2 (QGIS Development Team, 2025). Gęstość rozmieszczenia rdzeni oceniono w siatce 50 × 50 km, a każdy z nich przypisano do odpowiednich stref ekologicznych, obejmujących typy roślinności, typy torfowisk oraz strefy wieloletniej zmarzliny (Ivanov i Novikov, 1976; Olson i in., 2001; Brown i in., 2002; Kremenetski i in., 2003).

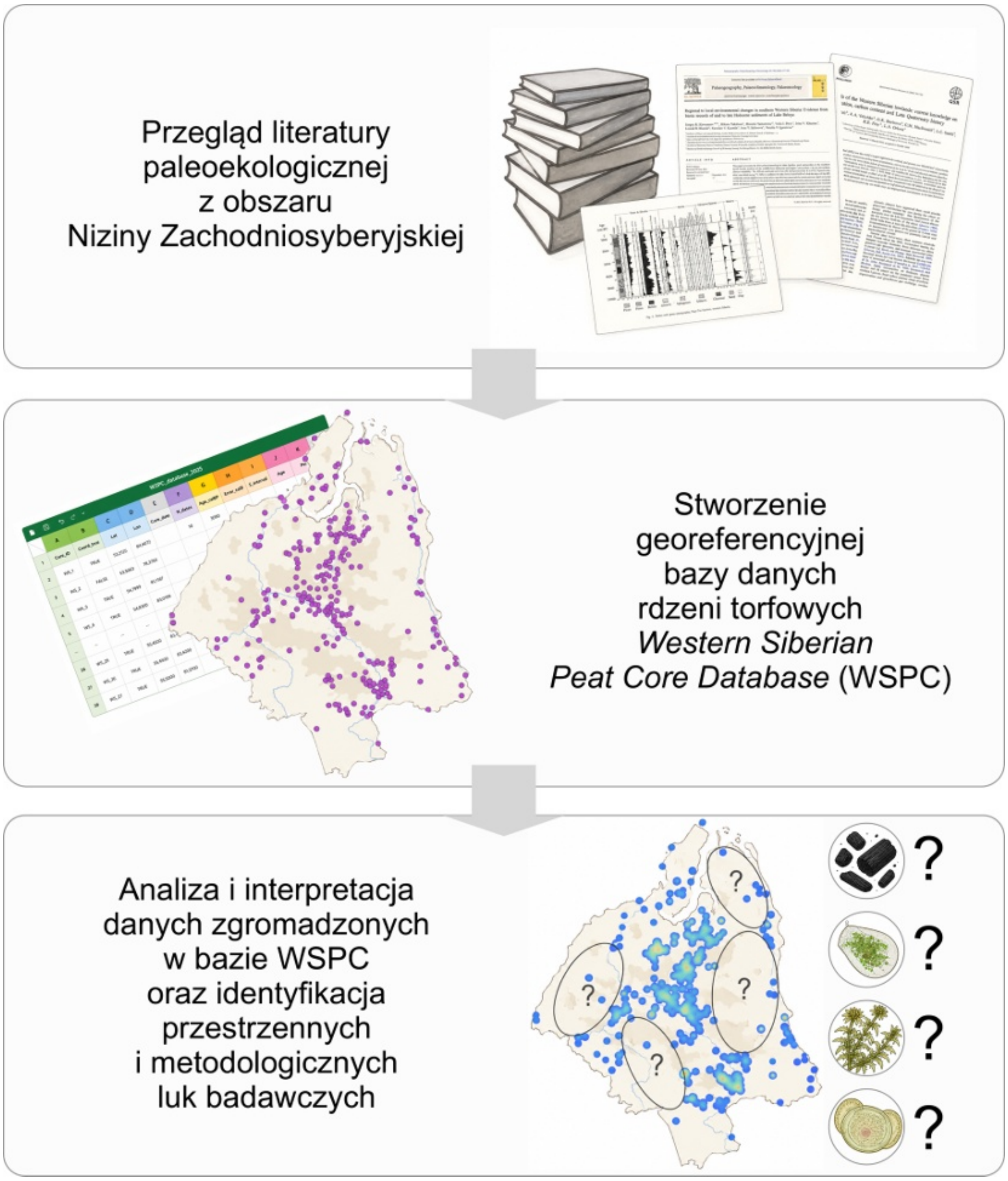

Ryc. 14 Schemat metodyki badań wykorzystany w artykule **III**.
Źródło: opracowanie własne; elementy graficzne ujednolicono stylistycznie przy użyciu ChatGPT (OpenAI).

Waloryzacja rdzeni torfowych pod kątem potencjału informacyjnego i wizualizacja przestrzenna

W celu oceny jakości i wartości informacyjnej każdego rdzenia opracowano autorski system punktacji, w którym poszczególnym wskaźnikom paleoekologicznym przypisano wagę odzwierciedlającą jego znaczenie w rekonstrukcjach środowiskowych (artykuł **III** – Tab. B3). Wskaźniki pogrupowano na trzy kategorie: biologiczne, fizyczne i chemiczne. Ostateczna ocena każdego rdzenia uwzględniała obecność chronologii, długość rekordu, liczbę zastosowanych wskaźników oraz ważoną sumę punktów w poszczególnych grupach (artykuł **III** – Tab. B4). Na tej podstawie wyznaczono cztery skumulowane indeksy: całkowity oraz trzy cząstkowe (odpowiednio dla wskaźników biologicznych, chemicznych i fizycznych). Wyższe wartości tych indeksów świadczą o lepszej kontroli chronologicznej, dłuższym pokryciu czasowym oraz większej różnorodności zastosowanych metod paleoekologicznych.

Wizualizację przestrzenną wyników przeprowadzono w programie QGIS z wykorzystaniem narzędzia Heatmap (ang. *Kernel Density Estimation*, KDE), przyjmując promień wygładzania wynoszący 30 km jako miarę średniej przestrzennej reprezentatywności pojedynczego rdzenia. Analizy wykonano zarówno dla skumulowanego indeksu całkowitego, jak i oddzielnie dla grup wskaźników biologicznych, chemicznych i fizycznych, co umożliwiło identyfikację obszarów o zróżnicowanym stopniu reprezentatywności danych paleoekologicznych.

Najważniejsze wyniki badań

Artykuł I - "*Developing a new testate amoeba hydrological transfer function for permafrost peatlands of NW Siberia*"

W artykule **I** przedstawiono kluczowe wyniki badań dotyczących relacji pomiędzy współczesnymi zbiorowiskami ameb skorupkowych (TA) a wybranymi elementami środowiska, przede wszystkim poziomem wód gruntowych (DWT) oraz typem roślinności, w kompleksie torfowiskowym Khanymei położonym w strefie nieciągłej wieloletniej zmarzliny. Na podstawie uzyskanych danych opracowano również pierwszą dla tego obszaru lokalną funkcję transferu, umożliwiającą bardziej szczegółową rekonstrukcję warunków hydrologicznych na badanych torfowiskach. Uzyskane wyniki stanowią istotną podstawę zarówno do interpretacji współczesnych zależności ekologicznych, jak i do rekonstrukcji przeszłych zmian hydrologicznych w ekosystemach torfowiskowych Niziny Zachodniosyberyjskiej.

W próbach powierzchniowych badanego kompleksu torfowiskowego zidentyfikowano łącznie 11 388 skorupek TA należących do 45 taksonów (artykuł **I** – Tab. 1). Zbiorowiska TA wykazywały wyraźne zróżnicowanie wzdłuż gradientu wilgotnościowego oraz typu mikrosiedliska, od suchych kęp i stanowisk porostowych *Cladonia* po silnie uwodnione obrzeża jeziorek termokrasowych (Ryc. 15A). Najliczniejszymi taksonami w całym zbiorze były *Corythion dubium*, *Archerella flavum*, *Cyclopyxis arcelloides* type oraz *Hyalosphenia papilio*, natomiast *Assulina muscorum* była najpowszechniej występującym taksonem.

Zbiorowiska TA na stanowiskach porostowych charakteryzowały się dominacją taksonów tolerujących suche warunki, niezależnie od lokalnego DWT. W przeciwieństwie do nich, pozostałe mikrosiedliska (kępy, dolinki, dywany mszarne i jeziorka) wykazywały wyraźne, stopniowe zmiany składu taksonomicznego zbiorowisk TA wzdłuż gradientu wilgotnościowego, z płynnym przejściem od taksonów charakterystycznych dla mikrosiedlisk suchych do form tolerujących warunki wilgotne i wodne.

Wskaźnik Shannona wykazał, że różnorodność taksonomiczna zbiorowisk TA różniła się istotnie pomiędzy mikrosiedliskami. Najwyższe i najbardziej wyrównane wartości wskaźnika odnotowano na kępach (płaskowyżach torfowych), natomiast największe zróżnicowanie wewnątrzgrupowe występowało w próbach porostowych oraz dolinkach (artykuł **I** – Ryc. 3).

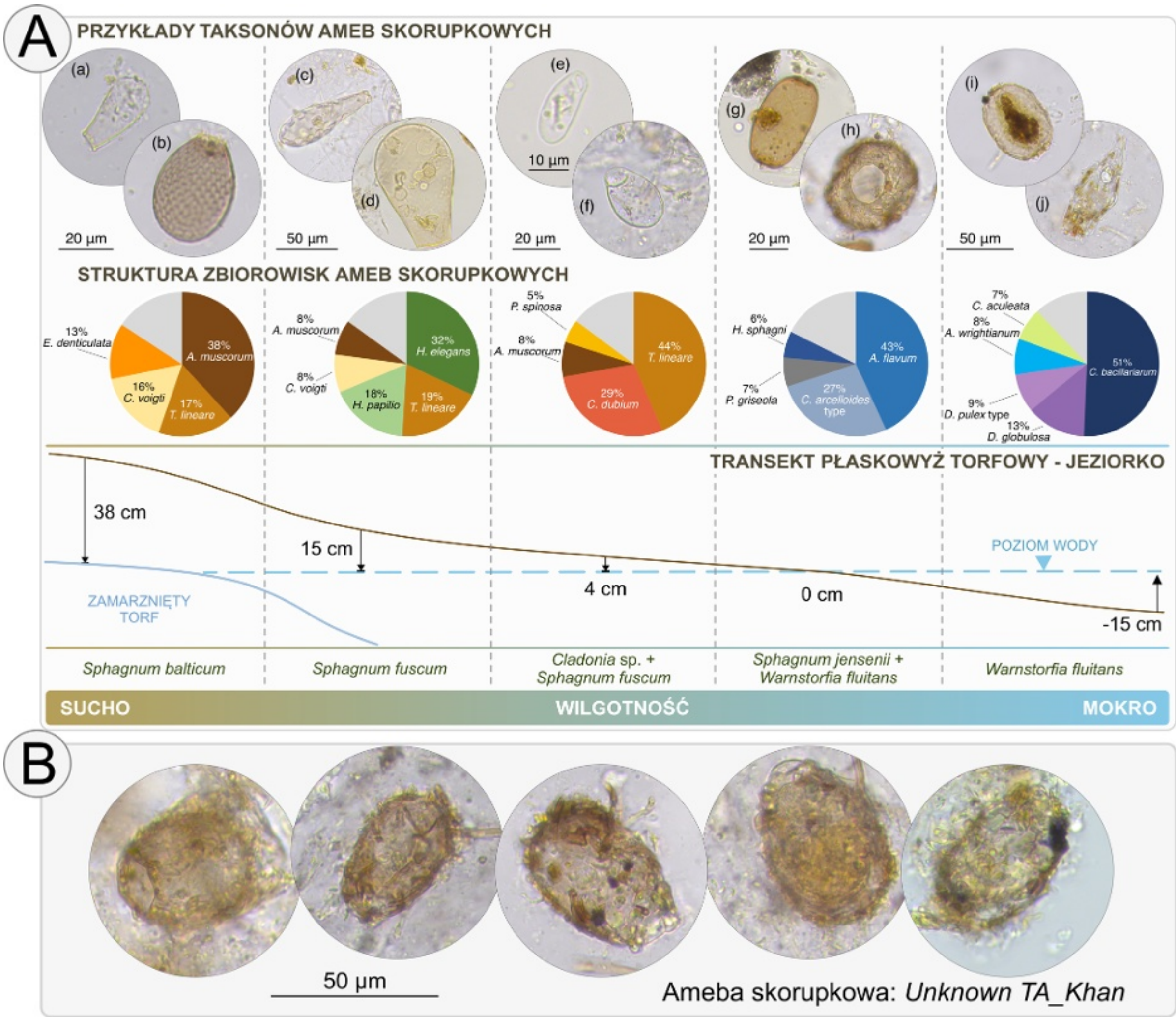

Ryc. 15 Charakterystyka zbiorowisk ameb skorupkowych (TA) z kompleksu torfowiskowego Khanymei: **(A)** zbiorowiska TA wzdłuż uproszczonego transektu A-B przedstawionego na ryc. 10C (próby użyte w transekcie od lewej do prawej: M3_13, M3_10, M3_7, M3_2, M3_3). Przykłady pospolitych taksonów TA: (a) *Cryptodifflugia voigti*, (b) *Assulina muscorum*, (c) *Hyalosphenia elegans*, (d) *Hyalosphenia papilio*, (e) *Trinema lineare*, (f) *Corythion dubium*, (f) *Archerella flavum*, (h) typ *Cyclopyxis arcelloides*, (i) *Amphitrema wrightianum*, (n) *Cylindrifflugia bacillariarum*; **(B)** zdjęcia niezidentyfikowanego taksonu ameby skorupkowej (*Unknown TA_Khan*) znalezionej w próbach z kompleksu torfowiskowego Khanymei.
Źródło: Panel A został przetłumaczony i zaadaptowany z artykułu **I**, natomiast panel B z artykułu **II**.

Analiza ordynacyjna NMDS potwierdziła, że DWT jest głównym czynnikiem kontrolującym strukturę zbiorowisk TA na tym obszarze (artykuł **I** – Ryc. 4A). Dopasowanie wektora zmiennej środowiskowej wykazało, że gradient DWT był silnie i istotnie statystycznie powiązany z układem prób, tłumacząc 51,59% zmienności w strukturze zbiorowisk ($p<0,001$), a próby układały się wzdłuż osi ordynacji zgodnie z wilgotnością siedliska. Wykluczenie prób porostowych zwiększyło siłę związku pomiędzy zbiorowiskami TA a gradientem DWT z 51,59% na 56,77%, potwierdzając specyficzny charakter warunków wilgotnościowych tych stanowisk. Najbardziej odrębną strukturą cechowały się zbiorowiska TA w próbach zatopionych, co było związane z wyraźnie wyższą wilgotnością tych mikrosiedlisk w porównaniu z pozostałymi analizowanymi powierzchniami (Ryc. 16B).

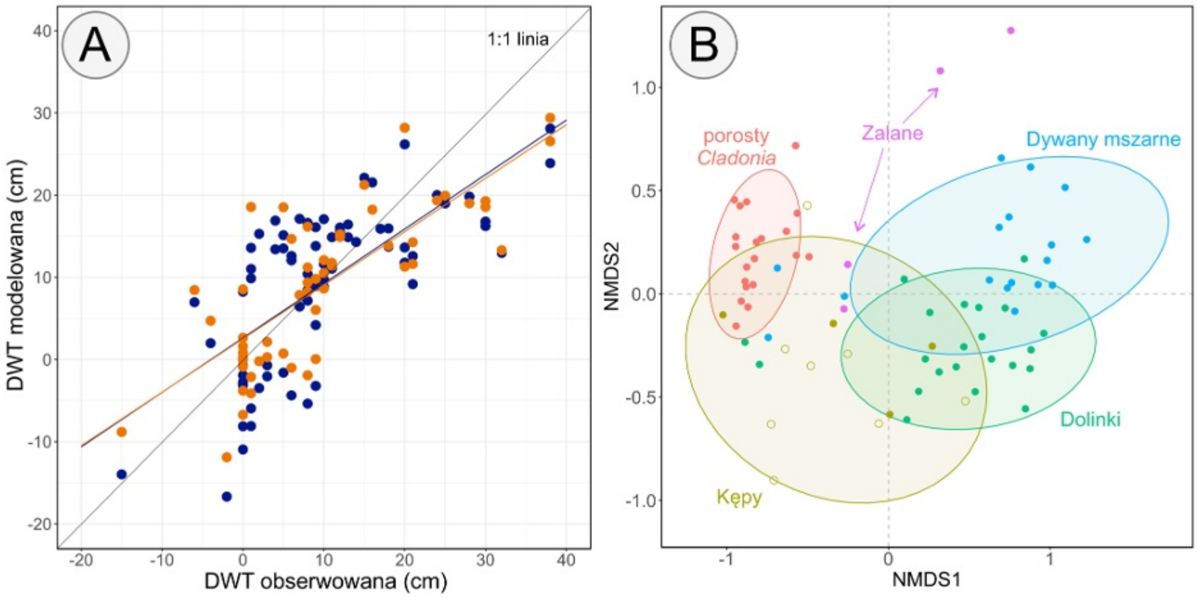

Ryc. 16 (A) Jakość dopasowania funkcji transferu (TF) Khanymei: obserwowane i modelowane wartości poziomu wód gruntowych (DWT) uzyskane z modelu WAtol.cla, wraz z liniowym trendem danych punktowych oraz linią 1:1 stanowiącą odniesienie. Ciemnoniebieskie kółka reprezentują TF dla całego zbioru danych (TF_{ALL}), natomiast pomarańczowe kółka – dla zbioru danych z wyłączeniem prób porostowych *Cladonia* ($TF_{NO.CLAD}$). **(B)** Dwuwymiarowy wykres porządkowania NMDS prób powierzchniowych, charakteryzujących się obecnością zwierciadła wód gruntowych (wypełnione kółka) lub zamarzniętego torfu (puste kółka), z elipsami 90% przedziałów ufności. Dla prób zalanych elipsa nie została przedstawiona ze względu na statystycznie niewystarczającą liczebność grupy.
Źródło: Rycina przetłumaczona i zaadaptowana z artykułu **I**.

Optima DWT dla najliczniejszych taksonów obejmowały zakres około 33–34 cm (Ryc. 17). Taksony tolerujące wilgotne mikrosiedliska (np. *Cylindrifflugia bacillariarum*, *Difflugia globulosa*) były związane z niskimi lub ujemnymi wartościami DWT, natomiast taksony tolerujące suchsze warunki (np. *Cryptodifflugia minuta*, *Trigonopyxis arcula*) – z wysokimi wartościami tego parametru (głębszym zaleganiem zwierciadła wody). Wykluczenie prób porostowych doprowadziło do przesunięcia optimów DWT części taksonów w kierunku warunków bardziej suchych, przy jednoczesnych niewielkich zmianach w grupie taksonów charakterystycznych dla mikrosiedlisk silnie uwodnionych.

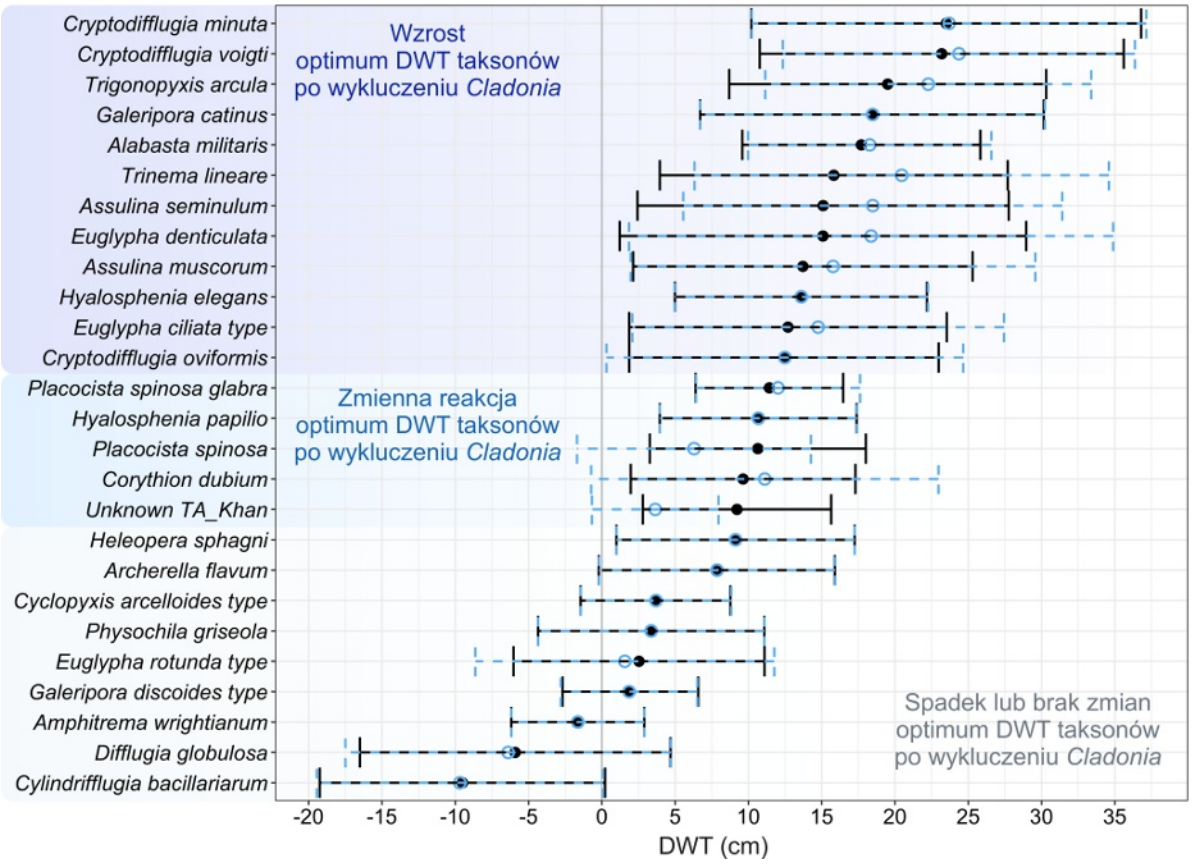

Ryc. 17 Optima poziomu wód gruntowych (DWT) oraz zakresy tolerancji obliczone dla wybranych taksonów TA metodą średnich ważonych dla pełnego zbioru danych (czarne linie ciągłe i pełne kółka) oraz dla zbioru danych z wyłączeniem prób porostowych *Cladonia* (niebieskie linie przerywane i puste kółka).
Źródło: Rycina przetłumaczona i zaadaptowana z artykułu **I**.

Analiza współczesnych zbiorowisk TA pozwoliła na opracowanie lokalnej funkcji transferu dla kompleksu torfowiskowego Khanymei, umożliwiającą rekonstrukcję warunków paleohydrologicznych. Cechą wyróżniającą opracowaną funkcję transferu było włączenie do zbioru testowego prób reprezentujących mikrosiedliska porostowe. Choć tego typu próby są często pomijane w badaniach paleoekologicznych, ich uwzględnienie ma istotne znaczenie dla torfowisk rozwijających się w strefie wieloletniej zmarzliny, gdzie porosty stanowią ważny (nieraz dominujący) i specyficzny komponent struktury mikrosiedliskowej.

Najlepsze parametry statystyczne uzyskano dla modelu średniej ważonej (WAtol.cla), zarówno dla pełnego zbioru danych ($TF_{Khan.ALL}$), jak i dla zbioru z wykluczeniem prób porostowych ($TF_{Khan.NO.CLAD}$) (artykuł **I** – Tab. 2). Wartości RMSEP (ok. 8,3-8,6 cm) były niskie w stosunku do zakresu i zmienności gradientu DWT, co wskazuje na dobrą jakość predykcyjną obydwu modeli.

Zastosowanie lokalnej funkcji transferu na danych subfosylnych z rdzenia torfowego Kh-K2 umożliwiło ilościową rekonstrukcję zmian DWT w profilu oraz porównanie uzyskanych wyników z rekonstrukcjami opartymi na kontynentalnych funkcjach transferu. Wszystkie zastosowane modele (TF_{Asian}, $TF_{Pan\text{-}European}$, $TF_{Khan.ALL}$, $TF_{Khan.NO.CLAD}$) wskazywały na ogólną tendencję do osuszania powierzchni torfowiska od podstawy rdzenia ku stropowi, z krótkotrwałymi fluktuacjami wilgotności (artykuł **I** – Ryc. 7). Zakres rekonstruowanych wartości DWT był mniejszy w opracowanej funkcji transferu niż w modelach kontynentalnych, co wynikało z węższego gradientu środowiskowego w lokalnym zbiorze testowym.

Podsumowując, opracowana lokalna funkcja transferu stanowi narzędzie lepiej dostosowane do specyfiki torfowisk rozwijających się w strefie nieciągłej wieloletniej zmarzliny. Uwzględnienie zróżnicowanych mikrosiedlisk, w tym powierzchni porostowych, pozwoliło pełniej uchwycić lokalną zmienność warunków hydrologicznych oraz ekologicznych. Uzyskane wyniki stanowią istotny wkład w rozwój regionalnych modeli paleoekologicznych dla Niziny Zachodniosyberyjskiej i podkreślają znaczenie lokalnych zbiorów testowych w rekonstrukcjach paleohydrologicznych prowadzonych na torfowiskach związanych z występowaniem wieloletniej zmarzliny.

Artykuł II – "*Peatland development reconstruction and complex biological responses to permafrost thawing in Western Siberia*"

Wyniki przedstawione w artykule **II** stanowią jedną z pierwszych tak szczegółowych wielowskaźnikowych analiz paleoekologicznych torfowisk z tego regionu. Zastosowanie lokalnej funkcji transferu (opracowanej w artykule **I**), umożliwiło wykonanie ilościowej rekonstrukcji zmian hydrologicznych z ostatnich 200 lat z uwzględnieniem lokalnych uwarunkowań środowiskowych.

Analiza wielowskaźnikowa dwóch rdzeni torfowych z kompleksu torfowiskowego Khanymei (Kh-K1 – obrzeże jeziora oraz Kh-K2 – płaskowyż torfowy) pozwoliła na odtworzenie zróżnicowanych trajektorii zmian hydrologicznych i ekologicznych w obrębie dwóch kontrastujących mikrosiedlisk torfowiskowych. Dodatkowo zapis paleoekologiczny obejmujący ostatnie 70 lat, obecny w obu rdzeniach, umożliwił analizę ich reakcji na postępującą zmianę klimatu i degradację wieloletniej zmarzliny, które szczególnie wyraźnie nasiliły się w drugiej połowie XX wieku (Rantanen i in., 2022). Pozwoliło to na zaproponowanie trzyetapowego schematu postępującego rozmarzania wieloletniej zmarzliny w strefie nieciągłej oraz odtworzenie hydrologicznych i środowiskowych reakcji mikrosiedlisk ekosystemu torfowiskowego na zachodzące zmiany.

Kompleks torfowiskowy Khanymei od 1815 do 1950 roku

Na początku XIX wieku w zapisie torfowym dominowały taksony TA uznawane za wskaźniki wilgotnych lub umiarkowanie wilgotnych mikrosiedlisk, takie jak *Unknown TA_Khan* (Ryc. 15B), *Difflugia pulex* type oraz *Centropyxis aculeata* type, a także glony z rodzaju *Botryococcus* (Ryc. 18A) (Halaś i in., 2023; Pandey i in., 2023). Dodatkowo obecność skorupek TA o większych rozmiarach apertur oraz bardziej sferycznym (kulistym) kształcie potwierdza wyższą wilgotność środowiska. Na tej podstawie zrekonstruowane wartości DWT oraz pH wyniosły odpowiednio około 4 cm oraz około 5,1 (artykuł **II** – Ryc. 3A). W tym samym okresie zapis paleoekologiczny wskazuje również na wysokie tempo akumulacji węgla oraz zwiększoną aktywność pożarową.

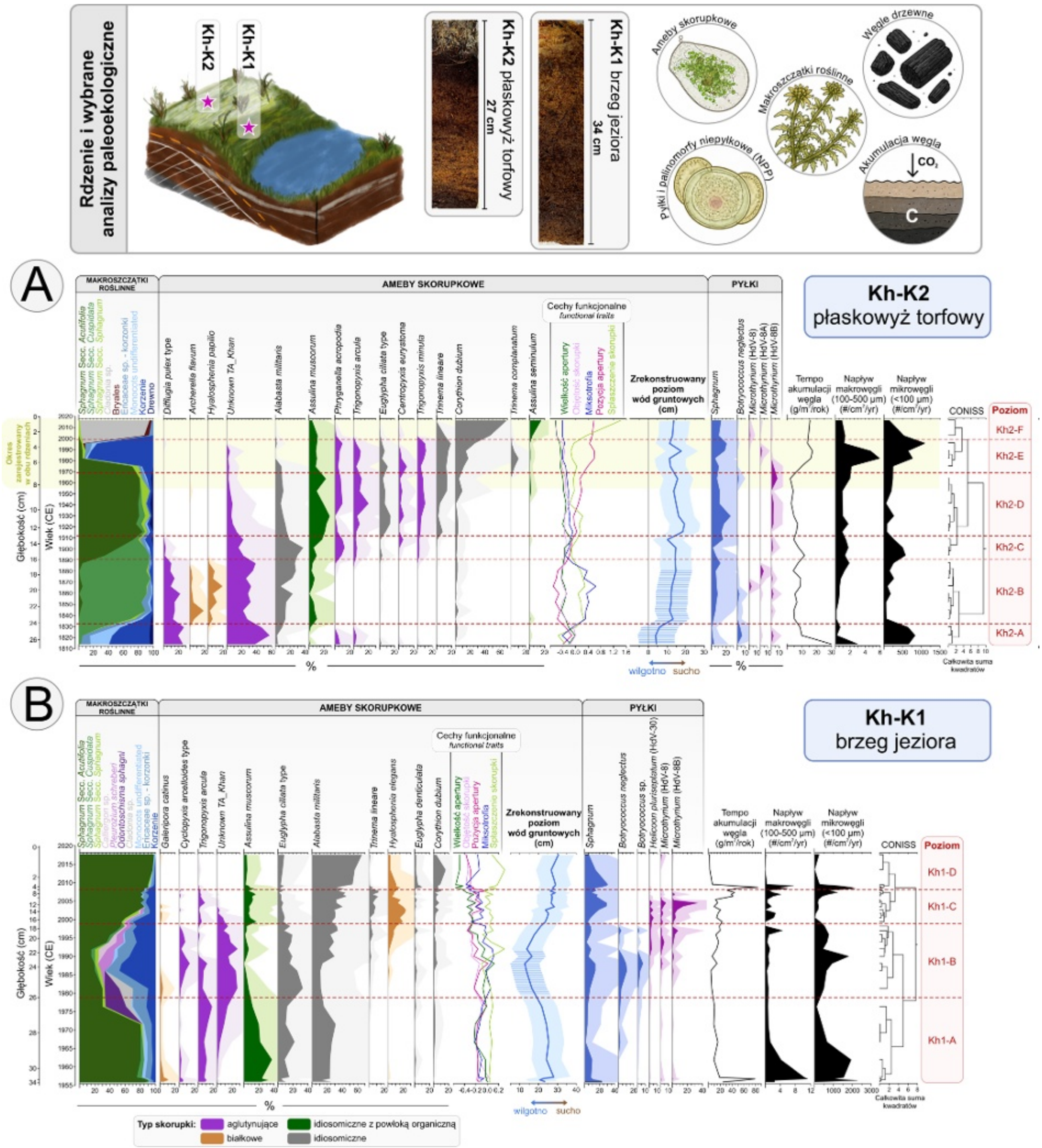

Ryc. 18 Diagramy stratygraficzne rdzeni **(A)** Kh-K2 – płaskowyż torfowy oraz **(B)** Kh-K1 – brzeg jeziora. Przedstawiono procentowy udział makroszczątków roślinnych oraz wybranych taksonów ameb skorupkowych (5-krotne przeskalowanie). Taksony TA pogrupowano według typu budowy skorupki, zgodnie z legendą barw poniżej wykresu. Diagram obejmuje również średnie ważone cech funkcjonalnych dla całej społeczności oraz rekonstrukcję poziomu wód gruntowych (DWT). Zacieniowane obszary przy krzywej DWT przedstawiają błędy rekonstrukcji, natomiast zakreskowanie wskazuje przedziały potencjalnie obarczone większą niepewnością rekonstrukcji z uwagi na obecność >25% nowego taksonu TA (*Unknown TA_Khan*). Dodatkowo przedstawiono wybrane taksony pyłkowe i palinomorfów niepyłkowych (5-krotne przeskalowanie), tempo akumulacji węgla, napływ makrowęgli (100-500 µm) oraz mikrowęgli (<100 µm). Poziomy stratygraficzne wyznaczono na podstawie analizy CONISS zbiorowisk TA.

Źródło: Rycina przetłumaczona i zaadaptowana z artykułu **II**

Po około 1830 roku w zapisie torfowym zaczęły dominować taksony tolerujące suchsze warunki, takie jak *Assulina muscorum* i *Alabasta militaris*, podczas gdy wskaźniki wilgotnych mikrosiedlisk stopniowo zanikały (Bobrov i in., 1999). Jednocześnie pojawiły się gatunki miksotroficzne (*Archerella flavum* i *Hyalosphenia papilio*), charakterystyczne dla stabilnych, kwaśnych warunków torfowiskowych (Lamentowicz i in., 2020). Cechy funkcjonalne TA uległy zmianie, zaczynają dominować taksony o bardziej spłaszczonych skorupkach i mniejszych aperturach. Na podstawie tych zmian zrekonstruowano wzrost wartości DWT do około 12–15 cm oraz obniżenie pH do około 5,0–4,8 (artykuł **II** – Ryc. 3A). W tym okresie powierzchnię torfowiska zdominowały torfowce z sekcji *Cuspidata*. Jednocześnie w profilu palinologicznym obserwuje się spadek udziału krzewinek (Ericaceae, Vaccinium) oraz wzrost znaczenia roślin zielnych, szczególnie *Rubus chamaemorus* (artykuł **II** – Ryc. 5A).

W latach 1890–1910 rozpoczęła się wyraźna reorganizacja zbiorowisk TA. W zapisie wciąż dominowały wskaźniki suchych mikrosiedlisk, jednak pojawiły się również taksony tolerujące bardziej wilgotne warunki, m.in. *Cyclopyxis arcelloides* type oraz *Phryganella acropodia* (Warner i Charman, 1994; Halaś i in., 2023). Obecność wrotka *Habrotrocha angusticollis* w zapisie torfowym wskazuje na okresową stagnację wody na powierzchni torfowiska (Shumilovskikh i in., 2021). Na tej podstawie zrekonstruowano krótkotrwałe obniżenie wartości DWT do 10 cm (około 1910 roku). Impuls ten poprzedził wyraźne przejście od *Sphagnum* sekcja *Cuspidata* do *Sphagnum* sekcja *Acutifolia*, co wskazuje na zapoczątkowanie rozwoju bardziej wyniesionych form torfowiska i możliwą agradację zmarzliny (Sannel i Kuhry, 2009; Treat i Jones, 2018b).

Po 1910 roku w zapisie torfowym wciąż dominują wskaźniki suchych mikrosiedlisk, jednak skład taksonomiczny zbiorowisk TA uległ wyraźnej zmianie (Ryc. 18A). Reorganizacja ta może wskazywać na stabilizację wyniesionego płaskowyżu torfowego związanego z agradacją zmarzliny na badanym stanowisku. W strukturze TA pojawiło się więcej osobników *Trinema lineare*, *Trigonopyxis arcula* czy *Corythion dubium*, przy jednoczesnym zaniku taksonów tolerujących silniej uwodnione mikrosiedliska, m.in. *Unknown TA_Khan*. Dominacja taksonów o małych i bardziej „ukrytych" aperturach wskazuje na adaptację do niższej wilgotności środowiska. Na tej podstawie zrekonstruowana wartość DWT wzrosła do około 20 cm, a następnie stabilizowała się na poziomie około 15 cm. W tym okresie zrekonstruowano również najniższe wartości pH (~4.7) oraz całkowite zasiedlenie powierzchni torfowiska przez *Sphagnum* sekcja *Acutifolia*. Dodatkowo w latach 1930–1960 w profilu palinologicznym wzrasta udział pyłku sosny (*Pinus*), co pokrywało się z okresem ocieplenia klimatu z pierwszej połowy XX wieku (artykuł **II** – Ryc. 5A) (Bokuchava i Semenov, 2021). Na ten sam przedział czasowy przypada także odnotowany w zapisie torfowym spadek tempa akumulacji torfu i węgla (artykuł **II** – Ryc. 6A).

<u>Kompleks torfowiskowy Khanymei od 1950 roku – reakcja mikrosiedlisk na degradacje wieloletniej zmarzliny</u>

Zapis paleoekologiczny ostatnich 70 lat obecny w rdzeniach z płaskowyżu torfowego oraz brzegu jeziora termokrasowego pozwolił na zaproponowanie trzyetapowego schematu reakcji tych mikrosiedlisk na degradację wieloletniej zmarzliny. Na podstawie zmian zarejestrowanych w rdzeniu Kh-K1 (brzeg jeziora) etapy te zostały dopasowane do konkretnych przedziałów czasowych: faza I (ok. 1955-1979), faza II (ok. 1979-1999) i faza III (ok. 1999-2008).

Wyniki rekonstrukcji paleoekologicznej wskazują, że w okresie 1955–1979 oba stanowiska charakteryzowały się niską wilgotnością oraz dominacją *Sphagnum* sekcja *Acutifolia* oraz porostów *Cladonia* na powierzchni torfowiska, co pozwoliło określić okres ten jako fazę „przed rozmarzaniem" (Ryc. 18, 19A). Prawdopodobnie oba badane stanowiska stanowiły w tym czasie fragment płaskowyżu torfowego, przy czym stanowisko Kh-K1 zlokalizowane było w jego strefie brzeżnej. Niskie wartości tempa akumulacji torfu i węgla zrekonstruowane w tym czasie, można powiązać z obecnością porostów, które rozwijając się na torfowisku ograniczają tym samym wzrost mchów (Harris i in., 2018). Mimo że porosty są charakterystycznym elementem roślinności dojrzałych pagórków palsa i płaskowyżów torfowych (Railton i Sparling, 1973), ich długotrwała obecność może negatywnie wpływać na stabilność wieloletniej zmarzliny, szczególnie w połączeniu z ociepleniem klimatu. Niskie albedo oraz ograniczona ewapotranspiracja sprzyjają zatrzymywaniu wody pochodzącej z rozmarzającej zmarzliny w warstwach torfu, co prowadzi do osłabienia właściwości izolacyjnych podłoża i dalszego pogłębiania procesu rozmarzania (Rönkkö i Seppälä, 2003; Romanovsky i in., 2010).

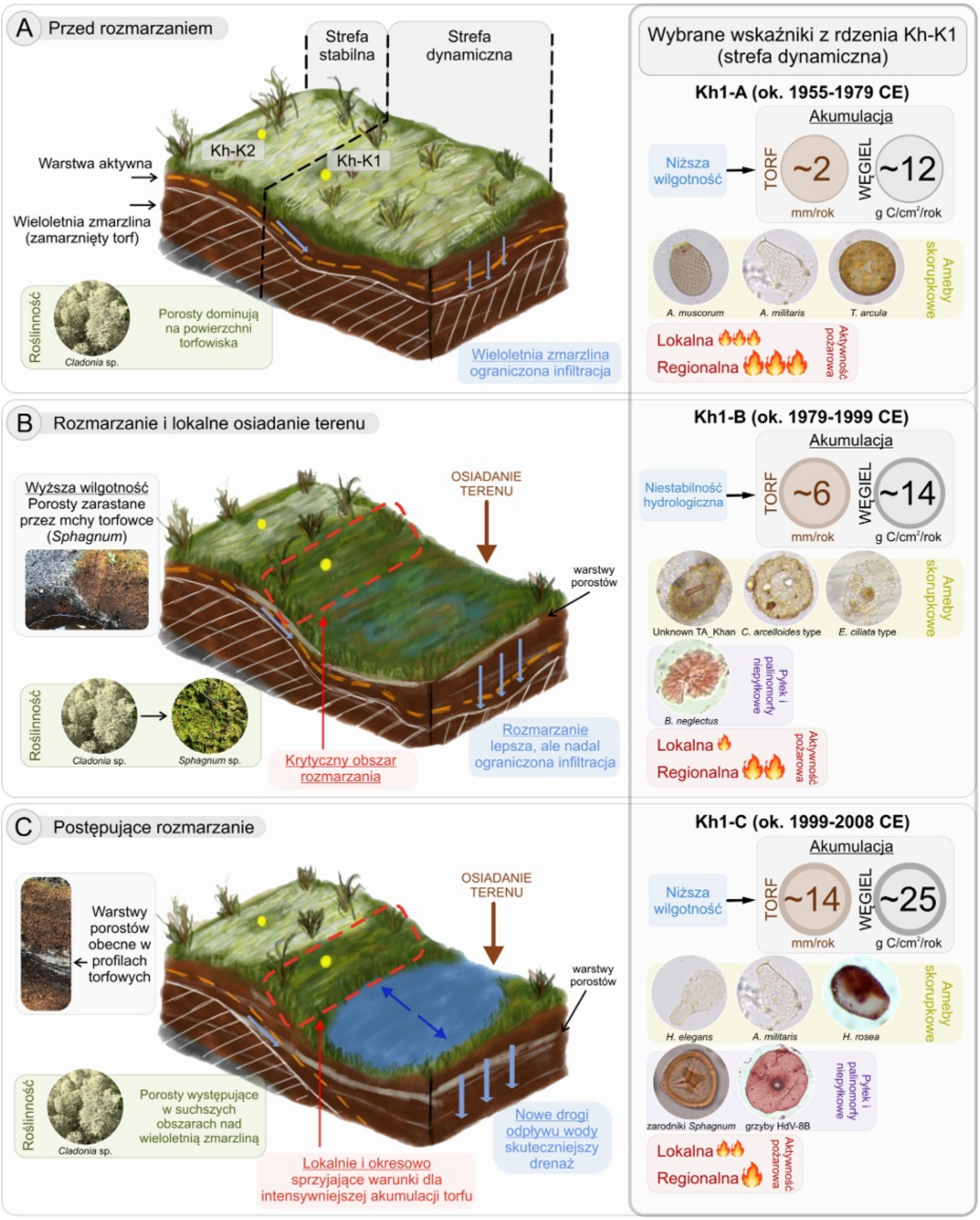

Ryc. 19 Schematyczne przedstawienie etapów postępującego rozmarzania wieloletniej zmarzliny na torfowisku w strefie nieciągłej zmarzliny, opracowana na podstawie rdzeni Kh-K1 (brzeg jeziora) oraz Kh-K2 (płaskowyż torfowy) z wykorzystaniem wybranych wskaźników paleoekologicznych. Na rycinie rdzeń Kh-K1 reprezentuje strefę dynamiczną, natomiast rdzeń Kh-K2 strefę stabilną. Wartości tempa akumulacji torfu i węgla przedstawione w prawym panelu oznaczają średnie wartości z wybranych poziomów rdzenia Kh-K1. Zdjęcia porostów, mchów i profili torfowych w lewym panelu pochodzą z różnych obszarów kompleksu torfowiskowego Khanymei i zostały wykorzystane w celu lepszego przedstawienia cyklicznej rotacji porostów i mchów *Sphagnum* na powierzchni torfowiska.
Źródło: Rycina przetłumaczona i zaadaptowana z artykułu **II.**

Pogłębianie warstwy aktywnej prowadzi do uwalniania znacznych ilości wody, która akumuluje się w obniżeniach terenu, powodując lokalne podtopienia oraz zapadanie się powierzchni torfowiska (Quinton i in., 2009; Olefeldt i in., 2021). Prawdopodobnie proces ten rozpoczął się na badanym obszarze po 1979 roku, kiedy zapis paleoekologiczny obu mikrosiedlisk zaczyna wykazywać wyraźne zróżnicowanie (Ryc. 18). W rdzeniu Kh-K1 zrekonstruowano obniżenie wartości DWT o ok. 12 cm, co było bezpośrednio uwarunkowane wzrostem udziału taksonów *Unknown TA_Khan* oraz *Cyclopyxis arcelloides* type w zapisie paleoekologicznym. Wynik ten, zestawiony z jednoczesnym całkowitym zanikiem porostów oraz liczniejszym pojawieniu się glonów z rodzaju *Botryococcus*, pozwolił uznać, że strefa brzeżna płaskowyżu uległa w tym czasie zapadnięciu (Ryc. 18B, 19B). Wyższa wilgotność zapadniętej powierzchni ograniczyła dalszy rozwój porostów, które zostały stopniowo zastąpione przez mchy *Sphagnum*. Zwiększona dostępność wody przyczyniła się również do wzrostu tempa akumulacji torfu i węgla, co zostało zrekonstruowane zarówno na płaskowyżu torfowym jak i jego świeżo zapadniętym brzegu.

Analiza zapisu paleoekologicznego po 1999 roku wskazuje na ponowną zmianę warunków hydrologicznych i ekologicznych, szczególnie wyraźną w rdzeniu z brzegu jeziora (Ryc. 19C). Rekonstrukcja poziomu wody sugeruje przesuszenie strefy brzegowej jeziora, podczas gdy na płaskowyżu torfowym utrzymywały się względnie stabilne, wilgotne warunki (Ryc. 18). Obserwacja ta odbiega od klasycznego schematu „wyniesienie – suche, obniżenie – wilgotne", co można tłumaczyć charakterystyką zbiorowisk TA wykorzystywanych do rekonstrukcji DWT. Ameby skorupkowe reagują przede wszystkim na wilgotność powierzchniową torfowiska (Woodland i in., 1998), dlatego obecność płytko zalegającej zmarzliny w płaskowyżu torfowym (ok. 27 cm) mogła podczas rozmarzania zwiększać uwilgotnienie warstw powierzchniowych mchów i wpływać na skład zbiorowisk TA. Natomiast w strefie brzegowej jeziora, gdzie zmarzlina była już nieobecna (lub zalegała znacznie głębiej), powierzchnia torfowiska była bardziej podatna na przesuszanie związane ze zwiększoną ewapotranspiracją.

Choć zrekonstruowane po 1999 roku wartości DWT wskazują na przesuszenie strefy brzegowej jeziora, w zapisie paleoekologicznym z tego stanowiska odnotowano wyraźny wzrost tempa akumulacji torfu i węgla (Ryc. 18B, 19C, artykuł **II** – Ryc.6B). Może to sugerować, że wcześniejsze rozmarzanie wieloletniej zmarzliny doprowadziło do zwiększenia dostępności wody i umożliwiło kolonizację stanowiska przez mchy *Sphagnum*.

W początkowej fazie warunki mogły być jednak zbyt wilgotne dla osiągnięcia przez nie wysokiej produktywności. Dopiero późniejsze częściowe przesuszenie powierzchni torfowiska, przy jednoczesnym utrzymaniu odpowiedniej dostępności wody, stworzyło bardziej optymalne warunki dla intensywnego wzrostu *Sphagnum* i zwiększenia produkcji biomasy. Utrzymująca się wysoka produktywność mogła być dodatkowo związana z dominacją mchów *Sphagnum* z sekcji *Acutifolia*, które dzięki zwartej strukturze są zdolne do utrzymania wysokiej aktywności fotosyntetycznej nawet przy obniżającej się wilgotności (Rydin i Jeglum, 2013). Interpretację tę potwierdza również zwiększony udział zarodników *Sphagnum* w profilu palinologicznym. Jednak, jak wskazuje zapis paleoekologiczny, warunki sprzyjające zwiększonej akumulacji torfu i węgla miały charakter krótkotrwały i obecnie nie występują już na badanym stanowisku.

Dane paleoekologiczne sugerują zatem, że dalsza degradacja wieloletniej zmarzliny doprowadziła do lepszego drenażu oraz akumulacji wody w obrębie misy jeziornej, co skutkowało przesuszeniem jej obrzeży. Bez współczesnych zobrazowań satelitarnych oraz rozpoznania terenowego zapis ten mógłby zostać zinterpretowany jednak odmiennie, co podkreśla znaczenie łączenia danych paleoekologicznych z obserwacjami współczesnych procesów zachodzących w ekosystemach torfowiskowych.

Zaproponowany schemat reakcji mikrosiedlisk na degradację wieloletniej zmarzliny w strefie nieciągłej stanowi przykład zmian zachodzących w warunkach lokalnych, których przebieg oraz intensywność mogą różnić się w zależności od specyfiki danego obszaru. Pomimo obserwowanego współcześnie wzrostu temperatury powietrza związanego ze zmianą klimatu, reakcja torfowisk na ocieplenie nie ma charakteru jednorodnego przestrzennie. Nawet w torfowiskach niezwiązanych z występowaniem wieloletniej zmarzliny struktura kępkowo-dolinkowa powoduje zróżnicowaną odpowiedź poszczególnych mikrosiedlisk na czynniki zewnętrzne. W torfowiskach rozwijających się w strefie wieloletniej zmarzliny zależności te są dodatkowo komplikowane przez wpływ zmarzliny na lokalne warunki hydrologiczne, co może prowadzić do odmiennych kierunków oraz tempa zmian nawet w obrębie jednego kompleksu torfowiskowego.

Obserwowane procesy, takie jak zmiany w zbiorowiskach TA, obecność charakterystycznych palinomorfów niepyłkowych czy tempo akumulacji torfu, pozostają zatem silnie zależne od lokalnego reżimu hydrologicznego. Jednocześnie różne etapy degradacji wieloletniej zmarzliny mogą występować równocześnie w obrębie jednego regionu, a nawet pojedynczego kompleksu torfowiskowego (Swindles i in., 2015). Oznacza to, że mimo lokalnego charakteru uzyskanych wyników, przedstawiony schemat pozwala wskazywać potencjalne kierunki przemian środowiskowych zachodzących w różnych częściach regionu Khanymei oraz innych obszarach Niziny Zachodniosyberyjskiej znajdujących się w strefie nieciągłej wieloletniej zmarzliny.

Artykuł III – "*Peat core research in the Western Siberian Lowland: applications of palaeoecological proxies, regions studied, and future prospects*"

W artykule **III** przedstawiono pierwszą ogólnodostępną i kompleksową bazę metadanych rdzeni torfowych z Niziny Zachodniosyberyjskiej (*Western Siberian Peat Core Database* – WSPC) (Halaś i Słowiński, 2026). Baza została opracowana na podstawie 156 publikacji naukowych opublikowanych w latach 1953-2025 i obejmuje 654 rdzenie torfowe. Analiza i interpretacja zgromadzonych danych umożliwiła ocenę aktualnego stanu badań paleoekologicznych prowadzonych na torfowiskach Niziny Zachodniosyberyjskiej oraz identyfikację najważniejszych luk przestrzennych, czasowych i metodycznych występujących w dostępnych danych.

Analiza rozmieszczenia przestrzennego rdzeni torfowych wykazała wyraźną koncentrację badań wzdłuż głównych rzek regionu – Obu i Jeniseju – oraz na obszarze Bagna Wasiugan (ros. *Vasyuganskiye bolota*, ang. *Great Vasyugan Mire*) (Ryc. 20, artykuł **III** – Ryc. 4). W tych rejonach zlokalizowane są nie tylko liczne stanowiska badawcze, ale również rdzenie analizowane z wykorzystaniem największej liczby wskaźników paleoekologicznych. Szczególnie istotnym obszarem badań okazało się Bagno Wasiugan, które ze względu na swoje rozmiary, znaczenie ekologiczne oraz stosunkowo dobrą dostępność terenową od wielu lat stanowi jeden z najważniejszych obiektów badań paleoekologicznych na obszarze Niziny Zachodniosyberyjskiej (m.in. Syso i Peregon, 2009; Rudmin i in., 2018; Blyakharchuk i in., 2019; Lapshina i Zarov, 2023). Dodatkowe skupisko rdzeni torfowych analizowanych z wykorzystaniem licznych i zróżnicowanych wskaźników zidentyfikowano w centralnej części obszaru badań, pomiędzy dolinami Obu i Jeniseju, gdzie w latach 1999–2001 realizowano rosyjsko-amerykańskie kampanie terenowe (Smith i in., 2000).

W bazie WSPC udokumentowane zostało wykorzystanie 26 wskaźników paleoekologicznych pogrupowanych w cztery główne kategorie: biologiczne, fizyczne, chemiczne i chronologiczne (artykuł **III** – Tab. A1). Liczba zastosowanych wskaźników w poszczególnych rdzeniach była zróżnicowana i wynosiła od jednego do maksymalnie dwunastu (Ryc. 20, artykuł **III** – Ryc. 6A). Ponad połowę bazy stanowiły rdzenie, w których zastosowano jedynie jeden lub dwa wskaźniki paleoekologiczne. Wynik ten wskazuje, że pomimo rosnącej liczby badań wielowskaźnikowych, znaczna część dostępnych danych nadal opiera się na stosunkowo prostych schematach analitycznych.

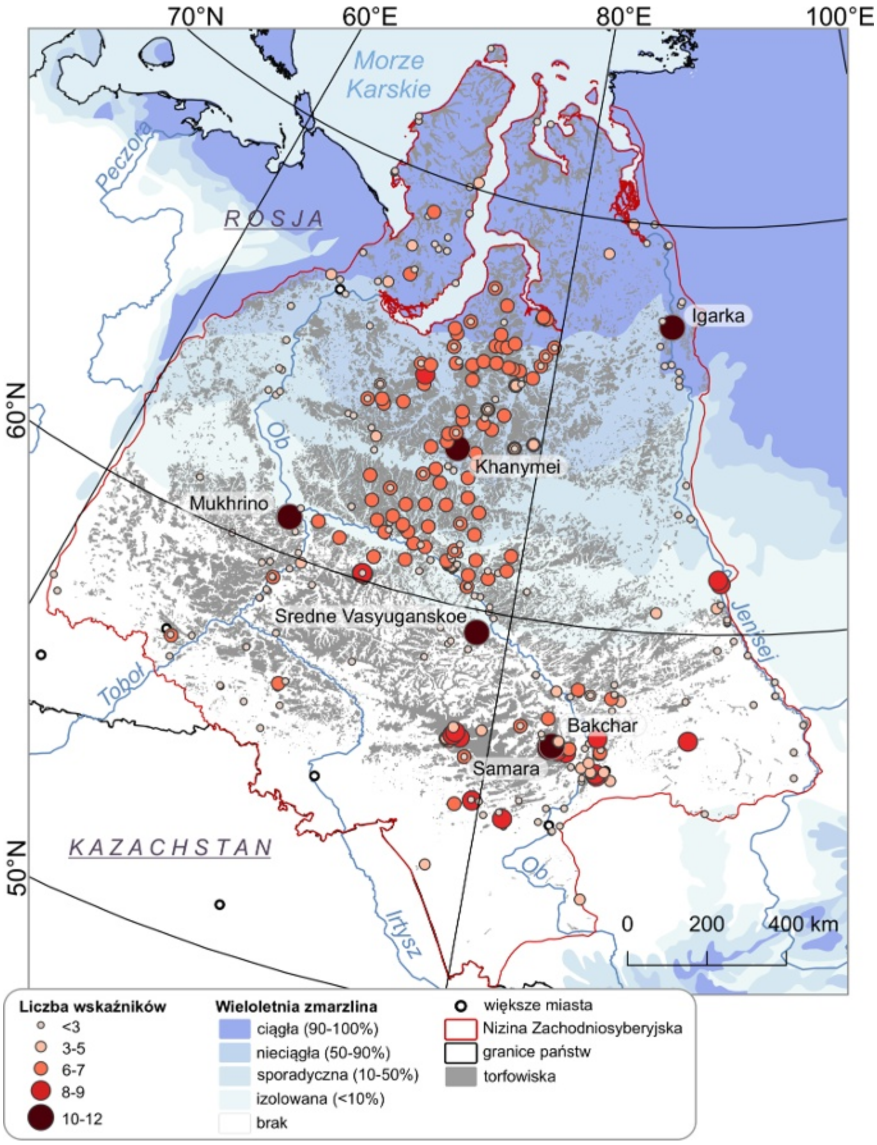

Ryc. 20 Przestrzenne rozmieszczenie rdzeni torfowych z Niziny Zachodniosyberyjskiej uwzględnionych w bazie *Western Siberian Peat Core Database* (WSPC), sklasyfikowanych według liczby zastosowanych wskaźników paleoekologicznych. Nazwami oznaczono stanowiska (rdzenie) o największej liczbie analizowanych wskaźników.
Źródło: opracowanie własne na podstawie: wieloletnia zmarzlina – Brown i in. (2002); torfowiska i granica niziny – Sheng i in. (2004). Rycina przetłumaczona i zaadaptowana z artykułu **III**.

Przeprowadzona analiza wykazała również znaczne różnice w częstości wykorzystania poszczególnych wskaźników paleoekologicznych oraz w ich rozmieszczeniu przestrzennym (Ryc. 21, artykuł **III** – Ryc. B1). Dominującą rolę odgrywają podstawowe wskaźniki fizyczne i chemiczne, takie jak głębokość zalegania spągu torfu, akumulacja węgla oraz zawartość materii organicznej (Ryc. 21A-B). Wśród wskaźników biologicznych najczęściej stosowane są pyłki i makroszczątki roślinne, natomiast ameby skorupkowe wykorzystywane są zdecydowanie rzadziej i ograniczają się do niewielkiej ilości stanowisk (Ryc. 21C-D). Najrzadziej wykorzystywane są zaawansowane analizy geochemiczne i izotopowe, takie jak fluorescencja rentgenowska (XRF), dyfrakcja rentgenowska (XRD) oraz analizy izotopów stabilnych (Ryc. 21E-F). Wyniki te wskazują na utrzymującą się nierównowagę pomiędzy powszechnie stosowanymi metodami a bardziej zaawansowanymi technikami badawczymi, które mogłyby dostarczyć dodatkowych informacji o historii rozwoju torfowisk i zmianach środowiskowych.

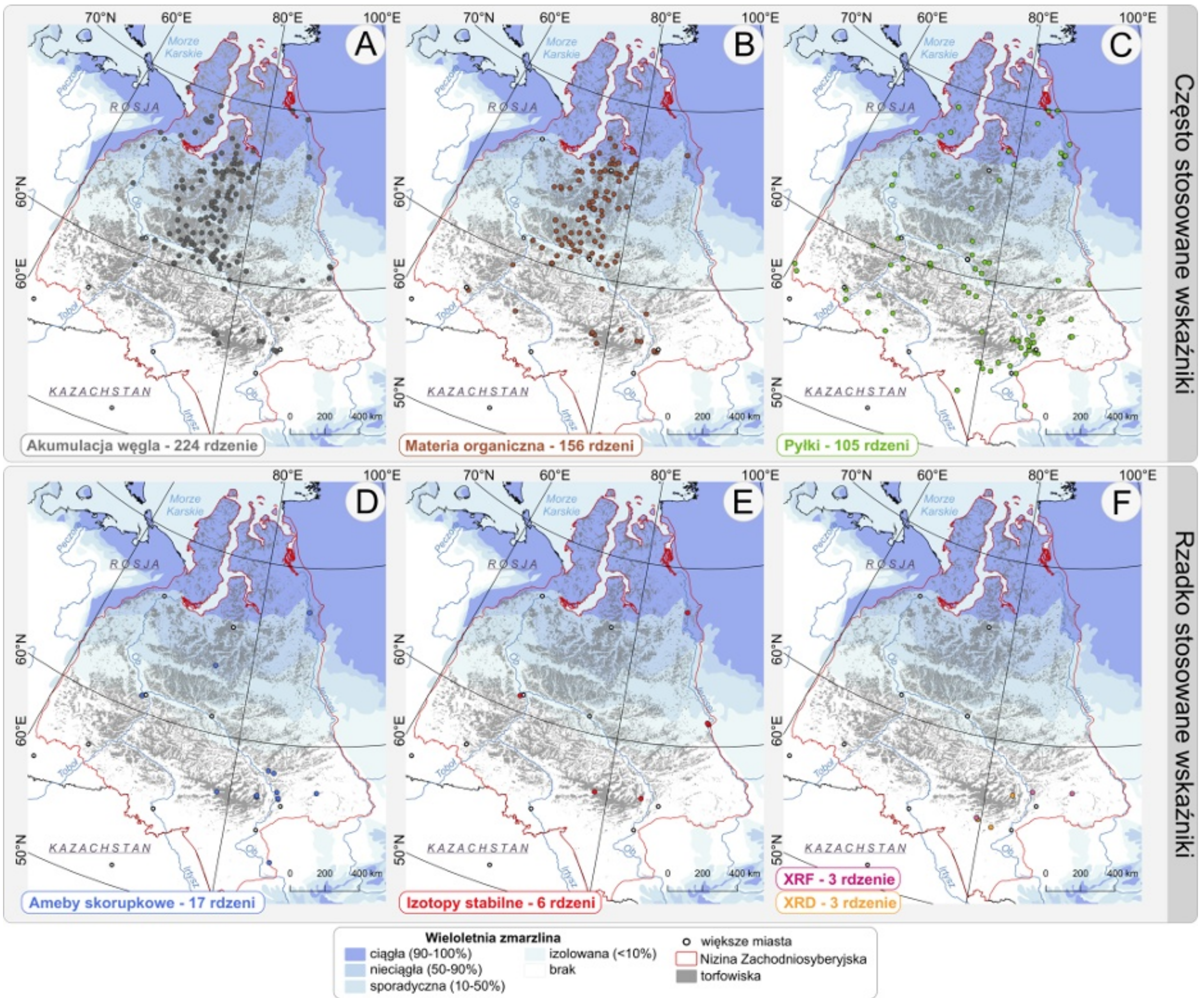

Ryc. 21 Rozmieszczenie przestrzenne rdzeni torfowych z Niziny Zachodniosyberyjskiej uwzględnionych w *Western Siberian Peat Core Database* (WSPC) zawierających zapisy wybranych wskaźników paleoekologicznych. Powszechnie stosowane wskaźniki paleoekologiczne przedstawiono na panelach **A-C** (A – akumulacja węgla; B – materia organiczna; C – pyłki), natomiast rzadziej wykorzystywane wskaźniki zaprezentowano na panelach **D-F** (D – ameby skorupkowe; E – izotopy stabilne; F – XRF/XRD).

Oznaczenia: XRF – fluorescencja rentgenowska (X-ray fluorescence); XRD – dyfrakcja rentgenowska (X-ray diffraction).

Źródło: opracowanie własne na podstawie: wieloletnia zmarzlina – Brown i in. (2002); torfowiska i granica niziny – Sheng i in. (2004). Rycina przetłumaczona i zaadaptowana z artykułu **III**.

Przestrzenna ocena potencjału informacyjnego rdzeni torfowych za pomocą map cieplnych wykazała istotną dysproporcję między liczbą stanowisk a rzeczywistą jakością i szczegółowością zapisów paleoekologicznych (Ryc. 22, artykuł **III** – Ryc. 10). Mimo stosunkowo dużej liczby rdzeni pozyskanych z Bagna Wasiugan, badania koncentrują się głównie wzdłuż jego obrzeży oraz dostępnych szlaków komunikacyjnych, podczas gdy rozległe obszary centralnej części tego kompleksu torfowiskowego pozostają słabo zbadane. Z kolei wysoki potencjał informacyjny obszaru między dolinami Obu i Jeniseju opiera się w głównej mierze na historycznych profilach pobranych blisko 30 lat temu, zorientowanych głównie na analizy fizyko-chemiczne osadu (artykuł **III** – Ryc. 10b). Najpoważniejszy deficyt danych, ilościowych i jakościowych, dotyczy północnej części Niziny Zachodniosyberyjskiej, pomimo jej kluczowego znaczenia dla badań nad zmianą klimatu i obiegiem węgla. Przeprowadzona walidacja wykazała również, że rzekomo wysoka reprezentatywność niektórych regionów opiera się głównie na starszych badaniach wykorzystujących pojedyncze wskaźniki paleoekologiczne oraz próbkowanie o stosunkowo niskiej rozdzielczości (np. co 10–25 cm).

Przeprowadzona synteza i interpretacja danych pozwoliła wyznaczyć priorytetowe cele dla przyszłych badań paleoekologicznych w obrębie Niziny Zachodniosyberyjskiej. Szczególnego znaczenia nabiera konieczność rozszerzenia ekspedycji terenowych na słabo rozpoznane obszary północne oraz tereny położone poza głównymi dolinami rzecznymi, które dotychczas pozostawały poza głównym nurtem badań. Wskazane jest również szersze wykorzystanie rzadziej stosowanych wskaźników biologicznych, takich jak ameby skorupkowe, mikrowęgle i makrowęgle drzewne oraz palinomorfy niepyłkowe. Wskaźniki te mogą dostarczyć unikalnych informacji o przeszłych zmianach hydrologicznych, aktywności pożarowej oraz lokalnych przemianach ekologicznych zachodzących w obrębie torfowisk. Istotnym kierunkiem dalszych prac jest także szersze wdrażanie nowoczesnych metod geochemicznych i izotopowych, zwłaszcza na torfowiskach objętych wieloletnią zmarzliną.

Na szczególne podkreślenie zasługuje duża wartość aplikacyjna opracowanej bazy metadanych. Dzięki planowanej corocznej aktualizacji może ona pełnić nie tylko funkcję narzędzia służącego wyszukiwaniu i integracji istniejących danych paleoekologicznych, lecz również wspierać planowanie przyszłych badań terenowych oraz identyfikację priorytetowych obszarów badawczych na terenie Niziny Zachodniosyberyjskiej.

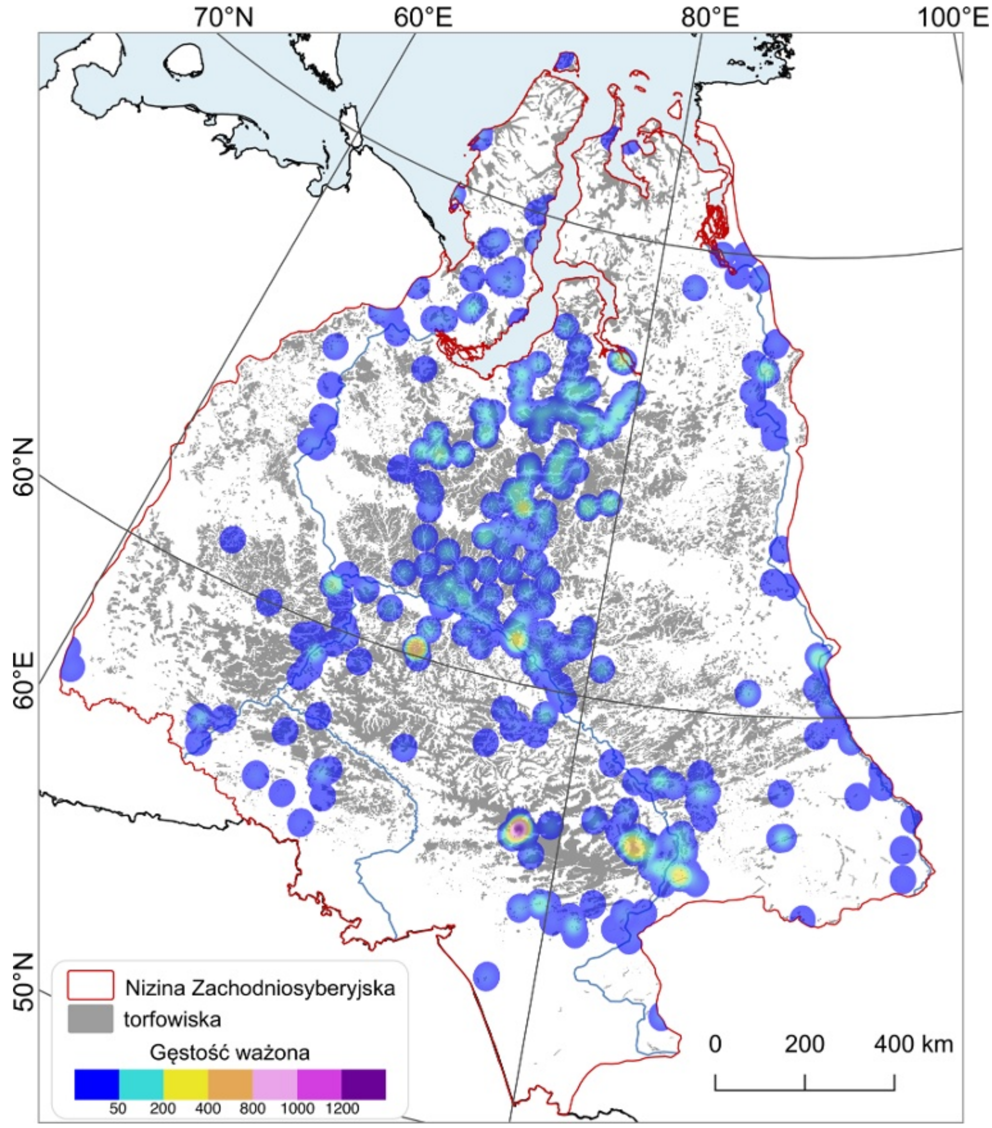

Ryc. 22 Przestrzenne rozmieszczenie badanych rdzeni torfowych na obszarze Niziny Zachodniosyberyjskiej oraz ich względny wkład informacyjny przedstawione w postaci mapy cieplnej łącznej punktacji wszystkich typów wskaźników paleoekologicznych. Mapa cieplna została wygenerowana z wykorzystaniem estymacji gęstości jądrowej (ang. *Kernel Density Estimation*, KDE), zakładając, że każdy rdzeń reprezentuje otaczający go obszar w promieniu 30 km. Wyniki ważono za pomocą wartości punktowych grup wskaźników w celu zobrazowania względnej gęstości danych. Punktacja rdzeni torfowych została określona na podstawie zarówno jakości chronologii, jak i liczby oraz rodzaju zastosowanych wskaźników paleoekologicznych.
Źródło: Rycina przetłumaczona i zaadaptowana z artykułu **III**.

Podsumowanie i wnioski

Głównym celem niniejszej rozprawy doktorskiej było rozpoznanie mechanizmów funkcjonowania i długoterminowych zmian hydrologicznych torfowisk Niziny Zachodniosyberyjskiej w strefie nieciągłej wieloletniej zmarzliny, ze szczególnym uwzględnieniem reakcji biotycznych wskaźników paleoekologicznych na procesy jej degradacji. Cel ten zrealizowano poprzez analizę współczesnych zbiorowisk ameb skorupkowych (TA) oraz określenie zależności pomiędzy ich strukturą a poziomem wód gruntowych (ang. *depth to water table*, DWT) w kompleksie torfowiskowym Khanymei. Uzyskane wyniki posłużyły do opracowania lokalnej funkcji transferu przeznaczonej do rekonstrukcji paleohydrologicznych na torfowiskach z tego obszaru.

Kolejnym celem badań była wielowskaźnikowa analiza dwóch rdzeni torfowych reprezentujących kontrastujące mikrosiedliska torfowiskowe – płaskowyż torfowy oraz strefę brzegową jeziora termokrasowego. Analizy te umożliwiły rekonstrukcję zmian środowiskowych zachodzących w obu mikrosiedliskach w ciągu ostatnich 70 lat, natomiast jeden z badanych rdzeni dostarczył również zapisu zmian w ostatnim 200-leciu. Zastosowane podejście wielowskaźnikowe (ang. *multi-proxy*) pozwoliło na identyfikację reakcji poszczególnych mikrosiedlisk ekosystemu torfowiskowego na postępującą degradację wieloletniej zmarzliny.

Ostatnim celem badań była synteza dotychczasowych badań paleoekologicznych prowadzonych na torfowiskach Niziny Zachodniosyberyjskiej. Jej rezultatem było stworzenie bazy metadanych rdzeni torfowych *Western Siberian Peat Core Database* (WSPC), dokumentującej lokalizacje stanowisk badawczych oraz wykorzystanie 26 wskaźników paleoekologicznych. Baza ta umożliwiła ocenę przestrzennego i metodologicznego zróżnicowania dotychczasowych badań oraz identyfikację głównych luk badawczych w skali całej Niziny Zachodniosyberyjskiej.

Realizacja przedstawionych celów pozwoliła na weryfikację postawionych hipotez badawczych oraz sformułowanie szeregu wniosków dotyczących współczesnych zależności ekologicznych kształtujących zbiorowiska TA, funkcjonowania torfowisk strefy nieciągłej wieloletniej zmarzliny i ich reakcji na współczesną zmianę klimatu, a także identyfikacji głównych luk badawczych oraz priorytetowych kierunków przyszłych badań paleoekologicznych na Nizinie Zachodniosyberyjskiej.

Na podstawie przeprowadzonych badań sformułowano następujące **wnioski szczegółowe**:

1. Poziom wód gruntowych (DWT) stanowi główny czynnik kształtujący zbiorowiska ameb skorupkowych (TA) w kompleksie torfowiskowym Khanymei, jednak zależność ta jest modyfikowana przez obecność wieloletniej zmarzliny, typ mikrosiedliska oraz skład roślinności. Wyniki sugerują, że w warunkach torfowisk strefy nieciągłej wieloletniej zmarzliny TA odzwierciedlają raczej ogólne warunki wilgotnościowe mikrosiedliska niż klasycznie definiowany DWT.
2. Włączenie do analiz zbiorowisk TA związanych z porostami rodzaju *Cladonia* wpływa na parametry statystyczne funkcji transferu oraz charakter rekonstruowanych zmian hydrologicznych. Wyniki wskazują, że porostowe zbiorowiska TA odzwierciedlają przede wszystkim specyficzne warunki wilgotnościowe występujące w obrębie porostów, a w mniejszym stopniu bezpośrednio reagują na położenie zwierciadła wody.
3. Opracowana lokalna funkcja transferu umożliwia bardziej precyzyjne rekonstrukcje zmian DWT niż modele oparte na kontynentalnych zbiorach testowych. Wynika to z lepszego odwzorowania lokalnych zależności pomiędzy zbiorowiskami TA a warunkami środowiskowymi oraz uwzględnienia specyfiki torfowisk rozwijających się w warunkach występowania wieloletniej zmarzliny.
4. Analiza materiału współczesnego i subfosylnego wykazała występowanie nieopisanego dotychczas taksonu TA (*Unknown TA_Khan*), którego obecność jest prawdopodobnie związana ze specyficznymi warunkami hydrochemicznymi powstającymi w wyniku degradacji wieloletniej zmarzliny. Wynik ten dowodzi, że bioróżnorodność TA w strefie nieciągłej wieloletniej zmarzliny pozostaje niedoszacowana, a dotychczasowe modele oparte na zbiorach testowych, które nie uwzględniają specyficznych mikrosiedlisk tych torfowisk, są niekompletne i mogą prowadzić do błędnych interpretacji paleoekologicznych.
5. Zastosowanie podejścia wielowskaźnikowego o wysokiej rozdzielczości czasowej pozwoliło na zredukowanie niepewności interpretacyjnej, właściwej dla analiz pojedynczych wskaźników, potwierdzając tym samym wysoką wartość archiwów torfowych w badaniach nad dynamiką środowiska. Integracja informacji pochodzących z różnych grup wskaźników umożliwiła kompleksowe odtworzenie nieliniowych zmian hydrologicznych, sukcesji roślinności oraz

mechanizmów funkcjonowania ekosystemów strefy nieciągłej wieloletniej zmarzliny, zachodzących pod wpływem współczesnego ocieplenia klimatu i degradacji wieloletniej zmarzliny.

6. Uzyskane wyniki wskazują, że pojedynczy rdzeń torfowy często nie odzwierciedla pełnego spektrum procesów zachodzących w obrębie całego kompleksu torfowiskowego. Znaczne zróżnicowanie mikrosiedlisk torfowiskowych prowadzi do powstawania odmiennych warunków wilgotnościowych, które wpływają na aktywność mikroorganizmów, tempo akumulacji torfu i węgla oraz skład gatunkowy roślinności. Szczególne znaczenie ma to w przypadku Niziny Zachodniosyberyjskiej, gdzie torfowiska tworzą rozległe, przestrzennie zróżnicowane kompleksy ekosystemów, a nie izolowane obiekty. W konsekwencji interpretacje oparte na pojedynczych rdzeniach mogą nie odzwierciedlać pełnej zmienności procesów zachodzących w skali całego kompleksu torfowiskowego, co ogranicza możliwość formułowania uogólnień dotyczących funkcjonowania torfowisk tego regionu.
7. Wyniki przeprowadzonych badań wskazują, że odpowiedź torfowisk strefy nieciągłej wieloletniej zmarzliny na postępujące ocieplenie klimatu jest silnie zróżnicowana przestrzennie i czasowo. Chociaż degradacja wieloletniej zmarzliny może lokalnie prowadzić do zwiększenia dostępności wody, wzrostu produktywności biologicznej oraz intensyfikacji akumulacji torfu i węgla, efekty te mają charakter przejściowy i są ograniczone do określonych mikrosiedlisk. Oznacza to, że potencjalne korzyści wynikające z rozmarzania zmarzliny nie występują równocześnie w całym ekosystemie torfowiskowym i nie mogą być traktowane jako uniwersalna odpowiedź tych ekosystemów na postępującą zmianę klimatu.
8. Stwierdzona heterogeniczność reakcji poszczególnych mikrosiedlisk na degradację wieloletniej zmarzliny wskazuje na konieczność uwzględniania zróżnicowania wewnętrznego torfowisk w modelach prognozujących przyszłe zmiany bilansu węgla i funkcjonowania ekosystemów torfowiskowych. Wyniki badań sugerują, że modele oparte na uśrednionych parametrach dla całych kompleksów torfowiskowych mogą nie odzwierciedlać rzeczywistej dynamiki zmian zachodzących w warunkach dalszego ocieplenia klimatu, co może wpływać na wiarygodność prognoz opartych m.in. na scenariuszach RCP (ang. *Representative Concentration Pathways*).

9. Analiza przestrzenna rozmieszczenia rdzeni torfowych ujawniła głęboką dysproporcję w stopniu zbadania Niziny Zachodniosyberyjskiej, wynikającą głównie z ograniczeń logistycznych. Dotychczasowe badania koncentrują się wzdłuż głównych dolin rzecznych (m.in. Ob, Jenisej), na obrzeżach Bagna Wasiugan oraz w rejonie dawnych kampanii rosyjsko-amerykańskich. W konsekwencji trudnodostępne rozległe obszary położone poza szlakami transportowymi pozostają słabo zbadane. Najpoważniejszy deficyt danych ilościowych i jakościowych dotyczy wschodniej części regionu (Nizina Taz-Pur, Równina Ketycko-Tymska) oraz północnej, z ciągłą wieloletnią zmarzliną, kluczowej dla badań nad współczesną zmianą klimatu.
10. Ocena potencjału informacyjnego rdzeni torfowych wykazała utrzymującą się nierównowagę metodologiczną, gdzie ponad połowa profili opiera się na prostych schematach analitycznych (1–2 wskaźniki). Dotychczasowe badania koncentrowały się głównie na podstawowych wskaźnikach dostarczających informacji o fizycznych i chemicznych właściwościach osadu torfowego (takich jak głębokość zalegania spągu, zawartość materii organicznej czy akumulacja węgla). Sytuacji tej towarzyszy wyraźny niedobór nowoczesnych wskaźników biologicznych (np. ameb skorupkowych, palinomorfów niepyłkowych) oraz zaawansowanych technik geochemicznych i izotopowych (np. XRF, FTIR), co ogranicza możliwość tworzenia zunifikowanych, wielowskaźnikowych modeli regionalnych.
11. Opracowana baza *Western Siberian Peat Core Database* (WSPC) stanowi pierwsze kompleksowe narzędzie integrujące rozproszone dotychczas informacje o profilach torfowych z Niziny Zachodniosyberyjskiej. Poprzez standaryzację metadanych o lokalizacji rdzeni i spektrum zastosowanych wskaźników, baza WSPC ułatwia prowadzenie wielkoskalowych syntez regionalnych oraz wspiera planowanie przyszłych, celowanych badań terenowych i projektów naukowych.

Przeprowadzone badania potwierdziły **główną hipotezę badawczą**, wskazując, że postępująca zmiana klimatu prowadzi do degradacji wieloletniej zmarzliny na Nizinie Zachodniosyberyjskiej oraz przekształceń hydrologicznych torfowisk. Zmiany te znajdują odzwierciedlenie w strukturze zbiorowisk biologicznych (przede wszystkim TA), składzie roślinności oraz dynamice akumulacji torfu i węgla, a procesy te są rejestrowane w archiwach torfowych, umożliwiając ich wysokorozdzielczą rekonstrukcję z wykorzystaniem metod paleoekologicznych.

Jednocześnie uzyskane wyniki pozwoliły na weryfikację postawionych **hipotez szczegółowych**:

- Potwierdzono hipotezę **H1**: Poziom wód gruntowych (DWT) jest głównym czynnikiem kształtującym strukturę zbiorowisk ameb skorupkowych (TA) na torfowiskach strefy nieciągłej wieloletniej zmarzliny, przy czym siła tej zależności jest modyfikowana przez typ mikrosiedliska oraz skład roślinności.
- Potwierdzono hipotezę **H2:** Funkcja transferu opracowana na podstawie lokalnego zbioru testowego umożliwia bardziej wiarygodne i precyzyjne rekonstrukcje zmian DWT niż funkcje transferu oparte na kontynentalnych zbiorach danych.
- Potwierdzono hipotezę **H3:** Uzyskane wyniki dostarczyły dowodów na obecność czytelnego sygnału degradacji wieloletniej zmarzliny zachowanego w archiwach torfowych (identyfikowalnego przy użyciu podejścia wielowskaźnikowego) oraz wykazały heterogeniczną i zróżnicowaną reakcję poszczególnych mikrosiedlisk na zachodzące zmiany środowiskowe.
- Potwierdzono hipotezę **H4:** Wykazano nierównomierny charakter dotychczasowych badań paleoekologicznych prowadzonych na Nizinie Zachodniosyberyjskiej, przejawiający się zarówno w dysproporcjach przestrzennych rozmieszczenia stanowisk, jak i nierównej reprezentacji stosowanych metod badawczych, co ogranicza możliwość formułowania uniwersalnych uogólnień regionalnych.

Bibliografia

Abe-Ouchi, A., Saito, F., Kageyama, M., Braconnot, P., Harrison, S. P., Lambeck, K., Otto-Bliesner, B. L., Peltier, W. R., Tarasov, L., Peterschmitt, J. Y., and Takahashi, K.: Ice-sheet configuration in the CMIP5/PMIP3 Last Glacial Maximum experiments, Geosci Model Dev, 8, 3621–3637, https://doi.org/10.5194/gmd-8-3621-2015, 2015.

Alexandrov, G. A., Brovkin, V. A., and Kleinen, T.: The influence of climate on peatland extent in Western Siberia since the Last Glacial Maximum, Sci. Rep., 6, 24784, https://doi.org/10.1038/srep24784, 2016.

Amesbury, M. J., Swindles, G. T., Bobrov, A., Charman, D. J., Holden, J., Lamentowicz, M., Mallon, G., Mazei, Y., Mitchell, E. A. D., Payne, R. J., Roland, T. P., Turner, T. E., and Warner, B. G.: Development of a new pan-European testate amoeba transfer function for reconstructing peatland palaeohydrology, Quat. Sci. Rev., 152, 132–151, https://doi.org/10.1016/j.quascirev.2016.09.024, 2016.

Amesbury, M. J., Booth, R. K., Roland, T. P., Bunbury, J., Clifford, M. J., Charman, D. J., Elliot, S., Finkelstein, S., Garneau, M., Hughes, P. D. M., Lamarre, A., Loisel, J., Mackay, H., Magnan, G., Markel, E. R., Mitchell, E. A. D., Payne, R. J., Pelletier, N., Roe, H., Sullivan, M. E., Swindles, G. T., Talbot, J., van Bellen, S., and Warner, B. G.: Towards a Holarctic synthesis of peatland testate amoeba ecology: Development of a new continental-scale palaeohydrological transfer function for North America and comparison to European data, Quat. Sci. Rev., 201, 483–500, https://doi.org/10.1016/j.quascirev.2018.10.034, 2018.

Beck, H. E., Zimmermann, N. E., McVicar, T. R., Vergopolan, N., Berg, A., and Wood, E. F.: Present and future Köppen-Geiger climate classification maps at 1-km resolution, Sci. Data, 5, 180214, https://doi.org/10.1038/sdata.2018.214, 2018.

Berglund, B. E. and Ralska-Jasiewiczowa, M.: Pollen analysis and pollen diagrams, Handb. Holocene Palaeoecol. Palaeohydrology, 455, 484–486, 1986.

Birks, H., Heiri, O., and Bjune, A.: Strengths and Weaknesses of Quantitative Climate Reconstructions Based on Late-Quaternary Biological Proxies, Open Ecol. J., 3, 68–110, https://doi.org/10.2174/1874213001003020068, 2010.

Birks, H. J. B.: Quantitative palaeoenvironmental reconstructions, in: Statistical Modelling of Quaternary Science Data. Technical guide 5, edited by: Maddy, D. and Brew, J. S., Quaternary Research Association, Cambridge, 271, 1995.

Biskaborn, B. K., Smith, S. L., Noetzli, J., Matthes, H., Vieira, G., Streletskiy, D. A., Schoeneich, P., Romanovsky, V. E., Lewkowicz, A. G., Abramov, A., Allard, M., Boike, J., Cable, W. L., Christiansen, H. H., Delaloye, R., Diekmann, B., Drozdov, D., Etzelmüller, B., Grosse, G., Guglielmin, M., Ingeman-Nielsen, T., Isaksen, K., Ishikawa, M., Johansson, M., Johannsson, H., Joo, A., Kaverin, D., Kholodov, A., Konstantinov, P., Kröger, T., Lambiel, C., Lanckman, J.-P., Luo, D., Malkova, G., Meiklejohn, I., Moskalenko, N., Oliva, M., Phillips, M., Ramos, M., Sannel, A. B. K., Sergeev, D., Seybold, C., Skryabin, P., Vasiliev, A., Wu, Q., Yoshikawa, K., Zheleznyak, M., and Lantuit, H.: Permafrost is warming at a global scale, Nat. Commun., 10, 264, https://doi.org/10.1038/s41467-018-08240-4, 2019.

Blyakharchuk, T.: Western Siberia, a review of Holocene climatic changes, J. Sib. Fed. Univ. - Biol., 2, 2009.

Blyakharchuk, T. A., Kurina, I. V., and Pologova, N. N.: Pozdnegolotsenovaya dinamika rastitel'nogo pokrova i uvlazhnennosti klimata yugo-vostochnogo sektora Zapadno-Sibirskoy ravniny po dannym palinologicheskogo i rizopodnogo issledovaniy torfyanykh otlozheniy [Late Holocene dynamics of vegetation cover and climate humidity in the southeastern sector of the West Siberian Plain based on palynological and rhizopod studies of peat deposits], Bull. Tomsk State Univ. Biol., 164–189, 2019.

Bobrov, A. A., Charman, D. J., and Warner, B. G.: Ecology of Testate Amoebae (Protozoa: Rhizopoda) on Peatlands in Western Russia with Special Attention to Niche Separation in Closely Related Taxa, Protist, 150, 125–136, https://doi.org/10.1016/S1434-4610(99)70016-7, 1999.

Bokuchava, D. D. and Semenov, V. A.: Mechanisms of the Early 20th Century Warming in the Arctic, Earth-Sci. Rev., 222, 103820, https://doi.org/10.1016/j.earscirev.2021.103820, 2021.

Booth, R. K., Lamentowicz, M., and Charman, D. J.: Preparation and analysis of testate amoebae in peatland palaeoenvironmental studies, Mires Peat, 7, 1–7, 2010.

Borge, A. F., Westermann, S., Solheim, I., and Etzelmüller, B.: Strong degradation of palsas and peat plateaus in northern Norway during the last 60 years, The Cryosphere, 11, 1–16, https://doi.org/10.5194/tc-11-1-2017, 2017.

Brown, J., Ferrians, O., Heginbottom, J. A., and Melnikov, E.: Circum-Arctic Map of Permafrost and Ground-Ice Conditions (2), https://doi.org/10.7265/SKBG-KF16, 2002.

Bulygina, O. N., Groisman, P. Y., Razuvaev, V. N., and Korshunova, N. N.: Changes in snow cover characteristics over Northern Eurasia since 1966, Environ. Res. Lett., 6, 045204, https://doi.org/10.1088/1748-9326/6/4/045204, 2011.

Carballeira, R. and Pontevedra-Pombal, X.: Diatoms in Paleoenvironmental Studies of Peatlands, Quaternary, 3, 10, https://doi.org/10.3390/quat3020010, 2020.

Chambers, F. M. and Charman, D. J.: Holocene environmental change: contributions from the peatland archive, The Holocene, 14, 1–6, https://doi.org/10.1191/0959683604hl684ed, 2004.

Chambers, F. M., Beilman, D. W., and Yu, Z.: Methods for determining peat humification and for quantifying peat bulk density, organic matter and carbon content for palaeostudies of climate and peatland carbon dynamics., Mires Peat, 7, 2011.

Charman, D. J.: Biostratigraphic and palaeoenvironmental applications of testate amoebae, Quat. Sci. Rev., 20, 1753–1764, https://doi.org/10.1016/S0277-3791(01)00036-1, 2001.

Charman, D. J., Hendon, D., and Woodland, W. A.: The identification of testate amoebae (Protozoa: Rhizopoda) in peats: QRA Technical Guide No. 9, Quaternary

Research Asociation, London, https://doi.org/10.1016/j.quascirev.2004.03.008, 2000.

Conedera, M., Tinner, W., Neff, C., Meurer, M., Dickens, A. F., and Krebs, P.: Reconstructing past fire regimes: methods, applications, and relevance to fire management and conservation, Quat. Sci. Rev., 28, 555–576, https://doi.org/10.1016/j.quascirev.2008.11.005, 2009.

Crichton, K. A., Anderson, K., Fewster, R. E., Charman, D. J., Garneau, M., Väliranta, M., Mleczko, M., Handley, J. N., Hodson, S., Parker, R. E., Swindles, G. T., Blaauw, M., and Gallego-Sala, A. V.: Satellite data indicates recent Arctic peatland expansion with warming, Commun. Earth Environ., 6, 461, https://doi.org/10.1038/s43247-025-02375-1, 2025.

Daly, A. J., Baetens, J. M., and De Baets, B.: Ecological Diversity: Measuring the Unmeasurable, Mathematics, 6, 119, https://doi.org/10.3390/math6070119, 2018.

Duchkov, A. D.: Characteristics of permafrost in Siberia, in: Advances in the Geological Storage of Carbon Dioxide, 81–91, https://doi.org/10.1007/1-4020-4471-2_08, 2006.

Faegri, K., Iversen, J., Kaland, P. E., and Krzywinski, K.: Textbook of pollen analysis, 4th ed., Blackburn Press, Caldwell, N.J., 328 pp., 1989.

Fournier, B., Lara, E., Jassey, V. E., and Mitchell, E. A.: Functional traits as a new approach for interpreting testate amoeba palaeo-records in peatlands and assessing the causes and consequences of past changes in species composition, The Holocene, 25, 1375–1383, https://doi.org/10.1177/0959683615585842, 2015.

Frolking, S. and Roulet, N. T.: Holocene radiative forcing impact of northern peatland carbon accumulation and methane emissions, Glob. Change Biol., 13, 1079–1088, https://doi.org/10.1111/j.1365-2486.2007.01339.x, 2007.

Frolking, S., Talbot, J., Jones, M. C., Treat, C. C., and Et., A.: Peatlands in the Earth's 21st century climate system, Environ. Rev., https://doi.org/10.1139/a11-014, 2011.

Greifswald Mire Centre: Global Peatland Map 2.0. Underlying dataset of the UNEP Global Peatland Assessment - The State of the World's Peatlands: Evidence for action toward the conservation, restoration, and sustainable management of peatlands, Global Peatlands Initiative, 2022.

Groisman, P. Y., Blyakharchuk, T. A., Chernokulsky, A. V., Arzhanov, M. M., Marchesini, L. B., Bogdanova, E. G., Borzenkova, I. I., Bulygina, O. N., Karpenko, A. A., Karpenko, L. V., Knight, R. W., Khon, V. C., Korovin, G. N., Meshcherskaya, A. V., Mokhov, I. I., Parfenova, E. I., Razuvaev, V. N., Speranskaya, N. A., Tchebakova, N. M., and Vygodskaya, N. N.: Climate Changes in Siberia, in: Regional Environmental Changes in Siberia and Their Global Consequences, edited by: Groisman, P. Y. and Gutman, G., Springer Netherlands, Dordrecht, 57–109, https://doi.org/10.1007/978-94-007-4569-8_3, 2013.

Halaś, A. and Słowiński, M.: Western Siberian Peat Core Database (WSPC), https://doi.org/10.5281/zenodo.20323517, 2026.

Halaś, A., Lamentowicz, M., Łuców, D., and Słowiński, M.: Developing a new testate amoeba hydrological transfer function for permafrost peatlands of NW Siberia, Quat. Sci. Rev., 308, 108067, https://doi.org/10.1016/j.quascirev.2023.108067, 2023.

Hantemirov, R. M., Corona, C., Guillet, S., Shiyatov, S. G., Stoffel, M., Osborn, T. J., Melvin, T. M., Gorlanova, L. A., Kukarskih, V. V., Surkov, A. Y., von Arx, G., and Fonti, P.: Current Siberian heating is unprecedented during the past seven millennia, Nat. Commun., 13, 4968, https://doi.org/10.1038/s41467-022-32629-x, 2022.

Harris, L. I., Moore, T. R., Roulet, N. T., and Pinsonneault, A. J.: Lichens: A limit to peat growth?, J. Ecol., 106, 2301–2319, https://doi.org/10.1111/1365-2745.12975, 2018.

Haslett, J. and Parnell, A. C.: A simple monotone process with application to radiocarbon-dated depth chronologies, J. R. Stat. Soc. Ser. C Appl. Stat., 57, 399–418, 2008.

Heiri, O., Lotter, A. F., and Lemcke, G.: Loss on ignition as a method for estimating organic and carbonate content in sediments: reproducibility and comparability of results, J. Paleolimnol., 25, 101–110, https://doi.org/10.1023/A:1008119611481, 2001.

Hendon, D. and Charman, D. J.: The preparation of testate amoebae (Protozoa: Rhizopoda) samples from peat, The Holocene, 7, 199–205, https://doi.org/10.1177/095968369700700207, 1997.

Hua, Q., Barbetti, M., and Rakowski, A. Z.: Atmospheric Radiocarbon for the Period 1950–2010, Radiocarbon, 55, 2059–2072, https://doi.org/10.2458/azu_js_rc.v55i2.16177, 2013.

Hugelius, G., Loisel, J., Chadburn, S., Jackson, R. B., Jones, M., MacDonald, G., Marushchak, M., Olefeldt, D., Packalen, M., Siewert, M. B., Treat, C., Turetsky, M., Voigt, C., and Yu, Z.: Large stocks of peatland carbon and nitrogen are vulnerable to permafrost thaw, Proc. Natl. Acad. Sci., 117, 20438–20446, https://doi.org/10.1073/pnas.1916387117, 2020.

IPCC: Climate Change 2021 – The Physical Science Basis: Working Group I Contribution to the Sixth Assessment Report of the Intergovernmental Panel on Climate Change, Cambridge University Press, Cambridge, https://doi.org/10.1017/9781009157896, 2023.

Ivanov, K. E. and Novikov, S. M.: Bolota Zapadnoi Sibiri, ikh stroenie i gidrologicheskiy rezhim [Bogs of West Siberia, their structure and hydrology], Gidrometeoizdat, Leningrad, 447 pp., 1976.

Jeong, S.-J., Bloom, A. A., Schimel, D., Sweeney, C., Parazoo, N. C., Medvigy, D., Schaepman-Strub, G., Zheng, C., Schwalm, C. R., Huntzinger, D. N., Michalak, A. M., and Miller, C. E.: Accelerating rates of Arctic carbon cycling revealed by long-term atmospheric CO2 measurements, Sci. Adv., 4, eaao1167, https://doi.org/10.1126/sciadv.aao1167, 2018.

Jones, B. M., Grosse, G., Farquharson, L. M., Roy-Léveillée, P., Veremeeva, A., Kanevskiy, M. Z., Gaglioti, B. V., Breen, A. L., Parsekian, A. D., Ulrich, M., and Hinkel, K. M.: Lake and drained lake basin systems in lowland permafrost regions, Nat. Rev. Earth Environ., 3, 85–98, https://doi.org/10.1038/s43017-021-00238-9, 2022.

Jones, M. C., Harden, J., O'Donnell, J., Manies, K., Jorgenson, T., Treat, C., and Ewing, S.: Rapid carbon loss and slow recovery following permafrost thaw in boreal peatlands, Glob. Change Biol., 23, 1109–1127, https://doi.org/10.1111/gcb.13403, 2017.

Juggins, S.: C2 Version 1.5. Software for ecological and palaeoecological data analysis and visualisation, 2007.

Juggins, S.: rioja: Analysis of Quaternary Science Data, R package version 0.9-26, 2020.

Kanevskiy, M., Jorgenson, T., Shur, Y., O'Donnell, J. A., Harden, J. W., Zhuang, Q., and Fortier, D.: Cryostratigraphy and Permafrost Evolution in the Lacustrine Lowlands of West-Central Alaska, Permafr. Periglac. Process., 25, 14–34, https://doi.org/10.1002/ppp.1800, 2014.

Karlsson, J., Serikova, S., Vorobyev, S. N., Rocher-Ros, G., Denfeld, B., and Pokrovsky, O. S.: Carbon emission from Western Siberian inland waters, Nat. Commun., 12, 825, https://doi.org/10.1038/s41467-021-21054-1, 2021.

Katz, N. J., Katz, S. V., and Skobiejeva, E. I.: Atlas rastitielnych ostatkov v torfach, Nedra, Moscow, Russia, 370 pp., 1977.

Kirpotin, S., Polishchuk, Y., Bryksina, N., Sugaipova, A., Kouraev, A., Zakharova, E., Pokrovsky, O. S., Shirokova, L., Kolmakova, M., Manassypov, R., and Dupre, B.: West Siberian palsa peatlands: distribution, typology, cyclic development, present day climate-driven changes, seasonal hydrology and impact on CO2 cycle, Int. J. Environ. Stud., 68, 603–623, https://doi.org/10.1080/00207233.2011.593901, 2011.

Kirpotin, S. N., Berezin, A., Bazanov, V., Polishchuk, Y., Vorobiov, S., Mironycheva-Tokoreva, N., Kosykh, N., Volkova, I., Dupre, B., Pokrovsky, O., Kouraev, A., Zakharova, E., Shirokova, L., Mognard, N., Biancamaria, S., Viers, J., and Kolmakova, M.: Western Siberia wetlands as indicator and regulator of climate change on the global scale, Int. J. Environ. Stud., 66, 409–421, https://doi.org/10.1080/00207230902753056, 2009.

Kluge, M., Wauthy, M., Clemmensen, K. E., Wurzbacher, C., Hawkes, J. A., Einarsdottir, K., Rautio, M., Stenlid, J., and Peura, S.: Declining fungal diversity in Arctic freshwaters along a permafrost thaw gradient, Glob. Change Biol., 27, 5889–5906, https://doi.org/10.1111/gcb.15852, 2021.

van der Kolk, H. J., Heijmans, M. M. P. D., van Huissteden, J., Pullens, J. W. M., and Berendse, F.: Potential Arctic tundra vegetation shifts in response to changing temperature, precipitation and permafrost thaw, Biogeosciences, 13, 6229–6245, https://doi.org/10.5194/bg-13-6229-2016, 2016.

Kondratjeva, K. A., Khrutzky, S. F., and Romanovsky, N. N.: Changes in the extent of permafrost during the late quaternary period in the territory of the former Soviet Union, Permafr. Periglac. Process., 4, 113–119, https://doi.org/10.1002/ppp.3430040204, 1993.

Kremenetski, K. V., Velichko, A. A., Borisova, O. K., MacDonald, G. M., Smith, L. C., Frey, K. E., and Orlova, L. A.: Peatlands of the Western Siberian lowlands: current knowledge on zonation, carbon content and Late Quaternary history, Quat. Sci. Rev., 22, 703–723, https://doi.org/10.1016/S0277-3791(02)00196-8, 2003.

Kujala, K., Seppälä, M., and Holappa, T.: Physical properties of peat and palsa formation, Cold Reg. Sci. Technol., 52, 408–414, https://doi.org/10.1016/j.coldregions.2007.08.002, 2008.

Kurakova, A. A.: Landscape-Hydrological Zoning of the Flat Areas of Western Siberia and Its Application in the Analysis of River Bank Erosion, Geogr. Nat. Resour., 45, 397–409, https://doi.org/10.1134/S1875372824700720, 2024.

Laliberté, E., Legendre, P., and Shipley, B.: FD: measuring functional diversity from multiple traits, and other tools for functional ecology. R package version 1.0-12.1., 2014.

Lamarre, A., Magnan, G., Garneau, M., and Boucher, É.: A testate amoeba-based transfer function for paleohydrological reconstruction from boreal and subarctic peatlands in northeastern Canada, Quat. Int., 306, 88–96, https://doi.org/10.1016/j.quaint.2013.05.054, 2013.

Lamentowicz and Mitchell, E. a. D.: Testate amoebae (protists) as palaeoenvironmental indicators in peatlands, Pol. Geol. Inst. Spec. Pap., Vol. 16, 2005.

Lamentowicz, Ł., Lamentowicz, M., and Gąbka, M.: Testate amoebae ecology and a local transfer function from a peatland in western Poland, Wetlands, 28, 164–175, https://doi.org/10.1672/07-92.1, 2008.

Lamentowicz, M.: Kopalne ameby skorupkowe (Protista) - źródło informacji o historii zmian klimatycznych i wpływie człowieka na przyrodę, vol. 1, Seria wydawnicza Stowarzyszenia Archeologii Środowiskowej, 253–264, 2007.

Lamentowicz, M., Słowiński, M., Marcisz, K., Zielińska, M., Kaliszan, K., Lapshina, E., Gilbert, D., Buttler, A., Fiałkiewicz-Kozieł, B., Jassey, V. E. J., Laggoun-Defarge, F., and Kołaczek, P.: Hydrological dynamics and fire history of the last 1300 years in western Siberia reconstructed from a high-resolution, ombrotrophic peat archive, Quat. Res., 84, 312–325, https://doi.org/10.1016/j.yqres.2015.09.002, 2015.

Lamentowicz, M., Kajukało-Drygalska, K., Kołaczek, P., Jassey, V. E. J., Gąbka, M., and Karpińska-Kołaczek, M.: Testate amoebae taxonomy and trait diversity are coupled along an openness and wetness gradient in pine-dominated Baltic bogs, Eur. J. Protistol., 73, 125674, https://doi.org/10.1016/j.ejop.2020.125674, 2020.

Lapshina, E. D. and Zarov, E. A.: Stratigraphy of peat deposits and mire development in the southernpart of the forest zone of Western Siberia in Holocene., Environ.

Dyn. Glob. Clim. Change, 14, 70–101, https://doi.org/10.18822/edgcc568688, 2023.

Leppänen, J. J., Piilo, S., Li, Y., Zhang, H., and Väliranta, M.: Paleoecological assessment of cladoceran community dynamics in two subarctic peatlands, Wetlands, 39, 831–839, https://doi.org/10.1007/s13157-018-1118-2, 2019.

Loisel, J. and Yu, Z.: Recent acceleration of carbon accumulation in a boreal peatland, south central Alaska, J. Geophys. Res. Biogeosciences, 118, 41–53, https://doi.org/10.1029/2012JG001978, 2013.

López-Blanco, E., Topp-Jørgensen, E., Christensen, T. R., Rasch, M., Skov, H., Arndal, M. F., Bret-Harte, M. S., Callaghan, T. V., and Schmidt, N. M.: Towards an increasingly biased view on Arctic change, Nat. Clim. Change, 14, 152–155, https://doi.org/10.1038/s41558-023-01903-1, 2024.

Martini, I. P., Cortizas, A. M., and Chesworth, W.: Peatlands: Evolution and Records of Environmental and Climate Changes, Elsevier, 606 pp., 2007.

Masyagina, O. V. and Menyailo, O. V.: The impact of permafrost on carbon dioxide and methane fluxes in Siberia: A meta-analysis, Environ. Res., 182, 109096, https://doi.org/10.1016/j.envres.2019.109096, 2020.

Mauquoy, D. and Geel, B.: Mire and peat macros, in: Encyclopedia of Quaternary Science, vol. 3, Elsevier, Amsterdam, 2315–2336, 2007.

Mazei, Y. A. and Tsyganov, A. N.: Freshwater Testate Amoebae, KMK Scientific press, Moscow, Russia, 2006.

Miles, V. V. and Esau, I.: Spatial heterogeneity of greening and browning between and within bioclimatic zones in northern West Siberia, Environ. Res. Lett., 11, 115002, https://doi.org/10.1088/1748-9326/11/11/115002, 2016.

Milner, A. M., McKeown, M. M., Ruwaimana, M., Gallego-Sala, A., Loisel, J., Menges, J., Roland, T. P., Ahiable, C. A. E., Akwany, L. O., Alarcon-Prado, P., Anshari, G., Alappat, L., Baird, A. J., Bąk, M., Bambuta Boole, J. J., Batten, S. E., Beaudoin, Y., Bechtold, M., Bu, Z.-J., Budisusanti, S. P. M., Benavides, J. C., Chawchai, S., Chimner, R. A., Cobb, A. R., Cole, L. E. S., Connolly, J., Calvo Vargas, J. C., Courtney-Mustaphi, C. J., Davidson, S. J., de la Peña, A., Duley, E., Elshehawi, S., Espinoza León, I., Finkelstein, S. A., Garneau, M., Girkin, N. T., Glen, E., Grover, S., Grundling, P.-L., Handley, J. N., Helfter, C., Hergoualc'h, K., Hoyt, A. M., Huang, X., Imani, G., James, A., Kabonyi Nzabandora, C., Kagaba Kairumba, C., Kansiime, F., Kolka, R. K., Koren, G., Korhola, A., Krisnawati, H., Kumar, R., Lamentowicz, M., Lång, K., Larmola, T., Lewis, S. L., Lopez, O. R., López-Blanco, E., Lupascu, M., Maldonado-Fonken, M., Marchant, R., Marcisz, K., Mazei, N. G., Mazei, Y. A., Mbasi, M., Melling, L., Miles, L., Montanarella, L., Moss, P. T., Murgía-Flores, F., NGuyen, M.-K., Novita, N., Oliver, D. J. S., Orijemie, E. A., Osaki, M., Page, S. E., Pancost, R. D., Pandey, S., Püschel Hoeneisen, N., Quintana Zagaceta, C. H., Ratnayake, A. S., Reed, M. S., Rochefort, L., Saavedra, B., Samuel, J., Scheel, P., Schutten, H., Siegert, F., Signori-Müller, C., Strack, M., Stolle, F., Swindles, G. T., Tanneberger, F., Turetsky, M. R., Urciuolo, A. B., Väliranta, M., Verstraeten, G., et al.: Priority research questions in global peatland science, Commun. Earth Environ., 7, 349, https://doi.org/10.1038/s43247-026-03321-5, 2026.

Minayeva, T. Yu. and Sirin, A. A.: Peatland biodiversity and climate change, Biol. Bull. Rev., 2, 164–175, https://doi.org/10.1134/S207908641202003X, 2012.

Mitchell, E. A. D.: A brief history of testate amoebae research and introducing the International Society for Testate Amoeba Research (ISTAR), Acta Protozool., 2024, 1–14, 2025.

Mitchell, E. A. D., Payne, R. J., and Lamentowicz, M.: Potential implications of differential preservation of testate amoeba shells for paleoenvironmental reconstruction in peatlands, J. Paleolimnol., 40, 603–618, https://doi.org/10.1007/s10933-007-9185-z, 2008.

Mitchell, E. A. D., Lamentowicz, M., Payne, R. J., and Mazei, Y.: Effect of taxonomic resolution on ecological and palaeoecological inference – a test using testate amoeba water table depth transfer functions, Quat. Sci. Rev., 91, 62–69, https://doi.org/10.1016/j.quascirev.2014.03.006, 2014.

Mooney, S. and Radford, K.: A simple and fast method for the quantification of macroscopic charcoal from sediments, Quat. Australas., 19, 43–46, 2001.

Moore, P. D., Collinson, M., and Webb, J. A.: Pollen Analysis, 2nd edition., Wiley, 216 pp., 1994.

Nieminen, M., Sallantaus, T., and Sarkkola, S.: Natural peatlands as buffers for protection of water quality in boreal forested catchments, For. Ecol. Manag., 606, 123533, https://doi.org/10.1016/j.foreco.2026.123533, 2026.

Ogden, E. L., Cumming, S. G., Smith, S. L., Turetsky, M. R., and Baltzer, J. L.: Permafrost thaw induces short-term increase in vegetation productivity in northwestern Canada, Glob. Change Biol., 29, 5352–5366, https://doi.org/10.1111/gcb.16812, 2023.

Oksanen, J., Simpson, G., Blanchet, F., Kindt, R., Legendre, P., Minchin, P., O'Hara, R., Solymos, P., Stevens, M., Szoecs, E., Wagner, H., Barbour, M., Bedward, M., Bolker, B., Borcard, D., Carvalho, G., Chirico, M., De Caceres, M., Durand, S., Evangelista, H., FitzJohn, R., Friendly, M., Furneaux, B., Hannigan, G., Hill, M., Lahti, L., McGlinn, D., Ouellette, M., Ribeiro Cunha, E., Smith, T., Stier, A., Ter Braak, C., and Weedon, J.: vegan: Community Ecology Package. R package version 2.6-2, 2022.

Olefeldt, D., Heffernan, L., Jones, M. C., Sannel, A. B. K., Treat, C. C., and Turetsky, M. R.: Permafrost Thaw in Northern Peatlands: Rapid Changes in Ecosystem and Landscape Functions, in: Ecosystem Collapse and Climate Change, edited by: Canadell, J. G. and Jackson, R. B., Springer International Publishing, Cham, 27–67, https://doi.org/10.1007/978-3-030-71330-0_3, 2021.

Olson, D. M., Dinerstein, E., Wikramanayake, E. D., Burgess, N. D., Powell, G. V. N., Underwood, E. C., D'amico, J. A., Itoua, I., Strand, H. E., Morrison, J. C., Loucks, C. J., Allnutt, T. F., Ricketts, T. H., Kura, Y., Lamoreux, J. F., Wettengel, W. W., Hedao, P., and Kassem, K. R.: Terrestrial Ecoregions of the World: A New Map of

Life on Earth: A new global map of terrestrial ecoregions provides an innovative tool for conserving biodiversity, BioScience, 51, 933–938, https://doi.org/10.1641/0006-3568(2001)051%5B0933:TEOTWA%5D2.0.CO;2, 2001.

Page, S. E. and Baird, A. J.: Peatlands and Global Change: Response and Resilience, Annu. Rev. Environ. Resour., 41, 35–57, https://doi.org/10.1146/annurev-environ-110615-085520, 2016.

Pandey, A., Tripathi, S., and Basumatary, S.: Non-Pollen Palynomorphs from the Late-Holocene Sediments of Majuli Island, Assam (Indo-Burma Region): Implications to Palaeoenvironmental Studies, 63–81, https://doi.org/10.1007/978-3-031-13119-6_5, 2023.

Pissart, A., Harris, S. A., Prick, A., and Vliet-Lanoë, B. V.: La signification paleoclimatique des lithalses (palses minerales) [Znaczenie paleoklimatyczne form litalsa (palsa mineralne)], Biul. Peryglac., 37, 141–154, https://doi.org/10.26485/BP/1998/37/11, 1998.

Płóciennik, M., Self, A., Birks, H. J. B., and Brooks, S. J.: Chironomidae (Insecta: Diptera) succession in Żabieniec bog and its palaeo-lake (central Poland) through the Late Weichselian and Holocene, Palaeogeogr. Palaeoclimatol. Palaeoecol., 307, 150–167, https://doi.org/10.1016/j.palaeo.2011.05.010, 2011.

Polishchuk, Y. M., Bogdanov, A. N., Polishchuk, V. Yu., Manasypov, R. M., Shirokova, L. S., Kirpotin, S. N., and Pokrovsky, O. S.: Size Distribution, Surface Coverage, Water, Carbon, and Metal Storage of Thermokarst Lakes in the Permafrost Zone of the Western Siberia Lowland, Water, 9, 228, https://doi.org/10.3390/w9030228, 2017.

QGIS Development Team: QGIS Geographic Information System, 2025.

Qin, Y., Li, H., Mazei, Y., Kurina, I., Swindles, G. T., Bobrov, A., Tsyganov, A. N., Gu, Y., Huang, X., Xue, J., Lamentowicz, M., Marcisz, K., Roland, T., Payne, R. J., Mitchell, E. A. D., and Xie, S.: Developing a continental-scale testate amoeba hydrological transfer function for Asian peatlands, Quat. Sci. Rev., 258, 106868, https://doi.org/10.1016/j.quascirev.2021.106868, 2021.

Quinton, W. L., Hayashi, M., and Chasmer, L. E.: Peatland Hydrology of Discontinuous Permafrost in the Northwest Territories: Overview and Synthesis, Can. Water Resour. J. Rev. Can. Ressour. Hydr., 34, 311–328, https://doi.org/10.4296/cwrj3404311, 2009.

R Core Team: R: A language and environment for statistical computing, 2022.

Railton, J. B. and Sparling, J. H.: Preliminary studies on the ecology of palsa mounds in northern Ontario, Can. J. Bot., 51, 1037–1044, https://doi.org/10.1139/b73-128, 1973.

Ramsey, C. B.: Development of the Radiocarbon Calibration Program, Radiocarbon, 43, 355–363, https://doi.org/10.1017/S0033822200038212, 2001.

Rantanen, M., Karpechko, A. Y., Lipponen, A., Nordling, K., Hyvärinen, O., Ruosteenoja, K., Vihma, T., and Laaksonen, A.: The Arctic has warmed nearly four times faster than the globe since 1979, Commun. Earth Environ., 3, 1–10, https://doi.org/10.1038/s43247-022-00498-3, 2022.

Raudina, T. V., Loiko, S. V., Lim, A. G., Krickov, I. V., Shirokova, L. S., Istigechev, G. I., Kuzmina, D. M., Kulizhsky, S. P., Vorobyev, S. N., and Pokrovsky, O. S.: Dissolved organic carbon and major and trace elements in peat porewater of sporadic, discontinuous, and continuous permafrost zones of western Siberia, Biogeosciences, 14, 3561–3584, https://doi.org/10.5194/bg-14-3561-2017, 2017.

Reimer, P. J., Austin, W. E. N., Bard, E., Bayliss, A., Blackwell, P. G., Ramsey, C. B., Butzin, M., Cheng, H., Edwards, R. L., Friedrich, M., Grootes, P. M., Guilderson, T. P., Hajdas, I., Heaton, T. J., Hogg, A. G., Hughen, K. A., Kromer, B., Manning, S. W., Muscheler, R., Palmer, J. G., Pearson, C., Plicht, J. van der, Reimer, R. W., Richards, D. A., Scott, E. M., Southon, J. R., Turney, C. S. M., Wacker, L., Adolphi, F., Büntgen, U., Capano, M., Fahrni, S. M., Fogtmann-Schulz, A., Friedrich, R., Köhler, P., Kudsk, S., Miyake, F., Olsen, J., Reinig, F., Sakamoto, M., Sookdeo, A., and Talamo, S.: The IntCal20 Northern Hemisphere Radiocarbon Age Calibration Curve (0–55 cal kBP), Radiocarbon, 62, 725–757, https://doi.org/10.1017/RDC.2020.41, 2020.

Roe, H. M., Elliott, S. M., and Patterson, R. T.: Re-assessing the vertical distribution of testate amoeba communities in surface peats: Implications for palaeohydrological studies, Eur. J. Protistol., 60, 13–27, https://doi.org/10.1016/j.ejop.2017.03.006, 2017.

Romanovsky, V. E., Drozdov, D. S., Oberman, N. G., Malkova, G. V., Kholodov, A. L., Marchenko, S. S., Moskalenko, N. G., Sergeev, D. O., Ukraintseva, N. G., Abramov, A. A., Gilichinsky, D. A., and Vasiliev, A. A.: Thermal state of permafrost in Russia, Permafr. Periglac. Process., 21, 136–155, https://doi.org/10.1002/ppp.683, 2010.

Rönkkö, M. and Seppälä, M.: Surface characteristics affecting active layer formation in palsas, Finnish Lapland, 2003.

Rudmin, M., Ruban, A., Savichev, O., Mazurov, A., Dauletova, A., and Savinova, O.: Authigenic and Detrital Minerals in Peat Environment of Vasyugan Swamp, Western Siberia, Minerals, 8, 500, https://doi.org/10.3390/min8110500, 2018.

Rydin, H. and Jeglum, J. K.: Peatland habitats, in: The Biology of Peatlands, edited by: Rydin, H. and Jeglum, J. K., Oxford University Press, 1–20, https://doi.org/10.1093/acprof:osobl/9780199602995.003.0001, 2013.

Rydin, H., Jeglum, J. K., and Bennett, K. D.: The Biology of Peatlands, OUP Oxford, 397 pp., 2013.

Sachs, H., Iii, T., and Clark, D.: Paleoecological Transfer Functions, Annu. Rev. Earth Planet. Sci., 5, 159–178, https://doi.org/10.1146/annurev.ea.05.050177.001111, 1977.

Safronova, I. and Yurkovsksya, T.: The latitudinal distribution of vegetation cover in Siberia, BIO Web Conf, 16, 00047, https://doi.org/10.1051/bioconf/20191600047, 2019.

Sannel, A. B. K. and Kuhry, P.: Holocene peat growth and decay dynamics in sub-arctic peat plateaus, west-central Canada, Boreas, 38, 13–24, https://doi.org/10.1111/j.1502-3885.2008.00048.x, 2009.

Scharlemann, J. P., Tanner, E. V., Hiederer, R., and Kapos, V.: Global soil carbon: understanding and managing the largest terrestrial carbon pool, Carbon Manag., 5, 81–91, https://doi.org/10.4155/cmt.13.77, 2014.

Scheffer, M., Carpenter, S., Foley, J. A., Folke, C., and Walker, B.: Catastrophic shifts in ecosystems, Nature, 413, 591–596, https://doi.org/10.1038/35098000, 2001.

Schuur, E. A. G., McGuire, A. D., Schädel, C., Grosse, G., Harden, J. W., Hayes, D. J., Hugelius, G., Koven, C. D., Kuhry, P., Lawrence, D. M., Natali, S. M., Olefeldt, D., Romanovsky, V. E., Schaefer, K., Turetsky, M. R., Treat, C. C., and Vonk, J. E.: Climate change and the permafrost carbon feedback, Nature, 520, 171–179, https://doi.org/10.1038/nature14338, 2015.

Schuur, E. A. G., Pallandt, M., and Göckede, M.: Russian collaboration loss risks permafrost carbon emissions network, Nat. Clim. Change, 14, 410–411, https://doi.org/10.1038/s41558-024-02001-6, 2024.

Seneviratne, S. I., Zhang, X., Adnan, M., Badi, W., Dereczynski, C., Di Luca, A., Ghosh, S., Iskandar, I., Kossin, J., Lewis, S., Otto, F., Pinto, I., Satoh, M., Vicente-Serrano, S. M., Wehner, M., and Zhou, B.: Weather and Climate Extreme Events in a Changing Climate, in: Climate Change 2021: The Physical Science Basis. Contribution of Working Group I to the Sixth Assessment Report of the Intergovernmental Panel on Climate Change, edited by: Pörtner, H.-O., Roberts, D. C., Tignor, M., Poloczanska, E. S., Mintenbeck, K., Alegría, A., Craig, M., Langsdorf, S., Löschke, S., Möller, V., Okem, A., and B., R., Cambridge University Press, Cambridge, United Kingdom and New York, NY, USA, 1513–1766, https://doi.org/10.1017/9781009157896.013, 2021.

Serikova, S., Pokrovsky, O. S., Laudon, H., Krickov, I. V., Lim, A. G., Manasypov, R. M., and Karlsson, J.: High carbon emissions from thermokarst lakes of Western Siberia, Nat. Commun., 10, 1552, https://doi.org/10.1038/s41467-019-09592-1, 2019.

Sheng, Y., Smith, L. C., MacDonald, G. M., Kremenetski, K. V., Frey, K. E., Velichko, A. A., Lee, M., Beilman, D. W., and Dubinin, P.: A high-resolution GIS-based inventory of the west Siberian peat carbon pool, Glob. Biogeochem. Cycles, 18, https://doi.org/10.1029/2003GB002190, 2004.

Shumilovskikh, L., Schlütz, F., Achterberg, I., Bauerochse, A., and Leuschner, H.: Non-Pollen Palynomorphs from Mid-Holocene Peat of the Raised Bog Borsteler Moor (Lower Saxony, Germany), Stud. Quat., 32, 5–18, https://doi.org/10.1515/squa-2015-0001, 2015.

Shumilovskikh, L., O'Keefe, J. M. K., and Marret, F.: An overview of the taxonomic groups of non-pollen palynomorphs, Geol. Soc. Lond. Spec. Publ., 511, 13–61, https://doi.org/10.1144/SP511-2020-65, 2021.

Siemensma, F. J.: Microworld, world of amoeboid organisms. World-wide electronic publication, 2022.

Słowiński, M., Marcisz, K., Płóciennik, M., Obremska, M., Pawłowski, D., Okupny, D., Słowińska, S., Borówka, R., Kittel, P., Forysiak, J., Michczyńska, D. J., and Lamentowicz, M.: Drought as a stress driver of ecological changes in peatland - A palaeoecological study of peatland development between 3500BCE and 200BCE in central Poland, Palaeogeogr. Palaeoclimatol. Palaeoecol., 461, 272–291, https://doi.org/10.1016/j.palaeo.2016.08.038, 2016.

Smith, L. C., MacDonald, G., Frey, K. E., Velichko, A. A., Kremenetski, K., Borisova, O. K., Dubinin, P., and Forster, R. R.: U.S.-Russia venture probes Siberian peatlands' sensitivity to climate, Eos Trans. Am. Geophys. Union, https://doi.org/https://doi.org/10.1029/00EO00357, 2000.

Smith, S. L., O'Neill, H. B., Isaksen, K., Noetzli, J., and Romanovsky, V. E.: The changing thermal state of permafrost, Nat. Rev. Earth Environ., 3, 10–23, https://doi.org/10.1038/s43017-021-00240-1, 2022.

Solomeshch, A. I.: The West Siberian Lowland, in: The World's Largest Wetlands: Ecology and Conservation, edited by: Fraser, L. H. and Keddy, P. A., Cambridge University Press, Cambridge, 11–62, https://doi.org/10.1017/CBO9780511542091.003, 2005.

Spiller, A., Kallenbach, C. M., Burnett, M. S., Olefeldt, D., Schulze, C., Maranger, R., and Douglas, P. M. J.: Gradual drying of permafrost peat decreases carbon dioxide in drier peat plateaus but not in wetter fens and bogs, EGUsphere, 1–15, https://doi.org/10.5194/egusphere-2024-2248, 2024.

Stockmarr, J.: Tablets with Spores used in Absolute Pollen Analysis, Pollen Spores, 13, 615–621, 1971.

Streletskiy, D., Anisimov, O., and Vasiliev, A.: Permafrost Degradation, in: Snow and Ice-Related Hazards, Risks, and Disasters, edited by: Shroder, J. F., Haeberli, W., and Whiteman, C., Academic Press, Boston, 303–344, https://doi.org/10.1016/B978-0-12-394849-6.00010-X, 2015.

Swindles, G. T., Morris, P. J., Mullan, D., Watson, E. J., Turner, T. E., Roland, T. P., Amesbury, M. J., Kokfelt, U., Schoning, K., Pratte, S., Gallego-Sala, A., Charman, D. J., Sanderson, N., Garneau, M., Carrivick, J. L., Woulds, C., Holden, J., Parry, L., and Galloway, J. M.: The long-term fate of permafrost peatlands under rapid climate warming, Sci. Rep., 5, 17951, https://doi.org/10.1038/srep17951, 2015.

Syso, A. I. and Peregon, A. M.: The features of peat-accumulation process at the southern slope of the Great Vasyugan Bog, Contemp. Probl. Ecol., 2, 124–127, https://doi.org/10.1134/S1995425509020064, 2009.

Tobolski, K.: Przewodnik do oznaczania torfów i osadów jeziornych, Wydawnictwo Naukowe PWN, Warszawa, 2000.

Treat, C. C. and Jones, M. C.: Near-surface permafrost aggradation in Northern Hemisphere peatlands shows regional and global trends during the past 6000 years, The Holocene, 28, 998–1010, https://doi.org/10.1177/0959683617752858, 2018a.

Treat, C. C. and Jones, M. C.: Near-surface permafrost aggradation in Northern Hemisphere peatlands shows regional and global trends during the past 6000 years, The Holocene, 28, 998–1010, https://doi.org/10.1177/0959683617752858, 2018b.

Treat, C. C., Jones, M. C., Camill, P., Gallego-Sala, A., Garneau, M., Harden, J. W., Hugelius, G., Klein, E. S., Kokfelt, U., Kuhry, P., Loisel, J., Mathijssen, P. J. H., O'Donnell, J. A., Oksanen, P. O., Ronkainen, T. M., Sannel, A. B. K., Talbot, J., Tarnocai, C., and Väliranta, M.: Effects of permafrost aggradation on peat properties as determined from a pan-Arctic synthesis of plant macrofossils, J. Geophys. Res. Biogeosciences, 121, 78–94, https://doi.org/10.1002/2015JG003061, 2016.

Treat, C. C., Jones, M. C., Alder, J., and Frolking, S.: Hydrologic Controls on Peat Permafrost and Carbon Processes: New Insights From Past and Future Modeling, Front. Environ. Sci., 10, https://doi.org/10.3389/fenvs.2022.892925, 2022.

Trofimova, I. E. and Balybina, A. S.: Classification of climates and climatic regionalization of the West-Siberian plain, Geogr. Nat. Resour., 35, 114–122, https://doi.org/10.1134/S1875372814020024, 2014.

Van Geel, B.: Non-Pollen Palynomorphs, in: Tracking Environmental Change Using Lake Sediments: Terrestrial, Algal, and Siliceous Indicators, edited by: Smol, J. P., Birks, H. J. B., Last, W. M., Bradley, R. S., and Alverson, K., Springer Netherlands, Dordrecht, 99–119, https://doi.org/10.1007/0-306-47668-1_6, 2001.

Vasiliev, A. A., Drozdov, D. S., Gravis, A. G., Malkova, G. V., Nyland, K. E., and Streletskiy, D. A.: Permafrost degradation in the Western Russian Arctic, Environ. Res. Lett., 15, 045001, https://doi.org/10.1088/1748-9326/ab6f12, 2020.

Velichko, A. A., Timireva, S. N., Kremenetski, K. V., MacDonald, G. M., and Smith, L. C.: West Siberian Plain as a late glacial desert, Quat. Int., 237, 45–53, https://doi.org/10.1016/j.quaint.2011.01.013, 2011.

Volkova, I. I., Kolesnichenko, L. G., Kirpotin, S. N., Pokrovsky, O. S., and Vorobyev, S. N.: Peat deposits and peat-forming plants in the mires of the West Siberian northern taiga (based on studies of the Khanymei site), IOP Conf. Ser. Earth Environ. Sci., 232, 012018, https://doi.org/10.1088/1755-1315/232/1/012018, 2019.

Walvoord, M. A. and Kurylyk, B. L.: Hydrologic Impacts of Thawing Permafrost—A Review, Vadose Zone J., 15, vzj2016.01.0010, https://doi.org/10.2136/vzj2016.01.0010, 2016.

Warner, B. G. and Charman, D. J.: Holocene changes on a peatland in northwestern Ontario interpreted from testate amoebae (Protozoa) analysis, Boreas, 23, 270–279, https://doi.org/10.1111/j.1502-3885.1994.tb00949.x, 1994.

Witze, A.: Russia's war in Ukraine forces Arctic climate projects to pivot, Nature, 607, 432–432, https://doi.org/10.1038/d41586-022-01868-9, 2022.

Woodland, W. A., Charman, D. J., and Sims, P. C.: Quantitative estimates of water tables and soil moisture in Holocene peatlands from testate amoebae, The Holocene, 8, 261–273, https://doi.org/10.1191/095968398667004497, 1998.

Xu, J., Morris, P. J., Liu, J., and Holden, J.: PEATMAP: Refining estimates of global peatland distribution based on a meta-analysis, CATENA, 160, 134–140, https://doi.org/10.1016/j.catena.2017.09.010, 2018.

Yu, Z., Loisel, J., Brosseau, D. P., Beilman, D. W., and Hunt, S. J.: Global peatland dynamics since the Last Glacial Maximum, Geophys. Res. Lett., 37, https://doi.org/10.1029/2010GL043584, 2010.

Zhang, H., Väliranta, M., Swindles, G. T., Aquino-López, M. A., Mullan, D., Tan, N., Amesbury, M., Babeshko, K. V., Bao, K., Bobrov, A., Chernyshov, V., Davies, M. A., Diaconu, A.-C., Feurdean, A., Finkelstein, S. A., Garneau, M., Guo, Z., Jones, M. C., Kay, M., Klein, E. S., Lamentowicz, M., Magnan, G., Marcisz, K., Mazei, N., Mazei, Y., Payne, R., Pelletier, N., Piilo, S. R., Pratte, S., Roland, T., Saldaev, D., Shotyk, W., Sim, T. G., Sloan, T. J., Słowiński, M., Talbot, J., Taylor, L., Tsyganov, A. N., Wetterich, S., Xing, W., and Zhao, Y.: Recent climate change has driven divergent hydrological shifts in high-latitude peatlands, Nat. Commun., 13, 4959, https://doi.org/10.1038/s41467-022-32711-4, 2022.

Spis rycin

Kopie artykułów wchodzących w skład rozprawy doktorskiej

Quaternary Science Reviews 308 (2023) 108067

Contents lists available at ScienceDirect

Quaternary Science Reviews

journal homepage: www.elsevier.com/locate/quascirev

Developing a new testate amoeba hydrological transfer function for permafrost peatlands of NW Siberia

Agnieszka Halaś [a, *], Mariusz Lamentowicz [b], Dominika Łuców [a], Michał Słowiński [a]

[a] Department of Past Landscape Dynamics, Institute of Geography and Spatial Organization Polish Academy of Sciences, Twarda 51/55, 00-818, Warsaw, Poland

[b] Climate Change Ecology Research Unit, Faculty of Geographical and Geological Sciences, Adam Mickiewicz University, Bogumiła Krygowskiego 10, 61-680, Poznań, Poland

ARTICLE INFO

Article history:
Received 30 January 2023
Received in revised form
21 March 2023
Accepted 24 March 2023
Available online 11 April 2023

Handling Editor: Donatella Magri

Keywords:
Calibration data set
Wetlands
Climate change
Permafrost thawing
Siberia

ABSTRACT

The vast areas of permafrost peatlands in the West Siberian Lowland (WSL) hold a significant amount of carbon currently at risk due to human-caused global warming. The rapid thawing of about 20–60% of the frozen soils of Western Siberia adds to the destruction of the region's signature palsa landscape and the development of thermokarst lakes or fens. Due to the complex interactions between climate and the ecosystem that shape its formation and degradation, permafrost reacts in different ways to environmental changes. Understanding recent changes in Western Siberia requires knowledge of previous environmental transitions, which needs to be enhanced further. This study, aimed to create a hydrological testate amoebae (TA) transfer function (TF) from the Khanymei area in the WSL to reconstruct past hydrological conditions in permafrost peatlands. In addition, this research intended to examine the influence of TA communities living in lichens (genus *Cladonia*) on the performance of TF by integrating these data with a calibration data set. In the summer of 2019, 76 modern samples of *Sphagnum*, *Cladonia*, and vascular plants from permafrost and non-permafrost sites were collected. Moreover, one peat core was extracted from the same area to reconstruct the depth to water table (DWT) quantitatively. The Shannon's diversity index, a quantitative measure of species richness, was calculated for each sample to estimate the TA species diversity in a community. Non-metric multidimensional scaling ordination was applied to the dataset to explore the similarities in TA communities between samples and determine whether the DWT controls the TA community structure. Results showed that the typical transition of TA species along the microtopographic (wet–dry) gradient is influenced by the presence of lichens on the surface of the peatland. Statistical analysis confirmed that TA communities in *Cladonia* are less affected by DWT. Therefore, the TF was constructed on the entire dataset ($n = 75$) and the dataset with *Cladonia* excluded ($n = 55$). Both these TFs showed satisfactory results. Even though the TF constructed on the entire dataset showed fewer predictive abilities, it provided a complete picture of the current vegetation conditions of Khanymei peatlands, where lichens are an essential element of the ecosystem. Therefore, it is assumed that TF with local environment traits may be more suitable for quantitative reconstruction, particularly in the newly explored permafrost area of Western Siberia.

1. Introduction

Currently, scientists are highly interested in the high latitudes of the Northern Hemisphere – especially the large permafrost peatland areas of Siberia and Canada, which have experienced significant changes in the past decades due to rapid climate change (e.g. Turetsky et al., 2007; Kirpotin et al., 2011; Vincent et al., 2017; Biskaborn et al., 2019; Fewster et al., 2022; Zhang et al., 2022). Northern peatlands (including Siberia) store about 415±150PgC, nearly half of which is accumulated in permafrost areas (Hugelius et al., 2020). Currently, these permafrost areas are thawing due to the ongoing anthropogenic global warming (Fewster et al., 2022; Gudmundsson et al., 2022). The disturbance of permafrost stability causes an increase in active layer thickness (Quinton and Baltzer, 2013) and widespread changes in thermokarst ponds and lakes distribution (Marsh et al., 2009; Sannel and Kuhry, 2011; Jones

* Corresponding author.
E-mail address: aj.halas@twarda.pan.pl (A. Halaś).

https://doi.org/10.1016/j.quascirev.2023.108067

et al., 2016). Rapid thaw influences the carbon cycle differently depending on local permafrost conditions (Schuur et al., 2015). Post-thaw expansion of thermokarst lakes increases emissions of CH_4 by microbial processes, but anaerobic conditions facilitate the accumulation of new carbon (Meredith et al., 2019; Magnan et al., 2022). In contrast, thermokarst lakes drainage which prevails in the zone of discontinuous permafrost, due to aerobic conditions may lead to long-term loss of carbon, which is compensated only at the beginning by renewed peat accumulation and an increase in the carbon uptake (Sannel and Kuhry, 2011; Voigt et al., 2019).

It is presumed that permafrost peatlands could be on the edge of their climate niche (Zhang et al., 2018). With an increase in warming, northern areas will become climatically unsuitable for them to last (Fewster et al., 2022). Changes currently observed in northern peatlands, such as hydrological changes (Karlsson et al., 2012; Han and Menzel, 2022), vegetation cover shifts (Tchebakova et al., 2009, van der Kolk et al., 2016), and wildfire regime changes (Lamentowicz et al., 2015; Gibson et al., 2018; Feurdean et al., 2022) may lead to the development of new post-thaw landscape and transformation of this large terrestrial ecosystem, especially in discontinuous and sporadic permafrost zones (Olefeldt et al., 2021).

These changes are progressing rapidly in Western Siberia (Hantemirov et al., 2022). The uniqueness of its permafrost peatlands and their critical role in shaping the global climate have made researchers interested in the changes that occurred in this region in the past (Kirpotin et al., 2009, 2011). Scientists started investigating Western Siberian permafrost and its dynamics in the nineteenth century due to its impact on society and the economy (Shiklomanov, 2005). Currently, 20–60% of the frozen soils of Western Siberia are exposed to rapid thawing (Turetsky et al., 2019) and models predict that this process is unlikely to stop (Alexandrov et al., 2021; Fewster et al., 2022). The ongoing warming threatens the existence of the characteristic forms of palsas (Kirpotin et al., 2011; Könönen et al., 2022), which will become thermokarst lakes or fens after permafrost collapse (Borge et al., 2017). However, Western Siberian permafrost is “ecosystem-driven”, meaning its formation and degradation result from complex interactions between climate and the ecosystem (Shur and Jorgenson, 2007). In this region permafrost is protected by vegetation, the moss-organic layer, and the cooling effect of lichens and mosses can delay the expected thaw and permafrost retreat, whereas shrubs have the opposite impact (Lawrence and Swenson, 2011; Myers-Smith and Hik, 2013; Alexandrov et al., 2021). Despite the increase in studies on permafrost in the high latitudes of the Northern Hemisphere (e.g. Gudmundsson et al., 2022; Perrier et al., 2022), there is still an insufficiency of studies from Western Siberia. Therefore, better knowledge about recent observations and past environmental changes in this region is required to understand the current processes resulting from ongoing anthropogenic global warming (IPCC et al., 2022).

Numerous studies have reported the usefulness of testate amoebae (TA), a group of single-celled protists with a shell (test) found at the surface of peatlands, in the reconstruction of past hydrological conditions (e.g. Booth, 2002; Van Bellen et al., 2014). This is due to their sensitivity to changes in hydrological conditions, resistance to decomposition in peat and long fossil history (Charman et al., 2000; Mitchell et al., 2008). Over the past 30 years, TA-based hydrological transfer functions (TFs) have been developed for numerous peatlands in lower latitudes (Charman et al., 2007; Lamentowicz et al., 2008; Qin et al., 2013; Swindles et al., 2014; Amesbury et al., 2016). Recent studies on several permafrost peatlands have reported equally satisfactory results, for both continuous (Taylor et al., 2019) and discontinuous permafrost peatlands (Lamarre et al., 2013; Swindles et al., 2015a; Zhang et al., 2017; Sim et al., 2021). TA communities present in some parts of Western Siberia have been studied (Rakhleeva, 2002; Bobrov et al., 2015; Mazei et al., 2017), and even used in continental-scale Asian TF (Qin et al., 2021), but so far, no Western-Siberia-specific TF has been developed. Moreover, ecological and paleoecological studies analyzing TA are rare in the case of Western Siberia peatlands (Lamentowicz et al., 2015; Fiałkiewicz-Kozieł et al., 2016).

Therefore, this study aimed to (1) establish the relationship between TA communities, depth to water table (DWT), microhabitat, and vegetation type in *Sphagnum*-dominated peatlands of North-western Siberia, (2) build a new TF useful for future palaeohydrological reconstructions in thawing permafrost areas and apply it to new subfossil data, and (3) check the influence of TA communities from lichens (genus *Cladonia*) on TF performance.

2. Materials and methods

2.1. Study area

The studied permafrost peatlands (palsa bogs – flat peat mounds with permafrost cores) are located near the Khanymei Research Station in the south-east of the Yamal-Nenets Autonomous District, Russia (63°43′N, 75°57′E, 70 m a.s.l.), at the northern border of the taiga subzone with open stands and woodlands (Fig. 1). They are part of second largest wetland complex in the world – West Siberian Lowland, which extends from the Ural Mountains to the Middle Siberian Highland (Kremenetski et al., 2003). The two primary features of this region are discontinuous permafrost and thermokarst lakes.

According to the Köppen-Geiger climate classification, this region has a boreal climate (Peel et al., 2007), with long, cold, and snowy winters and short and cool summers. The mean annual air temperatures range between −3.5 and −6 °C. January air temperatures vary from −22 to −24 °C and July from 15.5 to 17 °C (Trofimova and Balybina, 2014). In the past century, Siberia experienced the highest increase in air temperatures in the Northern Hemisphere (1.39 °C/100 years), compared with the Arctic (1.28 °C/100 years) or the entire Northern Hemisphere (0.77 °C/100 years) (Groisman et al., 2013). There is also a significant increase in hot extremes and a decrease in cold extremes (Seneviratne et al., 2021). Such a drastic change compared with other northern regions is attributable to the continentality of the Western Siberian climate. Projections of present-day climate models suggest that this systematic trend in air temperature change will remain one of the largest in the world (Groisman et al., 2013). The average annual precipitation for Khanymei Research Station is 436 mm (Kluge et al., 2021). During the past decades, the characteristics of precipitation have changed. Significant intensification of heavy rainfall over Western Siberia in the warm season (Seneviratne et al., 2021) and a general increase in precipitation and snow water equivalent in the cold season have been observed (Bulygina et al., 2011; Groisman et al., 2013).

The northern border of the taiga subzone is occupied primarily by coniferous pine (*Pinus siberica* and *Pinus sylvestris*) and larch (*Larix sibirica*) open forests (Safronova and Yurkovsksya, 2019). The characteristic feature of this landscape is a combination of moss-lichen-shrub mound palsa with dense dwarf shrubs (e.g. *Ledum palustre*), as well as dwarf birch (*Betula nana*) (Safronova and Yurkovsksya, 2019; Volkova et al., 2019). The vegetation of raised bogs is well-developed and consists primarily of *Sphagnum* mosses (mainly *Sphagnum fuscum* and *Sphagnum medium/divinum*), but lichens are also an essential component of the vegetation cover. Lichens occupy 70–80% of the surface in the Khanymei region, primarily species of the genera *Cladonia* and *Cetraria* (Volkova et al., 2019). In contrast to more southern regions in WSL in the Khanymei

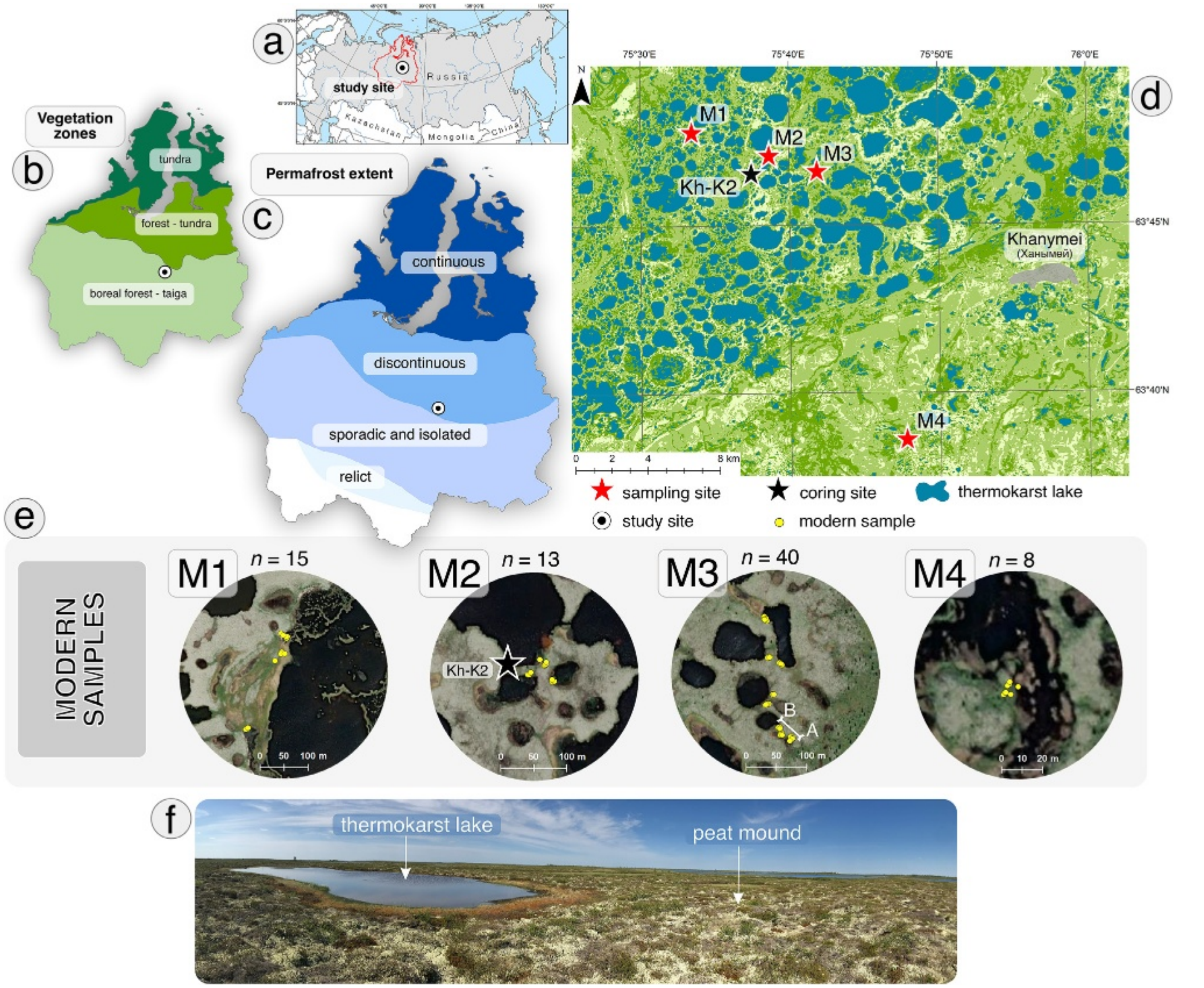

Fig. 1. Study area: a) location of West Siberian Lowland (WSL) b) WSL – vegetation zones based on Davydova and Rakovskaya (1990); c) WSL – permafrost extent based on Brown et al. (1997); d) the location of sampling and coring near the Khanymei Research Station with water bodies detected with the NDPI index from Landsat 8 imagery; e) approximate location of the sampling sites with peat mound-pond edge transect (A–B), background: ArcGIS World Imagery base map; f) the view on the peat mound/thermokarst lake complex in the area of sampling.

area lichens create a unique type of lichen peat (usually forming layers in the peat) (Volkova et al., 2019).

The formation of peatlands in Western Siberia started in the early Holocene (between 11,000 and 10,000 cal BP) due to the post-glacial warming of northern Siberia (Kremenetski et al., 2003). Many previous studies have attributed the late start of peat accumulation to the ice sheet cover over Western Siberia in the last glacial period. However, recent simulations have indicated that this region was ice-free (Abe-Ouchi et al., 2015). There is evidence of a vast cold desert in this region. Cryoarid environments were favored by the reduction in moisture supply from the North Atlantic caused by the expansion of the ice cover in the Arctic Ocean and the Siberian High (Velichko et al., 2011). These circumstances have resulted in summer dryness and moisture imbalance in Western Siberia, which is perceived as a critical factor blocking the formation of *Sphagnum*-dominated peatlands during the glacial period (Alexandrov et al., 2016). Peat deposits in the Khanymei region are usually 0.1–1.4 m in depth (Raudina et al., 2017). Epigenetic permafrost aggradation started in WSL during the Subatlantic period (after 2000 years BP) and resulted in the cryogenic lifting of peat deposits accumulated after deglaciation (Kondratjeva et al., 1993; Treat and Jones, 2018). Thermokarst lakes in the area developed under stable permafrost conditions ~2500 years ago (Lim et al., 2017; Raudina et al., 2017).

2.2. Fieldwork and sampling

From Khanymei permafrost peatlands (flat mound palsa bogs) 76 modern samples were collected at the turn of June and July 2019 in four different locations, indicated by letters M1 ($n = 15$), M2 ($n = 13$), M3 ($n = 40$) and M4 ($n = 8$) (Fig. 1). The modern samples were collected in transects toward the edges of thermokarst lakes covering various locations along microtopographic gradients: mounds (≥20 cm above the water table, $n = 14$), lawns (from 20 to 5 cm, $n = 34$), carpets (from 5 to 0 cm, $n = 23$) and ponds (inundated, edges of thermokarst ponds, $n = 5$) (Rydin and Jeglum, 2013) (Supplementary Table 1). The moisture gradient was from −15 cm (submerged) to +38 cm (dry) with a DWT standard deviation of 9.7 cm. Due to the discontinuous permafrost that generates specific conditions in the ground, some samples were taken from the above standard water table (non-permafrost sites) and others directly from above the frozen peat. Therefore, for simplification, the term depth to water table (DWT) was used concerning the depth of the water table and the permafrost in this study. Depth to water table or the frozen peat was measured in centimeters directly in the field using the measuring tape for each site. During measurements, the top of the moss/lichen layer or the water table (for inundated samples) was considered the "0" level. For TA analysis, the vegetation was sampled from 10 cm^2, and the plants upper part (0–3 cm) was collected and stored in plastic bags. The species composition of the vegetation in modern samples and peat core was determined in the laboratory using plant macrofossil analysis.

To test the performance of the TF, it was applied on the peat core (Kh-K2) taken from the same area as the modern samples (Fig. 1). A 26-cm long core was extracted from a peat mound with surface vegetation primarily consisting of lichens. The peat monolith with a diameter of 10 cm × 10 cm was extracted using a knife until the frozen peat was reached. It was used as a paleo-dataset of subfossil TA from the Khanymei region.

2.3. Modern and subfossil testate amoebae sampling

TA analysis followed the standard procedure without any chemical reagents (Hendon and Charman, 1997; Booth et al., 2010). Approximately 3 cm^3 of the material was extracted from each modern and paleo sample, and subfossil data were subsampled with a resolution of 1 cm (except for the first 0–2 cm sample). The prepared material was placed in 50 ml sample containers, shaken in distilled water, and sieved through a 300 μm mesh. The material was then spread on glass slides and examined using a ZEISS Axiolab 5 light microscope at a magnification of 200 × and 400 × . At least 150 individual tests were counted for each modern and subfossil sample. TA shells were identified to species (where possible) or "type" level based on the available taxonomic materials and identification guides (Charman et al., 2000; Clarke, 2003; Mazei & Tsyganov, 2006; Tsyganov et al., 2016; Todorov and Bankov, 2019; Siemensma, 2022). Some taxa were merged into groups based on morphological similarity, following the taxonomic harmonization developed by Amesbury et al. (2016). This procedure was applied to the following taxa: *Cyclopyxis arcelloides* type, *Euglypha rotunda* type, *Euglypha ciliata* type and *Difflugia lucida* type (Table 1). In modern samples, shells of rotifer *Habrotocha angusticollis* were also counted but excluded from the training set.

2.4. Statistical analysis

To measure the diversity of TA species in a community for each modern and subfossil sample, quantitative species richness/evenness Shannon's diversity index (Daly et al., 2018) was calculated using the *vegan* package (Oksanen et al., 2022) in R software (R Core Team, 2022). Box plots were created by dividing all samples into five groups based on the DWT and vegetation type: 1) *Cladonia* (n = 20), 2) *Sphagnum* spp. mounds DWT ≥20 cm (including permafrost samples) (n = 12), 3) *Sphagnum* spp. lawns DWT 20–5 cm (n = 22), 4) *Sphagnum* spp. carpets DWT 5–0 cm (n = 17), and 5) inundated samples (n = 4). *Cladonia* samples were treated separately due to their uniqueness in TA compositions. Statistics were not calculated for the inundated samples due to the insufficient group size.

To present the similarities in the community structures between sites, non-metric multidimensional scaling (NMDS) ordination on the Bray-Curtis dissimilarity (Ricotta and Podani, 2017) was applied on the data using *vegan* and plotted using the *ggplot2* package (Wickham et al., 2016) in R software. Non-linear species responses and only a few assumptions about the nature of the data were the reasons for selecting this method. The *decostand* function was used to standardize the TA abundance data using the Hellinger transformation to minimize the influence of common and rare species on the ordination (Legendre and Gallagher, 2001). To reduce the complexity of the NMDS plot, results for TA species and sites were plotted separately. For the species plot DWT vector was fitted into the ordination plot using the *envfit* function. For the sites plot, 90% confidence interval ellipses of multivariate *t*-distribution type were added for each sample group using the *stat_ellipse* function. NMDS ordination was carried out on three datasets: the entire dataset (n = 75 samples), the dataset with *Cladonia* excluded (n = 55 samples), and the dataset with only *Cladonia* (n = 20 samples).

2.5. Transfer function development

TFs for DWT were developed using the C2 program, version 1.7.7 (Juggins, 2007) for the entire dataset and then separately for the dataset with *Cladonia* excluded. The following commonly used model types available in the C2 program were implemented: four Weighted Averaging models with tolerance downweighting (WAtol) or without (WA), and using classical (cla) or inverse (inv) deshrinking; Weighted Averaging Partial Least Squares (WA-PLS); Modern Analogue Technique (MAT); Maximum Likelihood (ML); and Partial Least Squares (PLS). The implemented TF models were cross-validated using bootstrapping (1000 cycles) and leave-one-out methods. The performance of the models was evaluated using R-squared (R^2), root mean square error of prediction (RMSEP), average bias, and maximum bias. One modern sample (M1_11) was removed from the modern training set due to an extremely low concentration of shells, so all calculations were performed on TA from 75 (entire dataset) and 55 modern samples (with *Cladonia* excluded). Different configurations of taxonomic aggregation were applied to the dataset, from the actual resolution obtained during the microscope count to the lower taxonomic resolution previously proposed by various authors (e.g. Charman et al., 2000). The final grouping was made using the taxonomic aggregation proposed by Amesbury et al. (2016), with some changes. To eliminate the influence of potential recognition errors on the quality of the TF, difficult to identify taxa such as *Cyclopyxis arcelloides* type, *Difflugia lucida* type and *Difflugia pulex* type were grouped based on the morphological similarity approach (Mitchell et al., 2014). However, Amesbury et al. (2016) harmonization was not applied to taxa that, according to the authors, constitute an essential element of TA communities. Merging these taxa could lead to a loss of information and a reduction in taxonomic resolution (e.g. *Corythion dubium* and *Trinema lineare*, which in this study are considered separate taxa).

The best TF models for DWT were applied to a subfossil TA dataset from a peat monolith (Kh-K2) from Khanymei peatlands to test its usefulness. The reconstructed DWT using the created Khanymei TF was compared with the previously published Pan-European (Amesbury et al., 2016), and Asian (Qin et al., 2021) TFs. Reconstructions were carried out using the *rioja* package in R software (Juggins, 2020).

Tolerance ranges and optima statistics for the DWT were calculated for all species using WA in the C2 program. The calculations were carried out on the entire dataset, and the dataset with *Cladonia* was excluded and then compared.

3. Results

3.1. Testate amoebae communities along a microtopographic gradient

A total of 11 388 TA shells belonging to 45 taxa were identified in modern samples from Khanymei peatlands (Table 1). The most

Table 1
Overview of testate amoebae (TA) species identified in this study with acronyms, maximum abundance (%) in *Cladonia* and mosses samples, frequency of occurrences and percentage of all shells.

Full name	Acronym	Max (%)		In *n* samples (out of a total of 75 samples)	% of all shells
		in *Cladonia* samples	in moss samples		
Alabasta militaris	ALA MIL	2.9	**19.9**	36	1.79
Amphitrema wrightianum	AMP WRI	0.0	**63.3**	13	1.05
Archerella flavum	ARC FLA	1.3	**68.0**	46	13.49
Assulina muscorum	ASS MUS	25.8	**38.2**	64	7.90
Assulina seminulum	ASS SEM	21.3	**22.0**	40	2.35
Bullinularia indica	BUL IND	2.0	**3.9**	20	0.43
Centropyxis aculeata	CEN ACU	0.0	**9.3**	6	0.26
Centropyxis ecornis	CEN ECO	0.0	**3.7**	2	0.08
Centropyxis sp.	CEN SP	0.0	1.3	2	0.03
Corythion constricta	COR CON	**11.1**	2.0	19	1.00
Corythion dubium	COR DUB	**82.1**	50.6	48	16.96
Cryptodifflugia minuta	CRY MIN	0.7	**13.4**	12	0.68
Cryptodifflugia oviformis	CRY OVI	16.0	**30.0**	26	1.54
Cryptodifflugia voigti	CRY VOI	6.5	**16.4**	23	1.30
Cyclopyxis arcelloides type	CYC ARC	4.6	**92.1**	45	11.02
Cylindrifflugia bacillariarum	CYL BAC	1.3	**50.7**	13	0.21
Difflugia bacillifera	DIF BAC	0.0	**7.3**	5	0.99
Difflugia globulosa	DIF GLO	2.0	**13.3**	7	0.41
Difflugia lucida type	DIF LUC	**5.3**	5.1	15	0.09
Difflugia pulex type	DIF PUL	5.2	**18.7**	10	0.81
Difflugia sp.	DIF SP	0.0	0.7	2	0.02
Euglypha ciliata type	EUG CIL	10.6	**13.2**	32	1.88
Euglypha denticulata	EUG DEN	9.3	**21.0**	31	2.27
Euglypha leavis	EUG LEA	0.0	**2.6**	1	0.04
Euglypha rotunda type	EUG ROT	9.3	**16.7**	29	0.84
Euglypha sp.	EUG SP	2.0	3.1	16	0.28
Galeripora artocrea	GAL ART	0.0	**2.0**	4	0.06
Galeripora catinus	GAL CAT	0.7	**26.3**	22	1.39
Galeripora discoides type	GAL DIS	2.0	**22.0**	16	1.42
Galeripora sp.	GAL SP	0.7	0.7	4	0.04
Heleopera petricola	HEL PET	0.0	**7.3**	9	0.41
Heleopera sphagni	HEL SPH	0.0	**12.3**	30	0.05
Heleopera sylvatica	HEL SYL	**2.0**	1.3	4	1.15
Heleopera sp.	HEL SP	0.0	2.0	4	0.07
Hyalosphenia elegans	HYA ELE	4.0	**49.3**	41	5.72
Hyalosphenia ovalis	HYA OVA	0.0	**6.6**	5	0.20
Hyalosphenia papilio	HYA PAP	1.3	**61.2**	41	8.25
Hyalosphenia subflava	HYA SUB	0.0	**2.5**	4	0.08
Nebela collaris	NEB COL	**5.3**	0.0	8	0.28
Nebela tincta	NEB TIN	13.3	**22.4**	40	0.12
Nebela tincta var. *major*	NEB TINM	**6.0**	0.0	1	1.99
Nebela sp.	NEB SP	2.6	2.0	6	0.08
Physochila griseola	PHY GRI	0.0	**18.5**	30	2.14
Plagiopyxis labiata	PLA LAB	**16.8**	3.9	16	2.01
Placocista spinosa	PLA SPI	**16.8**	10.7	28	0.37
Placocista spinosa glabra	PLA SPI G	4.0	**6.0**	13	0.71
Planocarina carinata	PLA CAR	0.0	**2.0**	3	0.07
Trigonopyxis arcula	TRI ARC	**8.0**	6.4	25	0.73
Trigonopyxis minuta	TRI MIN	3.3	**8.9**	12	0.43
Trinema complanatum	TRI COM	0.0	**1.3**	2	0.03
Trinema lineare	TRI LIN	**43.5**	23.6	44	4.49

abundant taxa were: *Corythion dubium* (17.0% of all shells), *Archerella flavum* (13.5%), *Cyclopyxis arcelloides* type (11.0%), and *Hyalosphenia papilio* (8.2%). Taxa that were present in more than half of all samples were: *Assulina muscorum* (most common, present in 64 out of 75 samples), *C. dubium*, *A. flavum*, *C. arcelloides* type, *Trinema lineare*, *Hyalosphenia elegans*, *H. papilio*, *Assulina seminulum,* and *Nebela tincta*. Some species showed exceptional dominance in some samples, such as *C. arcelloides* type in sample M3_29 accounting for 92.1% of all shells, and *C. dubium,* which is dominant in *Cladonia* samples (from 20 to 82%).

The species richness of TA in modern samples varied from 5 to 20 species. *Cladonia* samples stood out from other modern samples (Supplementary Fig. 1). They occurred along a wide range of microtopographic gradients, from DWT = 20 cm at mounds to DWT = 1 cm at carpets (Supplementary Table 1), sometimes accompanied by mosses in wetter microhabitats. Despite the DWT, the most common TA species present in these samples were dry indicators such as *C. dubium*, *T. lineare,* and *A. muscorum* (Bobrov et al., 1999; Koenig et al., 2018) (Fig. 2). *Placocista spinosa* and *Placocista spinosa glabra* were also frequently observed. Taxa that occur almost only (*Plagiopyxis labiata* and *Corythion constricta*) or only (*Nebela collaris* and *Nebela tincta* var. major) in these samples were characteristic of *Cladonia*. Although the occurrence of the most frequent species was similar regardless of the DWT, in individual samples small numbers of species characteristic of the microstructure in which these lichens grew were observed, such as *Cylindrifflugia bacillariarum* (González-Miguéns et al., 2022) and *C. arcelloides* type in carpets, *Hyalosphenia* species in lawns and *Trigonopyxis arcula* in drier lawns and mounds.

Mounds (DWT ≥20 cm) covered mainly by *Sphagnum* mosses

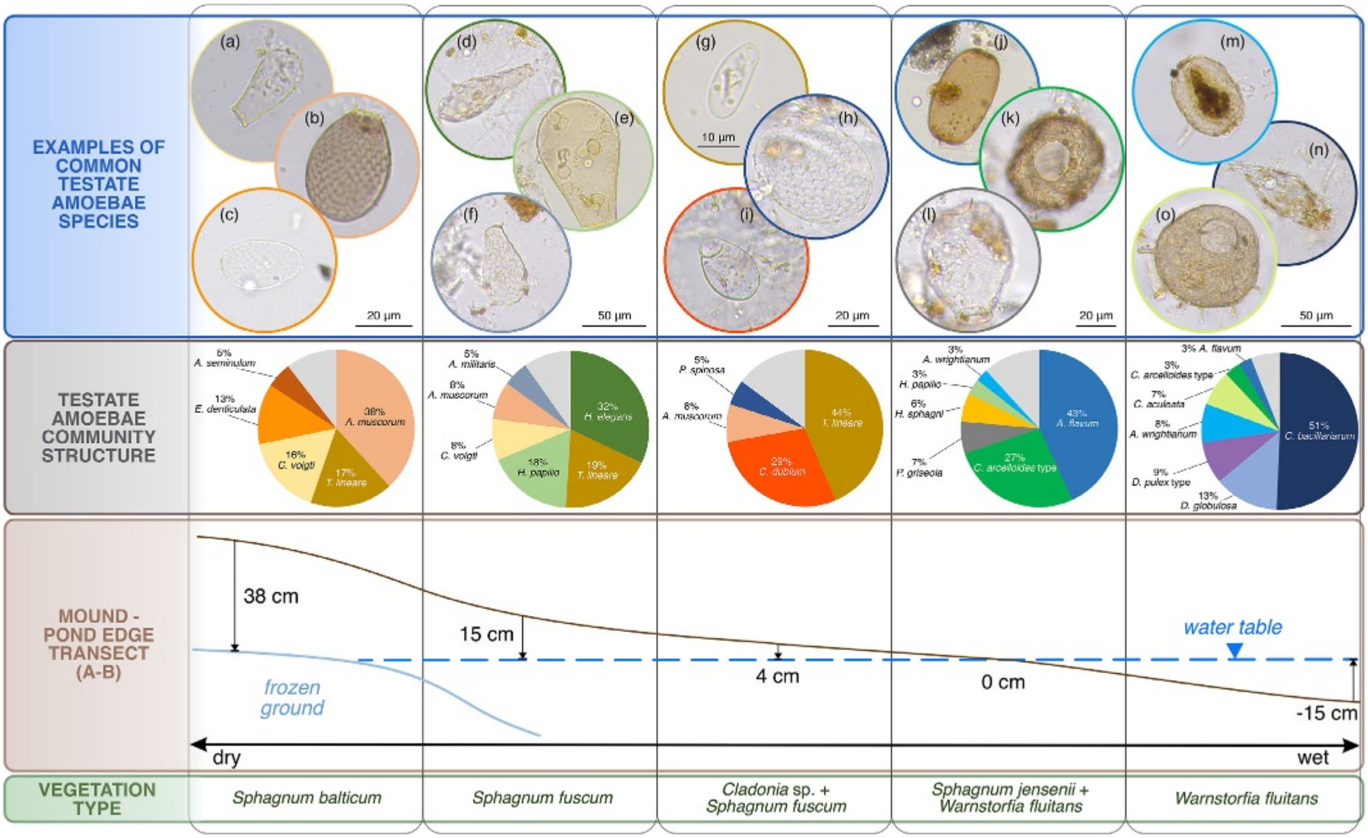

Fig. 2. Characteristics of testate amoebae (TA) communities along a simplified peat mound-lawn-carpet-pond edge transect A–B in Khanymei peatlands (samples used in the transect left-right: M3_13, M3_10, M3_7, M3_2, M3_3). Examples of common TA species (a) *Cryptodifflugia voigti*, (b) *Assulina muscorum*, (c) *Euglypha denticulata*, (d) *Hyalosphenia elegans*, (e) *Hyalosphenia papilio*, (f) *Alabasta militaris*, (g) *Trinema lineare*, (h) *Placocista spinosa glabra*, (i) *Corythion dubium*, (j) *Archerella flavum*, (k) *Cyclopyxis arcelloides* type, (l) *Physochila griseola*, (m) *Amphitrema wrightianum*, (n) *Cylindrifflugia bacillariarum*, (o) *Centropyxis aculeata*.

(*Sphagnum fuscum, Sphagnum majus, Sphagnum balticum*) showed a similar species composition as *Cladonia* with some significant differences and usually more species per sample (Fig. 3). Dry indicators also dominated, but *C. dubium* was not as dominant. A clear distinction was the higher presence of small taxa from the genus

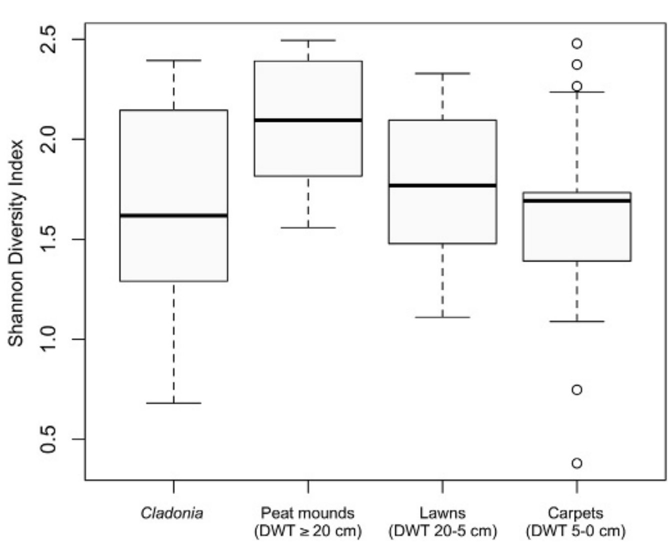

Fig. 3. Box plot with outliers of the Shannon's diversity index between groups of modern samples. (Note: peat mounds include all samples with frozen peat reached. Inundated samples were excluded from the graph due to the statistically insufficient size of the group).

Cryptodifflugia (*Cryptodifflugia voigti*, *Cryptodifflugia minuta*, *Cryptodifflugia oviformis*) and *A. seminulum*. A few shells of *Centropyxis ecornis* were only observed in this microstructure.

Wetter lawns (DWT 20–5 cm) covered by *Sphagnum* mosses (*Sphagnum jensenii*, *Sphagnum lindbergii*, *Sphagnum medium/divinum* and *Sphagnum cuspidatum*) and *Polytrichum strictum* were strongly dominated by *H. papilio*, *H. elegans, A. flavum* and *C. arcelloides* type (in sites below 10 cm to the water table). In addition, *Heleopera petricola* and colorless *Galeripora discoides* type were present. Two species – *Alabasta militaris* and *Galeripora catinus* – were observed in mounds and lawns more frequently than in other microhabitats.

Carpets (DWT 5–0 cm) covered by *Sphagnum* mosses (*S. jensenii*, *S. lindbergii*, *S. cuspidatum*) and *P. strictum*, and their TA species composition reflected their transitional character between lawns and ponds. Some taxa started to disappear (e.g. *A. militaris*, *G. catinus*, *T. lineare*), and others began to emerge (e.g. *Difflugia* species, *Amphitrema wrightianum*, *Centropyxis aculeata, Planocarina carinata*).

A characteristic feature of samples from the pond's edges (DWT <0 cm) was the species composition of vegetation. In this transect, stable and long-term submerged surfaces of the pond edges were covered with aquatic mosses *Warnstorfia fluitans* as the dominant vegetation type and were occupied by wet TA indicators such as *C. bacillariarum*, *Difflugia bacillifera*, *Difflugia globulosa* or *A. wrightianum* (Bobrov et al., 1999) (Fig. 2). However, samples from the pond edges with a recent permafrost collapse were covered with *P. strictum*, and their TA species composition was more similar to drier microhabitats (Fig. 4).

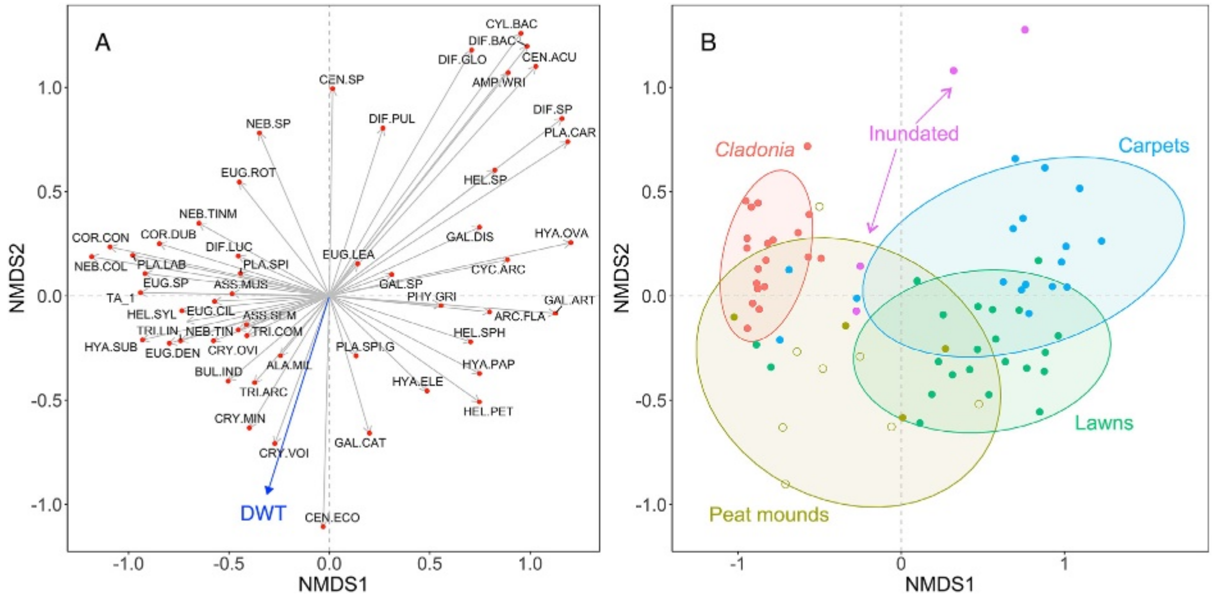

Fig. 4. Two-dimensional NMDS ordination plots of A) testate amoebae (TA) species with the depth to water table (DWT) vector, and B) samples with water table (filled circles) or frozen peat reached (open circles), with 90% confidence interval ellipses of multivariate *t*-distribution (stress = 0.13). For inundated samples, the ellipse has not been drawn due to the statistically insufficient size of the group.

3.2. Species richness among sites

The Shannon's diversity index ranged from 0.38 (low) to 2.51 (moderate diversity) (Fig. 3, Supplementary Table 1). Usually, it can reach values up to 3.5, rarely to 4.5 (Gaines et al., 1999). Between groups of samples, peat mounds were characterized by a higher median value of the Shannon's diversity index (M = 2.10) than other groups and a more similar number of species among samples. The index values for this group ranged from 1.56 to 2.50. Lawns showed a larger spectrum of index values (from 1.11 to 2.33, M = 1.77). The most significant differences in species richness between groups appeared in carpets and *Cladonia* sites. In these habitats, samples with low (5–6 species) and moderate diversity (20 species) were identified. The least diverse sample was *Sphagnum lindbergii* DWT 2 cm (M3_29), with only six species found and a high dominance of one – *Cyclopyxis arcelloides* type. The Shannon's diversity index values for inundated samples varied depending on the vegetation and ranged from 1.18 in *Warnstorfia fluitans* to 2.52 in *Polytrichum strictum* (Supplementary Table 1).

3.3. TA communities and gradients

A two-dimensional NMDS ordination plot with the lowest stress (stress = 0.13) provides a reliable illustration of the dataset (Fig. 4). Ordination provided a graphical representation of changes in TA assemblages along the DWT gradient, with a DWT vector explaining 51.59% of the variables ($p < 0.001$). TA species more associated with drier (negative NMDS values on the axis) and wetter microhabitats (positive values) were determined using an NMDS plot. Euclidean distances between samples in the *Cladonia* group showed similarities in their TA assemblages. The position at the lower end of axis 1 and span along axis 2 suggested the general domination of dry TA indicators with subtle species changes with DWT change. The overlapping ellipses indicated some similarities between the groups of modern samples. The most distinctive microhabitats were inundated samples with the highest outlier values on the ordination plot. Two subgroups were distinguished in this group: submerged aquatic mosses *Warnstorfia fluitans* and freshly collapsed permafrost with *Polytrichum strictum*. Euclidean distances between the samples in this group confirmed the dissimilarity of their TA communities. The results of NMDS for the dataset with *Cladonia* excluded changed the positions of species and samples on the ordination plot. However, the overall relationships remained identical (Supplementary Fig. 2), but the new DWT vector explained more variables (56.77%, $p < 0.001$), which confirms the influence TA communities in *Cladonia* have on TA optima and tolerance ranges. NMDS that was run only on *Cladonia* samples showed a weaker control of the DWT on their TA assemblages, with the DWT vector explaining 44.39% of the variables ($p < 0.009$).

Full names of the abbreviations used for TA species are included in Table 1.

3.4. Transfer function development and quantitative reconstruction

The ordination analysis performed on the dataset indicated that DWT is a significant environmental variable that controls modern TA assemblages; thus, a hydrological TF can be developed. Model evaluation based on R^2, RMSEP, and average and maximum bias showed that the best-performing model was: Weighted Averaging with tolerance downweighting and classical deshrinking (WAtol.-cla) for both the entire dataset (TF_{ALL}) and the dataset with *Cladonia* excluded ($TF_{NO.CLAD}$) (Table 2, Fig. 5). This model shows good performance for both datasets, with reliable RMSEP values. TF_{ALL} produced a lower average and maximum bias, whereas $TF_{NO.CLAD}$ showed a higher R^2. Compared with the DWT gradient range of 53 cm and the DWT standard deviation of 9.7 cm (entire dataset) and 10.8 cm (dataset with *Cladonia* excluded), $RMSEP_{BOOT}$ values of 8.6 and 8.3 cm (Table 2) were good results in both cases and indicating that the model has a reliable predictive performance (Payne et al., 2012). The $RMPEP_{BOOT}$ value could be influenced by an uneven number of samples in some moisture intervals (Supplementary Fig. 3).

The selected models were applied to a core extracted from Khanymei peatland area (Kh-K2), compared with the previously published continental TFs: Asian (Qin et al., 2021) and Pan-European (Amesbury et al., 2016) (Fig. 6, Fig. 7), and considered

Table 2
Performance statistics for transfer function models for the entire dataset (TF_{ALL}) and the dataset with *Cladonia* excluded ($TF_{NO.CLAD}$) based on 1000 bootstrap cycles cross-validation methods.

Model	*N* of samples	R^2_{BOOT}	Average Bias	Maximum Bias	$RMSEP_{BOOT}$
			TF$_{ALL}$		
WA.inv	75	0.427	− 0.011	18.789	7.814
WA.cla	75	0.441	0.065	17.814	9.241
WAtol.inv	75	0.468	0.460	18.053	7.767
WAtol.cla	**75**	**0.478**	**0.708**	**13.557**	**8.628**
			TF$_{NO.CLAD}$		
WA.inv	55	0.484	0.042	19.526	8.280
WA.cla	55	0.500	0.106	20.967	9.229
WAtol.inv	55	0.590	0.735	14.815	8.017
WAtol.cla	**55**	**0.598**	**0.931**	**14.450**	**8.322**

in the further discussion of the results. The TA assemblages of the Khanymei core (with a 2–3 cm layer of fresh *Cladonia* at the top) were characterized by the dominance of *Difflugia* species (*D. lucida* type, *D. pulex* type) in the bottom half of the core (Fig. 6). An almost constant presence of *Alabasta militaris* and *Assulina muscorum* and a higher abundance of *Archerella flavum*, *Hyalosphenia papilio* and *Nebela tincta* between 16 and 24 cm depth. Species considered as dry indicators, e.g. *Trinema lineare*, *Trigonopyxis arcula* and *Corythion dubium* (in more significant numbers) started to appear in the upper 13 cm of the core.

Only one subfossil species was absent in the modern training set (*Centropyxis laevigata*), but it was present in only one sample (1% of all shells); hence, the lack of it did not affect the reconstructions. *Cyclopyxis eurystoma* and *Phryganella acropodia* were grouped as *Cyclopyxis arcelloides* type according to the taxonomic scheme applied in this study (Table 1). There were no missing analogs between paleo-records and Asian and Pan-European calibration datasets and species were aggregated based on taxonomic harmonization applied in these studies.

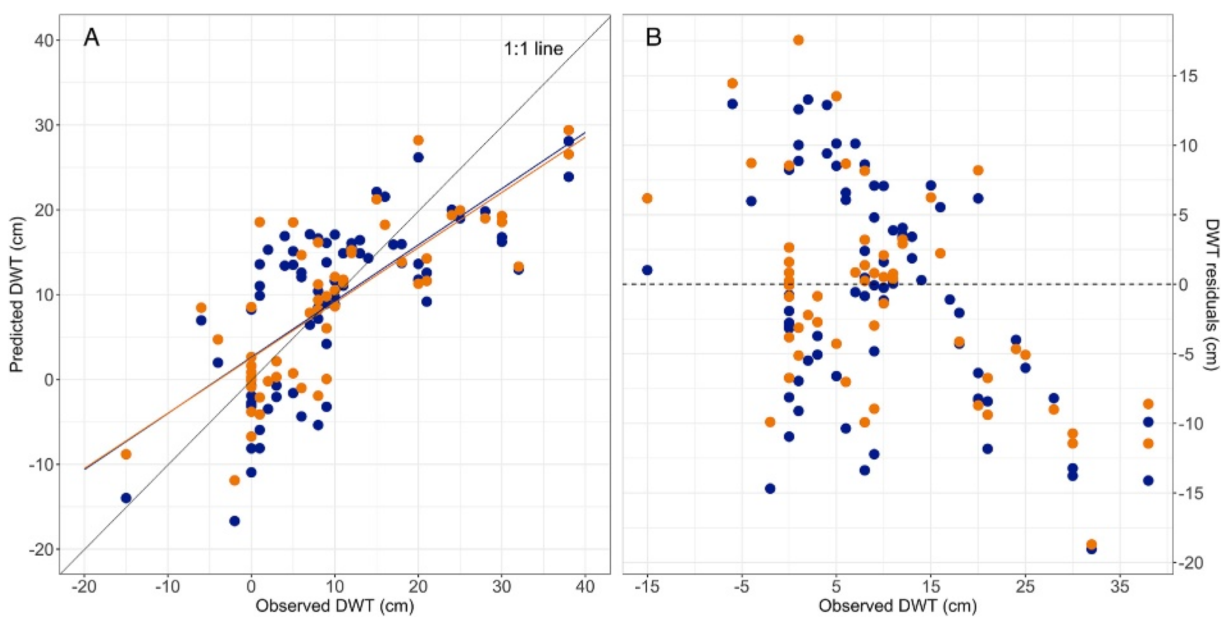

Fig. 5. Khanymei transfer function (TF) performance: a) observed and estimated (bootstrapping cross-validation) depth to water table (DWT) values from the WAtol.cla model with a linear trend of the points data and the 1:1 line for the reference, b) residual errors for each site. Dark blue circles represent the TF for the entire dataset (TF_{ALL}), and orange circles for the dataset with *Cladonia* excluded ($TF_{NO.CLAD}$).

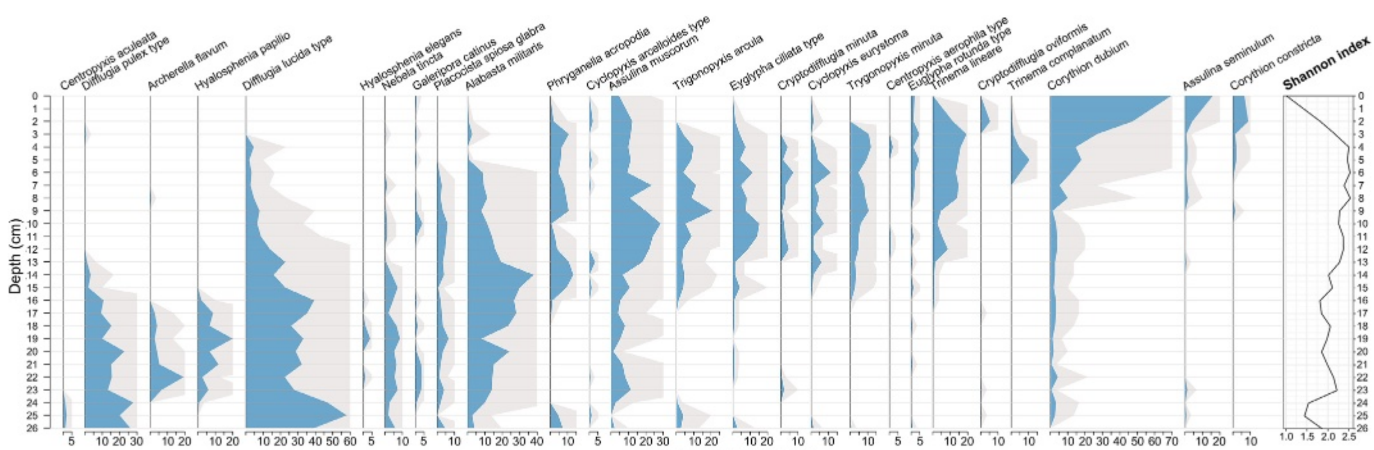

Fig. 6. Stratigraphic diagram of testate amoebae (TA) abundance with five times exaggeration in the Khanymei peat core (Kh-K2) with the Shannon's diversity index values. Species are sorted by weighted average (WA).

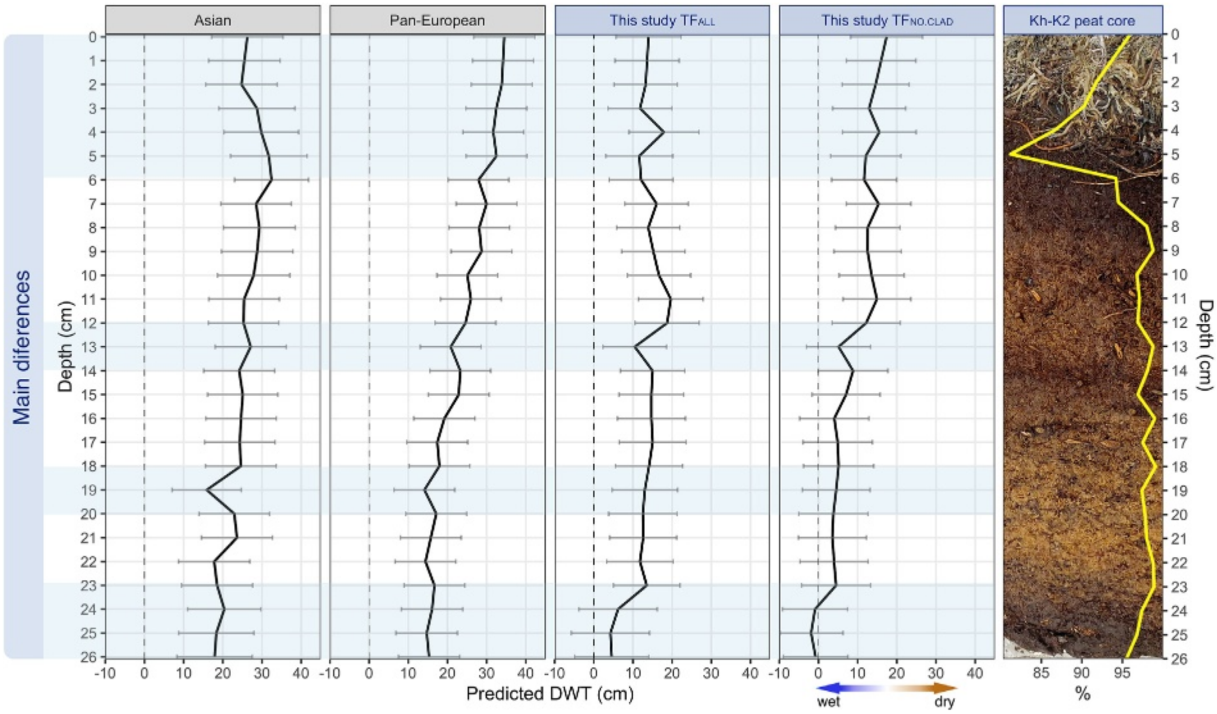

Fig. 7. Comparison of reconstructed DWT (cm) with bootstrap error bars for the Khanymei peat core (Kh-K2) from different transfer functions: Asian MAT_{BOOT} (Qin et al., 2021), Pan-European $WAtol.inv_{LOO}$ (Amesbury et al., 2016) and Khanymei $WAtol.cla_{BOOT}$ (this study) performed for the entire dataset (TF_{ALL}) and with *Cladonia* excluded ($TF_{NO.CLAD}$). Khanymei peat core (Kh-K2) photo with loss-on-ignition values (%).

Despite differences in the reconstructed values, all models showed a drying tendency from the base of the core to 12–13 cm with some fluctuations (Fig. 7). This study $TF_{NO.CLAD}$ and Pan-European TF reflected a relatively stable ~20 cm decrease in the DWT along the entire core, with the highest DWT at the top. For TF_{ALL} and Asian TF, overall changes in the DWT were more stable. In TF_{ALL} and $TF_{NO.CLAD,}$ there was a drier phase reconstructed at 23 cm related to an increase in *A. muscorum* and a decrease in *Difflugia* species and at the 13 cm wetter phase – an increase in *C. arcelloides* type was observed (Fig. 6). In the Asian model–based reconstruction, at 19 cm the wetter period was associated with an increase in the abundance of *H. papilio*. Apparent differences in the reconstructed DWT (~10 cm) at 13–23 cm depths between TF_{ALL} and $TF_{NO.CLAD}$ were due to a decrease in the DWT optima for *D. pulex* type and *D. lucida* type after removing *Cladonia* samples. These species were common in *Cladonia* samples, but mostly present in wetter microhabitats in other samples; hence, the decrease in the DWT was reconstructed with $TF_{NO.CLAD}$. From 13 cm to the top, TF_{ALL} showed the wetting trend but with some fluctuations, in the upper 6 cm of the core, $TF_{NO.CLAD}$ and Pan-European TF reconstructed further drying, Asian TF particular wetting, and TF_{ALL} stable DWT. The TF range of the reconstructed DWT values in this study was lower than those of the continental TFs due to the lower DWT gradient range in the modern training set.

The total range of DWT optima calculated for the most abundant taxa was 33 cm, ranging from −10 to 23 cm when the entire dataset was included and changed slightly when *Cladonia* was excluded (34 cm, −10 to 24 cm) (Fig. 8). *Cylindrifflugia bacillariarum*, *Difflugia globulosa*, *Difflugia bacilifera* and *Centropyxis aculeata* were associated with wet, inundated habitats, whereas *Cryptodifflugia minuta*, *Cryptodifflugia voigti*, as well as *Trigonopyxis minuta* and *T. arcula* were distinctive for drier sites. After excluding *Cladonia* samples, the DWT optima of dry and some intermediate taxa increased, and the optima of other intermediate species responded variously. In contrast, a decrease or almost no change was observed among the species inhabiting wetter microforms.

4. Discussion

4.1. Testate amoebae and environmental variables (DWT and vegetation)

The results obtained in this study confirmed the well-documented strong influence of hydrological variables (DWT) on TA communities in peatlands (e.g. Payne et al., 2006; Lamentowicz et al., 2008; Swindles et al., 2015a; Mazei et al., 2017). In general, the position of most species observed in this study along the DWT gradient was similar to those previously established in the literature (e.g. Charman et al., 2000). The wetter end of the moisture gradient was occupied by *Cylindrifflugia bacillariarum*, *Difflugia globulosa*, and *Centropyxis aculeata*, whereas *Cryptodifflugia minuta, Cryptodifflugia voigti, Trigonopyxis minuta* and *Trigonopyxis arcula* were related to drier conditions. However, some significant differences were observed, primarily in species considered as dry indicators, which was correlated with a high abundance of this species in *Cladonia* samples (Fig. 8).

In this study, several species with documented inconsistencies in their habitat preferences were identified. Taxa of the genus *Cryptodifflugia* (*C. minuta*, *C. voigti*) showed the highest DWT optima, and *Cryptodifflugia oviformis* was considered an intermediate species which contradicts the generally accepted characteristics of this species as freshwater ones (Bobrov and Mazei, 2017) (Fig. 8). However, drier preferences of *C. oviformis* have been reported by Lamentowicz and Mitchell (2005) in north-west Poland and Lamarre et al. (2013) in subarctic peatlands in Canada. Another significant difference was the DWT range of *Cyclopyxis arcelloides* type, which was found in wet sites (optima = 3.8 cm), but in previous studies, conflicting data about its preferences have been

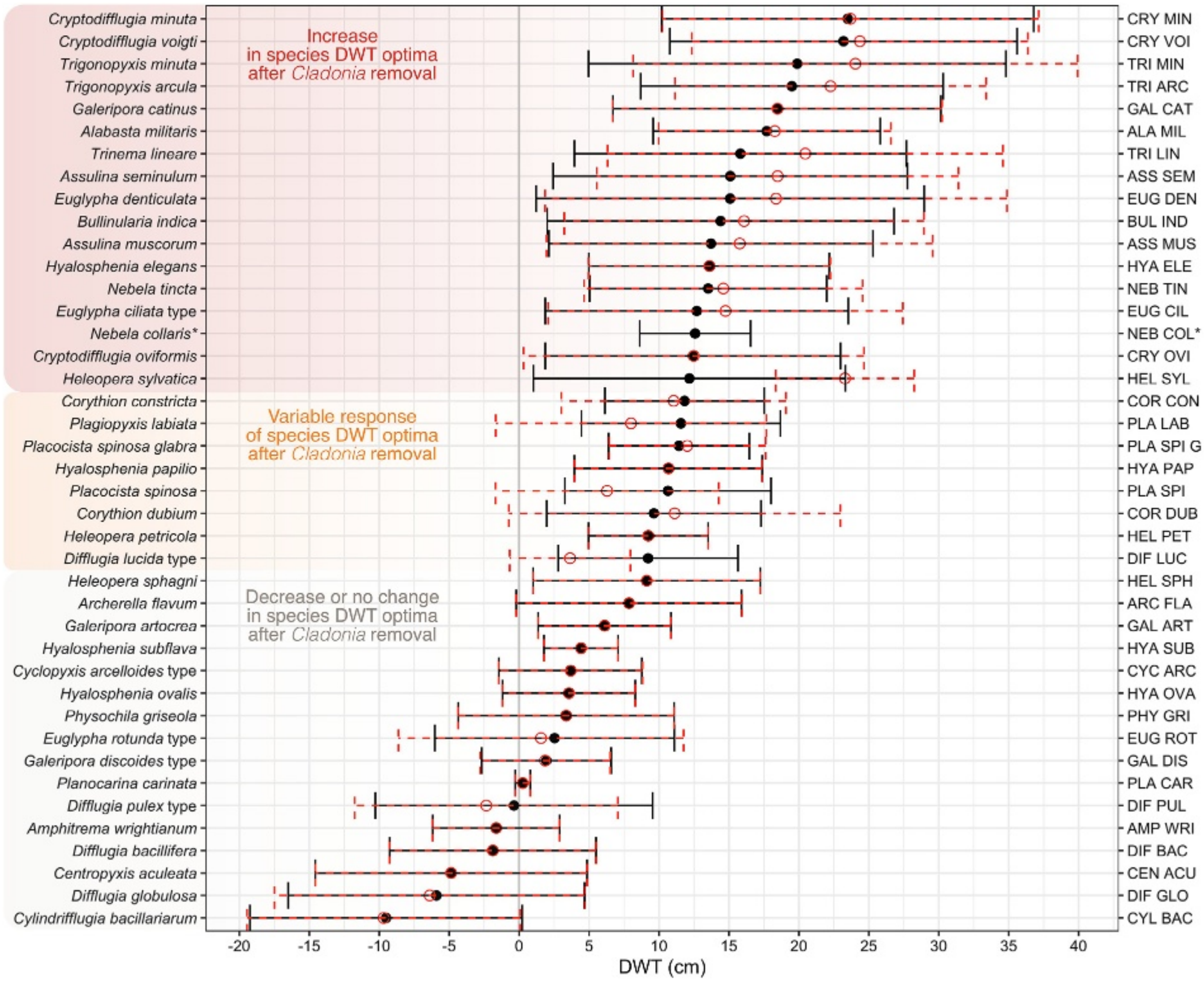

Fig. 8. Depth to water table (DWT) optima and tolerance ranges calculated using the weighted averaging model for the entire dataset (solid black lines and full circles) and the dataset with *Cladonia* excluded (red dashed lines and open circles). The graph shows groups of species based on their DWT optima response after the exclusion of *Cladonia* samples from the dataset
**Nebela collaris* was present only in *Cladonia* samples.

reported (Mitchell et al., 2008). *C. arcelloides* type is related to dry conditions in the USA and New Zealand (Wilmshurst et al., 2003; Booth, 2008), and to intermediate DWT in Sweden and the USA (Booth, 2001; Swindles et al., 2015a); however, in Poland, Switzerland, Canada and Turkey its optima are similar to those observed in this study (Warner and Charman, 1994; Mitchell et al., 1999; Lamentowicz and Mitchell, 2005; Payne et al., 2008). Disagreement often arises from treating *C. arcelloides* type as a species complex based on their morphological similarity (this study, Charman et al., 2000; Sullivan and Booth, 2011), not considering the variation in moisture preferences of the included taxa, e.g. *Phryganella acropodia* (e.g. Amesbury et al., 2013). Another species that has been differently classified by researchers and appeared in the modern and subfossil samples in this study was *Difflugia pulex* type with extremely low DWT optima (−0.3 cm). Some studies have considered this taxon as a dry or intermediate indicator (e.g. Schnitchen et al., 2003; Lamarre et al., 2013), whereas others have described it as characteristic of highly variable conditions (Sullivan and Booth, 2011). The DWT values obtained in this study defined it as more typical for wet conditions and were similar to those reported by Charman and Blundell (2007) and Payne and Mitchell (2007). An important factor that could have influenced the DWT optima in this study was the low percentage of *D. pulex* type in modern samples (0.81%). The dissimilarity between the abundance in subfossil assemblages from Khanymei (high) and the modern training set (low) could affect the TF reconstruction, and the same problem with this species has been identified by e.g. Booth (2008) and Charman and Blundell (2007). In addition, *D. pulex* type can be easily confused (Mitchell et al., 2014), and recent studies have suggested that due to its cryptic diversity, modern and subfossil individuals may belong to different taxa (Parfrey et al., 2008; Gomaa et al., 2012; Amesbury et al., 2013).

Cosmopolitan and generally associated with dry microhabitats, *Corythion dubium* (Lamentowicz and Mitchell, 2005; Lamarre et al., 2013; Koenig et al., 2018; Sim et al., 2021) was an important species in this study due to its high abundance in *Cladonia* samples (Table 1). This resulted in an increase in *C. dubium* DWT optima, placing it among intermediate species, with even lower optima than usually wetter *Hyalosphenia papilio* (Fig. 8). Lichen TA communities in Khanymei primarily consisted of dry indicators: *C. dubium*, *Assulina muscorum* and *Trinema lineare*. The same species were reported to dominate in lichens in the southern tundra of

Western Siberia (Mazei and Chernyshov, 2011), as well as in Greenland, Svalbard, and Alaska (Beyens et al., 1986; Beyens and Chardez, 1995; Pankratov et al., 2017).

Furthermore, it is worth mentioning that, as observed in the exemplary transect, the presence of *Cladonia* interrupts the common change in TA assemblages along the moisture gradient (Fig. 2). The range of *Cladonia* samples (DWT from 1 to 20 cm) and the high abundance of dry indicators (accounting for more than 50% of shells found) had an impact on species DWT optima, which was observed after the removal of *Cladonia* samples from the model (Fig. 8). Variables explained by the DWT vector confirmed that TA communities of *Cladonia* were less influenced by the DWT than TA communities in *Sphagnum* modern samples (Fig. 4). Although, the DWT is the major factor shaping the TA community structure (e.g. Payne et al., 2006; Lamentowicz et al., 2008; Swindles et al., 2015a), it is not so obvious in lichen TA communities, which tend to depend more on moisture rather than the DWT. The potential factor could be related to the low moisture content and quick wetting-drying cycles that are specific to the microhabitat of lichens (Beyens et al., 1986; Ray et al., 2020). *Cladonia* mats can easily dry out even near the water table, isolating TA communities from water and creating unique conditions for their growth.

In the literature, the influence of several other factors, not included in this study on TA communities has been confirmed, such as substrate moisture (Woodland et al., 1998; Mazei et al., 2017), pH (Payne and Mitchell, 2007; Booth, 2008), nutrient status (Tolonen et al., 1992; Lamentowicz et al., 2013), water chemistry (Mitchell et al., 2000; Carballeira and Pontevedra-Pombal, 2021), atmospheric pollution (Nguyen-Viet et al., 2004; Meyer et al., 2012), and seasonality (Sullivan and Booth, 2011; Tsyganov et al., 2012; Marcisz et al., 2014b). Vegetation type also influences the TA community similarly by shaping their environment's chemical and physical structures (Mazei et al., 2017), as confirmed by *Cladonia*.

Between peatland microforms, TA communities responded differently to hydrological changes, with assemblages of mounds and lawns being more sensitive to them (Marcisz et al., 2014a; Stastney and Black, 2020). Generally, the higher diversity of TA species in these microhabitats and the occasional co-occurrence of dry and wet species can be explained by the higher variability of moisture throughout the year (Booth, 2008; Tsyganov et al., 2012) (Fig. 3). This was also observed in this study, with higher values of the Shannon's diversity index in mounds and lawns compared with carpets and ponds. The appearance of wet species in mounds TA communities was more likely due to the ability of *Sphagnum* to retain water directly below the surface, even under temporary drought conditions rather than changes in the DWT (Woodland et al., 1998; Mazei et al., 2017). In addition, in permafrost peatlands exposure of mounds to seasonal thaw-freeze cycles may increase environmental variability, with drier conditions during freezing and wetter conditions after thawing (Lamarre et al., 2013). These two factors could explain the high diversity in samples above the permafrost in this study, but Lamarre et al. (2013) suggested this relationship needs further research. Another element influencing Shannon's index values in mounds and lawns is the nature of the flat mounds palsa in Khanymei (Fig. 1f). Due to the interspersion of microforms and the low elevation differences, there is a clear differentiation of microhabitats, which confirms the presence of different species of *Sphagnum*. The frozen peat and the surrounding thermokarst lakes influence the peat mounds, which may influence the species diversity during the thaw period.

The dynamics of thawing permafrost favors a rapid change in hydrological conditions of the peatland surface caused by permafrost collapse (Swindles et al., 2015b). Sudden shifts in the DWT produce intense stress for TA and force the exchange of species. Freshly collapsed permafrost was captured in the inundated samples. The samples from pond edges with *P. strictum* typically found in drier microhabitats (Bragazza, 2006) were characterized by the abundance of dry species (*C. dubium*, *A. muscorum*, *Assulina seminulum*) (Fig. 4). However, shifts in TA communities were more visible in higher occurrence of wet habitat species, like *Physochila griseola* (Koenig et al., 2018) and *C. arcelloides* type, as well as *Galeripora discoides* type, which is associated with rapid water table fluctuations (Lamentowicz et al., 2009). The higher species diversity in *Polytrichum strictum* samples than in *Warnstorfia fluitans* confirms their transitional character (Fig. 3, Supplementary Table 1).

4.2. Application of Khanymei transfer function

The results of this study confirmed that TA are good bioindicators of hydrological conditions in discontinuous permafrost peatlands and can be used to reconstruct past changes, which was also confirmed by previous studies conducted in the regions with present permafrost (Lamarre et al., 2013; Swindles et al., 2015a; Zhang et al., 2017; Taylor et al., 2019; Sim et al., 2021). The created TFs, for the entire dataset and with *Cladonia* excluded, was compared with two continental TFs: Pan-European (Amesbury et al., 2016) and Asian (Qin et al., 2021). Overall, the compared models reconstructed similar trajectories of DWT changes on the Khanymei core (Kh-K2). Still, the range of the modeled DWT varied between TFs (Fig. 7). A wider range of the DWT could explain it in continental training sets, which combine data from multiple locations and different types of peatlands. However, it is worth emphasizing that though drying to a certain point was reconstructed by all the models, the trajectory of changes in the most modern layers was more ambiguous, suggesting that the response pattern of Khanymei permafrost peatlands to current warming may be unstable (Zhang et al., 2022). Overall, continental TFs reconstructed changes in hydrological conditions along the Khanymei core (Kh-K2) from intermediate to dry, whereas the TFs of this study – reconstructed the same from wet to intermediate. Lower values of reconstructed DWT in this study TFs can result from sampling time at the beginning of the growing season when water level tend to be higher than in late summer (Marcisz et al., 2014b) mainly due to the seasonal thawing. However, an essential goal of the site-specific TF is to reconstruct local trends in DWT changes. This study TFs have caught these trends in contrast to continental TFs which smoothed and masked them.

Most certainly, wetter conditions reconstructed by Khanymei TF (TF_{ALL}, $TF_{NO.CLAD}$) at the bottom of the core were due to different ecological preferences of *D. pulex* type compared with other TFs. In this study it was considered a wet indicator. In contrast, in Asian (grouped as *Difflugia pristis* type) (Qin et al., 2021) and Pan-European (as *Cryptodifflugia sacculus* type) (Amesbury et al., 2016), it was considered an intermediate–dry species. As previously mentioned, poor modern analogs in the Khanymei training set could be the reason behind this, so the ecological preferences of this species in Western Siberian peatlands need further examination. Reconstructions also differ in the uppermost part of the core, where a significant decrease in the diversity and dominance of *Corythion dubium* was observed (Figs. 6 and 7). In the Pan-European TF, it belongs to *Corythion-Trinema* type and has much higher optima, whereas in the Asian TF, it is treated separately, with lower DWT optima. In this study, removal of *Cladonia* samples increased the optima of dry indicators and changed the reconstructed DWT from fluctuating to drying.

TA communities inhabiting lichens were characterized by a weaker dependence on the DWT, which led to worse performance of TF built on the entire dataset TF_{ALL} (Table 2). The statistics for the dataset with *Cladonia* excluded $TF_{NO.CLAD}$ were better, but this raises an important issue. TA communities in *Cladonia* are dominated mainly by weak idiosomic siliceous tests (WISTs), e.g. *Corythion*, *Trinema*, *Euglypha*, which are considered poorly preserved in subfossil samples and can be mostly found in the uppermost parts (Swindles et al., 2020). This raises the question of whether it is then necessary to include these data while creating the TF. However, since lichens are frequently observed in this region and they form lichen peat (Volkova et al., 2019), information on modern TA communities in *Cladonia* could be useful for a better exploration of peat archives from Western Siberia.

Hence, it can be concluded that using combined, regional, and supra-regional TFs is not always advantageous. Sometimes, meaningful information about unique local features of the environment may be lost by gaining versatility. Therefore, training sets that represent local conditions of the diverse mosaic structure of peatland ecosystems may be better suitable for such applications. In particular, this seems justified in areas where permafrost is or was present.

The Khanymei region with flat mound palsas is currently being dynamically transformed due to global warming with an increase in air temperature (Hantemirov et al., 2022) and changes in the characteristic, amount, and duration of precipitation (Bulygina et al., 2011; Morris et al., 2018). This directly induces an increase in permafrost temperature (Biskaborn et al., 2019), changes in the seasonal thaw-freeze cycle, and an increase in the active layer thickness (Romanovsky et al., 2010; Raudina et al., 2017). Thus, capturing these dynamics is crucial. The key advantage of this TA training set is its locality, which synthetically attempts to capture simultaneously various stages of permafrost degradation using space (microstructure). In addition, this study TFs captured local signals in DWT changes in the core Kh-K2 which were not visible in the compared continental TFs. Therefore, the Khanymei training set will be a valuable tool for reconstructing past climatic and hydrological changes in permafrost peatlands, especially, in tracking permafrost degradation and the response of peatlands ecosystems under anthropogenic global warming.

5. Conclusions

Permafrost creates specific hydrological conditions on peatlands and is recently under huge pressure due to global warming, especially in Siberia. Permafrost peatlands (flat mound palsas) in the Khanymei region are an ideal representation of vast Western Siberian wetlands on a microscale. The past hydrological conditions in this region are being explored and testate amoebae (TA) are a useful tool for this. Depth to water table (DWT) is an environmental variable that controls TA communities, but its influence depends on the vegetation type. TA communities in *Sphagnum* mosses are more dependent on the water table, where those in *Cladonia* are strongly shaped by hydrological conditions resulting from the properties of lichens. The results of this study confirm that TA communities in *Cladonia* influence TF performance and including them in the training set provides essential information on the environment of permafrost peatlands. Thawing permafrost causes TA shifts due to the sudden submersion of the peatland surface. The newly created TF is an effective tool for the paleo-hydrological reconstruction of peatlands in discontinuous permafrost areas. Nevertheless, research on TA in Western Siberia needs to be expanded due to the undeniably important role of these peatlands in shaping the global climate, especially in the long-term perspective.

Author contribution

All authors have made substantial contributions to a resubmission of this manuscript. AH wrote original draft and prepared revised version of the manuscript, performed testate amoebae and statistical analysis, created transfer function, and prepared all figures and tables. ML and DŁ helped in testate amoebae identification. ML helped in transfer function development and statistical analysis. MS performed plant macrofossil analysis and supervised the research. ML, DŁ and MS collected data in the field, as well as reviewed and edited the manuscript. All authors read and approved the final version of the revised manuscript and response to the reviewers.

Declaration of competing interest

The authors declare that they have no known competing financial interests or personal relationships that could have appeared to influence the work reported in this paper.

Data availability

Data will be made available on request.

Acknowledgments

This study was supported by the National Science Center in Poland, under the research projects *Pathways of permafrost thawing, fires, and decomposition processes recorded in the boreal peatlands on NW Siberia (PathThaw)*, no. 2019/35/O/ST10/02903 and *Tipping-points in boreal and permafrost peatland ecosystems of Western Siberia under the global climate crisis and increasing fire risk (PEAT-FLAMES)* no. 2021/41/B/ST10/00060. Field research at the Khanymei Research Station was possible thanks to the INTERACT project PEATHOT-Siberian peatlands as an archives of climate warming and longterm carbon dynamics, no. 730938. The authors thank Sergey Loiko, Alexandr O. Konstantinov, and Ivan Kritskov for help during the fieldwork, and Michał Brzozowski, for help in identifying liverworts.

Appendix A. Supplementary data

Supplementary data to this article can be found online at https://doi.org/10.1016/j.quascirev.2023.108067.

References

Abe-Ouchi, A., Saito, F., Kageyama, M., Braconnot, P., Harrison, S.P., Lambeck, K., Otto-Bliesner, B.L., Peltier, W.R., Tarasov, L., Peterschmitt, J.Y., Takahashi, K., 2015. Ice-sheet configuration in the CMIP5/PMIP3 last glacial maximum experiments. Geosci. Model Dev. (GMD) 8 (11), 3621–3637. https://doi.org/10.5194/gmd-8-3621-2015.

Alexandrov, G.A., Brovkin, V.A., Kleinen, T., 2016. The influence of climate on peatland extent in western Siberia since the last glacial maximum. Sci. Rep. 6 (1), 24784. https://doi.org/10.1038/srep24784.

Alexandrov, G.A., Ginzburg, V.A., Insarov, G.E., Romanovskaya, A.A., 2021. CMIP6 model projections leave no room for permafrost to persist in Western Siberia under the SSP5-8.5 scenario. Climatic Change 169 (3), 42. https://doi.org/10.1007/s10584-021-03292-w.

Amesbury, M.J., Mallon, G., Charman, D.J., Hughes, P.D.M., Booth, R.K., Daley, T.J., Garneau, M., 2013. Statistical testing of a new testate amoeba-based transfer function for water-table depth reconstruction on ombrotrophic peatlands in north-eastern Canada and Maine, United States. J. Quat. Sci. 28 (1), 27–39. https://doi.org/10.1002/jqs.2584.

Amesbury, M.J., Swindles, G.T., Bobrov, A., Charman, D.J., Holden, J., Lamentowicz, M., Mallon, G., Mazei, Y., Mitchell, E.A.D., Payne, R.J., Roland, T.P., Turner, T.E., Warner, B.G., 2016. Development of a new pan-European testate amoeba transfer function for reconstructing peatland palaeohydrology. Quat. Sci. Rev. 152, 132–151. https://doi.org/10.1016/j.quascirev.2016.09.024.

Beyens, L., Chardez, D., 1995. An annotated list of testate amoebae observed in the arctic between the longitudes 27° E and 168° W. Arch. Protistenkd. 146 (2), 219–233. https://doi.org/10.1016/S0003-9365(11)80114-4.

Beyens, L., Chardez, D., De Landtsheer, R., De Bock, P., Jacques, E., 1986. Testate amoebae populations from moss and lichen habitats in the Arctic. Polar Biol. 5 (3), 165–173. https://doi.org/10.1007/BF00441696.

Biskaborn, B.K., Smith, S.L., Noetzli, J., Matthes, H., Vieira, G., Streletskiy, D.A., Schoeneich, P., Romanovsky, V.E., Lewkowicz, A.G., Abramov, A., Allard, M., Boike, J., Cable, W.L., Christiansen, H.H., Delaloye, R., Diekmann, B., Drozdov, D., Etzelmüller, B., Grosse, G., Lantuit, H., 2019. Permafrost is warming at a global scale. Nat. Commun. 10 (1), 264. https://doi.org/10.1038/s41467-018-08240-4.

Bobrov, A., Mazei, Y.A., 2017. A review of testate amoeba genus Cryptodifflugia Penard, 1890 (Phryganellina: cryptodifflugiidae) with a key to species. Zootaxa 4282 (2), 292–308. https://doi.org/10.11646/zootaxa.4282.2.4.

Bobrov, A., Wilkinson, D.M., Qin, Y., 2015. Latitudinal diversity gradients in free-living microorganisms – hoogenraadia a key genus in testate amoebae biogeography. Acta Protozool. 54 (1), 1–8. https://doi.org/10.4467/16890027ap.15.001.2188.

Bobrov, A.A., Charman, D.J., Warner, B.G., 1999. Ecology of testate amoebae (Protozoa: rhizopoda) on peatlands in western Russia with special attention to niche separation in closely related taxa. Protist 150 (2), 125–136. https://doi.org/10.1016/S1434-4610(99)70016-7.

Booth, R.K., 2001. Ecology of testate amoebae (protozoa) in two Lake Superior coastal wetlands: implications for paleoecology and environmental monitoring. Wetlands 21 (4), 564–576. https://doi.org/10.1672/0277-5212(2001)021[0564:EOTAPI]2.0.CO.

Booth, R.K., 2002. Testate amoebae as paleoindicators of surface-moisture changes on Michigan peatlands: modern ecology and hydrological calibration. J. Paleolimnol. 28 (3), 329–348. https://doi.org/10.1023/A:1021675225099.

Booth, R.K., 2008. Testate amoebae as proxies for mean annual water-table depth in Sphagnum-dominated peatlands of North America. J. Quat. Sci. 23 (1), 43–57. https://doi.org/10.1002/jqs.1114.

Booth, R.K., Lamentowicz, M., Charman, D.J., 2010. Preparation and analysis of testate amoebae in peatland palaeoenvironmental studies. Mires Peat 7, 1–7.

Borge, A.F., Westermann, S., Solheim, I., Etzelmüller, B., 2017. Strong degradation of palsas and peat plateaus in northern Norway during the last 60 years. Cryosphere 11 (1), 1–16. https://doi.org/10.5194/tc-11-1-2017.

Bragazza, L., 2006. A decade of plant species changes on a mire in the Italian alps: vegetation-controlled or climate-driven mechanisms? Climatic Change 77 (3), 415–429. https://doi.org/10.1007/s10584-005-9034-x.

Brown, J., Ferrians Jr., O.J., Heginbottom, J.A., Melnikov, E.S., 1997. Circum-Arctic map of permafrost and ground-ice conditions. In: Circum-Pacific Map. https://doi.org/10.3133/cp45 [Report].

Bulygina, O.N., Groisman, P.Y., Razuvaev, V.N., Korshunova, N.N., 2011. Changes in snow cover characteristics over Northern Eurasia since 1966. Environ. Res. Lett. 6 (4), 045204. https://doi.org/10.1088/1748-9326/6/4/045204.

Carballeira, R., Pontevedra-Pombal, X., 2021. Diversity of testate amoebae as an indicator of the conservation status of peatlands in southwest Europe. Diversity 13 (6). https://doi.org/10.3390/d13060269.

Charman, D.J., Blundell, A., ACCROTELM, 2007. A new European testate amoebae transfer function for palaeohydrological reconstruction on ombrotrophic peatlands. J. Quat. Sci. 22 (3), 209–221. https://doi.org/10.1002/jqs.1026.

Charman, D.J., Hendon, D., Woodland, W.A., 2000. Quaternary Research Association. In: The Identification of Testate Amoebae (Protozoa: Rhizopoda) in Peats: QRA Technical Guide No. 9. https://doi.org/10.1016/j.quascirev.2004.03.008.

Clarke, K.J., 2003. Guide to the Identification of Soil Protozoa – Testate Amoebae. Freshwater Biological Association.

Daly, A.J., Baetens, J.M., De Baets, B., 2018. Ecological diversity: measuring the unmeasurable. Mathematics 6 (7), 119. https://doi.org/10.3390/math6070119.

Davydova, M.I., Rakovskaya, E.M., 1990. Phys. Geograp. USSR 2.

Feurdean, A., Diaconu, A.C., Pfeiffer, M., Gałka, M., Hutchinson, S.M., Butiseaca, G., Gorina, N., Tonkov, S., Niamir, A., Tantau, I., Zhang, H., Kirpotin, S., 2022. Holocene wildfire regimes in western Siberia: interaction between peatland moisture conditions and the composition of plant functional types. Clim. Past 18 (6), 1255–1274. https://doi.org/10.5194/cp-18-1255-2022.

Fewster, R.E., Morris, P.J., Ivanovic, R.F., Swindles, G.T., Peregon, A.M., Smith, C.J., 2022. Imminent loss of climate space for permafrost peatlands in Europe and Western Siberia. Nat. Clim. Change 12 (4), 373–379. https://doi.org/10.1038/s41558-022-01296-7.

Fiałkiewicz-Kozieł, B., Smieja-Król, B., Frontasyeva, M., Słowiński, M., Marcisz, K., Lapshina, E., Gilbert, D., Buttler, A., Jassey, V.E.J., Kaliszan, K., Laggoun-Défarge, F., Kołaczek, P., Lamentowicz, M., 2016. Anthropogenic- and natural sources of dust in peatland during the Anthropocene. Sci. Rep. 6 (1), 38731. https://doi.org/10.1038/srep38731.

Gaines, W.L., Harrod, J.R., Lehmkuhl, J.F., 1999. Monitoring Biodiversity: Quantification and Interpretation. USDA Forest Service Pacific North-West Research Station. *General Technical Report PNW-GTR-443*.

Gibson, C.M., Chasmer, L.E., Thompson, D.K., Quinton, W.L., Flannigan, M.D., Olefeldt, D., 2018. Wildfire as a major driver of recent permafrost thaw in boreal peatlands. Nat. Commun. 9 (1), 3041. https://doi.org/10.1038/s41467-018-05457-1.

Gomaa, F., Todorov, M., Heger, T.J., Mitchell, E.A.D., Lara, E., 2012. SSU rRNA phylogeny of Arcellinida (Amoebozoa) reveals that the largest arcellinid genus, Difflugia leclerc 1815, is not monophyletic. Protist 163 (3), 389–399. https://doi.org/10.1016/j.protis.2011.12.001.

González-Miguéns, R., Todorov, M., Blandenier, Q., Duckert, C., Porfirio-Sousa, A.L., Ribeiro, G.M., Ramos, D., Lahr, D.J.G., Buckley, D., Lara, E., 2022. Deconstructing Difflugia: the tangled evolution of lobose testate amoebae shells (Amoebozoa: Arcellinida) illustrates the importance of convergent evolution in protist phylogeny. Mol. Phylogenet. Evol. 175, 107557. https://doi.org/10.1016/j.ympev.2022.107557.

Groisman, P.Y., Blyakharchuk, T.A., Chernokulsky, A.V., Arzhanov, M.M., Marchesini, L.B., Bogdanova, E.G., Borzenkova, I.I., Bulygina, O.N., Karpenko, A.A., Karpenko, L.V., Knight, R.W., Khon, V.C., Korovin, G.N., Meshcherskaya, A.V., Mokhov, I.I., Parfenova, E.I., Razuvaev, V.N., Speranskaya, N.A., Tchebakova, N.M., Vygodskaya, N.N., 2013. Climate changes in Siberia. In: Groisman, P.Y., Gutman, G. (Eds.), Regional Environmental Changes in Siberia and Their Global Consequences. Springer Netherlands, pp. 57–109. https://doi.org/10.1007/978-94-007-4569-8_3.

Gudmundsson, L., Kirchner, J., Gädeke, A., Noetzli, J., Biskaborn, B.K., 2022. Attributing observed permafrost warming in the northern hemisphere to anthropogenic climate change. Environ. Res. Lett. 17 (9), 095014. https://doi.org/10.1088/1748-9326/ac8ec2.

Han, L., Menzel, L., 2022. Hydrological variability in southern Siberia and the role of permafrost degradation. J. Hydrol. 604, 127203. https://doi.org/10.1016/j.jhydrol.2021.127203.

Hantemirov, R.M., Corona, C., Guillet, S., Shiyatov, S.G., Stoffel, M., Osborn, T.J., Melvin, T.M., Gorlanova, L.A., Kukarskih, V.V., Surkov, A.Y., von Arx, G., Fonti, P., 2022. Current Siberian heating is unprecedented during the past seven millennia. Nat. Commun. 13 (1), 4968. https://doi.org/10.1038/s41467-022-32629-x.

Hendon, D., Charman, D.J., 1997. The preparation of testate amoebae (Protozoa: rhizopoda) samples from peat. Holocene 7 (2), 199–205. https://doi.org/10.1177/095968369700700207.

Hugelius, G., Loisel, J., Chadburn, S., Jackson, R.B., Jones, M., MacDonald, G., Marushchak, M., Olefeldt, D., Packalen, M., Siewert, M.B., Treat, C., Turetsky, M., Voigt, C., Yu, Z., 2020. Large stocks of peatland carbon and nitrogen are vulnerable to permafrost thaw. Proc. Natl. Acad. Sci. USA 117 (34), 20438–20446. https://doi.org/10.1073/pnas.1916387117.

IPCC, 2022. Climate change 2022: impacts, adaptation and vulnerability. In: Portner, H.-O., Roberts, D.C., Tignor, M., Poloczanska, E.S., Mintenbeck, K., Alegría, A., Craig, M., Langsdorf, S., Lochke, S., Moller, V., Okem, A., Rama, B. (Eds.), Contribution of Working Group II to the Sixth Assessment Report of the Intergovernmental Panel on Climate Change, p. 3056. https://doi.org/10.1017/9781009325844.

Jones, B.M., Baughman, C.A., Romanovsky, V.E., Parsekian, A.D., Babcock, E.L., Stephani, E., Jones, M.C., Grosse, G., Berg, E.E., 2016. Presence of rapidly degrading permafrost plateaus in south-central Alaska. Cryosphere 10 (6), 2673–2692. https://doi.org/10.5194/tc-10-2673-2016.

Juggins, S., 2007. C2 Version 1.5. Software for Ecological and Palaeoecological Data Analysis and Visualisation. https://www.staff.ncl.ac.uk/stephen.juggins/software.htm.

Juggins, S., 2020. Rioja: Analysis of Quaternary Science Data, R Package Version 0.9, 26. https://cran.r-project.org/package=rioja.

Karlsson, J.M., Lyon, S.W., Destouni, G., 2012. Thermokarst lake, hydrological flow and water balance indicators of permafrost change in Western Siberia. J. Hydrol. 464–465, 459–466. https://doi.org/10.1016/j.jhydrol.2012.07.037.

Kirpotin, S., Polishchuk, Y., Bryksina, N., Sugaipova, A., Kouraev, A., Zakharova, E., Pokrovsky, O.S., Shirokova, L., Kolmakova, M., Manassypov, R., Dupre, B., 2011. West Siberian palsa peatlands: distribution, typology, cyclic development, present day climate-driven changes, seasonal hydrology and impact on CO2 cycle. Int. J. Environ. Stud. 68 (5), 603–623. https://doi.org/10.1080/00207233.2011.593901.

Kirpotin, S.N., Berezin, A., Bazanov, V., Polishchuk, Y., Vorobiov, S., Mironycheva-Tokoreva, N., Kosykh, N., Volkova, I., Dupre, B., Pokrovsky, O., Kouraev, A., Zakharova, E., Shirokova, L., Mognard, N., Biancamaria, S., Viers, J., Kolmakova, M., 2009. Western Siberia wetlands as indicator and regulator of climate change on the global scale. Int. J. Environ. Stud. 66 (4), 409–421. https://doi.org/10.1080/00207230902753056.

Kluge, M., Wauthy, M., Clemmensen, K.E., Wurzbacher, C., Hawkes, J.A., Einarsdottir, K., Rautio, M., Stenlid, J., Peura, S., 2021. Declining fungal diversity in Arctic freshwaters along a permafrost thaw gradient. Global Change Biol. 27 (22), 5889–5906. https://doi.org/10.1111/gcb.15852.

Koenig, I., Mulot, M., Mitchell, E.A.D., 2018. Taxonomic and functional traits responses of Sphagnum peatland testate amoebae to experimentally manipulated water table. Ecol. Indicat. 85, 342–351. https://doi.org/10.1016/j.ecolind.2017.10.017.

Kondratjeva, K.A., Khrutzky, S.F., Romanovsky, N.N., 1993. Changes in the extent of permafrost during the late quaternary period in the territory of the former Soviet Union. Permafr. Periglac. Process. 4 (2), 113–119. https://doi.org/10.1002/ppp.3430040204.

Könönen, O.H., Karjalainen, O., Aalto, J., Luoto, M., Hjort, J., 2022. Environmental spaces for palsas and peat plateaus are disappearing at a circumpolar scale. Cryosphere Discuss. 2022, 1–37. https://doi.org/10.5194/tc-2022-135.

Kremenetski, K.V., Velichko, A.A., Borisova, O.K., MacDonald, G.M., Smith, L.C., Frey, K.E., Orlova, L.A., 2003. Peatlands of the Western Siberian lowlands: current knowledge on zonation, carbon content and Late Quaternary history. Quat. Sci. Rev. 22 (5), 703–723. https://doi.org/10.1016/S0277-3791(02)00196-8.

Lamarre, A., Magnan, G., Garneau, M., Boucher, É., 2013. A testate amoeba-based transfer function for paleohydrological reconstruction from boreal and subarctic peatlands in northeastern Canada. Quat. Int. 306, 88–96. https://doi.org/10.1016/j.quaint.2013.05.054.

Lamentowicz, Ł., Lamentowicz, M., Gąbka, M., 2008. Testate amoebae ecology and a local transfer function from a peatland in western Poland. Wetlands 28 (1), 164–175. https://doi.org/10.1672/07-92.1.

Lamentowicz, M., Bragazza, L., Buttler, A., Jassey, V.E.J., Mitchell, E.A.D., 2013.

Seasonal patterns of testate amoeba diversity, community structure and species—environment relationships in four Sphagnum-dominated peatlands along a 1300 m altitudinal gradient in Switzerland. Soil Biol. Biochem. 67, 1—11. https://doi.org/10.1016/j.soilbio.2013.08.002.
Lamentowicz, M., Milecka, K., Gałka, M., Cedro, A., Pawlyta, J., Piotrowska, N., Lamentowicz, Ł., Van Der Knaap, W.O., 2009. Climate and human induced hydrological change since AD 800 in an ombrotrophic mire in Pomerania (N Poland) tracked by testate amoebae, macro-fossils, pollen and tree rings of pine. Boreas 38 (2), 214—229. https://doi.org/10.1111/j.1502-3885.2008.00047.x.
Lamentowicz, M., Mitchell, E.A.D., 2005. The ecology of testate amoebae (protists) in Sphagnum in northNorth-western Poland in relation to peatland ecology. Microb. Ecol. 50 (1), 48—63. https://doi.org/10.1007/s00248-004-0105-8.
Lamentowicz, M., Słowiński, M., Marcisz, K., Zielińska, M., Kaliszan, K., Lapshina, E., Gilbert, D., Buttler, A., Fiałkiewicz-Kozieł, B., Jassey, V.E.J., Laggoun-Defarge, F., Kołaczek, P., 2015. Hydrological dynamics and fire history of the last 1300 years in western Siberia reconstructed from a high-resolution, ombrotrophic peat archive. Quat. Res. 84 (3), 312—325. https://doi.org/10.1016/j.yqres.2015.09.002.
Lawrence, D.M., Swenson, S.C., 2011. Permafrost response to increasing Arctic shrub abundance depends on the relative influence of shrubs on local soil cooling versus large-scale climate warming. Environ. Res. Lett. 6 (4), 045504. https://doi.org/10.1088/1748-9326/6/4/045504.
Legendre, P., Gallagher, E.D., 2001. Ecologically meaningful transformations for ordination of species data. Oecologia 129 (2), 271—280. https://doi.org/10.1007/s004420100716.
Lim, A., Loiko, S.V., Kritckov, I.V., Kuzmina, D.M., 2017. Structural-functional features of landscapes with active thermocarst in the northern taiga of Western Siberia. Ukrainian J. Ecol. 7, 414—423.
Magnan, G., Sanderson, N.K., Piilo, S., Pratte, S., Väliranta, M., van Bellen, S., Zhang, H., Garneau, M., 2022. Widespread recent ecosystem state shifts in high-latitude peatlands of northeastern Canada and implications for carbon sequestration. Global Change Biol. 28 (5), 1919—1934. https://doi.org/10.1111/gcb.16032.
Marcisz, K., Fournier, B., Gilbert, D., Lamentowicz, M., Mitchell, E.A.D., 2014a. Response of Sphagnum peatland testate amoebae to a 1-year transplantation experiment along an artificial hydrological gradient. Microb. Ecol. 67 (4), 810—818. https://doi.org/10.1007/s00248-014-0367-8.
Marcisz, K., Lamentowicz, Ł., Słowińska, S., Słowiński, M., Muszak, W., Lamentowicz, M., 2014b. Seasonal changes in Sphagnum peatland testate amoeba communities along a hydrological gradient. Eur. J. Protistol. 50 (5), 445—455. https://doi.org/10.1016/j.ejop.2014.07.001.
Marsh, P., Russell, M., Pohl, S., Haywood, H., Onclin, C., 2009. Changes in thaw lake drainage in the Western Canadian Arctic from 1950 to 2000. Hydrol. Process. 23 (1), 145—158. https://doi.org/10.1002/hyp.7179.
Mazei, Y.A., Chernyshov, V., Bukhkalo, S., Mazei, N., Creevy, A.L., Payne, R.J., 2017. Exploring the diversity and ecology of testate amoebae in West Siberian peatlands. Acta Protozool. 56 (1), 59—70. https://doi.org/10.4467/16890027ap.17.005.6969.
Mazei, Y.A., Chernyshov, V.A., 2011. Testate amoebae communities in the southern tundra and forest-tundra of Western Siberia. Biol. Bull. 38 (8), 789—796. https://doi.org/10.1134/S1062359011080036.
Mazei, Y.A., Tsyganov, A.N., 2006. Freshwater Testate Amoebae. KMK Scientific press.
Meredith, M., Sommerkorn, M., Cassotta, S., Derksen, C., Ekaykin, A., Hollowed, A., Kofinas, G., Mackintosh, A., Melbourne-Thomas, J., Muelbert, M.M.C., Ottersen, G., Pritchard, H., Schuur, E.A.G., 2019. Polar regions. In: Portner, H.-O., Roberts, D.C., Masson-Delmotte, V., Zhai, P., Tignor, M., Poloczanska, E., Mintenbeck, K., Alegría, A., Nicolai, M., Okem, A., Petzold, J., Rama, B., Weyer, N.M. (Eds.), IPCC Special Report on the Ocean and Cryosphere in a Changing Climate. Cambridge University Press, pp. 203—320. https://doi.org/10.1017/9781009157964.005.
Meyer, C., Gilbert, D., Gillet, F., Moskura, M., Franchi, M., Bernard, N., 2012. Using "bryophytes and their associated testate amoeba" microsystems as indicators of atmospheric pollution. Ecol. Indicat. 13 (1), 144—151. https://doi.org/10.1016/j.ecolind.2011.05.020.
Mitchell, E.A.D., Buttler, A., Grosvernier, P., Rydin, H., Albinsson, C., Greenup, A.L., Heijmans, M.M.P.D., Hoosbeek, M.R., Saarinen, T., 2000. Relationships among testate amoebae (Protozoa), vegetation and water chemistry in five Sphagnum-dominated peatlands in Europe. New Phytol. 145 (1), 95—106. https://doi.org/10.1046/j.1469-8137.2000.00550.x.
Mitchell, E.A.D., Buttler, A.J., Warner, B.G., Gobat, J.-M., 1999. Ecology of testate amoebae (Protozoa: rhizopoda) in Sphagnum peatlands in the Jura mountains, Switzerland and France. Ecoscience 6 (4), 565—576. https://doi.org/10.1080/11956860.1999.11682555.
Mitchell, E.A.D., Charman, D.J., Warner, B.G., 2008. Testate amoebae analysis in ecological and paleoecological studies of wetlands: past, present and future. Biodivers. Conserv. 17 (9), 2115—2137. https://doi.org/10.1007/s10531-007-9221-3.
Mitchell, E.A.D., Lamentowicz, M., Payne, R.J., Mazei, Y., 2014. Effect of taxonomic resolution on ecological and palaeoecological inference — a test using testate amoeba water table depth transfer functions. Quat. Sci. Rev. 91, 62—69. https://doi.org/10.1016/j.quascirev.2014.03.006.
Morris, P.J., Swindles, G.T., Valdes, P.J., Ivanovic, R.F., Gregoire, L.J., Smith, M.W., Tarasov, L., Haywood, A.M., Bacon, K.L., 2018. Global peatland initiation driven by regionally asynchronous warming. Proc. Natl. Acad. Sci. USA 115 (19), 4851—4856. https://doi.org/10.1073/pnas.1717838115.
Myers-Smith, I.H., Hik, D.S., 2013. Shrub canopies influence soil temperatures but not nutrient dynamics: an experimental test of tundra snow—shrub interactions. Ecol. Evol. 3 (11), 3683—3700. https://doi.org/10.1002/ece3.710.
Nguyen-Viet, H., Gilbert, D., Bernard, N., Mitchell, E., Badot, P.-M., 2004. Relationship between atmospheric pollution characterized by NO2 concentrations and testate amoebae density and diversity. Acta Protozool. 43 (3), 233—239. https://hal.inrae.fr/hal-02675671.
Oksanen, J., Simpson, G., Blanchet, F., Kindt, R., Legendre, P., Minchin, P., O'Hara, R., Solymos, P., Stevens, M., Szoecs, E., Wagner, H., Barbour, M., Bedward, M., Bolker, B., Borcard, D., Carvalho, G., Chirico, M., De Caceres, M., Durand, S., Weedon, J., 2022. vegan: Community Ecology Package. R package version 2.6-2. https://CRAN.R-project.org/package=vegan.
Olefeldt, D., Heffernan, L., Jones, M.C., Sannel, A.B.K., Treat, C.C., Turetsky, M.R., 2021. Permafrost thaw in northern peatlands: rapid changes in ecosystem and landscape functions. In: Canadell, J.G., Jackson, R.B. (Eds.), Ecosystem Collapse and Climate Change. Springer International Publishing, pp. 27—67. https://doi.org/10.1007/978-3-030-71330-0_3.
Pankratov, T.A., Kachalkin, A.V., Korchikov, E.S., Dobrovol'skaya, T.G., 2017. Microbial communities of lichens. Microbiology 86 (3), 293—309. https://doi.org/10.1134/S0026261717030134.
Parfrey, L.W., Lahr, D.J., Katz, L.A., 2008. The dynamic nature of eukaryotic genomes. Mol. Biol. Evol. 25 (4), 787—794. https://doi.org/10.1093/molbev/msn032.
Payne, R.J., Charman, D.J., Matthews, S.M., Eastwood, W.J., 2008. Testate amoebae as palaeohydrological proxies in Sürmene Ağaçbaşi Yaylasi peatland (northeast Turkey). Wetlands 28 (2), 311—323. https://doi.org/10.1672/07-42.1.
Payne, R.J., Kishaba, K., Blackford, J.J., Mitchell, E.A.D., 2006. Ecology of testate amoebae (Protista) in south-central Alaska peatlands: building transfer-function models for palaeoenvironmental studies. Holocene 16 (3), 403—414. https://doi.org/10.1191/0959683606hl936rp.
Payne, R.J., Mitchell, E.A.D., 2007. Ecology of testate amoebae from mires in the central rhodope mountains, Greece and development of a transfer function for palaeohydrological reconstruction. Protist 158 (2), 159—171. https://doi.org/10.1016/j.protis.2006.11.003.
Payne, R.J., Telford, R.J., Blackford, J.J., Blundell, A., Booth, R.K., Charman, D.J., Lamentowicz, Ł., Lamentowicz, M., Mitchell, E.A.D., Potts, G., Swindles, G.T., Warner, B.G., Woodland, W., 2012. Testing peatland testate amoeba transfer functions: appropriate methods for clustered training-sets. Holocene 22 (7), 819—825. https://doi.org/10.1177/0959683611430412.
Peel, M.C., Finlayson, B.L., McMahon, T.A., 2007. Updated world map of the Köppen-Geiger climate classification. Hydrol. Earth Syst. Sci. 11 (5), 1633—1644. https://doi.org/10.5194/hess-11-1633-2007.
Perrier, L., Garneau, M., Pratte, S., Sanderson, N.K., 2022. Climate-driven Holocene ecohydrological and carbon dynamics from maritime peatlands of the Gulf of St. Lawrence, eastern Canada. Holocene 32 (8), 749—763. https://doi.org/10.1177/09596836221095978.
Qin, Y., Li, H., Mazei, Y., Kurina, I., Swindles, G.T., Bobrov, A., Tsyganov, A.N., Gu, Y., Huang, X., Xue, J., Lamentowicz, M., Marcisz, K., Roland, T., Payne, R.J., Mitchell, E.A.D., Xie, S., 2021. Developing a continental-scale testate amoeba hydrological transfer function for Asian peatlands. Quat. Sci. Rev. 258, 106868. https://doi.org/10.1016/j.quascirev.2021.106868.
Qin, Y., Mitchell, E.A.D., Lamentowicz, M., Payne, R.J., Lara, E., Gu, Y., Huang, X., Wang, H., 2013. Ecology of testate amoebae in peatlands of central China and development of a transfer function for paleohydrological reconstruction. J. Paleolimnol. 50 (3), 319—330. https://doi.org/10.1007/s10933-013-9726-6.
Quinton, W.L., Baltzer, J.L., 2013. The active-layer hydrology of a peat plateau with thawing permafrost (Scotty Creek, Canada). Hydrogeol. J. 21 (1), 201—220. https://doi.org/10.1007/s10040-012-0935-2.
R Core Team, 2022. R: a language and environment for statistical computing. In: R Foundation for Statistical Computing. http://www.R-project.org/.
Rakhleeva, A.A., 2002. Testaceans (testacea, Protozoa) of taiga soils in western Siberia (surgut polesye). Biol. Bull. Russian Acad. Sci. 29 (6), 618—627. https://doi.org/10.1023/A:1021784429342.
Raudina, T.V., Loiko, S.V., Lim, A.G., Krickov, I.V., Shirokova, L.S., Istigechev, G.I., Kuzmina, D.M., Kulizhsky, S.P., Vorobyev, S.N., Pokrovsky, O.S., 2017. Dissolved organic carbon and major and trace elements in peat porewater of sporadic, discontinuous, and continuous permafrost zones of western Siberia. Biogeosciences 14 (14), 3561—3584. https://doi.org/10.5194/bg-14-3561-2017.
Ray, D.G., Cahalan, G.D., Lendemer, J.C., 2020. Factors influencing the persistence of reindeer lichens (Cladonia subgenus Cladina) within frequent-fire environments of the Mid-Atlantic Coastal Plain, USA. Fire Ecol. 16 (1), 1. https://doi.org/10.1186/s42408-019-0063-7.
Ricotta, C., Podani, J., 2017. On some properties of the Bray-Curtis dissimilarity and their ecological meaning. Ecol. Complex. 31, 201—205. https://doi.org/10.1016/j.ecocom.2017.07.003.
Romanovsky, V.E., Drozdov, D.S., Oberman, N.G., Malkova, G.V., Kholodov, A.L., Marchenko, S.S., Moskalenko, N.G., Sergeev, D.O., Ukraintseva, N.G., Abramov, A.A., Gilichinsky, D.A., Vasiliev, A.A., 2010. Thermal state of permafrost in Russia. Permafr. Periglac. Process. 21 (2), 136—155. https://doi.org/10.1002/ppp.683.
Rydin, H., Jeglum, J.K., 2013. Peatland habitats. In: Rydin, H., Jeglum, J.K. (Eds.), The Biology of Peatlands. Oxford University Press, pp. 1—20. https://doi.org/10.1093/acprof:osobl/9780199602995.003.0001.
Safronova, I., Yurkovsksya, T., 2019. The latitudinal distribution of vegetation cover in Siberia. BIO Web Conf 16, 00047. https://doi.org/10.1051/bioconf/20191600047.

Sannel, A.B.K., Kuhry, P., 2011. Warming-induced destabilization of peat plateau/thermokarst lake complexes. J. Geophys. Res.: Biogeosciences 116 (G3). https://doi.org/10.1029/2010JG001635.
Schuur, E.A.G., McGuire, A.D., Schädel, C., Grosse, G., Harden, J.W., Hayes, D.J., Hugelius, G., Koven, C.D., Kuhry, P., Lawrence, D.M., Natali, S.M., Olefeldt, D., Romanovsky, V.E., Schaefer, K., Turetsky, M.R., Treat, C.C., Vonk, J.E., 2015. Climate change and the permafrost carbon feedback. Nature 520 (7546), 171–179. https://doi.org/10.1038/nature14338.
Schnitchen, C., Magyari, E., Tóthmérész, B., Grigorszky, I., Braun, M., 2003. Micropaleontological observations on a Sphagnum bog in East Carpathian region – testate amoebae (Rhizopoda: testacea) and their potential use for reconstruction of micro- and macroclimatic changes. Hydrobiologia 506 (1), 45–49. https://doi.org/10.1023/B:HYDR.0000008553.82554.c2.
Seneviratne, S.I., Zhang, X., Adnan, M., Badi, W., Dereczynski, C., Di Luca, A., Ghosh, S., Iskandar, I., Kossin, J., Lewis, S., Otto, F., Pinto, I., Satoh, M., Vicente-Serrano, S.M., Wehner, M., Zhou, B., 2021. Weather and climate extreme events in a changing climate. In: Pörtner, H.-O., Roberts, D.C., Tignor, M., Poloczanska, E.S., Mintenbeck, K., Alegría, A., Craig, M., Langsdorf, S., Löschke, S., Möller, V., Okem, A., R, B. (Eds.), Climate Change 2021: the Physical Science Basis. Contribution of Working Group I to the Sixth Assessment Report of the Intergovernmental Panel on Climate Change. Cambridge University Press, pp. 1513–1766. https://doi.org/10.1017/9781009157896.013.
Shiklomanov, N.I., 2005. From exploration to systematic investigation: development of geocryology in 19th- and early—20th-century Russia. Phys. Geogr. 26 (4), 249–263. https://doi.org/10.2747/0272-3646.26.4.249.
Shur, Y.L., Jorgenson, M.T., 2007. Patterns of permafrost formation and degradation in relation to climate and ecosystems. Permafr. Periglac. Process. 18 (1), 7–19. https://doi.org/10.1002/ppp.582.
Siemensma, F.J., 2022. Microworld, World of Amoeboid Organisms. World-wide electronic publication. https://arcella.
Sim, T.G., Swindles, G.T., Morris, P.J., Baird, A.J., Charman, D.J., Amesbury, M.J., Beilman, D., Channon, A., Gallego-Sala, A.V., 2021. Ecology of peatland testate amoebae in Svalbard and the development of transfer functions for reconstructing past water-table depth and pH. Ecol. Indicat. 131, 108122. https://doi.org/10.1016/j.ecolind.2021.108122.
Stastney, P., Black, S., 2020. Bog microtopography and the climatic sensitivity of testate amoeba communities: implications for transfer function-based paleo-water table reconstructions. Microb. Ecol. 80 (2), 309–321. https://doi.org/10.1007/s00248-020-01499-5.
Sullivan, M.E., Booth, R.K., 2011. The potential influence of short-term environmental variability on the composition of testate amoeba communities in Sphagnum peatlands. Microb. Ecol. 62 (1), 80–93. https://doi.org/10.1007/s00248-011-9875-y.
Swindles, G.T., Amesbury, M.J., Turner, T.E., Carrivick, J.L., Woulds, C., Raby, C., Mullan, D., Roland, T.P., Galloway, J.M., Parry, L., Kokfelt, U., Garneau, M., Charman, D.J., Holden, J., 2015a. Evaluating the use of testate amoebae for palaeohydrological reconstruction in permafrost peatlands. Palaeogeogr. Palaeoclimatol. Palaeoecol. 424, 111–122. https://doi.org/10.1016/j.palaeo.2015.02.004.
Swindles, G.T., Morris, P.J., Mullan, D., Watson, E.J., Turner, T.E., Roland, T.P., Amesbury, M.J., Kokfelt, U., Schoning, K., Pratte, S., Gallego-Sala, A., Charman, D.J., Sanderson, N., Garneau, M., Carrivick, J.L., Woulds, C., Holden, J., Parry, L., Galloway, J.M., 2015b. The long-term fate of permafrost peatlands under rapid climate warming. Sci. Rep. 5 (1), 17951. https://doi.org/10.1038/srep17951.
Swindles, G.T., Reczuga, M., Lamentowicz, M., Raby, C.L., Turner, T.E., Charman, D.J., Gallego-Sala, A., Valderrama, E., Williams, C., Draper, F., Honorio Coronado, E.N., Roucoux, K.H., Baker, T., Mullan, D.J., 2014. Ecology of testate amoebae in an amazonian peatland and development of a transfer function for palaeohydrological reconstruction. Microb. Ecol. 68 (2), 284–298. https://doi.org/10.1007/s00248-014-0378-5.
Swindles, G.T., Roland, T.P., Amesbury, M.J., Lamentowicz, M., McKeown, M.M., Sim, T.G., Fewster, R.E., Mitchell, E.A.D., 2020. Quantifying the effect of testate amoeba decomposition on peat-based water-table reconstructions. Eur. J. Protistol. 74, 125693. https://doi.org/10.1016/j.ejop.2020.125693.
Taylor, L.S., Swindles, G.T., Morris, P.J., Gałka, M., 2019. Ecology of peatland testate amoebae in the Alaskan continuous permafrost zone. Ecol. Indicat. 96, 153–162. https://doi.org/10.1016/j.ecolind.2018.08.049.
Tchebakova, N.M., Parfenova, E., Soja, A.J., 2009. The effects of climate, permafrost and fire on vegetation change in Siberia in a changing climate. Environ. Res. Lett. 4 (4), 045013. https://doi.org/10.1088/1748-9326/4/4/045013.
Todorov, M., Bankov, N., 2019. An Atlas of Sphagnum-Dwelling Testate Amoebae in Bulgaria, 1 ed. Pensoft Publishers. https://doi.org/10.3897/ab.e38685.
Tolonen, K., Warner, B.G., Vasander, H., 1992. Ecology of testaceans (Protozoa: rhizopoda) in mires in southern Finland: I. Autecology. Arch. Protistenkd. 142 (3), 119–138. https://doi.org/10.1016/S0003-9365(11)80076-X.
Treat, C.C., Jones, M.C., 2018. Near-surface permafrost aggradation in Northern Hemisphere peatlands shows regional and global trends during the past 6000 years. Holocene 28 (6), 998–1010. https://doi.org/10.1177/0959683617752858.
Trofimova, I.E., Balybina, A.S., 2014. Classification of climates and climatic regionalization of the West-Siberian plain. Geogr. Nat. Resour. 35 (2), 114–122. https://doi.org/10.1134/S1875372814020024.
Tsyganov, A.N., Aerts, R., Nijs, I., Cornelissen, J.H.C., Beyens, L., 2012. Sphagnum-dwelling testate amoebae in subarctic bogs are more sensitive to soil warming in the growing season than in winter: the results of eight-year field climate manipulations. Protist 163 (3), 400–414. https://doi.org/10.1016/j.protis.2011.07.005.
Tsyganov, A.N., Babeshko, K.V., Mazei, Y.A., 2016. A Guide to Testate Amoebae with the Keys to Genera. Pub. House PSU.
Turetsky, M.R., Abbott, B.W., Jones, M.C., Walter Anthony, K., Olefeldt, D., Schuur, E.A.G., Koven, C., McGuire, A.D., Grosse, G., Kuhry, P., Hugelius, G., Lawrence, D.M., Gibson, C., Sannel, A.B.K., 2019. Permafrost collapse is accelerating carbon release. Nature 569 (7754), 32–34. https://doi.org/10.1038/d41586-019-01313-4.
Turetsky, M.R., Wieder, R.K., Vitt, D.H., Evans, R.J., Scott, K.D., 2007. The disappearance of relict permafrost in boreal north America: effects on peatland carbon storage and fluxes. Global Change Biol. 13 (9), 1922–1934. https://doi.org/10.1111/j.1365-2486.2007.01381.x.
Van Bellen, S., Mauquoy, D., Payne, R.J., Roland, T.P., Daley, T.J., Hughes, P.D.M., Loader, N.J., Street-Perrott, F.A., Rice, E.M., Pancotto, V.A., 2014. Testate amoebae as a proxy for reconstructing Holocene water table dynamics in southern Patagonian peat bogs. J. Quat. Sci. 29 (5), 463–474. https://doi.org/10.1002/jqs.2719.
van der Kolk, H.J., Heijmans, M.M.P.D., van Huissteden, J., Pullens, J.W.M., Berendse, F., 2016. Potential Arctic tundra vegetation shifts in response to changing temperature, precipitation and permafrost thaw. Biogeosciences 13 (22), 6229–6245. https://doi.org/10.5194/bg-13-6229-2016.
Velichko, A.A., Timireva, S.N., Kremenetski, K.V., MacDonald, G.M., Smith, L.C., 2011. West Siberian Plain as a late glacial desert. Quat. Int. 237 (1), 45–53. https://doi.org/10.1016/j.quaint.2011.01.013.
Vincent, W.F., Lemay, M., Allard, M., 2017. Arctic permafrost landscapes in transition: towards an integrated Earth system approach. Arctic Sci. 3 (2), 39–64. https://doi.org/10.1139/as-2016-0027.
Voigt, C., Marushchak, M.E., Mastepanov, M., Lamprecht, R.E., Christensen, T.R., Dorodnikov, M., Jackowicz-Korczyński, M., Lindgren, A., Lohila, A., Nykänen, H., Oinonen, M., Oksanen, T., Palonen, V., Treat, C.C., Martikainen, P.J., Biasi, C., 2019. Ecosystem carbon response of an Arctic peatland to simulated permafrost thaw. Global Change Biol. 25 (5), 1746–1764. https://doi.org/10.1111/gcb.14574.
Volkova, I.I., Kolesnichenko, L.G., Kirpotin, S.N., Pokrovsky, O.S., Vorobyev, S.N., 2019. Peat deposits and peat-forming plants in the mires of the West Siberian northern taiga (based on studies of the Khanymei site). IOP Conf. Ser. Earth Environ. Sci. 232, 012018. https://doi.org/10.1088/1755-1315/232/1/012018.
Warner, B.G., Charman, D.J., 1994. Holocene changes on a peatland in northwestern Ontario interpreted from testate amoebae (Protozoa) analysis. Boreas 23 (3), 270–279. https://doi.org/10.1111/j.1502-3885.1994.tb00949.x.
Wickham, H., Chang, W., Wickham, M.H., 2016. Package 'ggplot2.' *Create Elegant Data Visualisations Using the Grammar of Graphics, version 2.1.1.* Springer-Verlag New York.
Wilmshurst, J.M., Wiser, S.K., Charman, D.J., 2003. Reconstructing Holocene water tables in New Zealand using testate amoebae: differential preservation of tests and implications for the use of transfer functions. Holocene 13 (1), 61–72. https://doi.org/10.1191/0959683603hl595rp.
Woodland, W.A., Charman, D.J., Sims, P.C., 1998. Quantitative estimates of water tables and soil moisture in Holocene peatlands from testate amoebae. Holocene 8 (3), 261–273. https://doi.org/10.1191/095968398667004497.
Zhang, H., Amesbury, M.J., Ronkainen, T., Charman, D.J., Gallego-Sala, A.V., Väliranta, M., 2017. Testate amoeba as palaeohydrological indicators in the permafrost peatlands of north-east European Russia and Finnish Lapland. J. Quat. Sci. 32 (7), 976–988. https://doi.org/10.1002/jqs.2970.
Zhang, H., Piilo, S.R., Amesbury, M.J., Charman, D.J., Gallego-Sala, A.V., Väliranta, M.M., 2018. The role of climate change in regulating Arctic permafrost peatland hydrological and vegetation change over the last millennium. Quat. Sci. Rev. 182, 121–130. https://doi.org/10.1016/j.quascirev.2018.01.003.
Zhang, H., Väliranta, M., Swindles, G.T., Aquino-López, M.A., Mullan, D., Tan, N., Amesbury, M., Babeshko, K.V., Bao, K., Bobrov, A., Chernyshov, V., Davies, M.A., Diaconu, A.-C., Feurdean, A., Finkelstein, S.A., Garneau, M., Guo, Z., Jones, M.C., Kay, M., …, Zhao, Y., 2022. Recent climate change has driven divergent hydrological shifts in high-latitude peatlands. Nat. Commun. 13 (1), 4959. https://doi.org/10.1038/s41467-022-32711-4.

Supplementary data

Table 1

Location and description of the sampling sites of 76 modern samples included in this study.

#	CODE	Lat (N)	Lon (E)	DTW (cm)	Vegetation	Shannon's Diversity Index of testate amoebae	Species count	Frozen peat reached	Microtopography/ microhabitat
1	M1_1	63°47'50,5	75°33'27,5	20	Lichen - *Cladonia* sp.	1.02	6		mound
2	M1_2	63°47'50,0	75°33'27,3	14	Lichen - *Cladonia* sp.	0.95	6		lawn
3	M1_3	63°47'49,9	75°33'27,2	8	*Sphagnum fuscum*	2.33	16		lawn
4	M1_4	63°47'50,0	75°33'27,2	0	*Sphagnum lindbergii*	1.72	11		carpet
5	M1_5	63°47'50,2	75°33'26,4	20	Lichen - *Cladonia* sp.	2.14	15		mound
6	M1_6	63°47'50,1	75°33'26,7	10	Lichen - *Cladonia* sp.	1.95	13		lawn
7	M1_7	63°47'49,0	75°33'26,4	28	*Sphagnum balticum*	2.50	20		mound
8	M1_8	63°47'48,8	75°33'26,3	11	*Sphagnum jensenii*	1.44	11	x	lawn
9	M1_9	63°47'48,8	75°33'26,9	9	*Sphagnum lindbergii*	1.73	12		lawn
10	M1_10	63°47'48,4	75°33'25,4	18	Lichen - *Cladonia* sp.	1.90	12		lawn
11	M1_11	63°47'43,8	75°33'21,2	–2	*Warnstorfia fluitans*, *Gymnocolea inflata*	no data	no data		pond
12	M1_12	63°47'43,8	75°33'21,2	–2	*Warnstorfia fluitans*, *Gymnocolea inflata*	1.18	6	x	pond
13	M1_13	63°47'43,8	75°33'20,9	0	*Sphagnum lindbergii*	1.59	13		carpet
14	M1_14	63°47'43,9	75°33'21,3	18	*Sphagnum fuscum*	2.10	16		lawn
15	M1_15	63°47'43,9	75°33'21,2	38	*Sphagnum fuscum*	2.06	11	x	mound
16	M2_1	63°47'07,2	75°38'40,5	30	*Sphagnum majus,* Lichen - *Cladonia* ssp.	1.86	10		mound
17	M2_2	63°47'07,2	75°38'40,3	20	*Sphagnum fuscum*	2.27	15		mound
18	M2_3	63°47'07,2	75°38'40,5	8	*Sphagnum cuspidatum*	1.70	11		lawn
19	M2_4	63°47'07,3	75°38'40,7	0	*Sphagnum jensenii*	1.73	14		carpet
20	M2_5	63°47'07,6	75°38'42,2	30	*Sphagnum majus*, *Warnstorfia fluitans* (10%)	2.13	13		mound
21	M2_6	63°47'07,7	75°38'42,2	25	*Sphagnum majus*, *Gymnocolea inflata* (40%)	2.43	17		mound
22	M2_7	63°47'07,7	75°38'42,3	20	*Sphagnum fuscum*	2.03	17		mound
23	M2_8	63°47'08,0	75°38'41,7	6	*Sphagnum lindbergii*	1.30	9		lawn
24	M2_9	63°47'07,8	75°38'42,4	0	*Sphagnum lindbergii*	1.09	7		carpet
25	M2_10	63°47'06,8	75°38'43,0	21	*Sphagnum fuscum*	2.37	18		mound
26	M2_11	63°47'06,9	75°38'43,3	0	*Sphagnum cuspidatum*	2.48	20		carpet
27	M2_12	63°47'07,0	75°38'43,0	8	*Sphagnum jensenii*	1.74	13		lawn
28	M2_13	63°47'07,0	75°38'43,0	0	*Sphagnum cuspidatum*	1.38	8		carpet
29	M3_1	63°46'36,9	75°41'56,6	9	Lichen - *Cladonia* sp.	2.07	16	x	lawn
30	M3_2	63°46'36,8	75°41'56,4	15	*Sphagnum fuscum*	1.92	11		lawn
31	M3_3	63°46'36,8	75°41'56,6	38	*Sphagnum balticum*	1.75	9		mound
32	M3_4	63°46'36,7	75°41'56,5	10	*Sphagnum fuscum*	1.83	11		lawn
33	M3_5	63°46'36,6	75°41'56,3	0	*Sphagnum jensenii*	1.72	13		carpet
34	M3_6	63°46'37,1	75°41'55,3	17	Lichen - *Cladonia* sp.	2.24	14		lawn

35	M3_7	63°46'37,1	75°41'55,2	4	Lichen - *Cladonia* sp., *Sphagnum fuscum* (10%)	1.63	12		carpet
36	M3_8	63°46'37,1	75°41'55,2	12	*Sphagnum fuscum*	2.18	16		lawn
37	M3_9	63°46'36,9	75°41'55,1	3	*Sphagnum jensenii*	1.59	12		carpet
38	M3_10	63°46'36,9	75°41'55,4	0	*Sphagnum jensenii*, *Warnstorfia fluitans* (20 %)	1.71	12		carpet
39	M3_11	63°46'37,3	75°41'55,1	11	*Sphagnum fuscum*	1.80	15		lawn
40	M3_12	63°46'37,4	75°41'55,1	8	*Sphagnum medium/divinum*	1.57	13		lawn
41	M3_13	63°46'37,3	75°41'55,1	–15	*Warnstorfia fluitans*	1.67	11		pond
42	M3_14	63°46'37,3	75°41'54,9	7	*Sphagnum majus*	1.48	10		lawn
43	M3_15	63°46'37,3	75°41'55,1	11	Lichen - *Cladonia* sp.	2.15	17	x	lawn
44	M3_16	63°46'38,6	75°41'53,8	1	Lichen - *Cladonia* sp., *Warnstorfia fluitans* (10%)	2.39	20		carpet
45	M3_17	63°46'38,6	75°41'53,6	9	*Sphagnum jensenii*	1.31	9		lawn
46	M3_18	63°46'38,6	75°41'53,4	1	*Sphagnum lindbergii*	2.24	20		carpet
47	M3_19	63°46'38,6	75°41'53,5	12	Lichen - *Cladonia* sp.	1.38	13		lawn
48	M3_20	63°46'38,6	75°41'53,4	3	*Sphagnum jensenii*	1.69	12		carpet
49	M3_21	63°46'39,1	75°41'54,3	7	Lichen - *Cladonia* sp.	2.28	16		lawn
50	M3_22	63°46'39,1	75°41'54,3	6	Lichen - *Cladonia* sp.	1.50	11	x	lawn
51	M3_23	63°46'39,1	75°41'54,3	4	Lichen - *Cladonia* sp.	1.48	13		carpet
52	M3_24	63°46'39,1	75°41'54,3	9	*Sphagnum lindbergii*	2.27	17		lawn
53	M3_25	63°46'39,1	75°41'54,4	13	Lichen - *Cladonia* sp.	2.17	14		lawn
54	M3_26	63°46'40,5	75°41'55,0	10	*Sphagnum jensenii*	1.50	9		lawn
55	M3_27	63°46'40,8	75°41'55,2	12	*Sphagnum majus*	2.19	18	x	lawn
56	M3_28	63°46'40,8	75°41'55,1	32	*Sphagnum fuscum*	1.56	12		mound
57	M3_29	63°46'40,7	75°41'55,4	2	*Sphagnum lindbergii*	0.38	6		carpet
58	M3_30	63°46'40,8	75°41'55,3	9	*Sphagnum jensenii*	1.25	9		lawn
59	M3_31	63°46'41,1	75°41'54,0	9	Lichen - *Cladonia* sp.	0.94	9		lawn
60	M3_32	63°46'41,1	75°41'53,9	2	Lichen - *Cladonia* sp.	1.61	15		carpet
61	M3_33	63°46'41,1	75°41'53,9	1	Lichen - *Cladonia* sp.	0.68	5		carpet
62	M3_34	63°46'41,1	75°41'53,7	5	*Sphagnum jensenii*	1.39	12		carpet
63	M3_35	63°46'41,1	75°41'53,9	5	Lichen - *Cladonia* sp.	1.34	13		carpet
64	M3_36	63°46'43,3	75°41'53,4	10	*Sphagnum jensenii*	1.11	10		lawn
65	M3_37	63°46'43,0	75°41'53,7	1	*Sphagnum cuspidatum*	0.75	7		carpet
66	M3_38	63°46'43,2	75°41'53,5	24	*Sphagnum fuscum*	2.42	18		mound
67	M3_39	63°46'43,1	75°41'53,4	12	*Sphagnum fuscum*	1.93	16	x	lawn
68	M3_40	63°46'43,1	75°41'53,4	13	Lichen - *Cladonia* ssp.	1.24	12		lawn
69	M4_1	63°38'34,1	75°47'47,3	21	*Polytrichum strictum*	1.77	10		mound
70	M4_2	63°38'34,1	75°47'47,4	6	*Polytrichum strictum*	1.82	14		lawn
71	M4_3	63°38'34,2	75°47'47,5	0	*Polytrichum strictum*, *Messia* ssp., *Sphagnum cuspidatum*	2.37	19		carpet
72	M4_4	63°38'34,2	75°47'47,4	–4	*Polytrichum strictum*, *Sphagnum balticum* (20%),	2.40	19		pond
73	M4_5	63°38'34,1	75°47'47,4	16	*Sphagnum balticum*	2.20	14		lawn
74	M4_6	63°38'34,1	75°47'47,6	5	*Polytrichum strictum* (50%), *Sphagnum balticum* (50%), *Gymnocolea inflata*	2.27	15		carpet

75	M4_7	63°38'34,3	75°47'47,5	1	*Polytrichum strictum* (70%), *Sphagnum balticum* (30%), *Gymnocolea inflata*	1.68	15		carpet
76	M4_8	63°38'34,2	75°47'47,8	–6	*Polytrichum strictum* (70%), *Sphagnum balticum* (30%), *Gymnocolea inflata*	2.52	18		pond

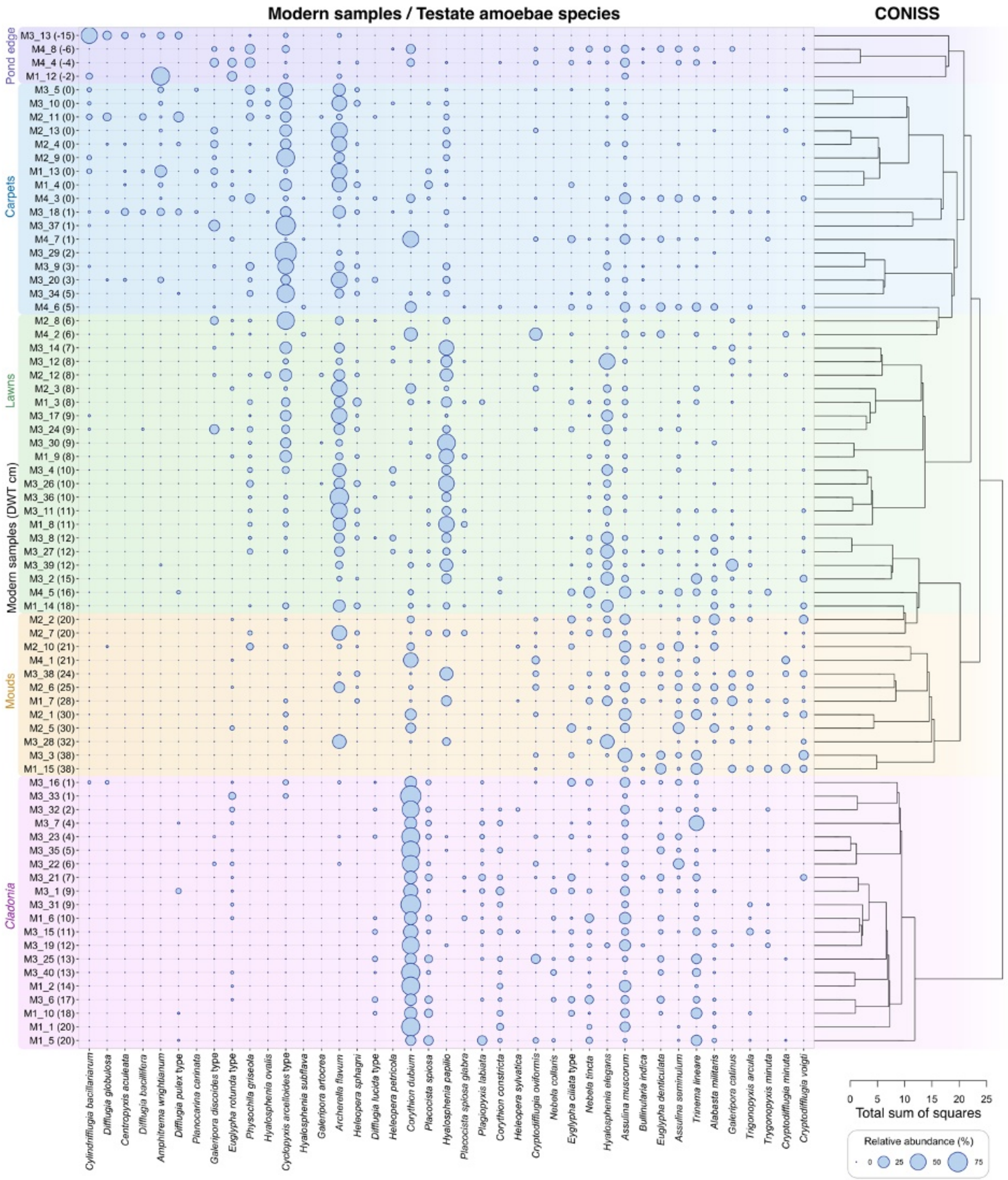

Fig. 1. Relative abundance (%) of common testate amoebae (TA) species in modern samples with samples groups used in this study and CONISS grouping based on TA relative abundance.

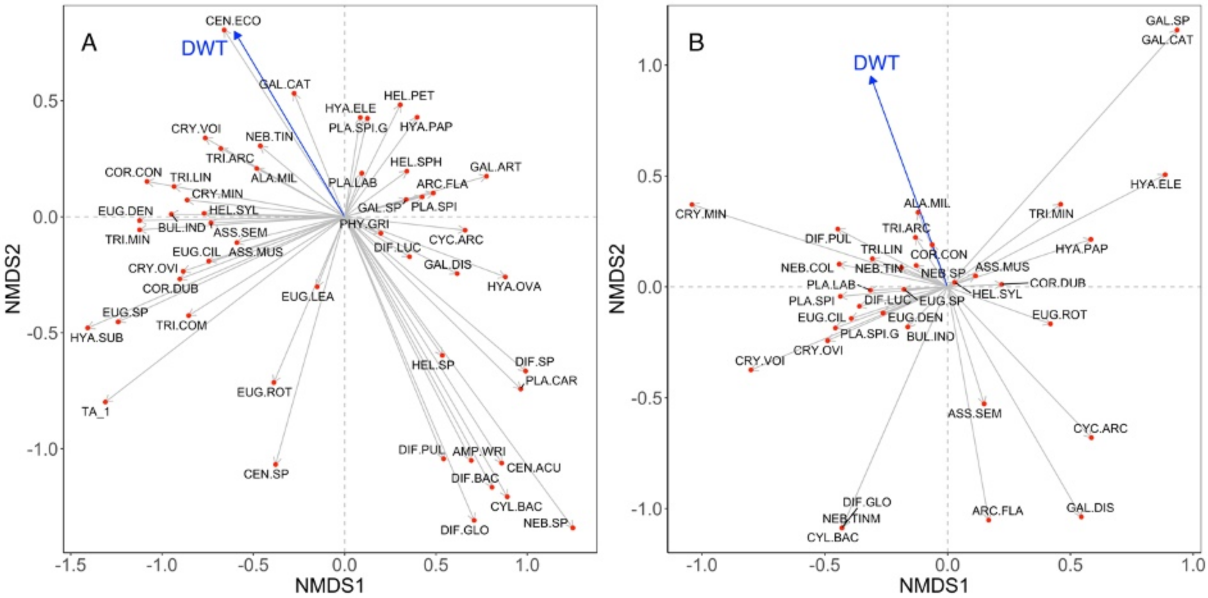

Fig. 2. Two-dimensional NMDS ordination plot of testate amoebae (TA) species with depth to water table (DWT) vector: A) the dataset with *Cladonia* excluded (stress = 0.13); B) only *Cladonia* samples (stress = 0.15).

Full names of the abbreviations used for TA species are included in Table 1.

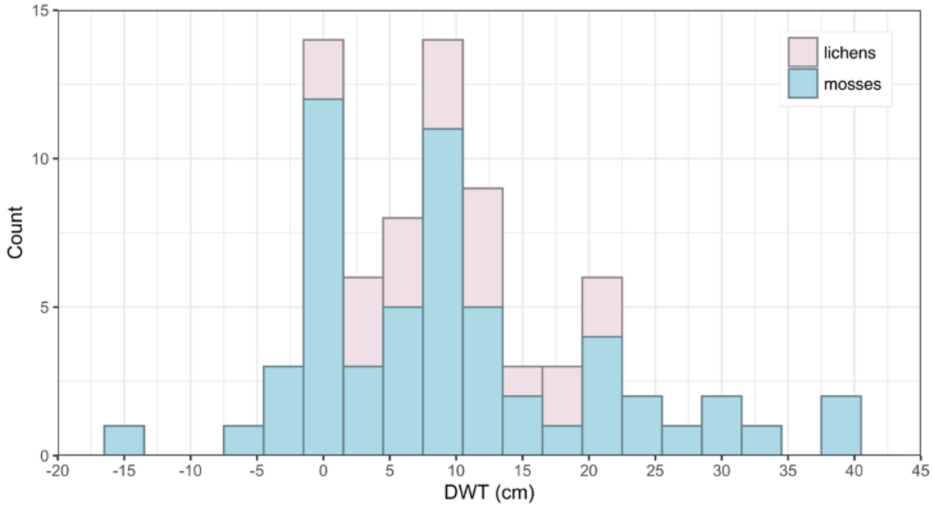

Fig. 3. Samples count – the depth to water table (DWT) intervals.

Biogeosciences, 22, 4797–4822, 2025
https://doi.org/10.5194/bg-22-4797-2025

Biogeosciences Open Access EGU

Research article

Peatland development reconstruction and complex biological responses to permafrost thawing in Western Siberia

Agnieszka Halaś[1], Mariusz Lamentowicz[2], Milena Obremska[3], Dominika Łuców[1], and Michał Słowiński[1]

[1]Department of Past Landscape Dynamics, Institute of Geography and Spatial Organization Polish Academy of Sciences, Warsaw, 00-818, Poland
[2]Climate Change Ecology Research Unit, Faculty of Geographical and Geological Sciences, Adam Mickiewicz University, Poznań, 61-680, Poland
[3]Institute of Geological Sciences, Polish Academy of Sciences, Research Centre in Warsaw, Warszawa, 00-818, Poland

Correspondence: Agnieszka Halaś (aj.halas@twarda.pan.pl)

Received: 26 March 2025 – Discussion started: 3 April 2025
Revised: 29 July 2025 – Accepted: 29 July 2025 – Published: 22 September 2025

Abstract. Western Siberian peatlands are among the largest peatland complexes in the world and play a crucial role in regulating the global climate. However, a lack of long-term, multi-proxy studies comprehensively examining the interactions between permafrost thaw and peatland ecosystems in Western Siberia hinders the ability to predict their response to future climate change. This research covers two centuries of the Khanymei peatlands history, situated within the discontinuous permafrost zone. In this study, a multi-proxy analysis (testate amoebae, plant macrofossil, pollen, micro- and macrocharcoal, loss on ignition) was conducted on two peat cores – one from a peat plateau and another from the edge of a thermokarst lake. We inferred peatland drying from the end of the Little Ice Age. The elevated peat plateau facilitated the aggradation of permafrost, which began to thaw in recent decades due to rising air temperatures, increasing peat moisture. The lake edge was the most dynamic part of the peatland, where more notable changes in hydrology, vegetation, and microbial composition occurred. Thawing led to significant *Sphagnum* growth and a shift in the testate amoebae community structure. We reconstructed the effects of permafrost thawing that resulted in a substantial but short-term and local increase in peat and carbon accumulation and an increased abundance of fungal communities. Our study reveals that thaw-induced terrain subsidence was subtle and spatially variable, yet these localized surface changes triggered complex hydrological, vegetational, and microbial responses, highlighting the nonlinear and multifaceted nature of permafrost degradation. The advantage of our research lies in the utilization of multi-proxy high-resolution palaeoecological techniques, enabling us to monitor even relatively minor permafrost transformations and identify early warning signals of climate-induced impacts on this invaluable ecosystem. We anticipate that further warming will contribute to the occurrence of these processes on a larger scale in Western Siberian peatlands, potentially significantly impacting ecosystem conditions and the global climate.

1 Introduction

Peatlands of Western Siberian Lowlands cover 592 440 km^2, with many underlain by permafrost (Sheng et al., 2004). Since the early Holocene, this region has been a carbon dioxide sink and during the last 11 ka has accumulated 70.2 Pg C, $\sim$ 26 % of all terrestrial carbon stored (Smith et al., 2004). Around half of this soil organic carbon is accumulated in permafrost-affected peat, making it vulnerable to climate change (Hugelius et al., 2020). Recent studies suggest that since 1979 CE, the Arctic has experienced warming almost four times as fast as lower latitudes due to a phenomenon known as Arctic amplification (Hantemirov et al., 2022; Rantanen et al., 2022; IPCC, 2023). Arctic warming accelerates permafrost thawing and significantly impacts Western Siberia, particularly peatland ecosystems (Hantemirov et al., 2022).

Permafrost peatlands are a unique environment with complex relationships between hydrological conditions, vegetation structures, peat accumulation and related carbon balance. The complexity of these interactions intensifies with permafrost thawing; however, many aspects remain unclear. During phases of stable permafrost, cold conditions make organic carbon relatively inactive (Swindles et al., 2015). Increased temperatures impact permafrost peatlands by inducing permafrost thaw, which leads to the release of little decomposed organic matter, and by triggering the activation of anaerobic decay processes (Jeong et al., 2018; Karlsson et al., 2021). The microbial decomposition of accumulated peat contributes to an increase in carbon dioxide (CO_2) and methane (CH_4) emissions from peatlands, which have positive feedback on climate (Jeong et al., 2018).

Thawing permafrost leads to an increase in the moisture content of the overlying peat layer. The increased water volume in circulation contributes to hydrologic modifications, especially in surface and subsurface hydrology of permafrost areas (Walvoord and Kurylyk, 2016). The enhanced wetness alters the thermal conductivity of peat (Kujala et al., 2008), diminishing peat insulation properties and facilitating easier and deeper heat penetration of underlying permafrost. This process creates a positive feedback loop, leading to further permafrost thawing and the amplification of climate warming (Schuur et al., 2015). A clear indication of thawing is an increase in active layer thickness (ALT), which has changed by 0.4 m in the Russian Arctic since 1990 CE (Smith et al., 2022). The changes in ALT lead to terrain subsidence (Ekici et al., 2019; O'Neill et al., 2023) and affect thermokarst lakes, a prominent feature of the Western Siberia landscape (Kremenetski et al., 2003). Initially, increased water supply leads to lake formation and expansion (Fewster et al., 2022; Luoto and Seppälä, 2003). However, new outflow channels created by continued permafrost degradation and increased evapotranspiration contribute to rapid lake drainage and disappearance (Webb and Liljedahl, 2023). This trend is visible especially in discontinuous and sporadic permafrost zones (Smith et al., 2005), where further thawing may shift these regions from surface water-dominated to groundwater-dominated systems (Frey et al., 2007).

The processes that are now observed in the Arctic-Boreal ecosystems are complex, scale-dependent, and determined by local conditions. The surface of permafrost peatlands often consists of microhabitats (palsa/peat plateau – depression), which are a result of complex interactions between vegetation growth, moisture, decomposition, peat accumulation, and permafrost (Nungesser, 2003; Rydin and Jeglum, 2013). The heterogeneous nature of permafrost peatlands facilitates the occurrence of various processes within short distances, which makes it difficult to predict how these peatlands will react to current warming (Sim et al., 2021). Numerous studies have emphasized their crucial role in global climate dynamics; however, these ecosystems remain unrepresented in climate models (Fewster et al., 2022; Sim et al., 2021; Swindles et al., 2015; Zhang et al., 2022).

The hydrological conditions of permafrost-affected peatlands following thaw will vary widely, and the trajectory of these changes is uncertain (Sim et al., 2021). As permafrost thaws, the destabilization of characteristic landscape features will lead to the formation of water-saturated areas with melting ice and elevated seasonal water tables (Sannel and Kuhry, 2011; Swindles et al., 2015). However, increased temperatures will also drive higher evapotranspiration rates, potentially causing drier conditions in certain areas depending on the microhabitat type and the season (Lawrence et al., 2015; Spiller et al., 2025). Bogs and fens may experience drier surface layers, particularly in summer, while faster drainage could occur following the thaw of ground ice (Sannel and Kuhry, 2011; Spiller et al., 2025). Observations already show that northern peatlands respond in diverse ways to warming, with no single, uniform trend of either wetting or drying (Sim et al., 2021; Zhang et al., 2022).

Many studies have indicated that permafrost thaw will have a beneficial effect on vegetation productivity in Arctic-Boreal ecosystems, causing so-called *greening* (Myers-Smith et al., 2020) and increased carbon accumulation (Heffernan et al., 2020). Greening dominates in northern regions, in Western Siberia above 64° N (Miles and Esau, 2016). Regions further south experience *browning*, characterized by decreased productivity (Miles and Esau, 2016; Phoenix and Bjerke, 2016), associated with disturbances such as drought (Magnússon et al., 2023), water stress (Li et al., 2021), insect outbreaks (Kurz et al., 2008) or wildfires (Zoltai et al., 1998). The transitional zone between these *greening*-dominated and *browning*-dominated regions is of particular interest, as it may reflect early signals of ecosystem change. Our study focuses on the permafrost peatlands, located within this transitional zone, which may indicate that some parts of these peatlands have already surpassed the period of post-thaw beneficial enhanced plant productivity (Ogden et al., 2023; Phoenix and Bjerke, 2016).

Palaeoecological reconstructions provide invaluable information about past environmental conditions and ecosystem responses to past climate changes (Bottjer, 2016). This is particularly important because palaeoecological records cover a much longer timeframe than observational data and, when using a multi-proxy approach, can offer a more comprehensive understanding of past ecosystem dynamics (Chambers and Charman, 2004). Different palaeoecological proxies can provide insights into peatland moisture conditions (Halaś et al., 2023; Lamentowicz et al., 2015), local (Feurdean et al., 2019; Volkova et al., 2019), and regional vegetation composition (De Klerk et al., 2009; Novenko et al., 2023) and fire activity (Conedera et al., 2009; Feurdean et al., 2019).

Western Siberian peatlands have been the subject of a spare number of studies comprehensively reconstructing their history (Beilman et al., 2009; Feurdean et al., 2019, 2020, 2022; Kurina et al., 2023; Lamentowicz et al., 2015; Peteet et al., 1998; Philben et al., 2014; Tikhonravova et al., 2023; Willis et al., 2015). Due to the vast area and challenging accessibility of Western Siberian peatlands, Russian paleoecologists began studying them in the early 20th century (Kremenetski et al., 2003). Most early research focused on peatland distribution, peat thickness, basal age, and fossil pollen and plant records (Kremenetski et al., 2003; Neustadt, 1967). More recent studies have focused on multi-proxy analyses (e.g., Feurdean et al., 2019; Kurina et al., 2023; Lamentowicz et al., 2015), vegetation reconstructions (Peteet et al., 1998; Philben et al., 2014; Tikhonravova et al., 2023), and carbon accumulation (Beilman et al., 2009). Fire history has also been investigated (Feurdean et al., 2020, 2022), while testate amoebae have been used to reconstruct peatland hydrology in only a few studies (Feurdean et al., 2020; Kurina et al., 2023; Lamentowicz et al., 2015; Willis et al., 2015). Due to the large area of the region, in situ data are primarily available from more accessible areas, emphasizing the need for further investigation. Despite an increase in publications on Western Siberian peatlands in recent decades, research in this region is expected to decline in the near future due to ongoing accessibility challenges (Schuur et al., 2024). Our research presents new insight into the history of peatlands in a poorly explored region of Western Siberia. The presented data covers an important period from the end of the Little Ice Age to modern times, providing information on how Khanymei peatland ecosystems and peatland's microhabitats have responded to recent warming.

Our study aimed to reconstruct past environmental changes on peatlands from the discontinuous permafrost zone based on two cores. The main objectives were to (1) reconstruct the 200-year history of Khanymei peatlands using a multi-proxy approach; (2) analyse differences in biological responses of peatland microhabitats to permafrost thaw; and (3) identify patterns of the progressive permafrost degradation in discontinuous permafrost zone.

2 Study area

The study area is located near Khanymei (Yamal-Nenets Autonomous District) (Fig. 1). The studied peatlands are situated at the northern border of the boreal forest taiga zone, which includes woodlands and open stands (Fig. 1b). Due to the presence of discontinuous permafrost, palsa and peat plateaus (with a frozen core) surrounded by thermokarst lakes are a characteristic feature of the study area.

The studied region has a boreal climate with short, cool summers and long, cold, snowy winters (Peel et al., 2007). The mean annual air temperature is between −3.5 and −6 °C, January air temperature ranges from −22 to −24 °C, and July from 15.5 to 17 °C (Trofimova and Balybina, 2014). The average annual precipitation in the Khanymei area is 436 mm (Kluge et al., 2021). Siberia stands out as one of the regions experiencing the most pronounced warming worldwide in recent years, and modern climate models project that this trend will continue (Groisman et al., 2013; Hantemirov et al., 2022). There has been a notable rise in hot extremes and a decline in cold extremes over recent decades (Seneviratne et al., 2021). Additionally, precipitation patterns have been altered significantly, with intensified heavy rainfall during the warm season (Seneviratne et al., 2021) and increased precipitation and snow water equivalent during the cold season (Bulygina et al., 2011; Groisman et al., 2013).

The northern border of the boreal forest taiga zone is characterized by coniferous pine (*Pinus sylvestris* and *Pinus siberica*) and larch (*Larix sibirica*) open forests (Safronova and Yurkovsksya, 2019). The palsas and peat plateaus are covered by moss-lichen mosaics with a presence of dwarf shrubs (e.g. *Rhododendron tomentosum*) and dwarf birch (*Betula nana*) (Safronova and Yurkovsksya, 2019; Volkova et al., 2019). Additionally, in permafrost peatland ecosystems in the Khanymei region, lichens (genera *Cladonia*) occupy 70 %–80 % of peatland surface and form a unique type of lichen peat (Volkova et al., 2019).

Peatlands started to form in Western Siberia in the early Holocene, between 11 000 and 10 000 cal BP (Kremenetski et al., 2003). Even though Western Siberia lacked ice sheet cover during the last glacial period, the initiation of peatlands formation did not occur until the post-glacial warming of this region (Abe-Ouchi et al., 2015). Unfavourable conditions for peat accumulation during the glacial period were caused by a limited moisture influx from the North Atlantic due to the spread of the ice cover in the Arctic Ocean and the Siberian High (Velichko et al., 2011). According to Alexandrov et al. (2016), summer dryness-induced moisture imbalance was an essential factor preventing the formation of *Sphagnum*-dominated peatlands during the glacial period in this part of Siberia. Peatlands in the Khanymei region were mostly formed on sandy and silty sediments, and peat deposits are usually 0.1–1.4 m deep (Raudina et al., 2017; Velichko et al., 2011).

Permafrost development in Western Siberia

The permafrost in Western Siberia was mainly developed in Late Pleistocene (18–27 ka BP), and during the most favourable conditions, the southern limit reached 48–49° N (Duchkov, 2006). The early Holocene warming led to a northward shift of the border up to 60° N. During the Subatlantic cooling (2–1.3 ka BP), an epigenetic permafrost aggradation started, and peat deposits accumulated after deglaciation were first to freeze (Kondratjeva et al., 1993). The good insulating properties of *Sphagnum* mosses allowed frost to persist during warmer seasons and extend into the deeper mineral layers. This process led to the development of permanently frozen peatlands and the formation of palsas due to the cryogenic lifting of the peatland's surface (Martini et al., 2007). The characteristic feature of discontinuous permafrost is thermokarst lakes, which developed in the Khanymei area around 2.5 ka BP under stable permafrost conditions (Martini et al., 2007; Raudina et al., 2017).

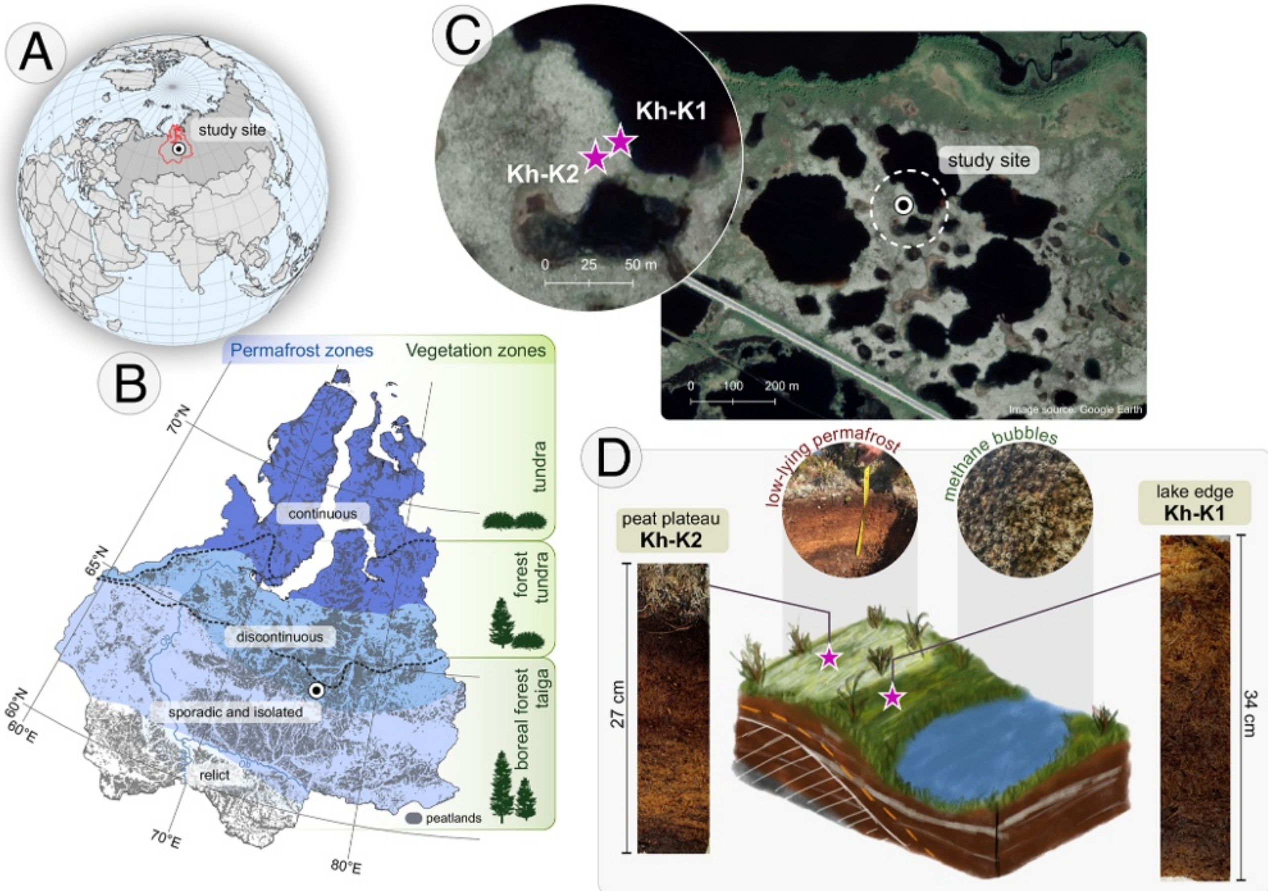

Figure 1. Study area: **(a)** location of West Siberian Lowland (WLS); **(b)** WSL – permafrost extent based on Brown et al. (1997), peatland extend based on Sheng et al. (2004) and vegetation zones based on Davydova and Rakovskaya (1990); **(c)** location of coring sites (background map source: © Google Earth 2015); **(d)** illustration of the peat plateau-lake edge microhabitat on study site with photos of peat cores.

3 Methods and materials

3.1 Coring and sediment sub-sampling

Two peat cores with a diameter of 10×10 cm were collected from Khanymei permafrost peatlands at the turn of June and July 2019. Cores were extracted from the peat plateau-lake edge complex 5 m apart from each other (Fig. 1c). The core Kh-K1 (34 cm, 63.7856° N, 75.6438° E) was taken from the lake edge and Kh-K2 (27 cm, 63.7855° N, 75.6434° E) from the peat plateau. The peat monoliths were extracted using a knife. The Kh-K2 core was sampled until the frozen peat was reached. Each peat core was then sub-sampled in 1 cm resolution (except for 0–2 cm in Kh-K2) for testate amoebae (sample volume: 3 cm^3), pollen and microcharcoal (1 cm^2), macrocharcoal (2 cm^2), plant macrofossils (4 cm^3), and loss on ignition (1 cm^3) analyses.

3.2 Chronology and peat accumulation rate

Eight samples from Kh-K1 and five from Kh-K2 of terrestrial plant macrofossils were selected for dating (Table 1). Cores chronology was based on ^{14}C dating using an Accelerator Mass Spectrometer (AMS) in the Poznań Radiocarbon Laboratory. The radiocarbon dates were calibrated with IntCal20 (Reimer et al., 2020) and NH1 post-bomb (Hua et al., 2013) atmospheric curves (Fig. 2). For models calculation with 1 cm resolution, the *P_Sequence* function with parameters $k0 = 10$ and $\log 10(k/k0) = 1$ was applied. One calendar year representing the date of coring 2019.6 at a depth of 0 cm, was introduced to the model. The age-depth models were calculated using the OxCal v4.4.4 software (Ramsey, 2001).

The peat accumulation rate (PAR, mm yr^{-1}) was calculated by dividing the sample thickness (mm) by the age difference between the top and bottom limits of the sample (CE years).

3.3 Testate amoebae analysis

Testate amoebae (TA) analysis was conducted following an established protocol (Booth et al., 2010). Sub-sampled material was shaken with distilled water and sieved through a

Table 1. Radiocarbon (^{14}C) dates from peat cores Kh-K1 and Kh-K2.

Core	Depth (cm)	Lab Number	^{14}C age or $F^{14}C$*	Material dated	Calibrated age (CE)	2σ range modelled age range (CE)
Kh-K1	2–3	Poz-150655	*101.58 ± 0.34*	*Sphagnum steams*	2009	2009–2009
	5–6	Poz-150725	*103.83 ± 0.32*	*Sphagnum steams*	2008	2007–2008
	9–10	Poz-150726	*106 ± 0.33*	*Sphagnum steams*	2006	2005–2007
	14–15	Poz-150728	*108.5 ± 0.39*	*Sphagnum steams*	2002	2000–2003
	19–20	Poz-150663	*111.55 ± 0.36*	*Sphagnum steams*	1996	1994–1997
	24–25	Poz-150664	*119.86 ± 0.37*	*Sphagnum steams*	1986	1984–1987
	30–31	Poz-157591	*102.87 ± 0.28*	*Sphagnum steams*	1957	1956–1957
	33–34	Poz-157563	*104.75 ± 0.31*	*Sphagnum steams*	1956	1955–1956
Kh-K2	6–7	Poz-150837	*125.66 ± 0.45*	*Sphagnum steams*	1975	1959–1982
	10–11	Poz-150665	105 ± 30	*Sphagnum steams*	1930	1902–1954
	15–16	Poz-150838	25 ± 30	*Sphagnum steams*	1894	1822–1920
	20–21	Poz-150666	105 ± 30	*Sphagnum steams*	1860	1756–1901
	26–27	Poz-150839	90 ± 30	*Sphagnum steams*	1814	1692–1875

* postbomb $F^{14}C$ values are shown in italics.

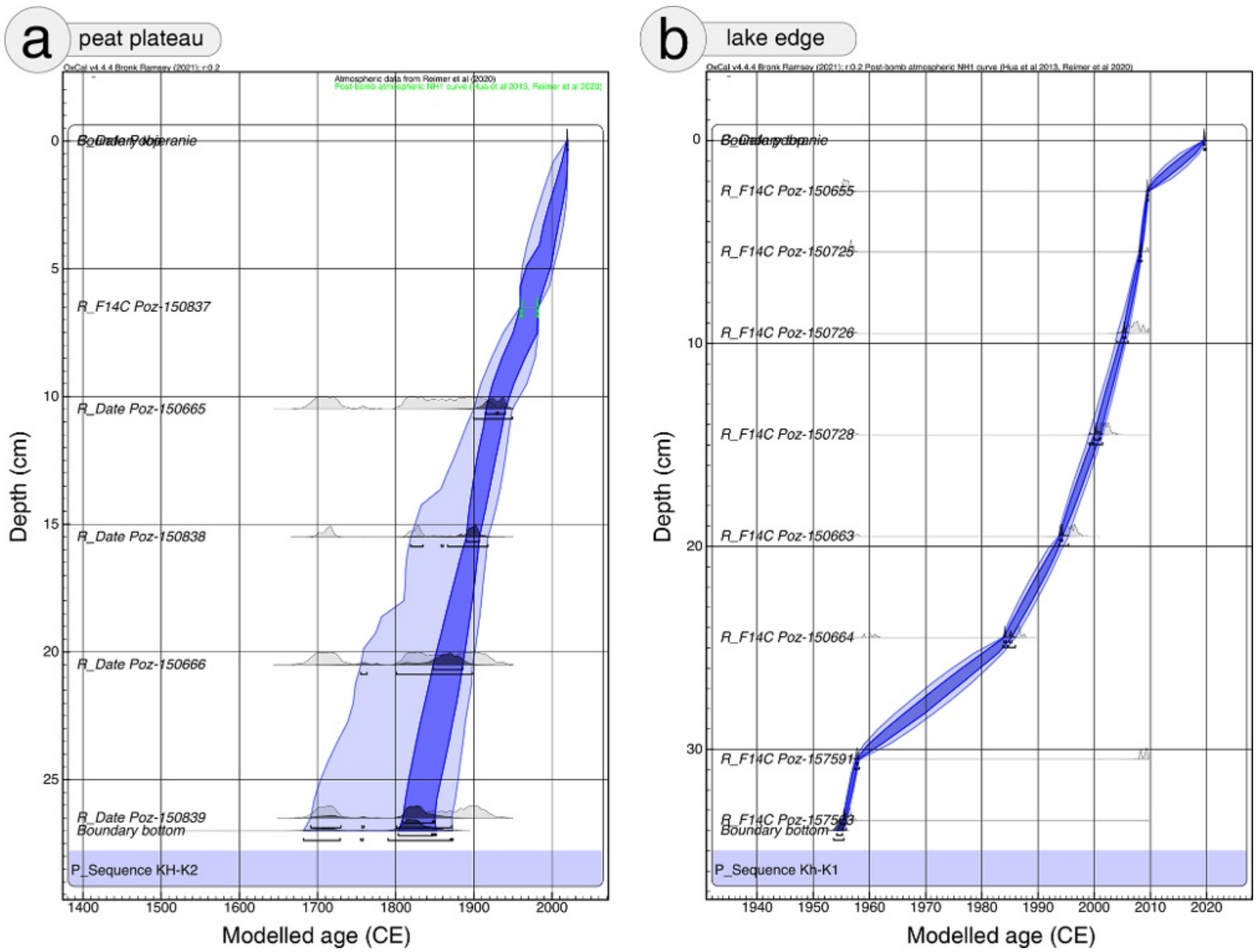

Figure 2. Age-depth models based on C^{14} dating for peat cores: **(a)** Kh-K2 – peat plateau and **(b)** Kh-K1 – lake edge. The dark and light blue areas provide the 68.3 % and 95.4 % confidence ranges of the model, respectively.

300 µm mesh. The material was examined using a light microscope at 200–400× magnification. For each sample, a minimum of 150 individual tests were counted and identified based on the available identification guides (e.g., Charman et al., 2000; Siemensma, 2022; Todorov and Bankov, 2019). The results of testate amoebae analysis were used for the quantitative depth to water table (DWT) and pH reconstructions.

3.4 Pollen, non-pollen palynomorphs (NPPs), and microcharcoal analysis

Pollen analysis was prepared following the standard procedure (Berglund and Ralska-Jasiewiczowa, 1986). To estimate the concentration of palynomorphs, *Lycopodium* markers were used (Stockmarr, 1971). For taxonomical identification, pollen keys (Beug, 2004; Faegri et al., 1989; Moore et al., 1994) and reference photographic collections were used. For each sample, at least 300–500 pollen grains of terrestrial plants were counted. The sum AP + NAP (arboreal and non-arboreal pollen) was calculated, excluding telmatic and aquatic taxa, spores, and non-pollen palynomorphs (NPPs). Microscopic charcoal particles (10–100 µm) and NPPs were counted during the analysis from the same slides. NPPs identification was based on Van Geel (2001) and Shumilovskikh et al. (2015). To determine regional fire activity, microcharcoal accumulation influx (MIC influx, particles $cm^{-2}\,yr^{-1}$) was calculated by dividing the microcharcoal concentration (particles cm^3) by peat accumulation rate ($cm\,yr^{-1}$).

3.5 Plant macrofossil analysis

Samples were washed and sieved with distilled water using 125 µm mesh. To estimate the percentage volume of mosses and vascular plants, samples were examined with a stereoscopic microscope. The macrofossils were identified using various identification guides (e.g., Katz et al., 1977; Mauquoy and Geel, 2007; Tobolski, 2000). The subfossil vegetative fragments and carpological remains were counted but excluded from volume percentages and noted as present or absent in each sample.

3.6 Macrocharcoal analysis

Macroscopic charcoal (particles ≥ 100 µm) analysis was used to conduct paleo fire reconstruction. All samples were bleached for 24 h (Mooney and Radford, 2001) and then wet-sieved through 100 µm and 500 µm meshes. Macrocharcoal particles were counted with a stereoscopic microscope and divided into two groups: 100–500 and > 500 µm to provide information about potential fire distance from the studied area (e.g., Conedera et al., 2009). To determine local fire activity, macrocharcoal accumulation influx (MAC influx, particles $cm^{-2}\,yr^{-1}$) was calculated by dividing the macrocharcoal concentration (particles cm^3) by peat accumulation rate ($cm\,yr^{-1}$).

3.7 Organic matter content and C content

The content of organic matter (OM, %) was determined by loss on ignition (LOI) analysis following standard protocol (Heiri et al., 2001). Samples were oven-dried at 105 °C for 12 h and then burned in a muffle furnace at 550 °C for 3 h. To estimate dry bulk density (BD, $g\,cm^{-3}$), the weight of the sample after drying was divided by the fresh sample volume. The organic matter content was calculated as the difference between dry and burned sample weight, divided by dry sample weight (Chambers et al., 2011). The carbon content (g) was converted from the OM by assuming that organic C is ∼ 50 % of OM by mass (Chambers et al., 2011; Treat et al., 2016). The carbon accumulation rate (CAR, $g\,C\,m^{-2}\,yr^{-1}$) was calculated following equation (Tolonen and Turunen, 1996):

$$\mathrm{CAR} = \frac{\mathrm{PAR}}{1000} \times \mathrm{BD} \times C \tag{1}$$

Where: CAR: carbon accumulation rate ($g\,m^{-2}\,yr^{-1}$), PAR: peat accumulation rate ($mm\,yr^{-1}$), BD: dry bulk density ($g\,m^{-3}$), C: C content ($g\,C\,g^{-1}$ dry weight)

3.8 Numerical analysis

All stratigraphic diagrams were plotted with Tilia graph software v3.0.1 (Grimm, 1991) and Grapher™ Golden Software. Peatlands' development stages were determined based on changes in TA community structure and related depth to water table (DWT) fluctuations. Zonation was based on CONISS using a *rioja* package in R (Juggins, 2020). The Shannon Diversity index was calculated for each TA sample using a *vegan* package (Oksanen et al., 2022) in R software (R Core Team, 2022). To understand the response of TA communities to past ecosystem disruptions, five TA functional traits were selected: mixotrophy, aperture size and position, shell compression, and biovolume. Based on TA functional traits, the community-level weighted means of trait values (CWM) was calculated for each community and each standardized trait to estimate their functional composition using the *FD* package (Laliberté et al., 2014) and TA functional traits established by Fournier et al. (2015). TA were also divided into four categories based on shell type: organic, organic-coated idiosomic, idiosomic, and agglutinated (Mitchell et al., 2008).

The Non-metric Multidimensional Scaling (NMDS) was applied to the TA species composition data from the Kh-K1 core using a *scikit-learn* library (Pedregosa et al., 2011) to detect temporal changes in community structure. Before the NMDS, the data were standardised using z-score standardization. The NMDS algorithm was set to use Euclidean distance and two dimensions. The K-Means clustering was applied to the transformed data and visualised with 95 % confidence interval ellipses. The optimal number of clusters that maximized the Silhouette Score was selected as the optimal clustering solution (Fig. S1 in the Supplement). Data visualization was carried out using a *matplotlib* (Hunter, 2007) and *seaborn* (Waskom, 2021) libraries. Calculations were conducted using Python in a Google Colaboratory (Google Colab) environment. The NMDS was performed only on core Kh-K1, as this core captures the most dynamic ecological transitions, and CONISS was considered sufficient for summarizing patterns in Kh-K2.

To reconstruct changes in DWT, Khanymei transfer function for discontinuous permafrost peatlands was applied (Halaś et al., 2023), and pH changes were reconstructed using Asian transfer function (Qin et al., 2021). Reconstructions were carried out using the C2 program, version 1.8.0 (Juggins, 2007).

4 Results

This section presents the outcomes of the multi-proxy analyses of two peat cores, Kh-K1 (lake edge) and Kh-K2 (peat plateau). The results are organized according to stratigraphic zones identified based on changes in testate amoeba (TA) community structure and associated fluctuations in depth to water table (DWT). For the peat core Kh-K1, four zones (Kh1-A to Kh1-D) were distinguished, and for Kh-K2, six zones (Kh2-A to Kh2-F). These zones provide a framework for describing and interpreting past hydrological and ecological dynamics (Figs. 3, 5, 6).

4.1 Kh-K2 – peat plateau

4.1.1 Zone Kh2-A (ca. 1814–1832 CE)

In the first zone Kh2-A there is a dominance of Unknown TA_Khan (Fig. 4), *Difflugia pulex* type, and the presence of *Centropyxis aculeata* type (Fig. 3a) – indicators of wet conditions (Halaś et al., 2023). Bigger TA aperture size, higher shell biovolumes, and more spherical shells also suggest wet conditions. TA species with agglutinated shells are the most abundant in this zone. Based on TA, this zone was characterized by wet conditions, with DWT around 4 cm and a pH of 5.1. The presence of green algae genera *Botryococcus* (Fig. 5a) also indicates a wetter environment (Pandey et al., 2023), while the presence of fungi *Helicoon pluriseptatum* HdV-30 a shift towards drier oligotrophic conditions (Kuhry, 1997). This period is characterized by a ligneous layer with roots and wood (Fig. 5a); however, ca. 1830 CE *Sphagnum* Secc. *Cuspidata* starts to take over the peatland surface. Numerous seeds of shrubs (*Vaccinium* sp.) and sedges (*Carex* sp.), as well as leaves of dwarf shrubs (*Betula nana*), are present in the sediment. In this zone, a high peak of *Betula* pollen was recorded, as well as the presence of shrubs *Rhododendron tomentosum*, Ericaceae, and *Vaccinium*. After ca. 1820 CE, a decrease in *Betula* pollen was inferred, which coincides with the period of high MIC that occurred between 1814 and 1835 CE (Figs. 5a, 6a). Peat accumulation in this period remains low and stable ($\sim 1.3\,\mathrm{mm\,yr^{-1}}$), while carbon accumulation decreases from 29.5 to $8.8\,\mathrm{g\,m^{-2}\,yr^{-1}}$.

4.1.2 Zone Kh2-B (ca. 1832–1890 CE)

In zone Kh2-B there is a disappearance of *Centropyxis aculeata* type and a decrease of *Difflugia pulex* type – wet indicators (Fig. 3a). Intermediate indicators such as Unknown TA_Khan, *Archerella flavum,* and *Hyalosphenia papilio* appear, and dry indicators are more abundant (e.g., *Alabasta militaris*, *Assulina muscorum*) (Bobrov et al., 1999; Halaś et al., 2023). The functional traits of TA change, shells become more compressed with smaller biovolume and smaller aperture in more terminal positions. Mixotrophic species (*Archerella flavum*, *Hyalosphenia papilio*), which survive and reproduce due to stable moisture conditions and low pH in *Sphagnum* (Lamentowicz et al., 2020), are the most abundant in this zone. In this zone DWT increases and stabilises between 12–15 cm, while peatland acidification continues (pH = 5.0) with periods of lower pH values (pH = 4.8). *Sphagnum* Secc. *Cuspidata* is a dominant peatland vegetation between 1835 and 1895 CE (Fig. 5a). HdV-83 associated with wet phases of *Sphagnum* becomes present after ca. 1845 CE (Shumilovskikh et al., 2015). NPP indicators of very wet conditions (HdV-30) and green algae *Botryococcus* decline after 1860 CE. We inferred the return of *Pinus* in pollen, which becomes similarly abundant as *Betula*. After 1865 CE, a decrease in shrubs (e.g. Ericaceae, *Vaccinium*) and an increase in herbs (e.g. *Rubus chamaemorus*) was inferred. Leaves and seeds of shrubs (e.g., *Betula nana*) and sedges (*Carex* sp.) are very abundant in this zone. This zone has a stable peat accumulation rate ($\sim 1.4\,\mathrm{mm\,yr^{-1}}$) and high content of organic matter ($\sim 98.3\,\%$) (Fig. 6a). Carbon accumulation rate oscillates between 4.3 and $9.2\,\mathrm{g\,m^{-2}\,yr^{-1}}$. Low MIC values indicate low regional fire activity; however, higher MAC ($> 500\,\mu\mathrm{m}$) values ca. 1890–1900 CE indicate a period of very local fires.

4.1.3 Zone Kh2-C (ca. 1890–1910 CE)

Zone Kh2-C was a 20-year transitional phase when a significant shift in TA community structure was inferred, and dry indicators like *Alabasta militaris* and *Assulina muscorum* become dominant (Bobrov et al., 1999) (Fig. 3a). There is also an increase in *Cyclopyxis arcelloides* type and *Phryganella acropodia*, which tolerate wetter conditions (Halaś et al., 2023). More species with larger apertures appear, while mixotrophic TA and species with organic shells almost disappear. Based on TA reconstruction, this zone was characterised by a short-term decrease in DWT to 10 cm ca. 1910 CE. The presence of rotifer *Habrotrocha angusticollis* (HdV-37) (Fig. 5a) also indicate periodic wetting (Shumilovskikh et al., 2021). A gradual transition in *Sphagnum* species from *Sphagnum* Secc. *Cuspidata* to *Sphagnum* Secc. *Acutifolia,* typically a hummock group of species

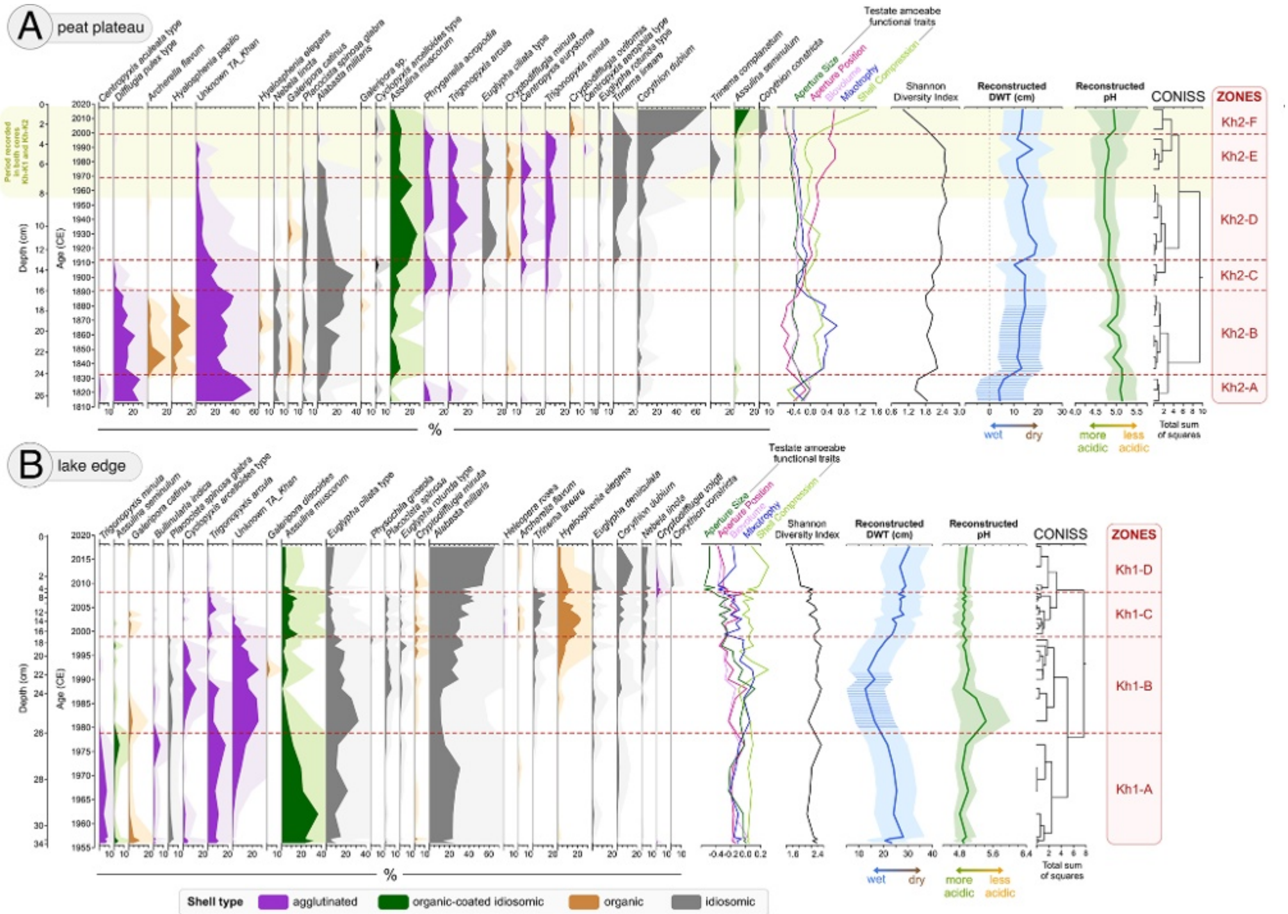

Figure 3. Testate amoebae (TA) diagram (abundance > 3 %) with 5× exaggeration for peat cores: **(a)** Kh-K2 – peat plateau and **(b)** Kh-K1 – lake edge. TA species are grouped by shell type, as indicated by the colour legend below the plot. The diagram includes community-weighted TA functional traits, Shannon Diversity index, reconstructed depth to water table (DWT) based on Halaś et al. (2023), and reconstructed pH based on Qin et al. (2021). Shaded areas for DWT and pH represent bootstrap reconstruction errors. The hatching on the DWT indicates a reconstruction potentially affected by error due to the presence of > 25 % of a new TA species. Species are sorted by weighted average (WA). Zonation was based on testate amoebae CONISS.

(Fig. 5a) (Malmer, 1988), was inferred together with a decrease in reconstructed pH (< 5). Leaves and seeds of shrubs and sedges become almost absent in the sediment after 1865 CE. Peat characteristics remain stable with no significant change in peat accumulation and organic matter content (Fig. 6a). Initially 11.9 $g\,m^{-2}\,yr^{-1}$, the carbon accumulation rate decreases to 4.7 $g\,m^{-2}\,yr^{-1}$ as DWT drops. An increase in MIC was inferred, which indicates higher regional fire activity.

4.1.4 Zone Kh2-D (ca. 1910–1970 CE)

In zone Kh2-D, *Difflugia pulex* type disappears, and the abundance of Unknown TA_Khan declines to below 10 % (Fig. 3a). At the same time, dry indicators, like *Cryptodifflugia minuta*, *Assulina muscorum*, or *Trigonopyxis arcula* appear in higher abundance (Bobrov et al., 1999). More species with idiosomic and organic-coated idiosomic shells appear. Taxa with smaller aperture sizes with cryptic positions become dominant (Fournier et al., 2015). At the beginning of this zone DWT significantly increases to 19.7 cm and later oscillates ∼ 15 cm. Acidification progresses reaching the lowest pH values in the record (pH = 4.7). This zone is dominated by *Sphagnum* Secc. *Acutifolia* (80 %) with some addition of *Sphagnum* Secc. *Sphagnum* (Fig. 5a). Less shrub remains were inferred; however, dead wood became more present in the sediment. Fungal fruit bodies of *Microthyrium* HdV-8B are more abundant, which has been associated with drier or more oligotrophic conditions (De Klerk et al., 2009). We inferred a lower frequency of shrubs and an increasing presence of herb *Rubus chamaemorus*. Between 1930 and 1960 CE, *Pinus pollen* is more abundant than *Betula* pollen. This coincides with a period of lower peat (∼ 0.9 $mm\,yr^{-1}$) and carbon accumulation 2.2–7.2 $g\,m^{-2}\,yr^{-1}$ (Fig. 6a). The low values of MIC and MAC indicate a period of low local and regional fire activity.

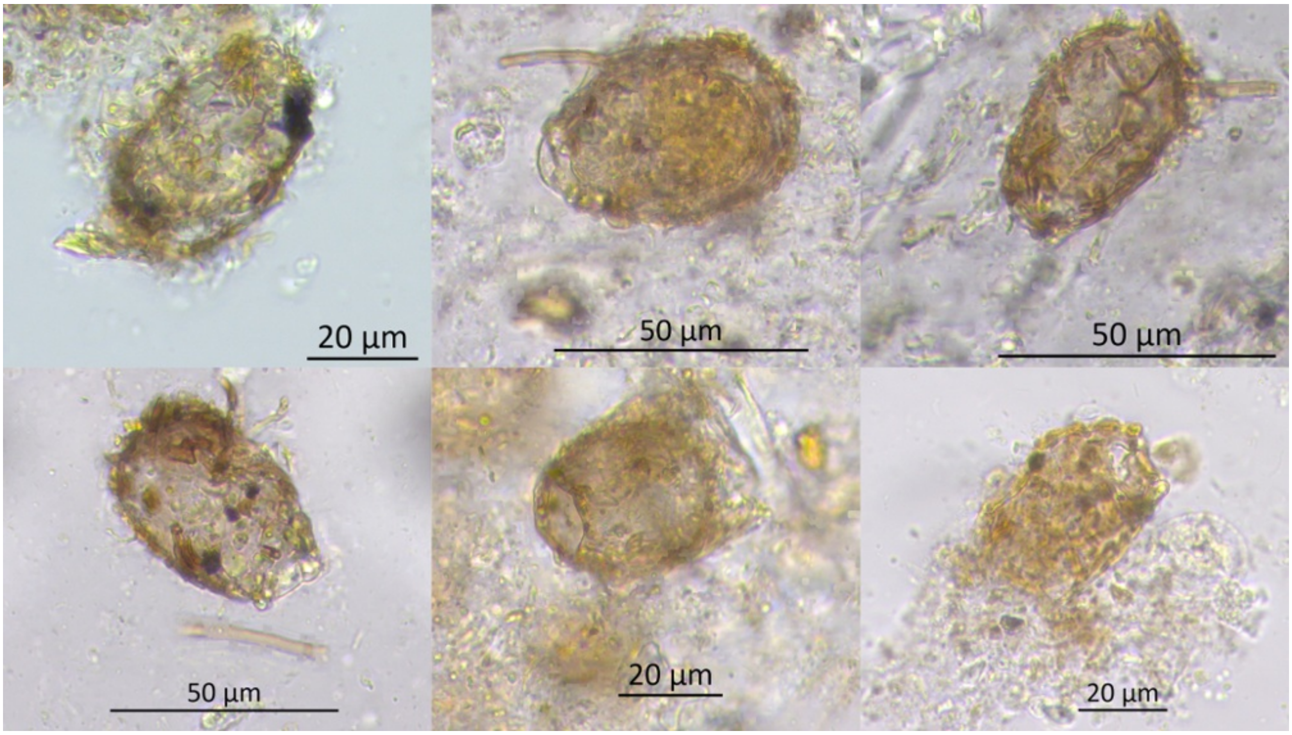

Figure 4. Light microscope images of an unidentified testate amoeba (Unknown TA_Khan) found in samples from Khanymei peatland. The taxon exhibits an ampulla-shaped test with a distinct collar or neck. The aperture is circular, and larger mineral particles are visible inside. Further taxonomic identification is needed.

4.1.5 Zone Kh2-E (ca. 1970–2000 CE)

In this zone, similar TA species are present as in the previous one but with a lower abundance of Unknown TA_Khan, *Assulina muscorum*, and *Alabasta militaris* (Fig. 3a). Species with drier moisture preferences like *Trinema lineare* or *Corythion dubium* appear more frequently (Bobrov et al., 1999). Functional traits adapting species to drier conditions were inferred, such as smaller aperture size, biovolume, compressed shells, and more cryptic aperture. Zone Kh2-E was characterized by fluctuating DWT, with an initial decrease to 12 cm and an increase to 18 cm by ca. 1990 CE. Acidification decreases slightly with high pH variability (reconstruction error 0.4 pH). We inferred a ligneous layer with $> 80\,\%$ of roots/rootlets and decrease in *Sphagnum* species after 1980 CE (Fig. 5a). After a period of domination of *Pinus* pollen between 1920 and 1960 CE, in this zone, the share of *Betula* and *Pinus* pollen remain, at a similar level of $\sim 35\,\%$. After 1990 CE, the shrub Ericaceae becomes more frequent while herbs *Rubus chamaemorus* and *Artemisia* almost disappear. Between 1975 and 2000 CE, high MIC and MAC values (high local and regional fire activity) and a decrease in organic matter content to 81 % were inferred (Fig. 6a). Peat and carbon accumulation increase to $1.4\,\mathrm{mm\,yr^{-1}}$ and $17.1\,\mathrm{g\,m^{-2}\,yr^{-1}}$, respectively.

4.1.6 Zone Kh2-F (ca. 2000–2019 CE)

In the last zone Kh2-F, the Shannon Diversity Index indicates low diversity in the TA community structure, which from 2000 CE is dominated by *Corythion dubium* ($> 50\,\%$) (Fig. 3a). The dominance of TA with idiosomic shells and the disappearance of species with agglutinated shells were inferred. TA shells become strongly compressed with small biovolumes and cryptic apertures. Reconstructed DWT is stable ~ 14 cm, and pH increases to 4.9 but with high model error (0.65). Surface vegetation consists mainly of *Cladonia* lichens ($> 85\,\%$), which appeared on peatland ca. 2000 CE (Fig. 5a). A peak in Ericaceae abundance was inferred, while other shrubs are absent. The low values of MIC indicate a decrease in regional fire activity; however, we found more MAC ($> 500\,\mu$m) particles in the sediment, which indicate that fire was present very locally (Fig. 6a). Organic matter content increases to 96 % and carbon accumulation to $\sim 15\,\mathrm{g\,m^{-2}\,yr^{-1}}$. Lichen and other moss accumulation rate is $1.4\,\mathrm{mm\,yr^{-1}}$.

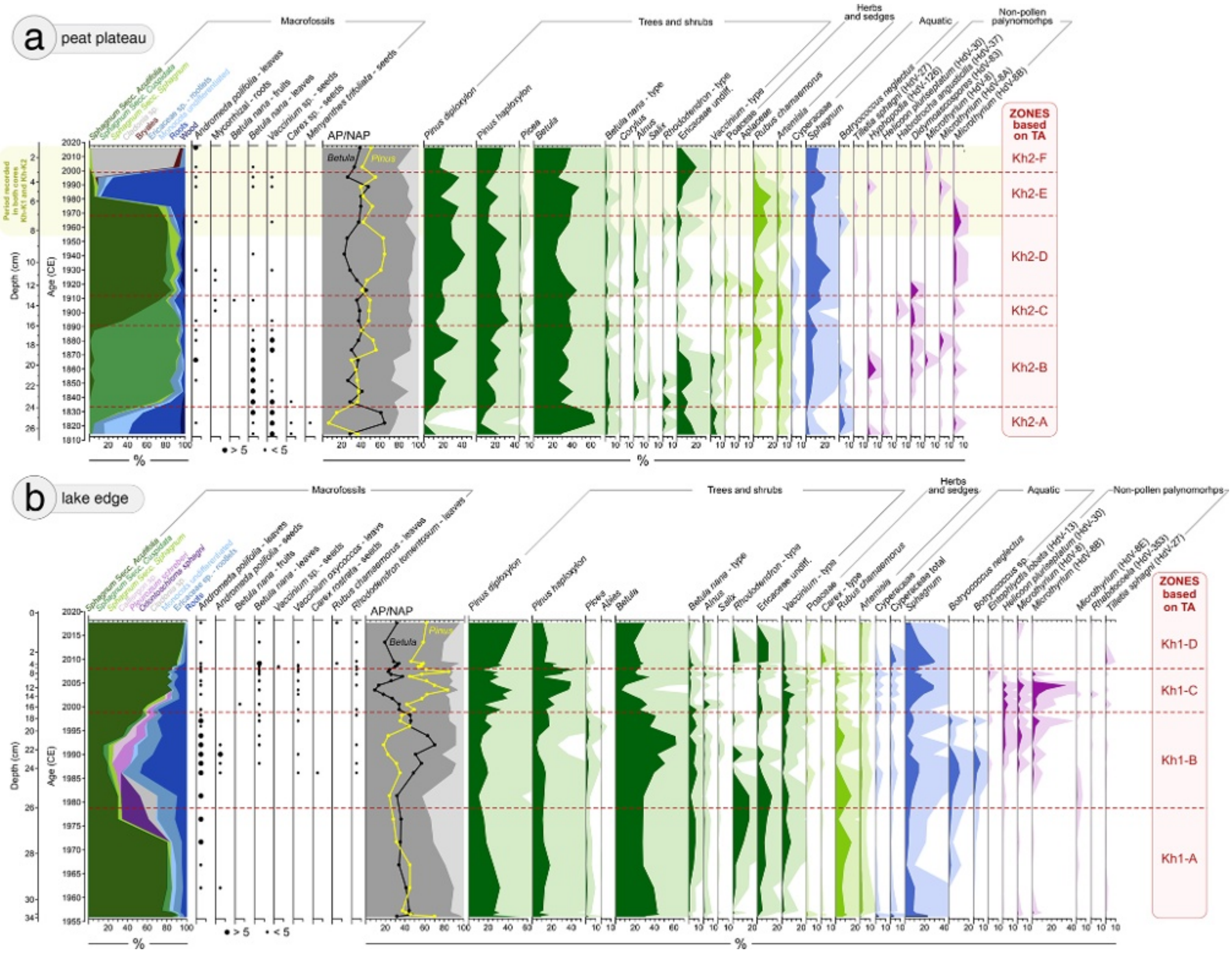

Figure 5. Macrofossils and pollen diagram with 5× exaggeration from peat cores: **(a)** Kh-K2 – peat plateau and **(b)** Kh-K1 – lake edge. The subfossil vegetative fragments and carpological remains are represented as either present or absent in each sample. Zonation based on testate amoebae CONISS was added to the graph.

4.2 Kh-K1 – lake edge (destabilised peat plateau margin)

4.2.1 Kh1-A (ca. 1955–1979 CE)

In the first zone Kh1-A, dry species *Alabasta militaris* and *Assulina muscorum* dominate at the beginning of the record (Bobrov et al., 1999). The abundance of *Assulina muscorum* subsequently decreases, while Unknown TA_Khan increases until 1979 CE. TA species with organic-coated idiosomic shells are highly abundant throughout the zone. Wet conditions were inferred at the beginning of the zone, followed by a rapid increase in DWT to 28 cm, which then slowly decreases to 17 cm by 1979 CE (Fig. 3b). The reconstructed pH indicates acidic conditions (pH = 4.8), with a slight increase in pH to 5.0 by 1979 CE. Local vegetation is dominated by *Sphagnum* Secc. *Acutifolia* with some addition of roots, rootlets, and monocots until ca. 1972 CE (Fig. 5b). As the DWT decreases liverworts *Odontoschisma sphagni* commonly found on *Sphagnum* hummocks/mounds but also on wet peat, appears (Blockeel et al., 2014), as well as lichens *Cladonia* sp. Both are present in the sediment between 1972 and 1986 CE. Shrubs pollen, particularly *Rhododendron*-type, and dwarf shrubs *Betula nana* increase after 1960 CE. An increase in abundance of green algae *Botryoccocus*, which indicates wetter conditions was inferred after ca. 1965 CE (Pandey et al., 2023). Peat and carbon accumulation is high initially (12.5–25 mm yr^{-1} and 24.4–79.0 g m^{-2} yr^{-1} respectively); however, as DWT increases after 1957 CE it slows down (2.1 mm yr^{-1} and 10 g m^{-2} yr^{-1}) (Fig. 6b). This zone is characterized by high MIC and MAC values until ca. 1965 CE, which indicates high local and regional fire activity.

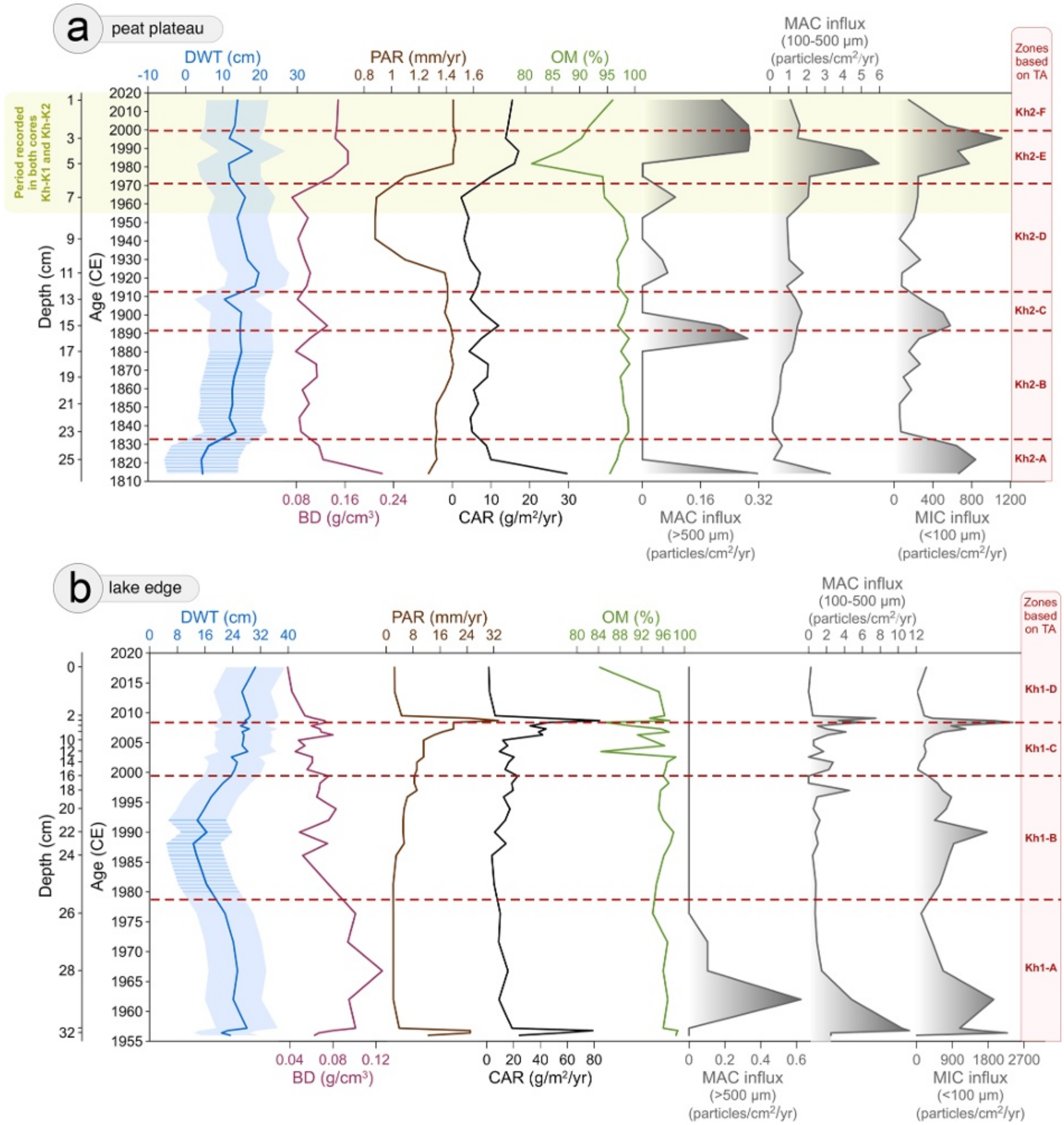

Figure 6. Changes in depth to water table (DWT) with bootstrap reconstruction errors (lighter blue), bulk density (BD), peat accumulation rate (PAR), carbon accumulation rate (CAR), organic matter content (OM), macrocharcoal influx > 500 and 100–500 µm (MAC), and microcharcoal influx < 100 µm (MIC) in peat cores **(a)** Kh-K2 – peat plateau and **(b)** Kh-K1 – lake edge. Zonation based on testate amoebae CONISS was added to the graph. The hatching on the DWT indicates a reconstruction potentially affected by error due to the presence of > 25 % of a new TA species.

4.2.2 Zone Kh1-B (ca. 1979–1999 CE)

In this zone, the structure of TA community changes (Figs. 7, 3b), TA species with agglutinated shells Unknown TA_Khan and *Cyclopyxis arcelloides* type, indicators of intermediate or relatively wet conditions, peak in abundance (Halaś et al., 2023; Warner and Charman, 1994). At the beginning of the zone *Euglypha ciliata* type is very abundant. *Galeripora discoides*, associated with rapid water table fluctuations (Lamentowicz et al., 2009), is present between 1992 and 1995 CE. After 1992 CE *Hyalosphenia elegans*, *Alabasta militaris*, and *Nebela tincta* start to appear more frequently in the record. TA shells become more compressed, and aperture size increases. Some mixotrophic species (e.g., *Placocista* *spinosa*) appear, which may indicate stable conditions, but heterotrophic species are still dominant. This zone is characterised by an initial decrease in DWT from 17 to 12 cm by 1988 CE, followed by a gradual increase, reaching 24 cm by 1999 CE. Higher pH was inferred on the site between 1980 and 1992 CE, but when drying starts, pH falls below 5.0 again. The peat is dominated by roots and Ericaceae sp. rootlets (Fig. 5b). *Sphagnum* Secc. *Acutifolia* accounts for ∼ 30 % of plant macrofossils. When lichens are present, more non-arboreal taxa, especially shrubs, e.g., Ericaceae and herb *Rubus chamaemorus*, were inferred. Lichens and liverworts are replaced ca. 1985 CE by *Calliergon* sp. and *Pleurozium schreberi*, which grows on drier hummocks/-mounds between wet *Sphagnum* (Street et al., 2013). More leaves and seeds of shrubs are found in the sediment after 1985 CE; however, the abundance of their pollen decreases. The most subfossil vegetative fragments belong to *Andromeda polifolia*, frequently found in low hummocks and lawns (Jacquemart, 1998). Abundance of green algae *Botryococcus* and *Sphagnum* spores starts to decline after ca. 1990 CE. Throughout the zone, a presence of fungi *Helicoon pluriseptatum* HdV-30, and fungal fruit bodies of *Microthyrium* HdV-8 and HdV-8B was inferred. Between 1980 and 1995 CE, *Betula* pollen is more abundant than *Pinus* pollen. The high MIC values indicate high regional fire activity, especially ca. 1990 CE (Fig. 6b). Organic matter content is high and stable ∼ 96 %. Peat and carbon accumulation is stable at the beginning of the zone but increases from 2.0 to 8.3 mm yr^{-1} and 3.8 to 23.1 g m^{-2} yr^{-1}, respectively, between 1988 and 2000 CE.

4.2.3 Kh1-C (ca. 1999–2008 CE)

In zone Kh1-C, the TA community structure changes again, with the most dominant species being *Alabasta militaris* (Figs. 3b, 7). We also inferred increased abundance of *Trigonopyxis arcula*, *Assulina muscorum*, and *Hyalosphenia elegans* in this period. Species with organic shells are more abundant, whilst agglutinated shells almost disappear. Characteristic of minerotrophic peatlands, *Heleopera rosea* is only present in this zone (Carballeira and Pontevedra-Pombal, 2021). The predominance of TA shells with smaller biovolume and aperture size with more cryptic position, indicate drier conditions. This zone is characterized by DWT ∼ 26 cm and pH 4.9. After 2003 CE, *Sphagnum* Secc. *Acutifolia* once again becomes a dominant species whilst other plant species disappear (Fig. 5b). Roots and leaves of shrubs are still abundant. The expansion of *Pinus* pollen, disappearance of shrub *Rhododendron*-type, and low frequency of herbs were inferred. Around 2000 CE, green algae *Botryococcus* disappears from the sediment. We inferred an increase of *Sphagnum* spores, which coincides with a peak in fungal fruit bodies of *Microthyrium* HdV-8B and HdV-8. *Helicoon pluriseptatum* HdV-30, indicators of a transition from wetter to drier conditions (Shumilovskikh et al., 2021), declines after 2008 CE, as well as other fungi. Throughout this zone, peat accumulation increases from 9.1 to 20.0 mm yr^{-1}, with the peak in 2008 CE (Fig. 6b). Organic matter content is unstable and varies from 84.4 % to 98.4 % between 2002 and 2008 CE. Periods with lower content of organic matter coincide with peaks in MAC (local fire activity). Carbon accumulation increases from 13.7 to 44.2 g m^{-2} yr^{-1} but decreases during periods when higher local fire activity was inferred.

4.2.4 Kh1-D (ca. 2008–2019 CE)

In the last zone, several TA species, e.g., *Cyclopyxis arcelloides* type and Unknown TA_Khan, disappear, while two new species *Cryptodifflugia voigti* (dry indicator) and *Corythion constricta* (intermediate) appear (Halaś et al., 2023) (Fig. 3b). The Shannon diversity index indicates a more homogeneous TA community structure dominated by *Alabasta militaris* (> 50 % of all shells). There is a dominance of TA species with smaller biovolume, more compressed shells, with smaller apertures, and idiosomic shells. In this zone the conditions are dry and stable with DWT ∼ 28 cm and pH 4.9 (Fig. 3b). Surface vegetation is dominated by *Sphagnum* Secc. *Acutifolia* with some roots, Ericaceae sp. rootlets, and monocots (Fig. 5b). Leaves of shrubs *Betula nana*, *Vaccinium oxycoccos*, and *Rhododendron tomentum* are still present, and *Pinus* pollen still dominates over *Betula* pollen. A high abundance of *Sphagnum* spores was inferred. The beginning of the zone is characterized by high peat (20.0–33.3 mm yr^{-1}) and carbon accumulation (45.0–84.0 g m^{-2} yr^{-1}) and high local and regional fire activity (high values of MIC and MAC) which significantly decrease after ca. 2009 CE (Fig. 6b). Following the intense fire period, peat and carbon accumulation slow down (2.5 mm yr^{-1} and 2.1 g m^{-2} yr^{-1}, respectively). Pollen of shrubs and sedges is more abundant after 2009 CE (Fig. 5b). Organic matter content for the top layer decreased to 84.2 %.

5 Discussion

5.1 Development of Western Siberian peatlands from the end of the Little Ice Age till modern times

Records from peat plateau core Kh-K2 show that at the beginning of the 19th century, the study site experienced wetter conditions with high carbon accumulation until ca. 1830 CE (Figs. 3a, 6a). On the Khanymei peatlands, this period was characterized by the presence of microalgae *Botryococcus*, typically found in fresh water wetlands (Pandey et al., 2023), which can also serve as an indicator of temporary water stagnation, as observed in Central European peatlands (Marcisz et al., 2015). Our results align with findings from more southeastern sites obtained by Feurdean et al. (2022) and Willis et al. (2015), where between 1400 and 1850 CE, an increase in water level was inferred. These reconstructions overlap with the presence of the Little Ice Age (LIA, 1600–1850 CE) in

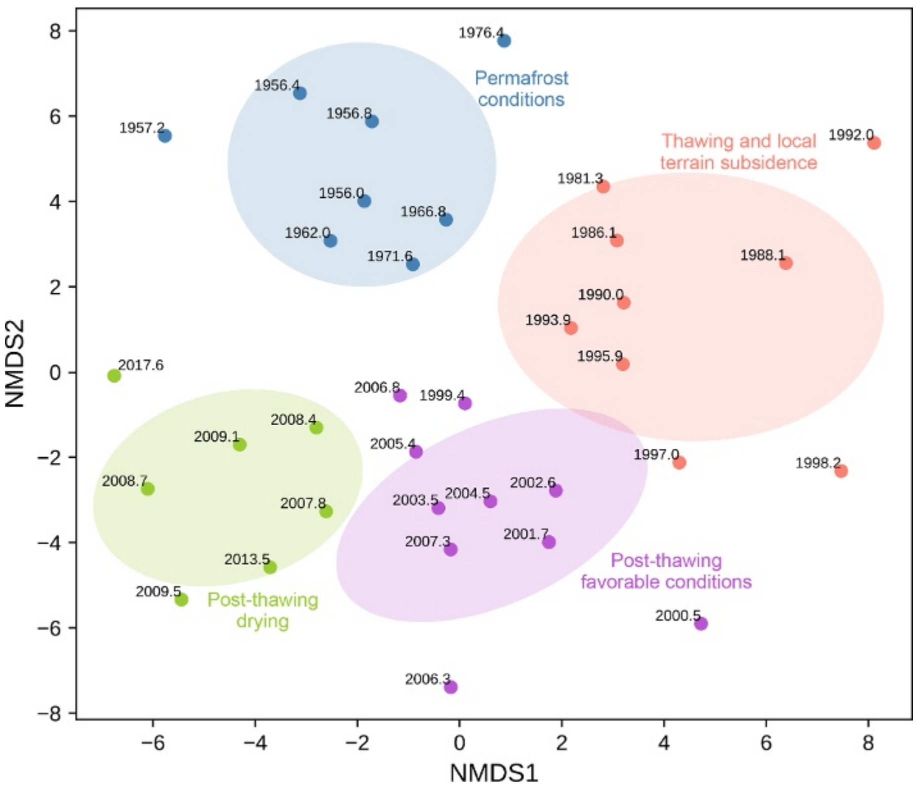

Figure 7. Two-dimensional NMDS ordination plot with K-Means clustering showing the distribution of testate amoebae samples from the Kh-K1 core (lake edge) over time. Ellipses represent the 95 % confidence interval based on the covariance matrix of each cluster. Each point represents a sample, with year labels indicating temporal changes.

the Northern Hemisphere (Mann, 2002). However, not all of the records from Western Siberia show the same trend; the LIA was a period of dry conditions on the southwest peatlands (Lamentowicz et al., 2015; Zakh et al., 2010). Although wetter conditions on a peatland usually limits fire activity (Nelson et al., 2021) on our site we inferred more local and regional fires (Fig. 6a). Higher fire activity and carbon accumulation at the end of LIA was also inferred on Plotnikovo Mire, where fires were associated with Russian exploration, which may also have affected the Khanymei region (Feurdean et al., 2019; Naumov, 2009).

After 1830 CE, the Khanymei site experienced drying, which resulted in the sudden disappearance of several TA species and increased acidification (Fig. 3a). The peatland was overtaken by *Sphagnum* Secc. *Cuspidata* and maintained a largely stable DWT till the end of the century (Fig. 3a). Period of drying (1830–1880 CE) overlaps with an increase in reconstructed mean June–July air temperature from tree rings in the Ob River valley (Gurskaya et al., 2012), and increased abundance of *Pinus* pollen. From 1885 CE, we inferred a transition of *Sphagnum* species from Secc. *Cuspidata* to *Acutifolia*, which indicate mound development (Malmer, 2014), this transition coincides with a decline of summer air temperature between 1880 and 1900 CE (Gurskaya et al., 2012) and follow a period of local fires (Fig. 6a). The post-fire recovery of *Sphagnum* Secc. *Acutifolia* was also observed on boreal peatlands in Western Canada (Kuosmanen et al., 2023) and Northern Europe (Sillasoo et al., 2011).

Different proxies like plant macrofossils, rhizopods, oribatid mites, diatoms, and testate amoebae have been tested as indicators of past environmental changes in permafrost peatlands (Lamarre et al., 2012; Markkula et al., 2018; Sannel and Kuhry, 2008; Wetterich et al., 2011). Markkula et al. (2018) demonstrated that some species of oribatid mites can be useful to detect past permafrost occurrence in peatlands; however, this proxy was not used in this study. Divergent plant succession trajectories in permafrost peatlands make it difficult to find a clear palaeoecological indicator of past aggradation (Treat et al., 2016). However, some studies suggest that the growth of *Sphagnum* Secc. *Acutifolia* in northern regions can precede permafrost aggradation (Pelletier et al., 2017; Sannel and Kuhry, 2009; Treat and Jones, 2018; Zoltai, 1993). This may indicate that on our site, permafrost started to aggrade ca. 1900 CE, taking advantage of the emergence of the denser and more insulating Secc. *Acutifolia* and periodic cooling in the summer months. Occurrence of *Sphagnum* Secc. *Acutifolia* and root/rootlet layers, which were considered by Sannel and Kuhry (2008) as indicators of permafrost conditions, can also serve as proof of permafrost presence on the study site after 1900 CE. However, because permafrost aggradation and degradation can co-occur within the same peatland (Zoltai, 1993), details regarding permafrost existence on the study site may be considered as a local process that needs more sites to be better understood in space.

The turn of the 19th century has also been marked by regional fires (Fig. 6a). Unfortunately, limited high-resolution fire records from Western Siberia make it difficult to compare if this fire period appears in a larger area. However, the increased regional fire activity may be linked to the fact that between 1896 and 1914 CE, Siberia became Russia's principal region of colonization (Goryushkin, 1991). Fire was widely used by new settlers for the construction of new roads and villages and the clearing of forests (Goryushkin, 1991). During dry and warm continental summers, these fires may have occasionally escaped control, leading to the spread of wildfires, that consumed drier peatland areas dominated by shrubs. After the period of higher fire activity, the region experienced a decrease in the shrub pollen, particularly Ericaceae and *Vaccinium*, as well as reduction in subfossil remains of *Betula nana* and *Vaccinium* on the peatland. This decrease in shrubs coincided with an increase in herbaceous species, particularly *Rubus chamaemorus* (Fig. 5a).

The beginning of the 20th century started with ca. 10 cm increase in DWT and an increased abundance of *Pinus* pollen (Figs. 3a, 5a). It is notable to mention that during *Pinus* pollen dominance (1920–1960 CE) there was a sequential emergence of fire-adapted Diploxylon pine species, followed by Haploxylon species that are better adapted to abiotic stress (Singh et al., 2023). Higher abundance of *Pinus* with higher resilience to drier conditions (Wei et al., 2019) and lower peat accumulation ($< 1.4\,\mathrm{mm\,yr^{-1}}$) may indicate the occurrence of a drier period in the Khanymei region. Although, the reduced peat accumulation may also be related to the presence of organic matter-decomposing fungi *Microthyrium* HdV-8B (Fig. 3a). Additionally, the period of increased presence of *Pinus* pollen coincides with the Early 20th Century Warming that started ca. 1910 CE and peaked in the 1940s, and could have contributed to the occurrence of drier conditions in the region (Bengtsson et al., 2004; Bokuchava and Semenov, 2021). However, the reconstruction of the DWT on peat plateau suggests that during this period, there was a gradual increase in moisture content (Fig. 3a). Potential explanations for the lower reconstructed DWT values on the peat plateau include the influence of low-lying permafrost, which creates different environmental conditions for testate amoebae – the microorganisms on which the reconstruction is based – compared to groundwater in non-permafrost peatlands (Zhang et al., 2017). In this context, the concept of a classic DWT level may not apply; rather, it reflects the specific moisture conditions of the mosses themselves. Notably, *Sphagnum* Sec. *Acutifolia*, which is present at the study site during that period, tends to grow in very dense patches, and its ability to maintain wet capitula through capillary water transport (Rydin and Jeglum, 2013) suggests that the reconstruction may not accurately represent commonly understood peatland ground water level (Baird and Low, 2022). On the other hand, higher air temperatures likely triggered permafrost thaw on the peat plateau, increasing peat moisture and ultimately leading to a decrease in the reconstructed DWT. As a result, reconstructing and interpreting water levels in permafrost peatlands requires caution due to the unique hydrological dynamics of these ecosystems.

Since 1970 CE, an increase in reconstructed summer mean air temperature in the Ob River valley and anomalies in surface annual temperature (SAT) in the Northern Hemisphere have been observed (Bokuchava and Semenov, 2021; Gurskaya et al., 2012). A warming climate also affects permafrost temperature, causing it to rise and leading to permafrost degradation, which can result in ground instability, altered hydrology, and changes in carbon dynamics (Streletskiy et al., 2015). Observations of permafrost temperature at 10 m in Nadym (260 km from Khanymei) showed increase of 1.3 °C between 1972 and 2009 CE (Romanovsky et al., 2010). These changes impacted the peatland ecosystems in Khanymei, where the marginal part of the peat plateau collapsed around 1980 CE (Fig. 3b). Between 1985 and 1995 CE, increasing moisture was inferred at the site, followed by a rise in peat and carbon accumulation rates (Fig. 6b). Similar, but more intensive patterns of collapse, followed by renewed productivity and peat accumulation, have been described in the Abisko region of Sweden (Swindles et al., 2015).

Increased regional fire activity recorded after 1970 CE indicates an overlap between natural fires and the human settlement expansion in the Khanymei region related to the construction of railways and oil exploration (Vaguet, 2013). Fires connected with gas and oil exploration were inferred at a similar time at the Mukhrino mire in the southern part of Western Siberia close to Khanty-Mansiysk (Lamentowicz et al., 2015). Excessive construction activity in the close vicinity of the study area (< 15 km) may have also contributed to a decrease in organic matter content, caused by a large supply of dust around 1980 CE (Fig. 6a). Data from the peat core Kh-K1 (1955–2020 CE) with higher temporal resolution, identified two distinct periods of higher fire activity in the region after 1970: 1985–1995 and 2006–2009 CE (Fig. 6b). Lower regional fire activity in our records in the last decades coincides with a decrease in burned area observed in Western Siberia after 2010 CE (Zhu et al., 2021). However, Zhu et al. (2021) noted that between 2003 and 2020 CE, wildfire extent in Siberia has been expanding westward, which may suggest that as climate change progresses, Western Siberia might be more affected by wildfires in the near future.

Fire activity in the peatland surroundings probably influenced shrub abundance in the area. We recognised a decrease in shrub pollen after 1880 CE, coinciding with a slight increase in local fire activity that persisted until 2000 CE, when shrubs, particularly Ericaceae, began to return (Figs. 5a, 6a).

Data from core Kh-K1 provide more detailed insights, showing that shrubs became more abundant after 1965 CE. However, increased local fires between 1990 and 2010 CE once again led to a decline in shrub presence, followed by their reappearance after 2010 CE (Figs. 5b, 6b). Although shrubification is more commonly discussed in the context of the Arctic tundra (Buttler et al., 2023; Mekonnen et al., 2021), Forbes et al. (2010) recorded the effect of warming on shrub rings in the northwest Russian Arctic, with correlations extending over long distances into the taiga zone of Western Siberia. Their findings revealed a clear *greening* trend at a regional scale from 1981 to 2005 CE, aligning with studies that have attributed a strong shrub component to the greening signal since 1980 CE. A similar signal is visible in our study site; however, it appears approximately 20 years earlier.

Increased air temperatures and higher fire activity in the past decades have impacted permafrost in Siberia, which remains in equilibrium with changing climate, continuous to alter peatland surface (Shur and Jorgenson, 2007). As permafrost gradually degrades, the height difference between the peat plateau and depression increases, exposing the peat plateau to environmental influences. A similar process occurs when ice aggrades within the peat, causing the bog surface to uplift (Thibault and Payette, 2009). This creates drier conditions at the uplifted peatland surface, leading to the replacement of *Sphagnum* mosses with lichens (Seppälä, 1988; Thibault and Payette, 2009), which happened on the study site ca. 2000 CE (Fig. 5a).

5.2 Patterns of progressive permafrost thawing

Permafrost peatlands underwent significant but divergent hydrological changes in recent decades due to rising air temperatures and related permafrost thaw (Olefeldt et al., 2021; Zhang et al., 2022). In Khanymei permafrost peatlands, thaw-related surface transformation triggered changes in various elements of the ecosystem. Paleoreconstructions from peat cores Kh-K1 and Kh-K2 that cover the period from 1955 CE allowed the reconstruction of biological responses of peatland's microhabitats and the creation of patterns of progressive permafrost thawing in a discontinuous permafrost zone (Fig. 8).

In the first stage, before thawing ca. 1979 CE, the peat plateau was characterized by dry conditions and lichen coverage (Fig. 8a). The presence of lichens temporarily constrains moss growth on peat plateau (Harris et al., 2018), which resulted in lower peat and carbon accumulation rates (Fig. 5a). Lichens are commonly found on mature peat mounds and palsas (Railton and Sparling, 1973), but their relatively low albedo reduces evapotranspiration, which can negatively affect ground cooling during the summer (Rönkkö and Seppälä, 2003). The underlying porous peat typically serves as an insulator for permafrost; however, thawing and melting water are strongly absorbed by the peat, and with limited evapotranspiration, this leads to a decreased insulating effect and the deepening of the active layer. With higher air temperatures and the occurrence of fires, these changes accelerate permafrost degradation, leading to further thawing and surface transformation (Biskaborn et al., 2019; Hantemirov et al., 2022; Romanovsky et al., 2010).

As thawing began after 1979 CE, the deepening of the active layer released water, which, due to limited drainage, accumulated in low-lying parts of the peat plateau, leading to terrain subsidence and local inundation (Fig. 8b). A simulation of ground subsidence run by Ekici et al. (2019) showed that between 2000–2010 some parts of Western Siberia experienced land subsidence of up to 0.7 m. This process has also been widely observed in permafrost areas in Canada (O'Neill et al., 2023; Wang et al., 2024). The higher moisture of subsided areas contributes to the submergence of lichens and their overgrowth by *Sphagnum* mosses. Wetter conditions also change the structure of TA communities to be dominated by wet (*C. arcelloides* type) and intermediate species (Unknown TA_Khan) and cause the emergence of various species of microalgae *Botryococcus* (Figs. 3b, 5b, 7).

Characteristic of this stage is the presence of new unidentified TA taxa (Unknown TA_Khan) (Fig. 4), which has an ampulla-shaped test with larger mineral particles, previously found in modern samples from Khanymei peatland and classified by Halaś et al. (2023) as *Difflugia lucida* type. This taxon was rare in modern samples and mainly present in lichens with an optimum water level of ∼ 9 cm, while in *Sphagnum* mosses mostly in wetter sites (∼ 3 cm). The unknown taxa is an agglutinated xenosomic TA type that constructs its shells using grains and diatoms from its environment (Ogden and Hedley, 1980), with its presence significantly influenced by the water chemistry of its surroundings (Mitchell et al., 2000). Typical processes associated with permafrost thaw, such as soil subsidence, lichen submergence, and peat abrasion, impact the water chemistry in the region (Manasypov et al., 2017). Experiments conducted by Manasypov et al. (2017) indicate that submerged lichens and peat abrasion efficiently enrich lake water with soluble organic constituents and alter the chemical composition of thaw water, with lichens having the greatest impact. Therefore, we hypothesize that this specific water chemistry may influence the appearance of this taxa in the Khanymei peatland; however, further research is needed.

Water availability is considered one of the most critical factors of *Sphagnum* growth and decay, and therefore carbon accumulation (Bengtsson et al., 2016; Thompson and Waddington, 2008). Compared to the pre-thawing phase, rising water levels caused by thawing and terrain subsidence boosted peat and carbon accumulation on the lake edge (Figs. 6b, 8b). The shift from drier to wetter conditions may reduce fire severity (Nelson et al., 2021), as inferred in this study, as local fire activity decreases with slight wetting (Fig. 6b).

Further thawing significantly altered the peatland ecosystem structure (Fig. 8c). Further subsidence contributes to the formation of depressions filled with thaw water, creating small thermokarst lakes. Although there is an overall decline in the area of thermokarst lakes in discontinuous permafrost zones (Smith et al., 2005; Webb and Liljedahl, 2023), small lakes are still being formed (Polishchuk et al., 2015). Our data suggests that further thawing led to better drainage and accumulation of thawed water in the lake basin, causing drying of the lake edges. These contradict the typical dry plateau-wet hollow pattern and can be explained by the characteristics of the TA that were used in DWT reconstruction. TA is widely used to reconstruct DWT on peatlands (e.g., Charman et al., 2007); however, the primary control of species abundance is surface wetness (Woodland et al., 1998). Wetter conditions reconstructed on the peat plateau resulted from low-lying permafrost ∼ 27 cm (Fig. 1d), which, during the thaw, increase peat moisture, influencing TA assemblages. Whereas on the lake edge, permafrost is absent, these assemblages are more vulnerable to *Sphagnum* surface drying, a process that is accelerated by increased evapotranspiration. Together with the drying of the peatland surface, we inferred an increase in local fire activity, similar to the pre-thawing period. Another important observation was that together with permafrost thawing we noted an increased abundance of several *Microthyrium* type fungal fruit bodies on the lake edge (type HdV-8 and HdV-8B) (Fig. 5b). In our study the highest abundance of HdV-8B fell in the period preceding the highest accumulation of peat and carbon but coincided with the greatest production of spores by *Sphagnum*. Given that fungi are involved in organic matter decomposition (Mitchell et al., 2003), this pattern may reflect a phase of active decomposition that preceded maximum peat accumulation. While we refrain from drawing firm conclusions, we consider this an intriguing signal that may warrant further investigation, particularly in light of the currently limited understanding of the ecological significance of these fungal remains.

Many studies have indicated that global warming and permafrost thawing will convert high-latitude peatlands from a net atmospheric carbon sink to a source (Abbott et al., 2016; Harris et al., 2023; Schuur et al., 2015). However, this shift may not be linear due to the complexity of plant-microbial-soil interactions and the potential mitigation of carbon losses through enhanced plant productivity (Berner et al., 2020; Epstein et al., 2013; Standen and Baltzer, 2021). In our study, increases in peat and carbon accumulation were inferred in both the peat plateau and lake edge sites after thawing began ca. 1979 CE, with the lake edge site being the most active in accumulation (Figs. 6, 8c). Although wetter conditions, considered better for *Sphagnum* growth (Clymo, 1973), occurred in the subside area in the previous stage, increased peat accumulation was still inferred even after the DWT increases. This suggests that thawing re-invigorated moss productivity by providing the necessary moisture, allowing them to continue benefiting from the additional water supply even many years after the collapse (Swindles et al., 2015). Vivid growth could also be explained by the dense structure of the dominant species of *Sphagnum* Secc. *Acutifolia* that could still maintain a high rate of photosynthesis after DWT increases (Rydin and Jeglum, 2013). A higher abundance of *Sphagnum* spores during this time confirms their robust potential for reproduction and colonization (Fenton and Bergeron, 2006). We hypothesize that the high values of peat and carbon accumulation inferred at the lake edge were a direct consequence of beneficial conditions created by thawing in the previous stage. Our study suggests that these favourable conditions have already happened on this part of the peatland, they were short-term and occurred in a limited area (Figs. 6b, 8c). However, it is important to note that different stages of permafrost degradation can occur simultaneously within the region, as shown by Swindles et al. (2015). Therefore, while our results are local, they highlight potential patterns of permafrost degradation and associated environmental consequences that may arise at different times in the Khanymei region or other areas with discontinuous permafrost in Western Siberia.

5.3 Same mire – different perspective

The majority of palaeoecological reconstructions on peatlands are based on one or a few cores located in the same area to study local history (e.g., Lamentowicz et al., 2015; Novenko et al., 2023) or hundreds of kilometres to reconstruct regional history or trends (e.g., Feurdean et al., 2022; Willis et al., 2015; Zhang et al., 2022). In this study, we focused on the differences between peat plateau-depression (lake edge, in this case) microhabitats. Our multi-proxy analysis showed that these microhabitats react differently, particularly in site-specific elements such as: peat and carbon accumulation, hydrology, plant macrofossil composition and occurrence of fungal NPPs (Figs. 3, 5, 6). The microhabitats described in our study are a characteristic feature of the landscape of discontinuous permafrost peatlands in Western Siberia. Our results show that peatland surface heterogeneity, especially in permafrost areas, leads to the occurrence of various simultaneous processes.

In non-permafrost regions, the typical hummock-hollow structure is in a certain state of equilibrium directly related to hydro-climatic conditions (Kulczyński, 1939; Rydin and Jeglum, 2013; Tobolski, 2000). Whereas in regions of discontinuous permafrost, palsa or peat plateaus/mounds are adjacent to the unfrozen peatlands or thermokarst lakes (Seppälä, 2011). The situation is specific because two very different environments are in close vicinity to each other. In this study, we distinguished two main zones within a short distance: stable and dynamic (Fig. 8).

The stable zone is characterized by the presence of permafrost in the ground, which creates stable conditions and an equilibrium on the peatland surface. In this zone, the water level was relatively stable or rising due to increase peat moisture from thawing. However, the processes occurring there were gradual and extended over time due to the pres-

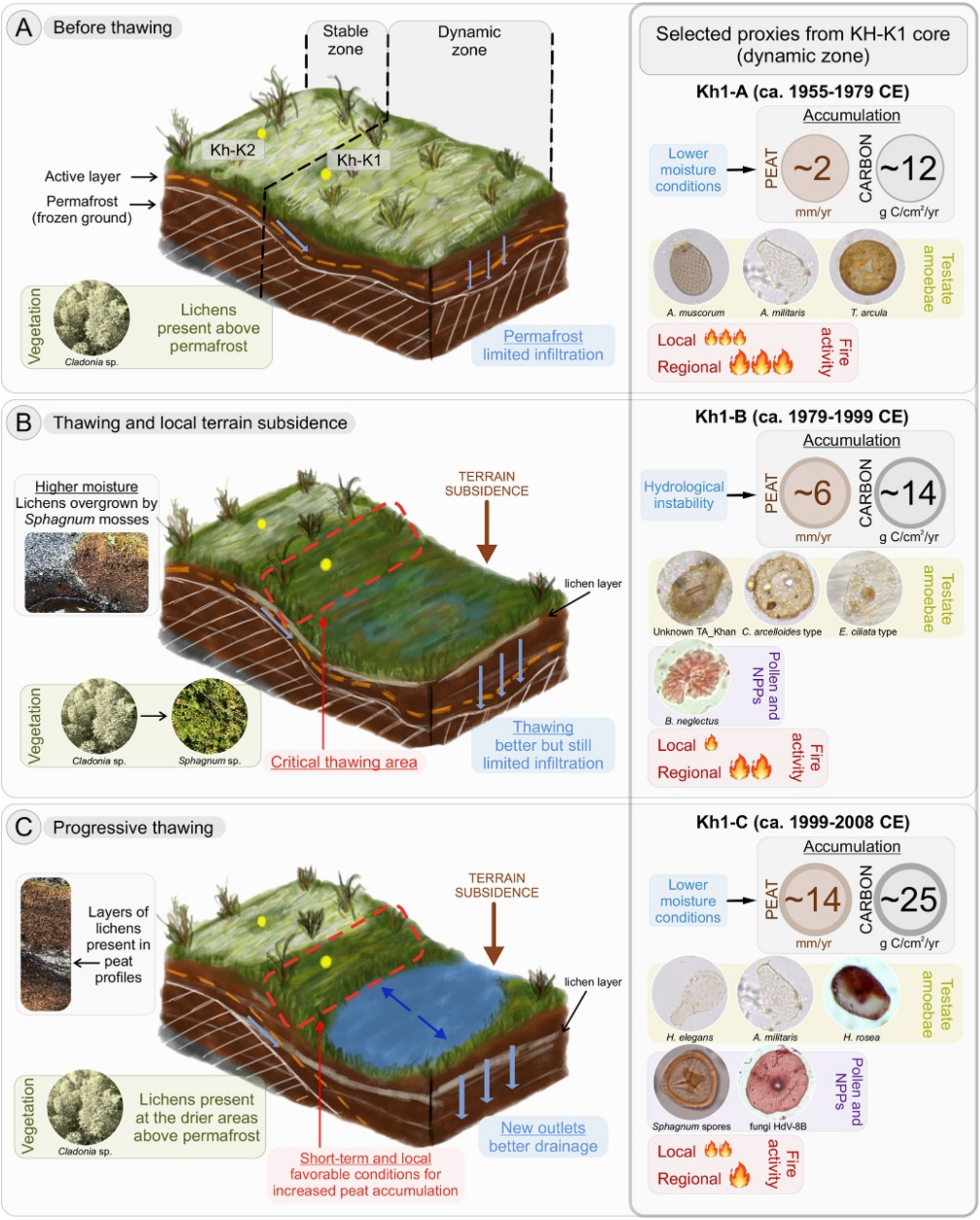

Figure 8. Illustration of stages of the progressive permafrost thawing in a discontinuous permafrost peatland based on cores Kh-K1 (lake edge) and Kh-K2 (peat plateau) with selected proxies. In the illustration, core Kh-K1 represents the dynamic zone, and core Kh-K2 represents the stable zone. The values for peat and carbon accumulation rates and intensity of fire activity shown in the right panel represent mean values from selected zones of core Kh-K1. Pictures of lichens, mosses, and peat profiles on the left panel come from the other peatlands in region to better present the process of lichen-*Sphagnum* shifts. Sources: photos of *Sphagnum* spores from Inglis et al. (2015).

ence of permafrost. In contrast, in the dynamic zone, thawing initially triggers cascading hydrological changes, consequently forcing habitat shifts (Figs. 3, 5, 6). These changes mostly occur in the lateral part of peat plateau, where data from the lake edge core (Kh-K1) allowed us to identify a critical thawing area (Fig. 8b). The described area is a part of the dynamic zone with the most noticeable and rapid changes due to its location between contrasting environments: a previously thawed and collapsed depression, and an ice-rich peat plateau (Fig. 8b). As a consequence of hydrological changes, expanding permafrost thawing leads to relatively rapid increase in DWT as a result of drainage towards the formed slough (Fig. 8c). However, only in this area a rapid but short-term improvement in hydrological conditions, with a simultaneous rapid increase in peat and carbon accumulation was reconstructed (Fig. 6b). This mechanism makes this area the most dynamic part of the peatland where permafrost thaw occurs.

The lateral part of the peat plateau (critical thawing area) where we inferred the most significant changes, although relatively small, has a significant impact on the permafrost core in the adjacent peat plateau. Post-thaw wetter peat conditions on the peat plateau margin allow higher heat penetration of the permafrost core (Railton and Sparling, 1973), accelerating its thaw and reducing plateau size. Currently, the shifting of this area and consequent increase in the area of drainless depressions and decrease in peat plateaus area is observed yearly, resembling a domino effect. These depressions eventually merge with adjacent ones to form larger lakes, which ultimately drain into a watercourse or river. Degradation of palsas and peat plateaus caused by lateral erosion and the formation of thermokarst lakes has also been observed in northern Norway, where since the 1950s, their total area has decreased by 33 %–71 %, depending on the region (Borge et al., 2017).

It is important to emphasize that the high variability of permafrost peatlands requires careful interpretation of environmental records. Without a comprehensive approach, changes inferred in the peat profile might be misattributed to incorrect factors. Therefore, conducting multi-proxy analyses is essential to ensure accurate reconstruction of past and present environmental conditions in areas with current or past permafrost.

6 Conclusions

Our multi-proxy reconstruction provided new insights into the history of peatlands in the understudied region of Western Siberia. On Khanymei peatlands, the end of the Little Ice Age was marked by wetter conditions that predominated until 1840 CE. This period was followed by peatland drying and an increase in regional fire activity. Later peaks of increased regional fires correspond to key historical events, including the Russian colonization of Siberia at the beginning of the 20th century and intensified oil and gas exploration after 1970 CE. Plant indicators suggest that permafrost likely began to aggrade on the study site around 1900 CE. The presence of an ice core within the peat plateau limited moss growth, leading to low peat and carbon accumulation. In recent decades, rising air temperatures have triggered permafrost thaw, transforming peatlands' ecosystem. Notably, the most dynamic changes occurred after 1979 CE, exhibiting considerable variation across different parts of the peatland. Our research highlights that permafrost thaw in the discontinuous permafrost zone in Western Siberia has driven significant but local transformations in peatland hydrology, vegetation, and microbial communities, with the lake edge being the most dynamic microhabitat. Thaw-related surface subsidence increased water availability, promoting *Sphagnum* growth and carbon accumulation, though these favourable conditions were short-term and limited to specific areas. Significant changes in testate amoebae communities and increased fungal activity indicate complex interactions between thaw dynamics and microbial processes, with potential implications for carbon cycling. Our findings underscore the nonlinear and spatially variable nature of permafrost thaw effects on peatlands, emphasizing that favourable conditions for carbon sequestration may only be temporary as warming continues.

Our study's strength lies in its comprehensive and high-resolution palaeoecological methodology, which enables the detection of even subtle alterations in permafrost conditions. However, these subtle changes can rapidly escalate into dramatic landscape transformations under continued warming. Our study serves as an early warning signal of climate-induced impacts on this fragile ecosystem. Ultimately, our results demonstrate the importance of incorporating microhabitat-specific responses to warming in climate models to more accurately predict future carbon gains or losses from northern peatlands.

Data availability. The dataset underlying this study is openly available at Zenodo: https://doi.org/10.5281/zenodo.15543975 (Halaś et al., 2025).

Supplement. The supplement related to this article is available online at https://doi.org/10.5194/bg-22-4797-2025-supplement.

Author contributions. AH wrote the original draft, performed testate amoebae, macrocharcoal, LOI analysis, conducted all statistical analysis and prepared all figures and tables. MS performed plant macrofossil analysis, selected material for AMS radiocarbon dating and supervised the research. MO performed pollen and microcharcoal analysis. ML, DŁ, and MS collected data in the field. All authors read, reviewed, edited, and approved the final version of the manuscript.

Competing interests. The contact author has declared that none of the authors has any competing interests.

Disclaimer. Publisher's note: Copernicus Publications remains neutral with regard to jurisdictional claims made in the text, published maps, institutional affiliations, or any other geographical representation in this paper. While Copernicus Publications makes every effort to include appropriate place names, the final responsibility lies with the authors. Also, please note that this paper has not received English language copy-editing.

Acknowledgements. The authors thank Sergey Loiko, Alexandr O. Konstantinov, and Ivan Kritskov for help during the fieldwork, Irena Hajdas (ETH Zürich, Switzerland) for help with the age-depth model calculation, Michał Brzozowski (Poznań University of Life Sciences, Poland) for help with liverworts identification, Jerzy Jonczak (SGGW, Poland) for help with LOI analysis, Chloé Giraud (UQAM, Canada) for help with testate amoebae photos, and Harry Roberts (IGSO PAS, Poland) for English corrections. We would like to thank the reviewers for their valuable comments and constructive suggestions, which improved the quality of this manuscript.

Financial support. This study was supported by the National Science Centre in Poland (grant nos. 2019/35/O/ST10/02903 and 2021/41/B/ST10/00060), and field research at the Khanymei Research Station was possible thanks to the EU Horizon 2020 INTERACT (project no. 730938).

Review statement. This paper was edited by Mark Lever and reviewed by Yuri Mazei and one anonymous referee.

References

Abbott, B. W., Jones, J. B., Schuur III, E. A. G.„ F. S. C., Bowden, W. B., Bret-Harte, M. S., Epstein, H. E., Flannigan, M. D., Harms, T. K., Hollingsworth, T. N., Mack, M. C., McGuire, A. D., Natali, S. M., Rocha, A. V., Tank, S. E., Turetsky, M. R., Vonk, J. E., Wickland, K. P., Aiken, G. R., Alexander, H. D., Amon, R. M. W., Benscoter, B. W., Bergeron, Y., Bishop, K., Blarquez, O., Bond-Lamberty, B., Breen, A. L., Buffam, I., Cai, Y., Carcaillet, C., Carey, S. K., Chen, J. M., Chen, H. Y. H., Christensen, T. R., Cooper, L. W., Cornelissen, J. H. C., Groot, W. J. de, DeLuca, T. H., Dorrepaal, E., Fetcher, N., Finlay, J. C., Forbes, B. C., French, N. H. F., Gauthier, S., Girardin, M. P., Goetz, S. J., Goldammer, J. G., Gough, L., Grogan, P., Guo, L., Higuera, P. E., Hinzman, L., Hu, F. S., Hugelius, G., Jafarov, E. E., Jandt, R., Johnstone, J. F., Karlsson, J., Kasischke, E. S., Kattner, G., Kelly, R., Keuper, F., Kling, G. W., Kortelainen, P., Kouki, J., Kuhry, P., Laudon, H., Laurion, I., Macdonald, R. W., Mann, P. J., Martikainen, P. J., McClelland, J. W., Molau, U., Oberbauer, S. F., Olefeldt, D., Paré, D., Parisien, M.-A., Payette, S., Peng, C., Pokrovsky, O. S., Rastetter, E. B., Raymond, P. A., Raynolds, M. K., Rein, G., Reynolds, J. F., Robards, M., Rogers, B. M., Schädel, C., Schaefer, K., Schmidt, I. K., Shvidenko, A., Sky, J., Spencer, R. G. M., Starr, G., Striegl, R. G., Teisserenc, R., Tranvik, L. J., Virtanen, T., Welker, J. M., and Zimov, S.: Biomass offsets little or none of permafrost carbon release from soils, streams, and wildfire: an expert assessment, Environ. Res. Lett., 11, 034014, https://doi.org/10.1088/1748-9326/11/3/034014, 2016.

Abe-Ouchi, A., Saito, F., Kageyama, M., Braconnot, P., Harrison, S. P., Lambeck, K., Otto-Bliesner, B. L., Peltier, W. R., Tarasov, L., Peterschmitt, J.-Y., and Takahashi, K.: Ice-sheet configuration in the CMIP5/PMIP3 Last Glacial Maximum experiments, Geosci. Model Dev., 8, 3621–3637, https://doi.org/10.5194/gmd-8-3621-2015, 2015.

Alexandrov, G. A., Brovkin, V. A., and Kleinen, T.: The influence of climate on peatland extent in Western Siberia since the Last Glacial Maximum, Sci. Rep., 6, 24784, https://doi.org/10.1038/srep24784, 2016.

Baird, A. J. and Low, R. G.: The water table: Its conceptual basis, its measurement and its usefulness as a hydrological variable, Hydrol. Process., 36, e14622, https://doi.org/10.1002/hyp.14622, 2022.

Beilman, D. W., MacDonald, G. M., Smith, L. C., and Reimer, P. J.: Carbon accumulation in peatlands of West Siberia over the last 2000 years, Glob. Biogeochem. Cycles, 23, https://doi.org/10.1029/2007GB003112, 2009.

Bengtsson, F., Granath, G., and Rydin, H.: Photosynthesis, growth, and decay traits in Sphagnum – a multispecies comparison, Ecol. Evol., 6, 3325–3341, https://doi.org/10.1002/ece3.2119, 2016.

Bengtsson, L., Semenov, V. A., and Johannessen, O. M.: The Early Twentieth-Century Warming in the Arctic—A Possible Mechanism, J. Climate, 17, 4045–4057, https://doi.org/10.1175/1520-0442(2004)017<4045:TETWIT>2.0.CO;2, 2004.

Berglund, B. E. and Ralska-Jasiewiczowa, M.: Pollen analysis and pollen diagrams, Handb. Holocene Palaeoecol. Palaeohydrology, 455, 484–486, 1986.

Berner, L. T., Massey, R., Jantz, P., Forbes, B. C., Macias-fauria, M., Myers-smith, I., Kumpula, T., Gauthier, G., Andreu-hayles, L., Gaglioti, B. V., Burns, P., Zetterberg, P., D'arrigo, R., and Goetz, S. J.: Summer warming explains widespread but not uniform greening in the Arctic tundra biome, Nat. Commun., 11, 4621, https://doi.org/10.1038/s41467-020-18479-5, 2020.

Beug, H.-J.: Leitfaden der Pollenbestimmung: für Mitteleuropa und angrenzende Gebiete, Pfeil, Dr. Friedrich, Munchen, 542 pp., ISBN 3 89937 043 0, 2004.

Biskaborn, B. K., Smith, S. L., Noetzli, J., Matthes, H., Vieira, G., Streletskiy, D. A., Schoeneich, P., Romanovsky, V. E., Lewkowicz, A. G., Abramov, A., Allard, M., Boike, J., Cable, W. L., Christiansen, H. H., Delaloye, R., Diekmann, B., Drozdov, D., Etzelmüller, B., Grosse, G., Guglielmin, M., Ingeman-Nielsen, T., Isaksen, K., Ishikawa, M., Johansson, M., Johannsson, H., Joo, A., Kaverin, D., Kholodov, A., Konstantinov, P., Kröger, T., Lambiel, C., Lanckman, J.-P., Luo, D., Malkova, G., Meiklejohn, I., Moskalenko, N., Oliva, M., Phillips, M., Ramos, M., Sannel, A. B. K., Sergeev, D., Seybold, C., Skryabin, P., Vasiliev, A., Wu, Q., Yoshikawa, K., Zheleznyak, M., and Lantuit, H.: Permafrost is warming at a global scale, Nat. Commun., 10, 264, https://doi.org/10.1038/s41467-018-08240-4, 2019.

Blockeel, T. L., Bosanquet, S. D. S., Hill, M. O., Preston, C. D., and Society, B. B.: Atlas of British & Irish Bryophytes: The Distribution and Habitat of Mosses and Liverworts in Britain and Ireland, Pisces Publications, 652 pp., ISBN 978-1-874357-66-7, 2014.

Bobrov, A. A., Charman, D. J., and Warner, B. G.: Ecology of Testate Amoebae (Protozoa: Rhizopoda) on Peatlands in Western Russia with Special Attention to Niche Separation in Closely Related Taxa, Protist, 150, 125–136, https://doi.org/10.1016/S1434-4610(99)70016-7, 1999.

Bokuchava, D. D. and Semenov, V. A.: Mechanisms of the Early 20th Century Warming in the Arctic, Earth-Sci. Rev., 222, 103820, https://doi.org/10.1016/j.earscirev.2021.103820, 2021.

Booth, R. K., Lamentowicz, M., and Charman, D. J.: Preparation and analysis of testate amoebae in peatland palaeoenvironmental studies, Mires Peat, 7, 1–7, 2010.

Borge, A. F., Westermann, S., Solheim, I., and Etzelmüller, B.: Strong degradation of palsas and peat plateaus in northern Norway during the last 60 years, The Cryosphere, 11, 1–16, https://doi.org/10.5194/tc-11-1-2017, 2017.

Bottjer, D. J.: Paleoecology: Past, Present and Future, John Wiley & Sons, 272 pp., ISBN 978-1-118-45584-5, 2016.

Brown, J., Ferrians Jr., O. J., Heginbottom, J. A., and Melnikov, E. S.: Circum-Arctic map of permafrost and ground-ice conditions, Circum-Pac. Map, USGS [data set], https://doi.org/10.3133/cp45, 1997.

Bulygina, O. N., Groisman, P. Y., Razuvaev, V. N., and Korshunova, N. N.: Changes in snow cover characteristics over Northern Eurasia since 1966, Environ. Res. Lett., 6, 045204, https://doi.org/10.1088/1748-9326/6/4/045204, 2011.

Buttler, A., Bragazza, L., Laggoun-Défarge, F., Gogo, S., Toussaint, M.-L., Lamentowicz, M., Chojnicki, B. H., Słowiński, M., Słowińska, S., Zielińska, M., Reczuga, M., Barabach, J., Marcisz, K., Lamentowicz, Ł., Harenda, K., Lapshina, E., Gilbert, D., Schlaepfer, R., and Jassey, V. E. J.: Ericoid shrub encroachment shifts aboveground–belowground linkages in three peatlands across Europe and Western Siberia, Glob. Change Biol., 29, 6772–6793, https://doi.org/10.1111/gcb.16904, 2023.

Carballeira, R. and Pontevedra-Pombal, X.: Diversity of Testate Amoebae as an Indicator of the Conservation Status of Peatlands in Southwest Europe, Diversity, 13, 269, https://doi.org/10.3390/d13060269, 2021.

Chambers, F. M. and Charman, D. J.: Holocene environmental change: contributions from the peatland archive, The Holocene, 14, 1–6, https://doi.org/10.1191/0959683604hl684ed, 2004.

Chambers, F. M., Beilman, D. W., and Yu, Z.: Methods for determining peat humification and for quantifying peat bulk density, organic matter and carbon content for palaeostudies of climate and peatland carbon dynamics, Mires Peat, 7, 1–10, http://www.mires-and-peat.net/, ISSN 1819-754X, 2011.

Charman, D. J., Hendon, D., and Woodland, W. A.: The identification of testate amoebae (Protozoa: Rhizopoda) in peats: QRA Technical Guide No. 9, Quaternary Research Asociation, London, https://doi.org/10.1016/j.quascirev.2004.03.008, 2000.

Charman, D. J., Blundell, A., and ACCROTELM: A new European testate amoebae transfer function for palaeohydrological reconstruction on ombrotrophic peatlands, J. Quat. Sci., 22, 209–221, https://doi.org/10.1002/jqs.1026, 2007.

Clymo, R. S.: The Growth of Sphagnum: Some Effects of Environment, J. Ecol., 61, 849–869, https://doi.org/10.2307/2258654, 1973.

Conedera, M., Tinner, W., Neff, C., Meurer, M., Dickens, A. F., and Krebs, P.: Reconstructing past fire regimes: methods, applications, and relevance to fire management and conservation, Quat. Sci. Rev., 28, 555–576, https://doi.org/10.1016/j.quascirev.2008.11.005, 2009.

Davydova, M. I. and Rakovskaya, E. M.: Fizičeskaja geografija SSSR [Physical Geography of the USSR], Prosveshenie, Moscow, USSR, 304 pp., ISBN 5-09-000965-1, 1990.

De Klerk, P., Donner, N., Joosten, H., Karpov, N. S., Minke, M., Seifert, N., and Theuerkauf, M.: Vegetation patterns, recent pollen deposition and distribution of non-pollen palynomorphs in a polygon mire near Chokurdakh (NE Yakutia, NE Siberia), Boreas, 38, 39–58, https://doi.org/10.1111/j.1502-3885.2008.00036.x, 2009.

Duchkov, A. D.: Characteristics of permafrost in Siberia, in: Advances in the Geological Storage of Carbon Dioxide, Dordrecht, 81–91, https://doi.org/10.1007/1-4020-4471-2_08, 2006.

Ekici, A., Lee, H., Lawrence, D. M., Swenson, S. C., and Prigent, C.: Ground subsidence effects on simulating dynamic high-latitude surface inundation under permafrost thaw using CLM5, Geosci. Model Dev., 12, 5291–5300, https://doi.org/10.5194/gmd-12-5291-2019, 2019.

Epstein, H. E., Myers-Smith, I., and Walker, D. A.: Recent dynamics of arctic and sub-arctic vegetation, Environ. Res. Lett., 8, 015040, https://doi.org/10.1088/1748-9326/8/1/015040, 2013.

Faegri, K., Iversen, J., Kaland, P. E., and Krzywinski, K.: Textbook of pollen analysis, 4th edn., Blackburn Press, Caldwell, N.J., 328 pp., edited by: Fægri, K., Kaland, P. E., and Krzywinski, K., ISBN 0 471 92178 5, 1989.

Fenton, N. J. and Bergeron, Y.: Sphagnum Spore Availability in Boreal Forests, The Bryologist, 109, 173–181, 2006.

Feurdean, A., Gałka, M., Florescu, G., Diaconu, A.-C., Tanţău, I., Kirpotin, S., and Hutchinson, S. M.: 2000 years of variability in hydroclimate and carbon accumulation in western Siberia and the relationship with large-scale atmospheric circulation: A multi-proxy peat record, Quat. Sci. Rev., 226, 105948, https://doi.org/10.1016/j.quascirev.2019.105948, 2019.

Feurdean, A., Florescu, G., Tanţău, I., Vannière, B., Diaconu, A.-C., Pfeiffer, M., Warren, D., Hutchinson, S. M., Gorina, N., Gałka, M., and Kirpotin, S.: Recent fire regime in the southern boreal forests of western Siberia is unprecedented in the last five millennia, Quat. Sci. Rev., 244, 106495, https://doi.org/10.1016/j.quascirev.2020.106495, 2020.

Feurdean, A., Diaconu, A.-C., Pfeiffer, M., Galka, M., Hutchinson, S. M., Butiseaca, G., Gorina, N., Tonkov, S., Niamir, A., Tantau, I., Zhang, H., and Kirpotin, S.: Holocene wildfire regimes in western Siberia: interaction between peatland moisture conditions and the composition of plant functional types, Clim. Past, 18, 1255–1274, https://doi.org/10.5194/cp-18-1255-2022, 2022.

Fewster, R. E., Morris, P. J., Ivanovic, R. F., Swindles, G. T., Peregon, A. M., and Smith, C. J.: Imminent loss of climate space for permafrost peatlands in Europe and Western Siberia, Nat. Clim. Change, 12, 373–379, https://doi.org/10.1038/s41558-022-01296-7, 2022.

Forbes, B. C., Fauria, M. M., and Zetterberg, P.: Russian Arctic warming and "greening" are closely tracked by tundra shrub willows, Glob. Change Biol., 16, 1542–1554, https://doi.org/10.1111/j.1365-2486.2009.02047.x, 2010.

Fournier, B., Lara, E., Jassey, V. E., and Mitchell, E. A.: Functional traits as a new approach for interpreting testate amoeba palaeorecords in peatlands and assessing the causes and consequences of past changes in species composition, The Holocene, 25, 1375–1383, https://doi.org/10.1177/0959683615585842, 2015.

Frey, K. E., Siegel, D. I., and Smith, L. C.: Geochemistry of west Siberian streams and their potential response to permafrost degradation, Water Resour. Res., 43, https://doi.org/10.1029/2006WR004902, 2007.

Goryushkin, L. M.: Migration, settlement and the rural economy of Siberia, 1861–1914, in: The History of Siberia: From Russian Conquest to Revolution, Routledge, edited by: Wood, A., 140–157, ISBN 0-415-05873-2, 1991.

Grimm, E. C.: Tilia and Tilia graphs computer programs, Illinois State Museum, Research and Collection Center, Springfield, 1991.

Groisman, P. Y., Blyakharchuk, T. A., Chernokulsky, A. V., Arzhanov, M. M., Marchesini, L. B., Bogdanova, E. G., Borzenkova, I. I., Bulygina, O. N., Karpenko, A. A., Karpenko, L. V., Knight, R. W., Khon, V. C., Korovin, G. N., Meshcherskaya, A. V., Mokhov, I. I., Parfenova, E. I., Razuvaev, V. N., Speranskaya, N. A., Tchebakova, N. M., and Vygodskaya, N. N.: Climate Changes in Siberia, in: Regional Environmental Changes in Siberia and Their Global Consequences, edited by: Groisman, P. Y. and Gutman, G., Springer Netherlands, Dordrecht, 57–109, https://doi.org/10.1007/978-94-007-4569-8_3, 2013.

Gurskaya, M., Hallinger, M., Singh, J., Agafonov, L., and Wilmking, M.: Temperature reconstruction in the Ob River valley based on ring widths of three coniferous tree species, Dendrochronologia, 30, 302–309, https://doi.org/10.1016/j.dendro.2012.04.002, 2012.

Halaś, A., Lamentowicz, M., Łuców, D., and Słowiński, M.: Developing a new testate amoeba hydrological transfer function for permafrost peatlands of NW Siberia, Quat. Sci. Rev., 308, 108067, https://doi.org/10.1016/j.quascirev.2023.108067, 2023.

Halaś, A., Lamentowicz, M., Obremska, M., Łuców, D., and Słowiński, M.: Data from: Peatland development reconstruction and complex biological responses to permafrost thawing in Western Siberia, Zenodo [data set], https://doi.org/10.5281/zenodo.15543975, 2025.

Hantemirov, R. M., Corona, C., Guillet, S., Shiyatov, S. G., Stoffel, M., Osborn, T. J., Melvin, T. M., Gorlanova, L. A., Kukarskih, V. V., Surkov, A. Y., von Arx, G., and Fonti, P.: Current Siberian heating is unprecedented during the past seven millennia, Nat. Commun., 13, 4968, https://doi.org/10.1038/s41467-022-32629-x, 2022.

Harris, L. I., Moore, T. R., Roulet, N. T., and Pinsonneault, A. J.: Lichens: A limit to peat growth?, J. Ecol., 106, 2301–2319, https://doi.org/10.1111/1365-2745.12975, 2018.

Harris, L. I., Olefeldt, D., Pelletier, N., Blodau, C., Knorr, K.-H., Talbot, J., Heffernan, L., and Turetsky, M.: Permafrost thaw causes large carbon loss in boreal peatlands while changes to peat quality are limited, Glob. Change Biol., 29, 5720–5735, https://doi.org/10.1111/gcb.16894, 2023.

Heffernan, L., Estop-Aragonés, C., Knorr, K.-H., Talbot, J., and Olefeldt, D.: Long-term Impacts of Permafrost Thaw on Carbon Storage in Peatlands: Deep Losses Offset by Surficial Accumulation, J. Geophys. Res.-Biogeo., 125, e2019JG005501, https://doi.org/10.1029/2019JG005501, 2020.

Heiri, O., Lotter, A. F., and Lemcke, G.: Loss on ignition as a method for estimating organic and carbonate content in sediments: reproducibility and comparability of results, J. Paleolimnol., 25, 101–110, https://doi.org/10.1023/A:1008119611481, 2001.

Hua, Q., Barbetti, M., and Rakowski, A. Z.: Atmospheric Radiocarbon for the Period 1950–2010, Radiocarbon, 55, 2059–2072, https://doi.org/10.2458/azu_js_rc.v55i2.16177, 2013.

Hugelius, G., Loisel, J., Chadburn, S., Jackson, R. B., Jones, M., MacDonald, G., Marushchak, M., Olefeldt, D., Packalen, M., Siewert, M. B., Treat, C., Turetsky, M., Voigt, C., and Yu, Z.: Large stocks of peatland carbon and nitrogen are vulnerable to permafrost thaw, P. Natl. Acad. Sci. USA, 117, 20438–20446, https://doi.org/10.1073/pnas.1916387117, 2020.

Hunter, J. D.: Matplotlib: A 2D Graphics Environment, Comput. Sci. Eng., 9, 90–95, https://doi.org/10.1109/MCSE.2007.55, 2007.

Inglis, G., Collinson, M., Wilde, V., Riegel, W., Robson, B., Lenz, O., and Pancost, R.: Ecological and biogeochemical change in an early Paleogene peat-forming environment: Linking biomarkers and palynology, Palaeogeogr. Palaeocl., 438, 245–255, https://doi.org/10.1016/j.palaeo.2015.08.001, 2015.

IPCC: Climate Change 2021 – The Physical Science Basis: Working Group I Contribution to the Sixth Assessment Report of the Intergovernmental Panel on Climate Change, Cambridge University Press, Cambridge, https://doi.org/10.1017/9781009157896, 2023.

Jacquemart, A.-L.: Andromeda polifolia L., J. Ecol., 86, 527–541, https://doi.org/10.1046/j.1365-2745.1998.00274.x, 1998.

Jeong, S.-J., Bloom, A. A., Schimel, D., Sweeney, C., Parazoo, N. C., Medvigy, D., Schaepman-Strub, G., Zheng, C., Schwalm, C. R., Huntzinger, D. N., Michalak, A. M., and Miller, C. E.: Accelerating rates of Arctic carbon cycling revealed by long-term atmospheric CO2 measurements, Sci. Adv., 4, eaao1167, https://doi.org/10.1126/sciadv.aao1167, 2018.

Juggins, S.: C2 Version 1.5. Software for ecological and palaeoecological data analysis and visualisation, University of Newcastle, Newcastle upon Tyne, UK, 2007.

Juggins, S.: rioja: Analysis of Quaternary Science Data, R package version 0.9-26, https://cran.r-project.org/package=rioja, 2020.

Karlsson, J., Serikova, S., Vorobyev, S. N., Rocher-Ros, G., Denfeld, B., and Pokrovsky, O. S.: Carbon emission from Western Siberian inland waters, Nat. Commun., 12, 825, https://doi.org/10.1038/s41467-021-21054-1, 2021.

Katz, N. J., Katz, S. V., and Skobiejeva, E. I.: Atlas rastitielnych ostatkov v torfach, Nedra, Moscow, Russia, 370 pp., 371–376, ISBN 5-7536-0126-X, 1977.

Kluge, M., Wauthy, M., Clemmensen, K. E., Wurzbacher, C., Hawkes, J. A., Einarsdottir, K., Rautio, M., Stenlid, J., and Peura, S.: Declining fungal diversity in Arctic freshwaters along a permafrost thaw gradient, Glob. Change Biol., 27, 5889–5906, https://doi.org/10.1111/gcb.15852, 2021.

Kondratjeva, K. A., Khrutzky, S. F., and Romanovsky, N. N.: Changes in the extent of permafrost during the late quaternary period in the territory of the former Soviet Union, Permafr. Periglac. Process., 4, 113–119, https://doi.org/10.1002/ppp.3430040204, 1993.

Kremenetski, K. V., Velichko, A. A., Borisova, O. K., MacDonald, G. M., Smith, L. C., Frey, K. E., and Orlova, L. A.: Peatlands of the Western Siberian lowlands: current knowledge on zonation, carbon content and Late Quaternary history, Quat. Sci. Rev., 22, 703–723, https://doi.org/10.1016/S0277-3791(02)00196-8, 2003.

Kuhry, P.: The palaeoecology of a treed bog in western boreal Canada: a study based on microfossils, macrofossils and physico-chemical properties, Rev. Palaeobot. Palynol., 96, 183–224, https://doi.org/10.1016/S0034-6667(96)00018-8, 1997.

Kujala, K., Seppälä, M., and Holappa, T.: Physical properties of peat and palsa formation, Cold Reg. Sci. Technol., 52, 408–414, https://doi.org/10.1016/j.coldregions.2007.08.002, 2008.

Kulczyński, S.: Torfowiska Polesia (tom I–II), PUA 37, Kraków, Poland, 1939.

Kuosmanen, N., Väliranta, M., Piilo, S., Tuittila, E.-S., Oksanen, P., and Wallenius, T.: Repeated fires in forested peatlands in sporadic permafrost zone in Western Canada, Environ. Res. Lett., 18, 094051, https://doi.org/10.1088/1748-9326/acf05b, 2023.

Kurina, I. V., Veretennikova, E. E., Il'ina, A. A., Egorova, M. L., Salisch, L. V., Dolgin, V. N., Udaloi, A. V., Golovatskaya, E. A., Dyukarev, E. A., and Smirnov, S. V.: Multi-proxy climate and environmental records from a Holocene eutrophic mire, southern taiga subzone, West Siberia, Boreas, 52, 223–239, https://doi.org/10.1111/bor.12604, 2023.

Kurz, W. A., Dymond, C. C., Stinson, G., Rampley, G. J., Neilson, E. T., Carroll, A. L., Ebata, T., and Safranyik, L.: Mountain pine beetle and forest carbon feedback to climate change, Nature, 452, 987–990, https://doi.org/10.1038/nature06777, 2008.

Laliberté, E., Legendre, P., and Shipley, B.: FD: measuring functional diversity from multiple traits, and other tools for functional ecology. R package version 1.0-12.1, Université de Montréal, Montréal, Canada, https://doi.org/10.32614/CRAN.package.FD, 2014.

Lamarre, A., Garneau, M., and Asnong, H.: Holocene paleohydrological reconstruction and carbon accumulation of a permafrost peatland using testate amoeba and macrofossil analyses, Kuujjuarapik, subarctic Québec, Canada, Rev. Palaeobot. Palynol., 186, 131–141, https://doi.org/10.1016/j.revpalbo.2012.04.009, 2012.

Lamentowicz, M., Milecka, K., Gałka, M., Cedro, A., Pawlyta, J., Piotrowska, N., Lamentowicz, Ł., and Van Der Knaap, W. O.: Climate and human induced hydrological change since AD 800 in an ombrotrophic mire in Pomerania (N Poland) tracked by testate amoebae, macro-fossils, pollen and tree rings of pine, Boreas, 38, 214–229, https://doi.org/10.1111/j.1502-3885.2008.00047.x, 2009.

Lamentowicz, M., Słowiński, M., Marcisz, K., Zielińska, M., Kaliszan, K., Lapshina, E., Gilbert, D., Buttler, A., Fiałkiewicz-Kozieł, B., Jassey, V. E. J., Laggoun-Defarge, F., and Kołaczek, P.: Hydrological dynamics and fire history of the last 1300 years in western Siberia reconstructed from a high-resolution, ombrotrophic peat archive, Quat. Res., 84, 312–325, https://doi.org/10.1016/j.yqres.2015.09.002, 2015.

Lamentowicz, M., Kajukało-Drygalska, K., Kołaczek, P., Jassey, V. E. J., Gąbka, M., and Karpińska-Kołaczek, M.: Testate amoebae taxonomy and trait diversity are coupled along an openness and wetness gradient in pine-dominated Baltic bogs, Eur. J. Protistol., 73, 125674, https://doi.org/10.1016/j.ejop.2020.125674, 2020.

Lawrence, D. M., Koven, C. D., Swenson, S. C., Riley, W. J., and Slater, A. G.: Permafrost thaw and resulting soil moisture changes regulate projected high-latitude CO2 and CH4 emissions, Environ. Res. Lett., 10, 094011, https://doi.org/10.1088/1748-9326/10/9/094011, 2015.

Li, J., Holmgren, M., and Xu, C.: Greening vs browning? Surface water cover mediates how tundra and boreal ecosystems respond to climate warming, Environ. Res. Lett., 16, 104004, https://doi.org/10.1088/1748-9326/ac2376, 2021.

Luoto, M. and Seppälä, M.: Thermokarst ponds as indicators of the former distribution of palsas in Finnish Lapland, Permafr. Periglac. Process., 14, 19–27, https://doi.org/10.1002/ppp.441, 2003.

Magnússon, R. Í., Groten, F., Bartholomeus, H., van Huissteden, K., and Heijmans, M. M. P. D.: Tundra Browning in the Indigirka Lowlands (North-Eastern Siberia) Explained by Drought, Floods and Small-Scale Vegetation Shifts, J. Geophys. Res.-Biogeo., 128, e2022JG007330, https://doi.org/10.1029/2022JG007330, 2023.

Malmer, N.: Patterns in the Growth and the Accumulation of Inorganic Constituents in the Sphagnum Cover on Ombrotrophic Bogs in Scandinavia, Oikos, 53, 105, https://doi.org/10.2307/3565670, 1988.

Malmer, N.: On the relations between water regime, mass accretion and formation of ombrotrophic conditions in Sphagnum mires, Mires Peat, 14, 1–23, 2014.

Manasypov, R. M., Shirokova, L. S., and Pokrovsky, O. S.: Experimental modeling of thaw lake water evolution in discontinuous permafrost zone: Role of peat, lichen leaching and ground fire, Sci. Total Environ., 580, 245–257, https://doi.org/10.1016/j.scitotenv.2016.12.067, 2017.

Mann, M.: Little Ice Age, Encycl. Glob. Environ. Change, The Earth system: physical and chemical dimensions of global environmental change, edited by: MacCracken, M. C. and Perry, J. S., John Wiley & Sons, Ltd, Chichester, UK,1, 504–509, ISBN 0-471-97796-9, 2002.

Marcisz, K., Tinner, W., Colombaroli, D., Kołaczek, P., Słowiński, M., Fiałkiewicz-Kozieł, B., Łokas, E., and Lamentowicz, M.: Long-term hydrological dynamics and fire history over the last 2000 years in CE Europe reconstructed from a high-resolution peat archive, Quat. Sci. Rev., 112, 138–152, https://doi.org/10.1016/j.quascirev.2015.01.019, 2015.

Markkula, I., Oksanen, P., and Kuhry, P.: Indicator value of oribatid mites in determining past permafrost dynamics in northern European sub-Arctic peatlands, Boreas, 47, 884–896, https://doi.org/10.1111/bor.12312, 2018.

Martini, I. P., Cortizas, A. M., and Chesworth, W.: Peatlands: Evolution and Records of Environmental and Climate Changes, Elsevier, 606 pp., ISBN 978-0-444-52883-4, 2007.

Mauquoy, D. and Geel, B.: Mire and peat macros, in: Encyclopedia of Quaternary Science, vol. 3, Elsevier, Amsterdam, 2315–2336, ISBN 978-0-444-51947-4, https://doi.org/10.1016/B0-44-452747-8/00229-5, 2007.

Mekonnen, Z. A., Riley, W. J., Berner, L. T., Bouskill, N. J., Torn, M. S., Iwahana, G., Breen, A. L., Myers-Smith, I. H., Criado, M. G., Liu, Y., Euskirchen, E. S., Goetz, S. J., Mack, M. C., and Grant, R. F.: Arctic tundra shrubification: a review of mechanisms and impacts on ecosystem carbon balance, Environ. Res. Lett., 16, 053001, https://doi.org/10.1088/1748-9326/abf28b, 2021.

Miles, V. V. and Esau, I.: Spatial heterogeneity of greening and browning between and within bioclimatic zones in northern West Siberia, Environ. Res. Lett., 11, 115002, https://doi.org/10.1088/1748-9326/11/11/115002, 2016.

Mitchell, E. A. D., Buttler, A., Grosvernier, P., Rydin, H., Albinsson, C., Greenup, A. L., Heijmans, M. M. P. D., Hoosbeek, M. R., and Saarinen, T.: Relationships among testate amoebae (Protozoa), vegetation and water chemistry in five Sphagnum-dominated peatlands in Europe, New Phytol., 145, 95–106, https://doi.org/10.1046/j.1469-8137.2000.00550.x, 2000.

Mitchell, E. A. D., Gilbert, D., Buttler, A., Amblard, C., Grosvernier, P., and Gobat, J. M.: Structure of Microbial Communities in Sphagnum Peatlands and Effect of Atmospheric Carbon Dioxide Enrichment, Microb. Ecol., 46, 187–199, 2003.

Mitchell, E. A. D., Payne, R. J., and Lamentowicz, M.: Potential implications of differential preservation of testate amoeba shells for paleoenvironmental reconstruction in peatlands, J. Paleolimnol., 40, 603–618, https://doi.org/10.1007/s10933-007-9185-z, 2008.

Mooney, S. and Radford, K.: A simple and fast method for the quantification of macroscopic charcoal from sediments, Quat. Australas., 19, 43–46, 2001.

Moore, P. D., Collinson, M., and Webb, J. A.: Pollen Analysis, 2nd edn., Wiley, 216 pp., ISBN 0-86542-895-6, ISBN 978-0-86542-895-9, 1994.

Myers-Smith, I. H., Kerby, J. T., Phoenix, G. K., Bjerke, J. W., Epstein, H. E., Assmann, J. J., John, C., Andreu-Hayles, L., Angers-Blondin, S., Beck, P. S. A., Berner, L. T., Bhatt, U. S., Bjorkman, A. D., Blok, D., Bryn, A., Christiansen, C. T., Cornelissen, J. H. C., Cunliffe, A. M., Elmendorf, S. C., Forbes, B. C., Goetz, S. J., Hollister, R. D., de Jong, R., Loranty, M. M., Macias-Fauria, M., Maseyk, K., Normand, S., Olofsson, J., Parker, T. C., Parmentier, F.-J. W., Post, E., Schaepman-Strub, G., Stordal, F., Sullivan, P. F., Thomas, H. J. D., Tømmervik, H., Treharne, R., Tweedie, C. E., Walker, D. A., Wilmking, M., and Wipf, S.: Complexity revealed in the greening of the Arctic, Nat. Clim. Change, 10, 106–117, https://doi.org/10.1038/s41558-019-0688-1, 2020.

Naumov, I. V.: The History of Siberia, Routledge, 242 pp., ISBN 978-0-415-54581-5, 2009.

Nelson, K., Thompson, D., Hopkinson, C., Petrone, R., and Chasmer, L.: Peatland-fire interactions: A review of wildland fire feedbacks and interactions in Canadian boreal peatlands, Sci. Total Environ., 769, 145212, https://doi.org/10.1016/j.scitotenv.2021.145212, 2021.

Neustadt, M. I.: On absolute age of peat bogs of Western Siberia., Rev. Roum. Biol. Ser. Bot., 12, 181–186, 1967.

Novenko, E. Y., Mazei, N. G., Kupriyanov, D. A., Babeshko, K. V., Kusilman, M. V., Zyuganova, I. S., Tsyganov, A. N., Mazei, Y. A., Phelps, L. N., and Davis, B. A.: A 1300-year multiproxy palaeoecological record from the northwest Putorana Plateau (Russian Subarctic): environmental changes, vegetation dynamics and fire history, The Holocene, 33, 181–193, https://doi.org/10.1177/09596836221131693, 2023.

Nungesser, M. K.: Modelling microtopography in boreal peatlands: hummocks and hollows, Ecol. Model., 165, 175–207, https://doi.org/10.1016/S0304-3800(03)00067-X, 2003.

Ogden, C. G. and Hedley, R. H.: An Atlas of Freshwater Testate Amoebae, Oxford University Press [for the] British Museum (Natural History), 236 pp., ISBN 978-0-198-58502-2, 1980.

Ogden, E. L., Cumming, S. G., Smith, S. L., Turetsky, M. R., and Baltzer, J. L.: Permafrost thaw induces short-term increase in vegetation productivity in northwestern Canada, Glob. Change Biol., 29, 5352–5366, https://doi.org/10.1111/gcb.16812, 2023.

Oksanen, J., Simpson, G., Blanchet, F., Kindt, R., Legendre, P., Minchin, P., O'Hara, R., Solymos, P., Stevens, M., Szoecs, E., Wagner, H., Barbour, M., Bedward, M., Bolker, B., Borcard, D., Carvalho, G., Chirico, M., De Caceres, M., Durand, S., Evangelista, H., FitzJohn, R., Friendly, M., Furneaux, B., Hannigan, G., Hill, M., Lahti, L., McGlinn, D., Ouellette, M., Ribeiro Cunha, E., Smith, T., Stier, A., Ter Braak, C., and Weedon, J.: vegan: Community Ecology Package. R package version 2.6-2, CRAN, https://doi.org/10.32614/CRAN.package.vegan, 2022.

Olefeldt, D., Heffernan, L., Jones, M. C., Sannel, A. B. K., Treat, C. C., and Turetsky, M. R.: Permafrost Thaw in Northern Peatlands: Rapid Changes in Ecosystem and Landscape Functions, in: Ecosystem Collapse and Climate Change, edited by: Canadell, J. G. and Jackson, R. B., Springer International Publishing, Cham, 27–67, https://doi.org/10.1007/978-3-030-71330-0_3, 2021.

O'Neill, H. B., Smith, S. L., Burn, C. R., Duchesne, C., and Zhang, Y.: Widespread Permafrost Degradation and Thaw Subsidence in Northwest Canada, J. Geophys. Res.-Earth Surf., 128, e2023JF007262, https://doi.org/10.1029/2023JF007262, 2023.

Pandey, A., Tripathi, S., and Basumatary, S.: Non-Pollen Palynomorphs from the Late-Holocene Sediments of Majuli Island, Assam (Indo-Burma Region): Implications to Palaeoenvironmental Studies, in: Climate Change and Environmental Impacts: Past, Present and Future Perspective, edited by: Phartiyal, B., Mohan, R., Chakraborty, S., Dutta, V., Gupta, A. K., Society of Earth Scientists Series. Springer, Cham, 63–81, https://doi.org/10.1007/978-3-031-13119-6_5, 2023.

Pedregosa, F., Varoquaux, G., Gramfort, A., Michel, V., Thirion, B., Grisel, O., Blondel, M., Prettenhofer, P., Weiss, R., Dubourg, V., Vanderplas, J., Passos, A., Cournapeau, D., Brucher, M., Perrot, M., and Duchesnay, É.: Scikit-learn: Machine Learning in Python, J. Mach. Learn. Res., 12, 2825–2830, 2011.

Peel, M. C., Finlayson, B. L., and McMahon, T. A.: Updated world map of the Köppen-Geiger climate classification, Hydrol. Earth Syst. Sci., 11, 1633–1644, https://doi.org/10.5194/hess-11-1633-2007, 2007.

Pelletier, N., Talbot, J., Olefeldt, D., Turetsky, M., Blodau, C., Sonnentag, O., and Quinton, W. L.: Influence of Holocene permafrost aggradation and thaw on the paleoecology and carbon storage of a peatland complex in northwestern Canada, The Holocene, 27, 1391–1405, https://doi.org/10.1177/0959683617693899, 2017.

Peteet, D., Andreev, A., Bardeen, W., and Mistretta, F.: Long-term Arctic peatland dynamics, vegetation and climate history of the Pur-Taz region, Western Siberia, Boreas, 27, 115–126, https://doi.org/10.1111/j.1502-3885.1998.tb00872.x, 1998.

Philben, M., Kaiser, K., and Benner, R.: Biochemical evidence for minimal vegetation change in peatlands of the West Siberian Lowland during the Medieval Climate Anomaly and Little Ice Age, J. Geophys. Res.-Biogeo., 119, 808–825, https://doi.org/10.1002/2013JG002396, 2014.

Phoenix, G. K. and Bjerke, J. W.: Arctic browning: extreme events and trends reversing arctic greening, Glob. Change Biol., 22, 2960–2962, https://doi.org/10.1111/gcb.13261, 2016.

Polishchuk, Y. M., Bryksina, N. A., and Polishchuk, V. Y.: Remote analysis of changes in the number of small thermokarst lakes and their distribution with respect to their sizes in the cryolithozone of Western Siberia, 2015, Izv. Atmospheric Ocean. Phys., 51, 999–1006, https://doi.org/10.1134/S0001433815090145, 2015.

Qin, Y., Li, H., Mazei, Y., Kurina, I., Swindles, G. T., Bobrov, A., Tsyganov, A. N., Gu, Y., Huang, X., Xue, J., Lamentowicz, M., Marcisz, K., Roland, T., Payne, R. J., Mitchell, E. A. D., and Xie, S.: Developing a continental-scale testate amoeba hydrological transfer function for Asian peatlands, Quat. Sci. Rev., 258, 106868, https://doi.org/10.1016/j.quascirev.2021.106868, 2021.

Railton, J. B. and Sparling, J. H.: Preliminary studies on the ecology of palsa mounds in northern Ontario, Can. J. Bot., 51, 1037–1044, https://doi.org/10.1139/b73-128, 1973.

Ramsey, C. B.: Development of the Radiocarbon Calibration Program, Radiocarbon, 43, 355–363, https://doi.org/10.1017/S0033822200038212, 2001.

Rantanen, M., Karpechko, A. Y., Lipponen, A., Nordling, K., Hyvärinen, O., Ruosteenoja, K., Vihma, T., and Laaksonen, A.: The Arctic has warmed nearly four times faster than the globe since 1979, Commun. Earth Environ., 3, 1–10, https://doi.org/10.1038/s43247-022-00498-3, 2022.

Raudina, T. V., Loiko, S. V., Lim, A. G., Krickov, I. V., Shirokova, L. S., Istigechev, G. I., Kuzmina, D. M., Kulizhsky, S. P., Vorobyev, S. N., and Pokrovsky, O. S.: Dissolved organic carbon and major and trace elements in peat porewater of sporadic, discontinuous, and continuous permafrost zones of western Siberia, Biogeosciences, 14, 3561–3584, https://doi.org/10.5194/bg-14-3561-2017, 2017.

R Core Team: R: A language and environment for statistical computing, R Foundation for Statistical Computing, Vienna, Austria, https://www.R-project.org/, 2022.

Reimer, P. J., Austin, W. E. N., Bard, E., Bayliss, A., Blackwell, P. G., Ramsey, C. B., Butzin, M., Cheng, H., Edwards, R. L., Friedrich, M., Grootes, P. M., Guilderson, T. P., Hajdas, I., Heaton, T. J., Hogg, A. G., Hughen, K. A., Kromer, B., Manning, S. W., Muscheler, R., Palmer, J. G., Pearson, C., Plicht, J. van der, Reimer, R. W., Richards, D. A., Scott, E. M., Southon, J. R., Turney, C. S. M., Wacker, L., Adolphi, F., Büntgen, U., Capano, M., Fahrni, S. M., Fogtmann-Schulz, A., Friedrich, R., Köhler, P., Kudsk, S., Miyake, F., Olsen, J., Reinig, F., Sakamoto, M., Sookdeo, A., and Talamo, S.: The IntCal20 Northern Hemisphere Radiocarbon Age Calibration Curve (0–55 cal kBP), Radiocarbon, 62, 725–757, https://doi.org/10.1017/RDC.2020.41, 2020.

Romanovsky, V. E., Drozdov, D. S., Oberman, N. G., Malkova, G. V., Kholodov, A. L., Marchenko, S. S., Moskalenko, N. G., Sergeev, D. O., Ukraintseva, N. G., Abramov, A. A., Gilichinsky, D. A., and Vasiliev, A. A.: Thermal state of permafrost in Russia, Permafr. Periglac. Process., 21, 136–155, https://doi.org/10.1002/ppp.683, 2010.

Rönkkö, M. and Seppälä, M.: Surface characteristics affecting active layer formation in palsas, Finnish Lapland, in: Proceedings of the 8th International Conference on Permafrost, edited by: Phillips, M., Springman, S. M., and Arenson, L. U., Zürich, Switzerland, 21–25 July 2003. Vol. 2, 995–1000, ISBN 978-90-5809-582-4, 2003. Rönkkö, M., and Seppälä, M.: Surface characteristics affecting active layer formation in palsas, Finnish Lapland, in: Proceedings of the 8th International Conference on Permafrost, edited by: Phillips, M., Springman, S. M., and Arenson, L. U., Vol. 2, pp. 995–1000, Zürich, Switzerland, 21–25 July 2003. ISBN: 978-90-5809-582-4.

Rydin, H. and Jeglum, J. K.: Peatland habitats, in: The Biology of Peatlands, edited by: Rydin, H. and Jeglum, J. K., Oxford University Press, 1–20, https://doi.org/10.1093/acprof:osobl/9780199602995.003.0001, 2013.

Safronova, I. and Yurkovsksya, T.: The latitudinal distribution of vegetation cover in Siberia, BIO Web Conf, 16, 00047, https://doi.org/10.1051/bioconf/20191600047, 2019.

Sannel, A. B. K. and Kuhry, P.: Long-term stability of permafrost in subarctic peat plateaus, west-central Canada, The Holocene, 18, 589–601, https://doi.org/10.1177/0959683608089658, 2008.

Sannel, A. B. K. and Kuhry, P.: Holocene peat growth and decay dynamics in sub-arctic peat plateaus, west-central Canada, Boreas, 38, 13–24, https://doi.org/10.1111/j.1502-3885.2008.00048.x, 2009.

Sannel, A. B. K. and Kuhry, P.: Warming-induced destabilization of peat plateau/thermokarst lake complexes, J. Geophys. Res.-Biogeo., 116, https://doi.org/10.1029/2010JG001635, 2011.

Schuur, E. A. G., McGuire, A. D., Schädel, C., Grosse, G., Harden, J. W., Hayes, D. J., Hugelius, G., Koven, C. D., Kuhry, P., Lawrence, D. M., Natali, S. M., Olefeldt, D., Romanovsky, V. E., Schaefer, K., Turetsky, M. R., Treat, C. C., and Vonk, J. E.: Climate change and the permafrost carbon feedback, Nature, 520, 171–179, https://doi.org/10.1038/nature14338, 2015.

Schuur, E. A. G., Pallandt, M., and Göckede, M.: Russian collaboration loss risks permafrost carbon emissions network, Nat. Clim. Change, 14, 410–411, https://doi.org/10.1038/s41558-024-02001-6, 2024.

Seneviratne, S. I., Zhang, X., Adnan, M., Badi, W., Dereczynski, C., Di Luca, A., Ghosh, S., Iskandar, I., Kossin, J., Lewis, S., Otto, F., Pinto, I., Satoh, M., Vicente-Serrano, S. M., Wehner, M., and Zhou, B.: Weather and Climate Extreme Events in a Changing Climate, in: Climate Change 2021: The Physical Science Basis. Contribution of Working Group I to the Sixth Assessment Report of the Intergovernmental Panel on Climate Change, edited by: Pörtner, H.-O., Roberts, D. C., Tignor, M., Poloczanska, E. S., Mintenbeck, K., Alegría, A., Craig, M., Langsdorf, S., Löschke, S., Möller, V., Okem, A., and B., R., Cambridge University Press, Cambridge, United Kingdom and New York, NY, USA, 1513–1766, https://doi.org/10.1017/9781009157896.013, 2021.

Seppälä, M.: Palsas and releated forms, in: Advances in Periglacial Geomorphology, edited by: M. J. Clark, John Wiley & Sons, Chichester, UK, 247–278, ISBN 978-0-471-90981-5, 1988.

Seppälä, M.: Synthesis of studies of palsa formation underlining the importance of local environmental and physical characteristics, Quat. Res., 75, 366–370, https://doi.org/10.1016/j.yqres.2010.09.007, 2011.

Sheng, Y., Smith, L. C., MacDonald, G. M., Kremenetski, K. V., Frey, K. E., Velichko, A. A., Lee, M., Beilman, D. W., and Dubinin, P.: A high-resolution GIS-based inventory of the west Siberian peat carbon pool, Glob. Biogeochem. Cycles, 18, https://doi.org/10.1029/2003GB002190, 2004.

Shumilovskikh, L., Schlütz, F., Achterberg, I., Bauerochse, A., and Leuschner, H.: Non-Pollen Palynomorphs from Mid-Holocene

Peat of the Raised Bog Borsteler Moor (Lower Saxony, Germany), Stud. Quat., 32, 5–18, https://doi.org/10.1515/squa-2015-0001, 2015.

Shumilovskikh, L., O'Keefe, J. M. K., and Marret, F.: An overview of the taxonomic groups of non-pollen palynomorphs, Geol. Soc. Lond. Spec. Publ., 511, 13–61, https://doi.org/10.1144/SP511-2020-65, 2021.

Shur, Y. L. and Jorgenson, M. T.: Patterns of permafrost formation and degradation in relation to climate and ecosystems, Permafr. Periglac. Process., 18, 7–19, https://doi.org/10.1002/ppp.582, 2007.

Siemensma, F. J.: Microworld, world of amoeboid organisms, World-wide electronic publication, Kortenhoef, the Netherlands, https://arcella.nl, 2022.

Sillasoo, Ü., Väliranta, M., and Tuittila, E.-S.: Fire history and vegetation recovery in two raised bogs at the Baltic Sea, J. Veg. Sci., 22, 1084–1093, https://doi.org/10.1111/j.1654-1103.2011.01307.x, 2011.

Sim, T. G., Swindles, G. T., Morris, P. J., Baird, A. J., Cooper, C. L., Gallego-Sala, A. V., Charman, D. J., Roland, T. P., Borken, W., Mullan, D. J., Aquino-López, M. A., and Gałka, M.: Divergent responses of permafrost peatlands to recent climate change, Environ. Res. Lett., 16, 034001, https://doi.org/10.1088/1748-9326/abe00b, 2021.

Singh, S. P., Gumber, S., Singh, R. D., and Pandey, R.: Differentiation of diploxylon and haploxylon pines in spatial distribution, and adaptational traits, Acta Ecol. Sin., 43, 1–10, https://doi.org/10.1016/j.chnaes.2021.07.007, 2023.

Smith, L. C., MacDonald, G. M., Velichko, A. A., Beilman, D. W., Borisova, O. K., Frey, K. E., Kremenetski, K. V., and Sheng, Y.: Siberian Peatlands a Net Carbon Sink and Global Methane Source Since the Early Holocene, Science, 303, 353–356, https://doi.org/10.1126/science.1090553, 2004.

Smith, L. C., Sheng, Y., MacDonald, G. M., and Hinzman, L. D.: Disappearing Arctic Lakes, Science, 308, 1429–1429, https://doi.org/10.1126/science.1108142, 2005.

Smith, S. L., O'Neill, H. B., Isaksen, K., Noetzli, J., and Romanovsky, V. E.: The changing thermal state of permafrost, Nat. Rev. Earth Environ., 3, 10–23, https://doi.org/10.1038/s43017-021-00240-1, 2022.

Spiller, A., Kallenbach, C. M., Burnett, M. S., Olefeldt, D., Schulze, C., Maranger, R., and Douglas, P. M. J.: Gradual drying of permafrost peat decreases carbon dioxide production in drier peat plateaus but not in wetter fens and bogs, SOIL, 11, 371–379, https://doi.org/10.5194/soil-11-371-2025, 2025.

Standen, K. M. and Baltzer, J. L.: Permafrost condition determines plant community composition and community-level foliar functional traits in a boreal peatland, Ecol. Evol., 11, 10133–10146, https://doi.org/10.1002/ece3.7818, 2021.

Stockmarr, J.: Tablets with Spores used in Absolute Pollen Analysis, Pollen Spores, 13, 615–621, 1971.

Street, L. E., Subke, J.-A., Sommerkorn, M., Sloan, V., Ducrotoy, H., Phoenix, G. K., and Williams, M.: The role of mosses in carbon uptake and partitioning in arctic vegetation, New Phytol., 199, 163–175, https://doi.org/10.1111/nph.12285, 2013.

Streletskiy, D., Anisimov, O., and Vasiliev, A.: Permafrost Degradation, in: Snow and Ice-Related Hazards, Risks, and Disasters, edited by: Shroder, J. F., Haeberli, W., and Whiteman, C., Academic Press, Boston, 303–344, https://doi.org/10.1016/B978-0-12-394849-6.00010-X, 2015.

Swindles, G. T., Morris, P. J., Mullan, D., Watson, E. J., Turner, T. E., Roland, T. P., Amesbury, M. J., Kokfelt, U., Schoning, K., Pratte, S., Gallego-Sala, A., Charman, D. J., Sanderson, N., Garneau, M., Carrivick, J. L., Woulds, C., Holden, J., Parry, L., and Galloway, J. M.: The long-term fate of permafrost peatlands under rapid climate warming, Sci. Rep., 5, 17951, https://doi.org/10.1038/srep17951, 2015.

Thibault, S. and Payette, S.: Recent permafrost degradation in bogs of the James Bay area, northern Quebec, Canada, Permafr. Periglac. Process., 20, 383–389, https://doi.org/10.1002/ppp.660, 2009.

Thompson, D. K. and Waddington, J. M.: Sphagnum under pressure: towards an ecohydrological approach to examining Sphagnum productivity, Ecohydrology, 1, 299–308, https://doi.org/10.1002/eco.31, 2008.

Tikhonravova, Y., Kuznetsova, A., Slagoda, E., and Koroleva, E.: Holocene permafrost peatland evolution in drained lake basins on the Pur-Taz Interfluve, North-Western Siberia, Quaternary Int., 669, 32–42, https://doi.org/10.1016/j.quaint.2023.07.005, 2023.

Tobolski, K.: Przewodnik do oznaczania torfów i osadów jeziornych, Wydawnictwo Naukowe PWN, Warszawa, 508 pp., ISBN 83-01-13215-9, 2000.

Todorov, M. and Bankov, N.: An Atlas of Sphagnum-Dwelling Testate Amoebae in Bulgaria, 1st edn., Pensoft Publishers, Sofia, Bulgaria, Advanced Books, https://doi.org/10.3897/ab.e38685, 2019.

Tolonen, K. and Turunen, J.: Accumulation rates of carbon in mires in Finland and implications for climate change, The Holocene, 6, 171–178, https://doi.org/10.1177/095968369600600204, 1996.

Treat, C. C. and Jones, M. C.: Near-surface permafrost aggradation in Northern Hemisphere peatlands shows regional and global trends during the past 6000 years, The Holocene, 28, 998–1010, https://doi.org/10.1177/0959683617752858, 2018.

Treat, C. C., Jones, M. C., Camill, P., Gallego-Sala, A., Garneau, M., Harden, J. W., Hugelius, G., Klein, E. S., Kokfelt, U., Kuhry, P., Loisel, J., Mathijssen, P. J. H., O'Donnell, J. A., Oksanen, P. O., Ronkainen, T. M., Sannel, A. B. K., Talbot, J., Tarnocai, C., and Väliranta, M.: Effects of permafrost aggradation on peat properties as determined from a pan-Arctic synthesis of plant macrofossils, J. Geophys. Res.-Biogeo., 121, 78–94, https://doi.org/10.1002/2015JG003061, 2016.

Trofimova, I. E. and Balybina, A. S.: Classification of climates and climatic regionalization of the West-Siberian plain, Geogr. Nat. Resour., 35, 114–122, https://doi.org/10.1134/S1875372814020024, 2014.

Vaguet, Y.: Oil and Gas towns in Western Siberia: past, present and future challenges, Nordregio, Stockholm, Sweden, WP 6:218, 125–132, 2013.

Van Geel, B.: Non-Pollen Palynomorphs, in: Tracking Environmental Change Using Lake Sediments: Terrestrial, Algal, and Siliceous Indicators, edited by: Smol, J. P., Birks, H. J. B., Last, W. M., Bradley, R. S., and Alverson, K., Springer Netherlands, Dordrecht, 99–119, https://doi.org/10.1007/0-306-47668-1_6, 2001.

Velichko, A. A., Timireva, S. N., Kremenetski, K. V., MacDonald, G. M., and Smith, L. C.: West Siberian Plain as a late glacial desert, Quaternary Int., 237, 45–53, https://doi.org/10.1016/j.quaint.2011.01.013, 2011.

Volkova, I. I., Kolesnichenko, L. G., Kirpotin, S. N., Pokrovsky, O. S., and Vorobyev, S. N.: Peat deposits and peat-forming plants in the mires of the West Siberian northern taiga (based on studies of the Khanymei site), IOP Conf. Ser. Earth Environ. Sci., 232, 012018, https://doi.org/10.1088/1755-1315/232/1/012018, 2019.

Walvoord, M. A. and Kurylyk, B. L.: Hydrologic Impacts of Thawing Permafrost—A Review, Vadose Zone J., 15, vzj2016.01.0010, https://doi.org/10.2136/vzj2016.01.0010, 2016.

Wang, Y., Way, R., Lewkowicz, A. G., Tutton, R., Beer, J., Colyn, V., and Forget, A.: Assessing recent thaw and subsidence of peatland permafrost in coastal Labrador, northeastern Canada, in: Proceedings of the 12th International Conference on Permafrost, edited by: Canadian Permafrost Association, Whitehorse, Yukon, Canada, 469–476, https://doi.org/10.52381/ICOP2024.155.1, 2024.

Warner, B. G. and Charman, D. J.: Holocene changes on a peatland in northwestern Ontario interpreted from testate amoebae (Protozoa) analysis, Boreas, 23, 270–279, https://doi.org/10.1111/j.1502-3885.1994.tb00949.x, 1994.

Waskom, M. L.: seaborn: statistical data visualization, J. Open Source Softw., 6, 3021, https://doi.org/10.21105/joss.03021, 2021.

Webb, E. E. and Liljedahl, A. K.: Diminishing lake area across the northern permafrost zone, Nat. Geosci., 16, 202–209, https://doi.org/10.1038/s41561-023-01128-z, 2023.

Wei, L., Xu, C., Jansen, S., Zhou, H., Christoffersen, B. O., Pockman, W. T., Middleton, R. S., Marshall, J. D., and McDowell, N. G.: A heuristic classification of woody plants based on contrasting shade and drought strategies, Tree Physiol., 39, 767–781, https://doi.org/10.1093/treephys/tpy146, 2019.

Wetterich, S., Rudaya, N., Tumskoy, V., Andreev, A. A., Opel, T., Schirrmeister, L., and Meyer, H.: Last Glacial Maximum records in permafrost of the East Siberian Arctic, Quat. Sci. Rev., 30, 3139–3151, https://doi.org/10.1016/j.quascirev.2011.07.020, 2011.

Willis, K. S., Beilman, D., Booth, R. K., Amesbury, M., Holmquist, J., and MacDonald, G.: Peatland paleohydrology in the southern West Siberian Lowlands: Comparison of multiple testate amoeba transfer functions, sites, and Sphagnum δ13C values, The Holocene, 25, 1425–1436, https://doi.org/10.1177/0959683615585833, 2015.

Woodland, W. A., Charman, D. J., and Sims, P. C.: Quantitative estimates of water tables and soil moisture in Holocene peatlands from testate amoebae, The Holocene, 8, 261–273, https://doi.org/10.1191/095968398667004497, 1998.

Zakh, V. A., Ryabogina, N. E., and Chlachula, J.: Climate and environmental dynamics of the mid- to late Holocene settlement in the Tobol–Ishim forest-steppe region, West Siberia, Quaternary Int., 220, 95–101, https://doi.org/10.1016/j.quaint.2009.09.010, 2010.

Zhang, H., Amesbury, M. J., Ronkainen, T., Charman, D. J., Gallego-Sala, A. V., and Väliranta, M.: Testate amoeba as palaeohydrological indicators in the permafrost peatlands of north-east European Russia and Finnish Lapland, J. Quat. Sci., 32, 976–988, https://doi.org/10.1002/jqs.2970, 2017.

Zhang, H., Väliranta, M., Swindles, G. T., Aquino-López, M. A., Mullan, D., Tan, N., Amesbury, M., Babeshko, K. V., Bao, K., Bobrov, A., Chernyshov, V., Davies, M. A., Diaconu, A.-C., Feurdean, A., Finkelstein, S. A., Garneau, M., Guo, Z., Jones, M. C., Kay, M., Klein, E. S., Lamentowicz, M., Magnan, G., Marcisz, K., Mazei, N., Mazei, Y., Payne, R., Pelletier, N., Piilo, S. R., Pratte, S., Roland, T., Saldaev, D., Shotyk, W., Sim, T. G., Sloan, T. J., Słowiński, M., Talbot, J., Taylor, L., Tsyganov, A. N., Wetterich, S., Xing, W., and Zhao, Y.: Recent climate change has driven divergent hydrological shifts in high-latitude peatlands, Nat. Commun., 13, 4959, https://doi.org/10.1038/s41467-022-32711-4, 2022.

Zhu, X., Xu, X., and Jia, G.: Asymmetrical Trends of Burned Area Between Eastern and Western Siberia Regulated by Atmospheric Oscillation, Geophys. Res. Lett., 48, e2021GL096095, https://doi.org/10.1029/2021GL096095, 2021.

Zoltai, S. C.: Cyclic Development of Permafrost in the Peatlands of Northwestern Alberta, Canada, Arct. Alp. Res., 25, 240, https://doi.org/10.2307/1551820, 1993.

Zoltai, S. C., Morrissey, L. A., Livingston, G. P., and Groot, W. J.: Effects of fires on carbon cycling in North American boreal peatlands, Environ. Rev., 6, 13–24, https://doi.org/10.1139/a98-002, 1998.

Supplement of Biogeosciences, 22, 4797–4822, 2025
https://doi.org/10.5194/bg-22-4797-2025-supplement

Biogeosciences
Open Access

Supplement of

Peatland development reconstruction and complex biological responses to permafrost thawing in Western Siberia

Agnieszka Halaś et al.

Correspondence to: Agnieszka Halaś (aj.halas@twarda.pan.pl)

Supplementary material

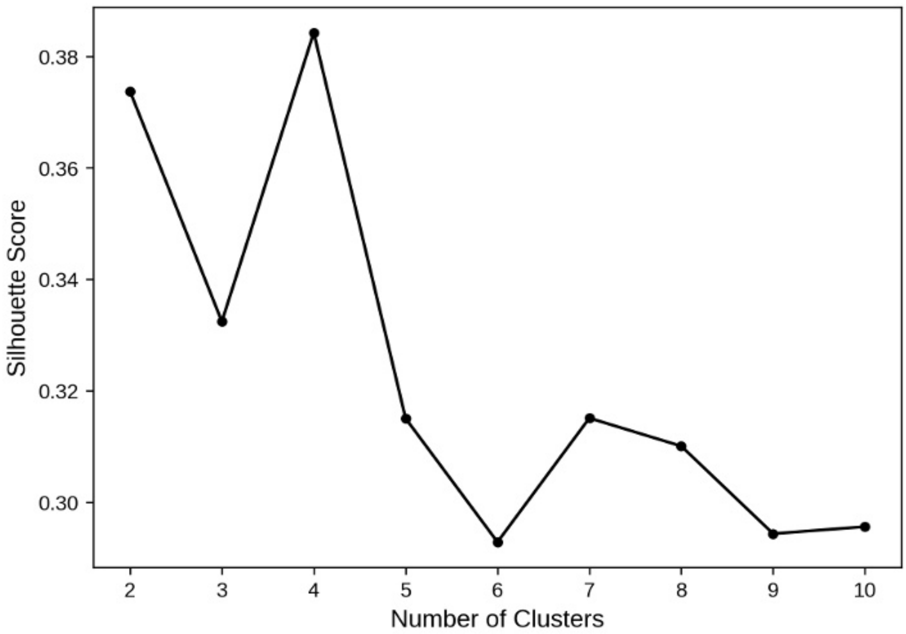

Figure S1 Silhouette Score for different number of clusters in testate amoebae samples from the Kh-K1 core. The highest silhouette score is observed at four clusters.

Earth Syst. Sci. Data, 18, 3853–3888, 2026
https://doi.org/10.5194/essd-18-3853-2026

Peat core research in the Western Siberian Lowland: applications of palaeoecological proxies, regions studied, and future prospects

Agnieszka Halaś and Michał Słowiński

Department of Past Landscape Dynamics, Institute of Geography and Spatial Organization, Polish Academy of Sciences, Warsaw, Poland

Correspondence: Agnieszka Halaś (aj.halas@twarda.pan.pl)

Received: 9 December 2025 – Discussion started: 30 January 2026
Revised: 22 May 2026 – Accepted: 26 May 2026 – Published: 5 June 2026

Abstract. Peatlands are natural archives that preserve information not only about their own development but also about past environmental conditions in surrounding landscapes. This study presents a comprehensive review of palaeoecological research based on peat cores from the Western Siberian Lowland (WSL). We compiled and georeferenced 654 peat cores and documented the application of 26 palaeoecological proxies, including chronological, physical, chemical, and biological indicators, resulting in the creation of the Western Siberian Peat Core Database (WSPC). The database synthesizes information from 156 publications spanning 1953–2025 and captures both the temporal and methodological evolution of peatland studies in the region, highlighting a clear shift from early single-proxy, low resolution investigations to modern multi-proxy high-resolution studies. Spatial analysis reveals high density of peat-core studies along major rivers and in the Great Vasyugan Mire, while remote northern continuous permafrost regions remain underrepresented. Temporal coverage indicates that most cores capture Holocene peatland dynamics, with the longest records in non-permafrost and isolated permafrost zones, extending into the Late Glacial ($\sim$ 15 600 cal. yr BP). The database underscores the dominant role of fundamental physical and chemical proxies, while highlighting the selective application of biological proxies and the limited use of specialized chemical analyses. In addition, the study identifies key research challenges in WSL, including narrow seasonal windows for fieldwork, presence of permafrost, limited transport infrastructure, permit requirements, and geopolitical barriers, which collectively constrain peatland sampling. The WSPC database represents the most extensive compilation of metadata on peat cores in the region, integrating georeferenced core locations, original core identifiers, applied palaeoecological proxies, and associated literature, offering critical guidance for targeted sampling and future research to address spatial, temporal, and proxy-specific gaps in the study of WSL peatlands. The database is available at https://doi.org/10.5281/zenodo.20323517 (Halaś and Słowiński, 2026).

1 Introduction

Peatlands are one of the most important terrestrial ecosystems in the world, acting as significant carbon sinks, regulating hydrology, and providing unique habitats for diverse species. Covering only about 3 % of the land surface, they store roughly one-third of the world's soil carbon, highlighting their critical role in the global carbon cycle (Greifswald Mire Centre, 2022; Scharlemann et al., 2014; Xu et al., 2018). In addition to their ecological importance, peat deposits constitute valuable natural archives due to the preservation of biological remains and physicochemical characteristics formed during peat accumulation under specific environmental conditions (Barber, 1993). Due to their stratified structure and often continuous accumulation, peat sequences provide long-term records of environmental and climatic changes.

The palaeoecological reconstructions from peat deposits are based on the analysis of palaeoecological proxies, which are indirect indicators of past environmental conditions preserved within peat sequences. Depending on their origin and the type of information they provide, these proxies can be broadly classified into biological, chemical, physical, and chronological proxies. The application of these proxies enables the reconstruction of past hydrological conditions, vegetation dynamics, fire activity, carbon accumulation patterns, and other aspects of ecosystem functioning, thereby providing detailed insights into Holocene environmental history (Chambers and Charman, 2004).

One of the largest peatland complexes in the world is found in Western Siberian Lowland (WSL), with almost 600 000 km^2 of peatlands and 70.2 Pg of carbon stored (Sheng et al., 2004). Peatlands across the WSL began accumulating almost simultaneously around 11 000–10 000 yr BP, as postglacial environmental conditions became favourable for peat formation, with only a few sites showing evidence of earlier initiation (Alexandrov et al., 2016; Kremenetski et al., 2003). Spanning the entire Holocene and extending over an exceptionally large geographical area, these peatlands preserve detailed records of environmental and climatic changes, documenting not only their own developmental history but also broader landscape-scale ecosystem dynamics. The scale and ecological significance of the WSL make it a key region for understanding long-term peatland dynamics and predicting peatland responses to ongoing climate change.

Comprehensive syntheses by Kremenetski et al. (2003) and Solomeshch (2005), who consolidated the extensive Russian-language literature and documented the legacy of scientific work in the WSL, provide the historical context for early exploration and peatland research. As summarized by them, the scientific study of WSL peatlands began in the early 20th century, initially through government botanical and pedological surveys in the southern WSL (Dranitsyn, 1914; Gordiagin, 1901; Zhilinsky, 1907), with more detailed investigations followed in the 1920s (Baryshnikov, 1929; Bronzov, 1930). During the 1930s, botanical expeditions to the Yamal and Gydan peninsulas generated the first scientific descriptions of arctic peatlands in the northern WSL (Gorodkov, 1932; Govorukhin, 1933). These early investigations, largely carried out along river valleys and exposed natural outcrops, formed the foundation for later palaeoecological research and represent a major legacy of early Soviet and Russian studies.

The discovery of significant oil reserves in the WSL in the 1950s triggered a wave of intensive peatland exploration aimed at assessing peat thickness, distribution, and suitability for infrastructure development. Exploration of the WSL have historically been difficult due to harsh climatic conditions, vast distances, and complex topography. Despite these challenges, the West Siberian Peat Exploratory Expedition (Glavtorffond RSFSR, 1956) produced the first large-scale estimates of peat stocks for the region, with similar work carried out in the Middle Taiga zone of the WSL in a following decade (Lapshina and Zarov, 2023). During the 1960s and 1970s, systematic surveys mapped the spatial distribution of peatlands and documented peat thickness, hydrology and vegetation cover (Ivanov and Novikov, 1976; Liss and Berezina, 1981; Neustadt, 1971). Important cartographic products, including Geoltorfrazvedka's peatland maps (Map of West Siberian wetlands, 1970, 1996) and Romanova's latitudinal zonation of Eurasian peatlands (Ivanov and Novikov, 1976), remain central references. This period also marked the beginning of modern paleoecology in the WSL, with the first radiocarbon dates (Liss and Kulikova, 1967; Neustadt, 1967) and the earliest pollen-dated peat stratigraphies (Glebov et al., 1974; Levkovskaya et al., 1970; Volkov et al., 1973). Evolution of paleoreconstruction methods started in the 1970s when more precise approach, including the method of retrospective ecological peat analysis with higher sampling resolution started to be implemented (Lapshina and Zarov, 2023; L'vov, 1974).

From the 1980s onward, research expanded into peatland ecology, carbon storage, and long-term accumulation dynamics (Botch et al., 1995; Botch and Masing, 1983; Neustadt, 1984). The first integrative, internationally accessible synthesis appeared in Kremenetski et al. (2003), who reviewed WSL peatland zonation, carbon stocks, and late-Quaternary development, highlighting major gaps in knowledge and the need to integrate the extensive Russian-language legacy. Solomeshch (2005) further refined understanding of WSL peatland ecology and provided an updated overview of their structure, distribution, and environmental significance. Together, these works emphasize the long-standing contributions of Russian scientists and underscore the global importance of the WSL for paleoclimate reconstruction and carbon-cycle research.

Despite the wealth of studies, much of the palaeoecological research in the WSL remains dispersed across numerous publications, often in older Russian-language journals or books. The variety of proxies, peatland types, and sampling locations complicates efforts to form a complete picture of the region's long-term ecological changes. Additionally, access to detailed site-level information, including peat core locations, stratigraphic data, and the specific proxies analysed, is limited, hindering cross-site comparisons and meta-analyses. These challenges underscore the need for a structured and accessible resource that consolidates existing information, providing a clear overview of what has been studied and where gaps in knowledge remain.

The goal of this review is to synthesize and organize existing palaeoecological research across the WSL by developing the Western Siberian Peat Core Database (WSPC). This database compiles information on peat core locations, the palaeoecological proxies analysed, and the original source references, providing a harmonized inventory of research in this globally significant peatland region. Beyond cataloguing peat cores and proxies, this synthesis addresses key questions about the development of peatland research in the WSL. How has the application of palaeoecological proxies evolved over time, from early single-proxy studies to modern multi-proxy approaches? Where are the main spatial gaps in the coverage of peat-core studies across vegetation and permafrost zones, and how have logistical constraints shaped sampling locations? Which proxies remain rarely used, where are these methods under-represented, and what are the implications for reconstructing peatland hydrology, fire regimes, and geochemical conditions at a regional scale? By framing the database around these questions, our review not only documents past research but also highlights priorities and strategies for future studies. Rather than serving as a tool for quantitative analysis, the WSPC database provides a comprehensive overview of what has been studied to date. By consolidating dispersed and often difficult-to-access data, the database facilitates identification of sites with comparable proxy records, helps researchers locate relevant datasets, and supports strategic planning of future fieldwork. Ultimately, the WSPC database aims to enhance accessibility, transparency, and coordination in WSL peatland research.

2 Study region

The geographical extent of the study region considered in this review follows the boundary of the Western Siberian Lowland (WSL) defined by Sheng et al. (2004). The natural boundaries of the region are marked by the Ural Mountains in the west, the Yenisey River in the east, the Altai Mountains and Kazakh steppes in the south, and the Kara Sea in the north (Fig. 1). The study region stretches from 60–93° E to 52–73° N and covers the area of approximately 2 600 000 km^2. The WSL is the flattest and lowest major physiographic region of Russia, characterized by an extensive plain that gently slopes northward and lies between 0 and 300 m a.s.l (Solomeshch, 2005). Geologically, the lowland is underlain by a young tectonic plate covered by thick sedimentary sequence that increases from around 3 km in the south to 11 km in the north (Kurakova, 2024). This succession consists of alternating continental and marine deposits and is capped by 200–250 m of Quaternary sediments, primarily clays, sands, and loams (Kremenetski et al., 2003; Kurakova, 2024). The topography of the WSL contributes to the occurrence of a clear latitudinal distribution of climatic zones and vegetation. According to the Köppen-Geiger climate classification, most of the WSL has a subarctic climate (Dfc), with mean annual air temperatures ranging from −11.5 °C in the Gyda Peninsula to 1 to −1 °C in the south, and annual precipitation between 390 and 600 mm (Beck et al., 2018; Solomeshch, 2005; Trofimova and Balybina, 2014). Vegetation mirrors this latitudinal pattern, transitioning from arctic tundra in the north through the extensive zone of boreal forest (taiga), to a narrow belt of temperate broadleaf and mixed forests, and ultimately temperate grasslands and shrublands in the far south (Olson et al., 2001). The characteristic feature of this region is presence of permafrost, which developed mostly in Late Pleistocene (Duchkov, 2006). Currently, permafrost extends southward to about 60° N, with continuous permafrost on the Yamal and Gyda Peninsulas reaching up to ∼ 67° N and ranging in thickness from 100 to over 500 m, whereas further south the permafrost becomes discontinuous, sporadic, isolated, and finally absent in the southernmost WSL (Solomeshch, 2005). The combination of flat terrain and fine-grained, poorly drained sediments promotes extensive waterlogging and widespread peatland development (Kirpotin et al., 2009). As a consequence, nearly 50 % of the WSL is covered by wetland ecosystems. Peatlands occupy 592 440 km^2 (20 %) of this area, with the largest peatland complex in the world, the Great Vasyugan Mire, covering 67 800 km^2 (Sheng et al., 2004; Vaganov et al., 2005). Most of the region lies within the Ob' River watershed, with smaller northern sectors draining to the Nadym, Pur, and Taz rivers, and limited areas contributing to the left-bank tributaries of the Yenisey. The region is also rich in thermokarst lakes, mostly shallow systems less than 1 km^2 in area and 2–5 m deep, mainly formed due to the thawing of permafrost (Kirpotin et al., 2009; Polishchuk et al., 2017). In the forest-swamp zone, basins can contain up to 40 %–50 % lake coverage, whereas lake density declines toward the southeast, though extensive marsh systems continue to regulate water tables and surface hydrology (Kurakova, 2024). Despite its vast area, population density in the WSL is low, especially in the northern sector where extensive peatland landscapes remain sparsely populated. However, since the mid-1960s, the region has undergone intensive oil and gas development, particularly in the mid- and lower Ob River basin. Consequently, although large areas in the north remain relatively undisturbed, industrial activity and land-use change across WSL have imposed substantial pressures on peatlands, altering their structure, hydrology, and ecological dynamics (Solomeshch, 2005).

2.1 Peatland extent mapping

Estimates of peatland extent in WSL have varied considerably over time due to differences in mapping methods, definitions, and data availability. Early studies reported smaller areas; for example, Neustadt (1971) as a first estimated peatland extent to 325 380 km^2, later Tiuremnov (1976) 341 000 km^2, and Efremov and Efremova (2001) 464 000 km^2, illustrating the progressive refinement of peatland inventories. Sheng et al. (2004) provided a more detailed assessment, estimating 592 440 km^2 of peatlands with a total carbon pool of 70.2 Pg C, based on a comprehensive GIS-based inventory combining decades of Geoltorfrazvedka field surveys, Russian wetland maps, satellite imagery, and extensive digitized peat depth and carbon data

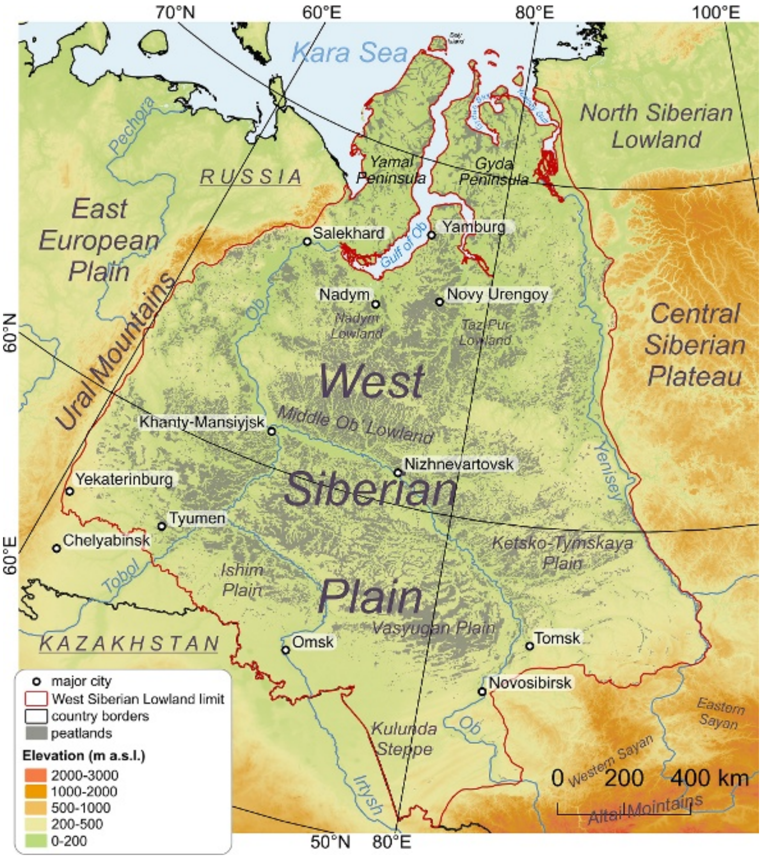

Figure 1. Topographic map of Western Siberian Lowland with the extent of peatlands based on Sheng et al. (2004), main rivers, selected cities, main geographic units and geographical extent of study area considered in this literature review. Elevation source: © DLR e.V. 2010–2014 and © Airbus Defence and Space GmbH 2014–2018 provided under COPERNICUS by the European Union and ESA; all rights reserved.

(Fig. 2a). However, the authors noted that this estimate should still be considered a minimum value because the Russian survey data used in the compilation did not include thin peat deposits (< 50 cm). Modern global products, such as the Global Peatland Map 2.0 (GPM2.0), classify regions as peat-dominated or peat-in-soil-mosaic at a 1×1 km resolution by integrating multiple regional and national datasets using proxy mapping, satellite classification, and expert judgement (Greifswald Mire Centre, 2022). The available version of GPM uses a peat depth threshold of ≥ 10 cm to account for climate-relevant peat carbon, rather than the conventional agricultural threshold of ≥ 30 cm, which increases Russia's estimated peatland area 2.6 times (UNEP, 2022). While GPM provides consistent and updated coverage, its ≥ 10 cm threshold overestimates the area of peatlands that are relevant for palaeoecological reconstruction. This overestimation is particularly visible in the continuous permafrost zone, where it shows nearly continuous peatland coverage; as well as along the western border and in the eastern parts of the region, including the Yenisey valley and the Ketsko-Tymskaya Plain (Fig. 2b). Therefore, for this review, the regional map created by Sheng et al. (2004) remains the most reliable source for WSL peatlands. Although this inventory likely underestimates the total peatland extent because peat deposits thinner than 50 cm were excluded, its methodological framework and closer correspondence to the ≥ 30 cm threshold commonly applied in palaeoecology make it more suitable for this review than GPM. Nevertheless, the selection of peatland datasets and peat depth thresholds should be considered in relation to the specific research objective. Inventories based on lower thresholds (e.g. ≥ 10 cm) may be more appropriate for large-scale carbon balance and climate-related studies, whereas thresholds closer to ≥ 30 cm are generally more applicable in palaeoecological investigations focused on sufficiently developed peat sequences suitable for long-term environmental reconstruction. Therefore, future field campaigns and research expeditions in WSL should evaluate peatland products and thresholds according to the aims of the study.

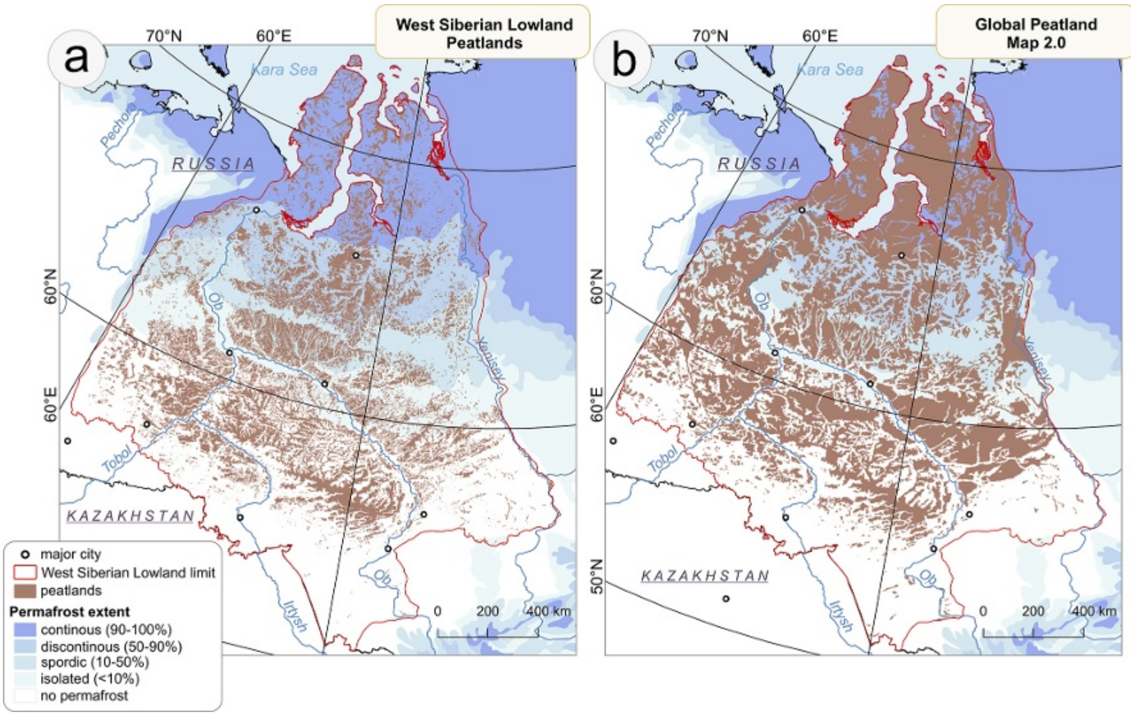

Figure 2. Spatial distribution of peatlands in the Western Siberian Lowland: **(a)** regional map by Sheng et al. (2004) with peat depth threshold > 50 cm; **(b)** Global Peatland Map 2.0 (Greifswald Mire Centre, 2022) with peat depth threshold ≥ 10 cm.

3 Methods and materials

3.1 Literature selection

The literature selection was based on two online databases of scientific papers: Google Scholar and Scopus, using the keywords "*Western Siberia*" AND "*reconstruction*" AND "*peatland*". The initial results were screened manually to identify relevant studies. We applied specific inclusion and exclusion criteria to select studies further used in this review:

- *Publication type*: only published articles and books were considered.
- *Time span*: studies published up to May 2025 were included.
- *Language*: only publications in English or Russian were considered.
- *Temporal coverage*: only stratigraphic peat cores or peat cross-sections were included, with a focus on Holocene records.
- *Geographical extent*: only studies in which at least one peat core was located within the borders of the Western Siberian Lowland (Fig. 1), as defined by Sheng et al. (2004) were included (Sheng, 2016).
- *Core location*: studies were included if they reported precise or approximate coring coordinates, or if approximate locations could be estimated from maps provided in the original publication. Studies lacking sufficient locational information were excluded.
- *Coring material*: only peat sediments (peat cores or peat cross-sections) were included. If the type of sediment could not be clearly determined, the core was excluded.
- *Study type*: eligible studies presented original palaeoecological data derived from peat cores, or meta-analyses synthesizing data from a defined set of peat core studies. Review articles and books that only summarized previously published data without referencing specific peat cores were excluded. We also excluded studies based solely on modelling or simulations not directly grounded in empirical peat core data.
- *Minimum information required*: to be eligible, peat cores had to provide at least one source of palaeoecological information (proxy), regardless of whether chronology was available (e.g., palynology, charcoal analysis, loss-on-ignition or bulk density). In addition, cores were also considered if they contained only chronological information or only basal depth data.

3.2 Data extraction and database creation

After compiling a database of relevant studies, we developed the Western Siberian Peat Core Database (WSPC) by extracting information on individual cores from each publication. For every peat core, we recorded the following required information: location, core name and applied proxies. Whenever available, we also collected supplementary details, including coring date, dating method, number of dated levels, temporal span of the record and sampling resolution. In total, 26 different proxies were identified (Table A1). To avoid duplication, we cross-checked all entries to identify peat cores reported in multiple publications. We first compared core names and reported coordinates (or approximate locations when exact coordinates were unavailable). When cores shared identical or nearly identical locations and had the same ages, lab numbers, basal depths, reference or any unique metadata that could be compared, we treated them as the same record. In cases where the same core was described across multiple publications, we merged the information into a single record. The ages of the records were obtained from the original publications, expressed in calibrated radiocarbon years (cal. yr BP) where available. For 27 sites with only uncalibrated ages, calibration was conducted in R Statistical Software (R Core Team, 2022) using the *bchron* package (Haslett and Parnell, 2008) and the IntCal20 calibration curve (Reimer et al., 2020) (Table A2). Peat cores were identified as basal (representing the complete peat sequence down to the mineral substrate) when such information was provided in the source publication, or when it could be inferred from the stratigraphic diagrams. In the WSPC database, each peat core was assigned a unique Core ID in the format WS_X (e.g., WS_001, WS_002, WS_003). Cores were numbered sequentially according to their geographic position, starting from the southernmost site and progressing northwards. In addition to the assigned Core IDs, we retained the original core names as reported in the source publications and databases to facilitate easier identification and cross-referencing. Each core includes also references to the original source from which the authors of this database obtained it, as well as information about the publication of the initial core source, if such details were provided in the reviewed publication.

3.3 Spatial analysis and data visualization

3.3.1 GIS data preparation and spatial datasets

To visualize and analyse the spatial distribution of peat cores, a shapefile (SHP) layer was created for WSPC database. All sites were georeferenced and compiled into a unified GIS layer using QGIS 3.16.2 software (QGIS Development Team, 2025), with the database attribute structure described in Table 1. The extent of the study region, as well as all subsequent spatial analyses, followed the WSL boundary as described by Sheng et al. (2004). Given the vast extent of the study region and clustering of coring sites, peat core density was assessed by dividing the area into 50 × 50 km grid cells. The number of cores within each cell was calculated using the *join attributes by location (summary)* tool (geometric predicate: *contains*) in QGIS. Besides the attributes obtained from the original publications, each peat core record was supplemented with information on its location within specific vegetation, permafrost, and peatland zones using the same tool in QGIS. Spatial data about vegetation zones were obtained from the map of terrestrial ecoregions by Olson et al. (2001), while permafrost extent was derived from the circum-Arctic map of permafrost and ground-ice conditions by Brown et al. (2002). The spatial extent of peatland zones was based on the map of major peatland zones originally published by Ivanov and Novikov (1976) and reproduced in Kremenetski et al. (2003). This map was georeferenced and digitized for use in this study.

3.3.2 Temporal coverage analysis and permafrost-related grouping

To analyse the percentage of peat cores covering each time interval, we assumed that the age of the record represents the period from the time of sampling back to the oldest dated level, although in some cases (particularly in the northern part of the study area) this may not have been the case. The same assumption was used to analyse the temporal coverage of individual proxies across WSL. Given the substantial influence of permafrost on sampling and data availability, peat cores were classified into three groups corresponding to different permafrost zones: (1) non-permafrost and isolated permafrost, (2) sporadic and discontinuous permafrost, and (3) continuous permafrost.

3.3.3 Scoring system and spatial visualization of proxy representation

To evaluate peat core datasets, we developed a quantitative scoring system to assess the quality and informational value of each peat core record. Proxies were grouped into three categories (biological, physical, and chemical) and each proxy was assigned an individual weight reflecting its relative contribution to environmental reconstructions (Table A3). In addition to proxy-specific weights, we also applied an additional weighting step when integrating proxy information into the final scores. For each proxy group (biological, physical, and chemical), the total sum of all proxy weights from a given group was multiplied by a factor of 4 to emphasize the contribution of group-level proxy richness. When calculating the overall proxy score, the total sum of all proxies across groups was instead multiplied by 5, giving greater influence to records that include a broad suite of proxy types. Each record was also evaluated based on (1) the presence of a chronology, (2) total record length, and (3) the number of proxy types available. These components were scaled to 0–1 and combined with the weighted proxy information to generate four aggregated scores (*combined_bio*, *combined_phys*, *combined_chem*, and *combined_all*) (Table A4).

Table 1. The column headers within Western Siberian Peat Core database and their meaning.

Column name	Description
Core_ID	Unique identifier for each or peat core
Core_name	Original names or identifiers used in the original publication with references
Coord_true	Information if exact geographical coordinates of the location of peat core were provided in the original publication
Lat	Latitude of the core location (in decimal degrees)
Lon	Longitude of the core location (in decimal degrees)
Core_date	Year or period when the core was collected
S_interval	Sampling interval (cm)
N_proxy	Number of proxy types analyzed in the core
P_type	Peatland type based on peatland zone by Kremenetski et al. (2003) after Ivanov and Novikov (1976)
Perm	Permafrost zone based on Brown et al. (2002)
Veg	Vegetation zone in WSL based on Olson et al. (2001)
Ref_n	Source publication reference ($n = 1$–12)
URL_n	DOI, repository link, or other online source corresponding to Ref_n ($n = 1$–12)
	Chronology
N_dates	Number of radiocarbon or other chronological dates available for the core
Age_calBP	Calibrated age in years before present (BP)
Error_calBP	Uncertainty or error range associated with the calibrated age
Age	Availability of data about core age
	Biological proxies
Pol	Availability of pollen data
NPP	Availability of non-pollen palynomorph data
Macro	Availability of plant macrofossil data
TA	Availability of testate amoebae data
MIC_char	Availability of microscopic charcoal data
MAC_char	Availability of macroscopic charcoal data
Orib	Availability of oribatid data
Moll	Availability of mollusc data
Diatom	Availability of diatom data
Arth	Availability of arthropod data
Zoo_rem	Availability of zoological remains data
	Physical proxies
BD	Availability of bulk density data
Moist	Availability of moisture content data
P_accum	Availability of peat accumulation data
Decomp	Availability of degree of decomposition data
Humif	Availability of peat humification data
B_depth	Availability of basal depth data
	Chemical proxies
Ash	Availability of ash content data
pH	Availability of pH data
OM	Availability of organic matter (loss on ignition) data
C_accum	Availability of carbon accumulation data
S_isotop	Availability of stable isotope data ($\delta^{13}C$, $\delta^{15}N$, δD, $\delta^{18}O$)
XRF_XRD	Availability of XRF (X-ray fluorescence) or XRD (X-ray diffraction) data
FTIR	Availability of FTIR (Fourier-transform infrared spectroscopy) data
Geochem	Availability of geochemical data (e.g., elemental analysis, trace element concentrations, radioisotopes, geochemical ratios)

Higher scores indicate records with greater chronological control, longer temporal coverage, and richer multiproxy data. All calculations were performed in R Statistical Software (R Core Team, 2022) using the *dplyr* package (Wickham et al., 2023) for data manipulation. Spatial patterns of combined scores were visualized using QGIS. We applied the Heatmap (Kernel Density Estimation, KDE) tool to each dataset, using a 30 km radius and a pixel size of 100×100 m. The KDE was weighted by the combined scores of all proxies as well as separately for the biological, chemical, and physical proxy groups. The resulting density maps provide a spatially smoothed representation of proxy distribution and highlight both well-sampled regions and areas with insufficient proxy coverage.

3.3.4 Literature-based data extraction and figure assembly

For the literature analysis, if the full text of publication was unavailable, information on the language and proxies used was inferred from the available title, abstract, or bibliographic data accessible to the authors. All plots and diagrams were prepared in R Statistical Software (R Core Team, 2022) using *ggplot2* (Wickham, 2016) package, and final figures were assembled in CorelDRAW Graphic Suite 2021.

4 Results and Discussion

4.1 Peat core studies in the Western Siberian Lowland – literature analysis

4.1.1 Source publications overview

The database was compiled from a total of 156 publications published between 1953 and 2025, which were classified into two categories. The first group *primary sources* included 99 publications identified through an extensive literature review, from which data were directly obtained and used to build the database. The second group *secondary sources* included 57 original publications that were not directly accessible, but were cited within the primary publications used for data extraction. For each core, references are provided both to the publication from which the data were obtained (primary source) and, where available, to the original source publication cited therein (secondary source). The WSPC database is based on 82 English-language, 73 Russian-language, and one German-language publications. The authors had direct access to 79 of the English-language and 20 of the Russian-language sources.

The publications used in the compilation of the database contained information on varying numbers of peat cores. The majority of studies (82 %) presented data from one to five cores, typically providing reconstructions at the local or regional scale. Another 13 % of the publications included results from six to fifty cores. These studies analysed various regions within the Western Siberian Lowland (WSL), often along transects across peatlands, or incorporated WSL data as part of larger datasets. Only eight publications contained datasets with more than fifty peat cores. These studies generally focused on large-scale syntheses addressing specific research questions at the global scale (such as carbon accumulation) or provided a more detailed analysis of the WSL, and include Kremenetski et al. (2003), Sheng et al. (2004), Smith et al. (2004, 2012), MacDonald et al. (2006), Loisel et al. (2014), Hugelius et al. (2020), and Lapshina and Zarov (2023).

Based on conducted literature review, it was observed that between 1950 and 1990, the number of peat core studies in WSL increased notably, with most results published in Russian-language journals or books and only a limited number appearing in English (Fig. 3a). This pattern reflects the early growth of peat research during the Soviet period and the dominance of domestic Soviet research activity, as the region remained largely inaccessible to the international scientific community. After 1990, this trend shifted, as the number of English-language publications increased rapidly, reflecting the onset of international collaboration after the collapse of the USSR. The decade 2010–2020 saw the highest number of publications, reflecting not only regional research dynamics but also the broader global growth in scientific output. Although the decade 2020–2030 is only halfway through, 28 papers on this topic have already been published. While this trend may suggest that the current decade will produce the highest number of publications, ongoing geopolitical tensions, limited accessibility of some areas, and difficulties in collaborating with Russian scientists may slow down further research activity.

4.1.2 Trends in palaeoecological proxy use in the Western Siberian Lowland

Based on the use of proxies, two distinct periods can be identified in WSL studies: an early stage (1950–2000), characterized by single-proxy studies, and the modern period (after 2000), marked by increasing integration of biological, physical, and chemical indicators (Fig. 3b). A major step forward in peatland research was the implementation of radiocarbon dating, developed in the 1940s (Olsson, 2009). Since the 1960s, it has become increasingly important in paleoenvironmental studies and remains the most widely applied chronological tool in peatland research in WSL (Kremenetski et al., 2003). Whereas earlier studies often reported results solely based on depth, radiocarbon dating is now used almost universally. Basal depth was an important physical parameter not only from a scientific perspective but also from an economic one. The discovery of oil in the 1950s initiated intensive studies of WSL peatlands, as information on peat thickness was essential for constructing roads and infrastructure required for oil exploration (Kremenetski et al., 2003). Early decades were dominated by classic palynological studies. Pollen was the first biological proxy applied in this re-

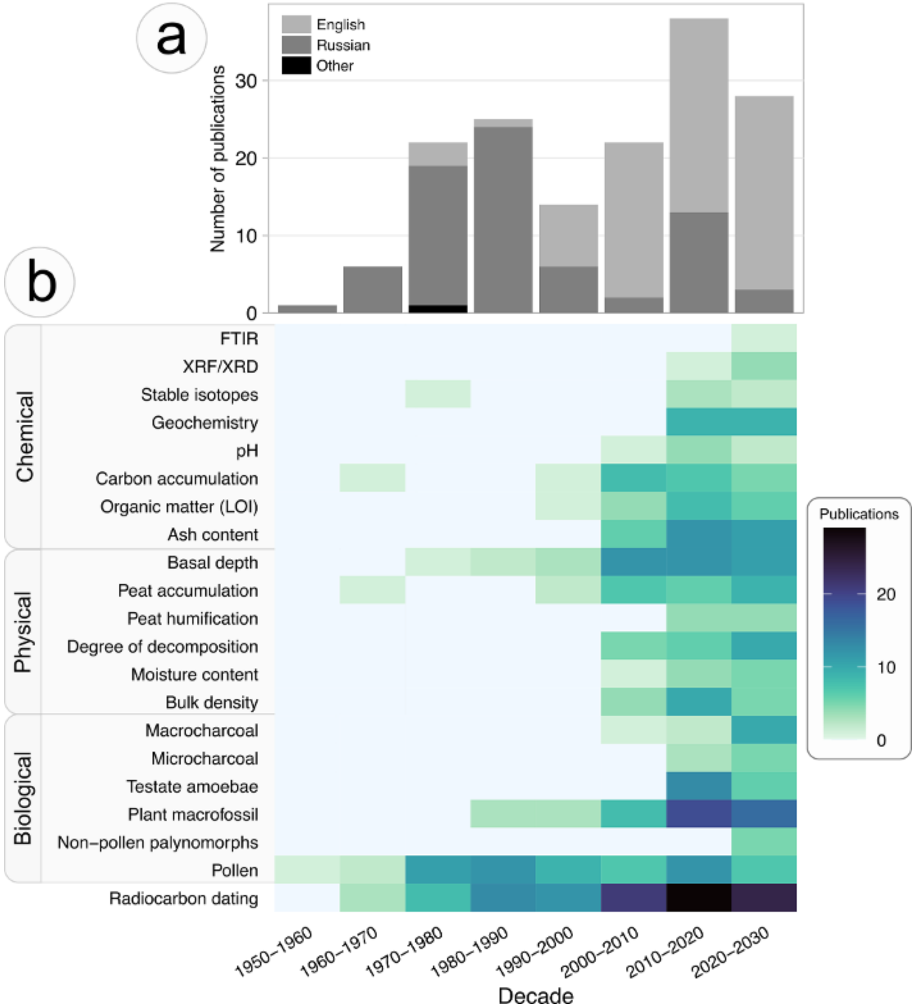

Figure 3. Temporal patterns in research output and methodological approaches: **(a)** trends in the number of publications in Russian and English per decade; **(b)** frequency of selected proxies used in studies across decades. Abbreviations: XRF – X-ray fluorescence; XRD – X-ray diffraction; FTIR – Fourier-transform infrared spectroscopy.

gion and has maintained its importance to the present day. However, although pollen analysis is widely used, it primarily provides information about the vegetation and environment surrounding the peatland rather than the peatland itself. Growing interest in peatland development led to the increasing use of plant macrofossil analysis, which began to be applied from the 1980s onward. After 2000, more proxies started to be implemented in research on WSL. New biological proxies, such as testate amoebae and micro- and macrocharcoal, were introduced, providing valuable tools for reconstructing changes in peatland hydrology and fire activity at different spatial scales. More laboratory analyses aimed at obtaining more precise data on the physical and chemical properties of peat began to be applied (e.g., bulk density, pH, ash content), along with newly developed technologies introduced over the past decade (e.g., XRF (X-ray fluorescence), FTIR (Fourier-transform infrared spectroscopy)). Peat and carbon accumulation were already studied in research conducted before 2000; however, their frequency had increased noticeably since then. The increased variety of applied proxies over the past 25 years, on one hand reflects the development of new research methods, and on the other, a growing awareness of the importance of peatland ecosystems and the desire to better understand their history.

4.2 Western Siberian Peat Core Database

4.2.1 General information and spatial distribution

The Western Siberian Peat Core Database (WSPC) includes information on the locations and applied palaeoecological proxies of 654 peat cores or peat cross-sections collected from the WSL (Fig. 4a). The spatial distribution of cores highlights the considerable challenges associated with conducting research in the WSL peatlands. Their vast extent, the widespread presence of permafrost, and limited transport accessibility largely determine the areas where sediment sampling is logistically feasible. Notably, 47 % of all peat cores (306 out of 654) included in the WSPC database were collected within a 100 km buffer zone of the major rivers: Ob, Yenisey, Irtysh, and Tobol, with high density of cores in the Middle Ob' Lowland (Fig. 4b). A distinct concentration of collected cores is observed in the Great Vasyugan Mire (west of Tomsk), which represents the largest contiguous peatland in the world (Fig. 4c) (Kirpotin et al., 2009). Various parts of this extensive complex have been the focus of numerous previous studies (e.g. Blyakharchuk et al., 2019; Lapshina and Zarov, 2023; Rudmin et al., 2018; Syso and Peregon, 2009) due to the absence of permafrost and the proximity to major cities facilitating field work organisation. Another distinct concentration of peat cores is observed in the central part of the study region, between the Ob and Yenisey rivers, where numerous cores were collected during extensive Russian-American field campaigns conducted between 1999 and 2001 (Sheng et al., 2004; Smith et al., 2000). Although the railway network in WSL is relatively sparse, a major line crosses this area, connecting Tyumen with Novy Urengoy, Nadym, and Yamburg, thereby facilitating logistical access to this part of the region. Peatlands in the northern part of the WSL have been studied mostly on the Yamal Peninsula, with a few coring sites on the Gyda Peninsula, mainly along the shore of the Gydan Bay. The northernmost core in the database was located on Bely Island (73.34190° N, 70.12760° E) and southernmost on Dolgon'koye swamp (53.21250° N, 84.40720° E).

The WSPC database includes peat cores, representing a broad range of environmental settings across the region. Peatlands in WSL occupy all major permafrost zones and vegetation types, although their spatial extent and sampling intensity vary (Fig. 5a, c). Peatlands are most extensive in the non-permafrost zone, which covers 41.5 % of the total peatland area, followed by the discontinuous (18.6 %), sporadic (14.1 %), isolated (13.9 %), and continuous (11.9 %) permafrost zones. In general, the number of peat cores reflects the relative area of peatlands in each zone. The two permafrost zones with the largest peatland areas also have the highest numbers of peat cores: the non-permafrost zone (278 cores, 42.5 % of the total) and the discontinuous permafrost zone (132 cores, 20.2 %). The number of peat cores in the isolated (94 cores, 14.4 %) and continuous (101 cores, 15.4 %) permafrost zones also corresponds closely to the proportion of peatland area in these zones. The main exception is the sporadic permafrost zone, which contains the third-largest share of peatland area (14.1 %) but is relatively underrepresented, accounting for only 7.5 % of all peat cores in the database.

Across vegetation types, the majority of WSL peatlands are associated with boreal forests/taiga (78.9 %), followed by tundra (13.7 %), temperate broadleaf and mixed forests (6.1 %), and temperate grasslands and shrublands (1.3 %). The distribution of peat cores reflects this pattern: cores from peatlands in boreal forests dominate the dataset (405 cores, 61.9 %), followed by tundra sites (118 cores, 18.0 %), while mixed forests (92 cores, 14.1 %) and shrubland peatlands (39 cores, 6.0 %) are considerably less represented by peat cores in the database.

Based on major peatland zones, polygonal peatlands, which dominate north of 67° N and are associated with continuous permafrost and tundra vegetation, are represented by 90 cores (13.8 %) in the database (Fig. 5b, c). Flat hill and large hill peatlands, which occur predominantly within the discontinuous permafrost zone and are associated with taiga vegetation between 61–67° N, account for 107 (16.4 %) and 49 (7.5 %) cores, respectively. Oligotrophic (*Sphagnum*-dominated) peatlands, concentrated between 56–61° N and typically associated with boreal forest/taiga areas exhibiting either non-permafrost, isolated or sporadic permafrost, represent the most frequent peatland type in WSL and are represented by the largest group of 337 cores (51.5 %). The two southernmost peatland zones, where permafrost is absent and temperate vegetation types predominate, are the least represented in the dataset. Flat eutrophic and mesotrophic peatlands, occurring in a narrow belt from 55–58° N in the east and up to 60° N in the west, include 34 cores (5.2 %), while eutrophic and brackish peatlands, located south of 55° N, form the smallest group, with 30 cores (4.6 %). Additionally, 7 cores (1.0 %) are outside the extent of the defined peatland zones.

4.2.2 Variation in the number of proxies per core

The WSPC database documents the application of 26 palaeoecological proxies in peat cores in the WSL, grouped into four categories: biological, physical, chemical and chronological (Fig. 6b, Table A1). Peat cores in the database differ substantially in the number of applied proxies, ranging from only one to a maximum of 12 per core (Figs. 6a, 8a). The most common in the database were cores containing one or two palaeoecological proxies, representing 26.3 % and 28.4 % of all records, respectively. Peat cores that include only a single proxy most commonly contain information on basal depth or sediment age; and in some cases, pollen or plant macrofossil data. For cores containing only biological proxies, this may be explained by the extraction of data from more recent, method-focused publications (e.g. palynology), whereas broader and potentially more comprehensive information may have been reported in earlier sources that were inaccessible for the authors of this database. In cores containing two proxies, the most frequent combinations include basal depth or age paired with either pollen or carbon accumulation data. Peat cores containing data from three to six proxies typically include several biological proxies combined with age or basal depth information, and in some cases supplemented with peat property measurements (e.g. peat or carbon accumulation, or organic matter content). The sec-

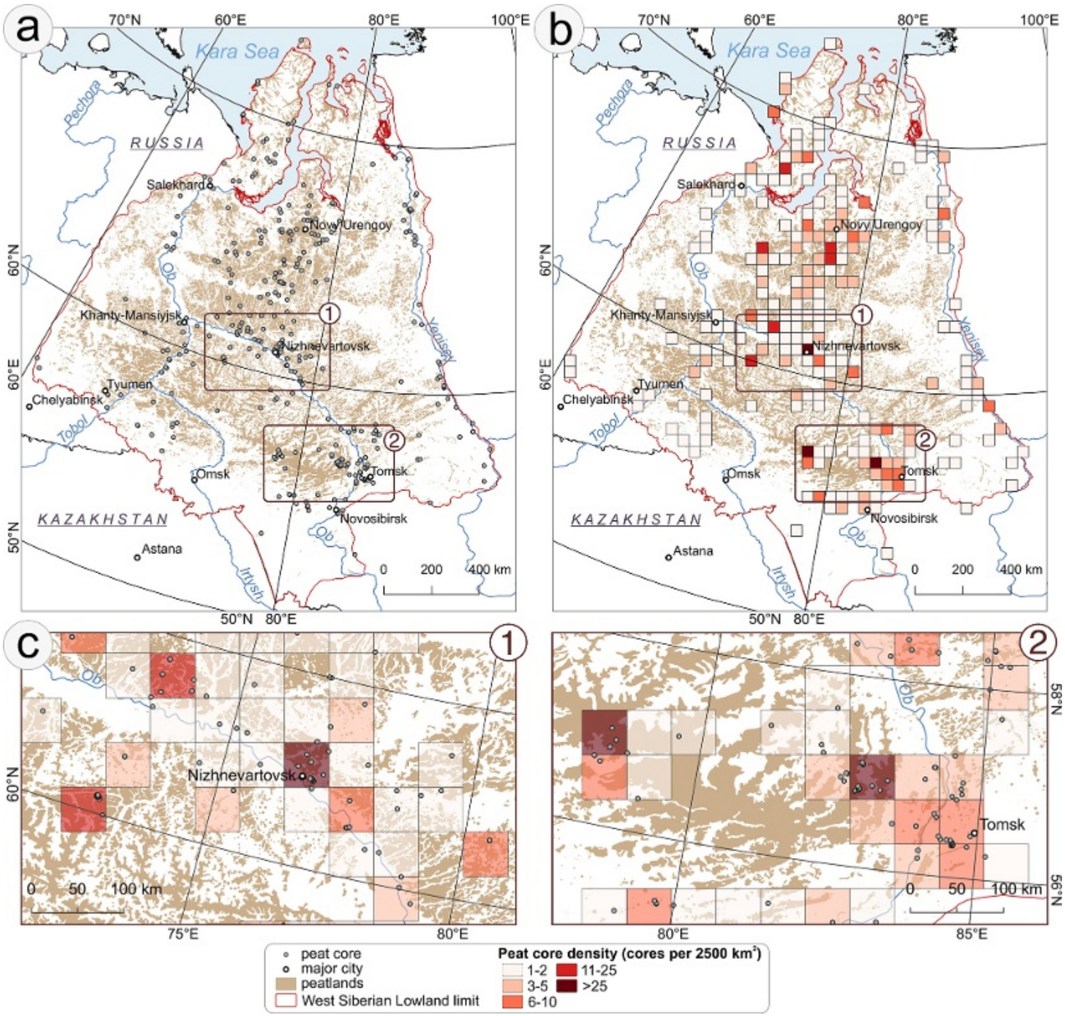

Figure 4. Distribution of peat cores in Western Siberian Peat Core Database: **(a)** spatial distribution of peat cores in Western Siberia Lowland (WSL), **(b)** peat core density (number of cores per 2500 km^2), **(c)** the zoomed maps of two regions within the WSL: (1) peatland complexes in the Middle Ob' Lowland near Nizhnevartovsk, and (2) the eastern part of the Great Vasyugan Mire. Maps include peatlands extent based on Sheng et al. (2004).

ond most common proxy count is seven (13.0 %). Within this group, two distinct core types can be distinguished: (1) cores that resemble the "3–6 proxy" category but incorporate more biological proxies, and (2) cores that lack biological proxies but provide more extensive data on the physical and chemical properties of peat. Cores containing eight or more proxies represent multi-proxy analyses, integrating biological, physical, and chemical data along with sediment dating, and thus provide the most comprehensive information on the history of the studied peatlands. Only 9.8 % of all cores include this number of proxies, while just 1.2 % contain ten or more. The spatial distribution of peat cores with a given number of proxies is also evident (Fig. 8a). High concentrations of well-studied peatlands occur along major rivers, particularly the Ob (Mukhrino, Sredne Vasyuganskoe, Samara, and Bakchar) and the Yenisey (Igarka). Given its large size and ecological significance, the Great Vasyugan Mire also contains numerous peat cores with a high number of proxies, reflecting its long-term use as a key site for multi-proxy palaeoecological research. Another cluster of cores analysed with multiple proxies is observed in the central part of the study region, between the Ob and Yenisey rivers. These cores were mostly collected during Russian-American field campaigns and include detailed physical and chemical analyses of peat, as well as cores described in single-core studies, such as the Khanymei peatland (Halaś et al., 2025).

4.2.3 Relative use of different proxy and their regional patterns

In the WSPC database, a total of 26 palaeoecological proxies has been applied to peat cores from WSL; however, their

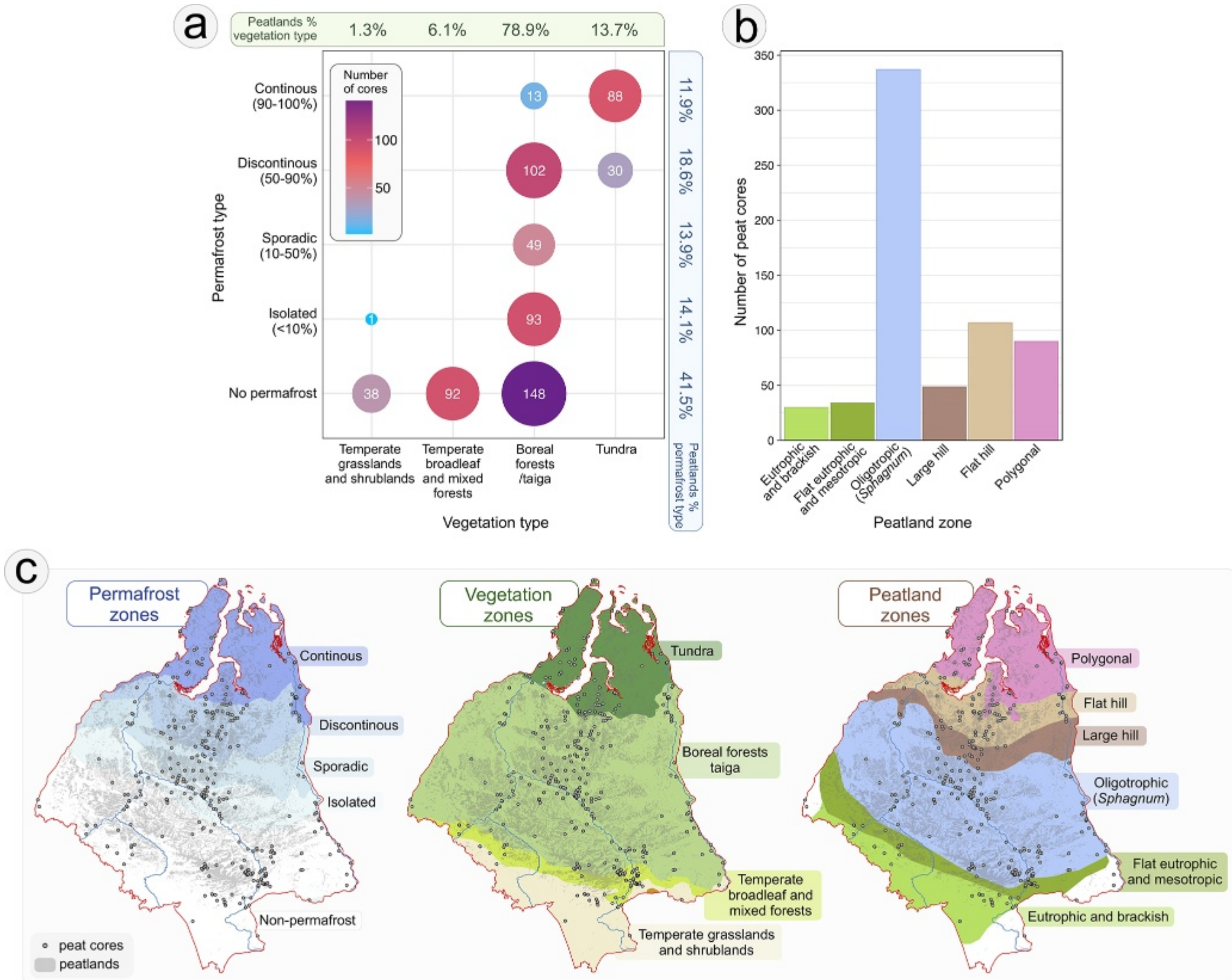

Figure 5. Distribution of peat cores in the Western Siberian Peat Cores Database by permafrost, vegetation, and peatland type; **(a)** number of peat cores within each permafrost zone and vegetation type, with percentages of peatlands occurring in each category; **(b)** number of peat cores by major peatland zones; **(c)** spatial distribution of peat cores in relation to permafrost zone, vegetation type and peatland type. Vegetation zones are based on Olson et al. (2001), permafrost extent on Brown et al. (2002), major peatland zones on Kremenetski et al. (2003) (after Ivanov and Novikov, 1976), and peatland extent on Sheng et al. (2004).

use varies significantly, both in quantitative frequency and in spatial distribution across the study area (Figs. 6b, 7, B1).

Chronological proxies

Chronological proxies are essential for reconstructing peatland development over time and were applied in 58.0 % of all peat cores. Radiocarbon dating is by far the most frequently used method in the region, enabling age-depth modelling and temporal correlation of palaeoecological data (Chambers and Charman, 2004). The resolution of dating varies considerably between cores: some cores were dated only at the basal level, whereas others include several dated horizons. This variability often reflects financial constraints, as multipoint dating remains relatively expensive. Nevertheless, in recent decades researchers have increasingly adopted multilevel dating within individual cores to achieve more robust reconstructions and to facilitate comparison with paleoclimate data (e.g. Feurdean et al., 2019; Lamentowicz et al., 2015; Leonova et al., 2022; Novenko et al., 2023). Due to its widespread application, the spatial distribution of this proxy is relatively uniform, and it is represented in peat cores across most of WSL (Fig. B1a).

Physical proxies

Physical proxies, which provide information on peat properties and stratigraphy, are frequently applied in the peat

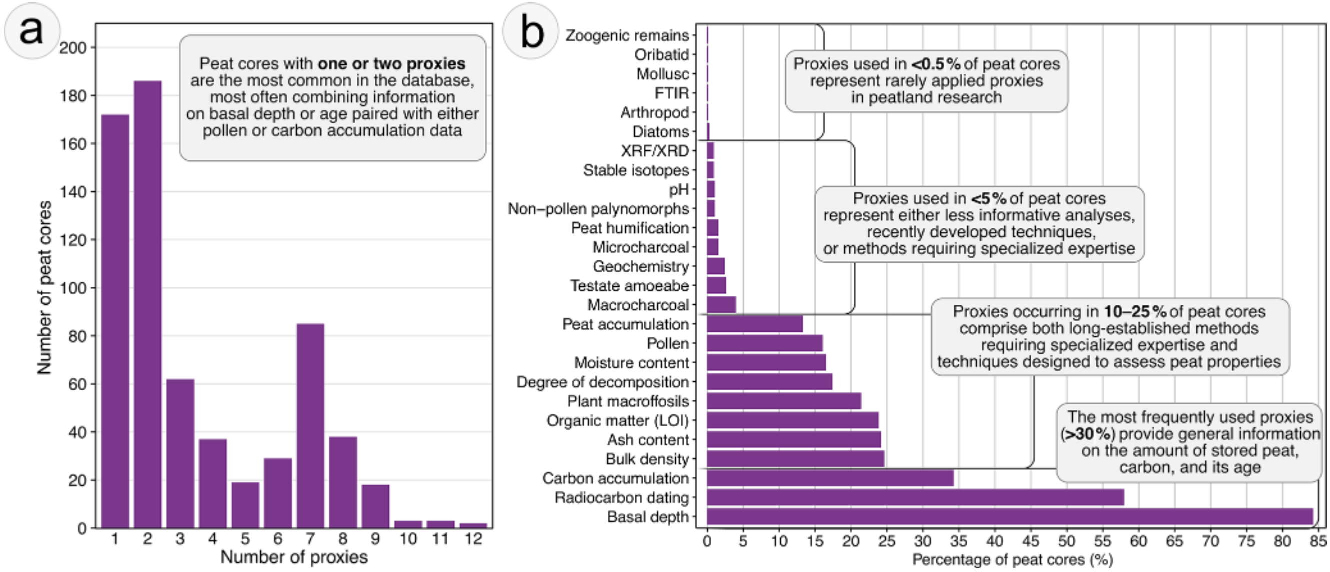

Figure 6. Summary of palaeoecological proxies applied in peat cores in the Western Siberian Peat Core Database; **(a)** number of proxies used and corresponding number of peat cores, **(b)** frequency (%) of use of individual proxies across the peat cores. Abbreviations: XRF – X-ray fluorescence; XRD – X-ray diffraction; FTIR – Fourier-transform infrared spectroscopy.

cores included in the database in the database. Basal depth is by far the most common proxy, present in 84.3 % of cores (Fig. 6b). Such a large number of basal depth measurements is primarily due to the fact that this parameter is relatively easy to obtain in the field and usually does not require specialist expertise (Parry et al., 2014). Many basal depth data were collected during geological prospecting campaigns or as part of detailed investigations of the development of individual peatland complexes (Kremenetski et al., 2003; Lapshina and Zarov, 2023). This widespread use reflects both its fundamental importance for peatland development studies and its relevance as an economically significant parameter (Fig. B1b). Another important physical proxy useful e.g. for carbon content calculations is bulk density, reported in 24.6 % of cores, mostly from the central part between the Ob and Yenisey rivers and from the Vasyugan Plain (Fig. B1c). Degree of decomposition and peat humification are both analyses that indicate the intensity of decay processes; however, the methods differ (Biester et al., 2014). Peat humification is an older technique and is rarely used (1.5 % of cores), whereas the degree of decomposition, usually assessed via the von Post scale – a traditional Russian field method – is much more common in WSL cores (17.4 %). Their occurrence within the study area is characterized by a clear concentration in the south, on the Vasyugan Plain, while in the remaining regions the proxy is represented only in a small number of sites (Fig. B1d, g). Moisture or water content, a proxy useful for interpreting decomposition processes or nutrient mobility (Rydin et al., 2006), was applied in 16.5 % of all cores, and its spatial distribution is similar to that of bulk density (Fig. B1e). Peat accumulation is an important proxy that not only provides information about peatland development but can also indirectly inform about past climate variability (Swindles et al., 2025). It was used in 13.3 % of the cores, which are distributed across the study region, with more sites located on the Vasyugan Plain (Fig. B1f). The form in which this information is reported varies depending on analytical resolution, sometimes it is a single value for the entire core, and its accuracy increases with increasing resolution. Nevertheless, accumulation rates in permafrost-affected peatlands should be interpreted with caution, as cryogenic structures and variable ice content may substantially influence peat accumulation and preservation processes (Treat et al., 2016). However, such information was not consistently reported in the analysed studies and therefore could not be systematically included in the database.

Chemical proxies

Chemical properties of accumulated peat in WSL have also been frequently analysed in peat cores. The most commonly used chemical proxy is carbon accumulation, applied in 34.3 % of all studied cores (Fig. 6b). This proxy provides valuable information about the total amount of stored carbon in the peat and about long-term changes in peatland carbon sink strength (Charman et al., 2015). WSL is recognized as a global carbon hotspot; therefore, many studies focus on carbon budgets and accumulation patterns, which explains the widespread use of this proxy. This proxy is predominantly reported in sites from the central part of the study region and the peatlands of the Vasyugan Plain; however, cores containing this information are also frequently found in river valleys

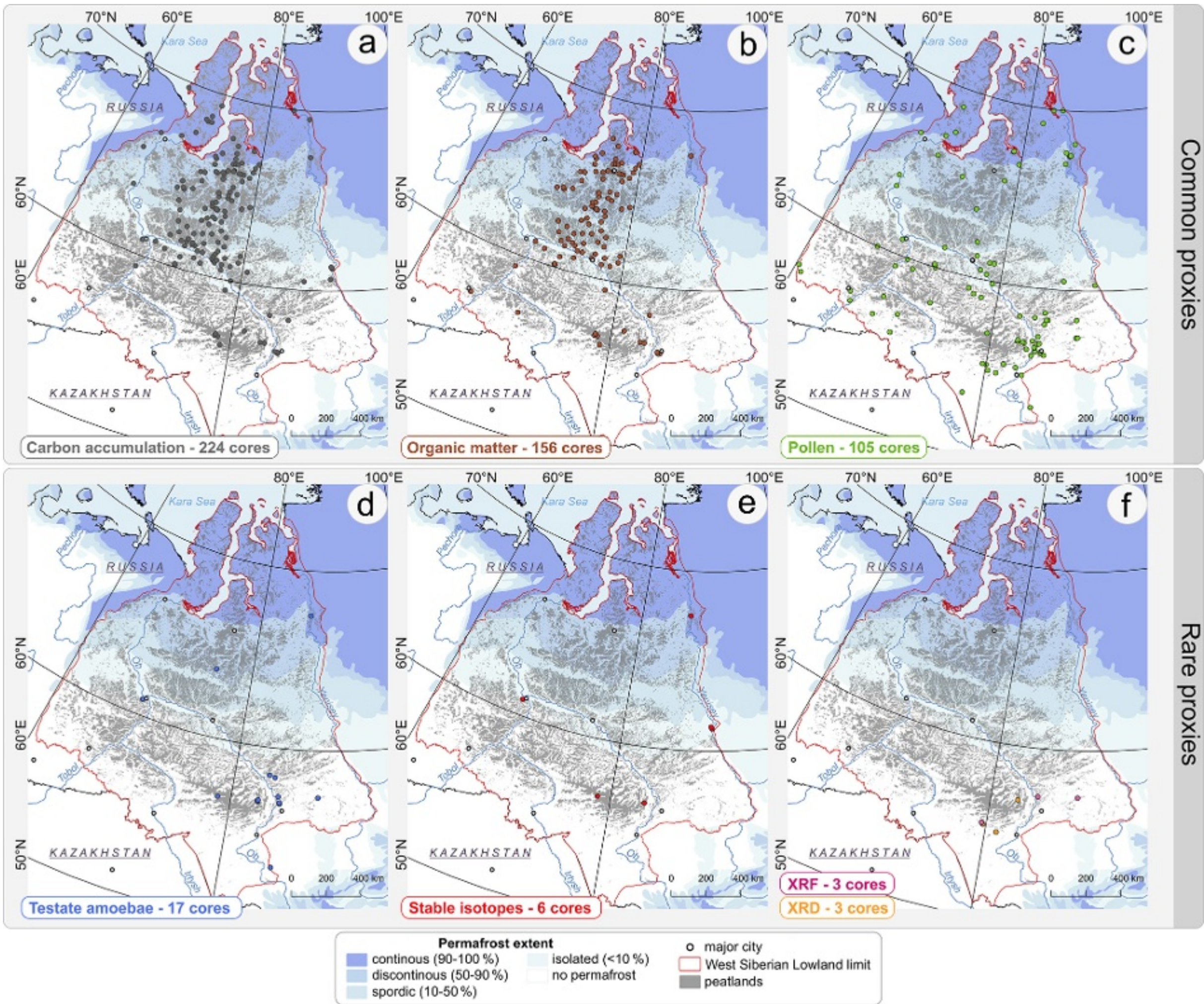

Figure 7. Spatial distribution of peat cores included in the Western Siberian Peat Core Database with records of selected proxies. Commonly used palaeoecological proxies are shown in panels **(a)**–**(c)** (**(a)** – carbon accumulation; **(b)** – organic matter; **(c)** – pollen), while rarely applied proxies are presented in panels **(d)**–**(f)** (**(d)** – testate amoebae; **(e)** – stable isotopes; **(f)** – XRF/XRD). Numbers indicate the total count of cores containing each proxy. Maps include peatlands extent based on Sheng et al. (2004) and permafrost extent based on Brown et al. (2002). Abbreviations: XRF – X-ray fluorescence; XRD – X-ray diffraction.

and on the Yamal Peninsula (Fig. 7a). Ash content and organic matter, typically measured via loss-on-ignition (LOI) analysis, are also commonly analysed in WSL peat cores, appearing in 24.2 % and 23.9 % of peat cores, respectively. These simple and low-cost methods are widely used in paleoecology and provide information about peat composition and the input of inorganic material (Chambers and Charman, 2004; Tolonen, 1984). Their spatial distribution is very similar and resembles the distribution pattern of bulk density (Figs. 7b, B1t). Other chemical proxies included in this database: geochemistry, pH, stable isotopes, XRF or XRD and FTIR have been rarely applied in WSL peat cores. Data on pH, which reflects peat acidity, are more characteristic of modern ecological surveys than of palaeoecological studies. Consequently, this proxy was used in only 1.1 % of all cores, exclusively in non-permafrost peatlands in the southern part of the region (Fig. B1w). Traditional geochemical analyses (2.4 %), stable isotopes (0.9 %), XRF/XRD (0.9 %), and FTIR (0.2 %) all require specialised expertise and laboratory infrastructure, which until recently were not widely accessible. Geochemical analyses and XRF/XRD are different methods for determining the elemental composition of peat. Geochemistry has become increasingly popular in recent years, whereas XRF and XRD, traditionally used in lake sediment studies, have only recently begun to be applied to peat (Longman et al., 2019; Shotyk, 1988). Geochemical analyses have been conducted in several peatlands south of 64° N, while XRF/XRD has been used primarily in peatlands near Tomsk in the south-eastern part of the study area (Figs. 7f, B1v). Stable isotopes in peat provide valuable in-

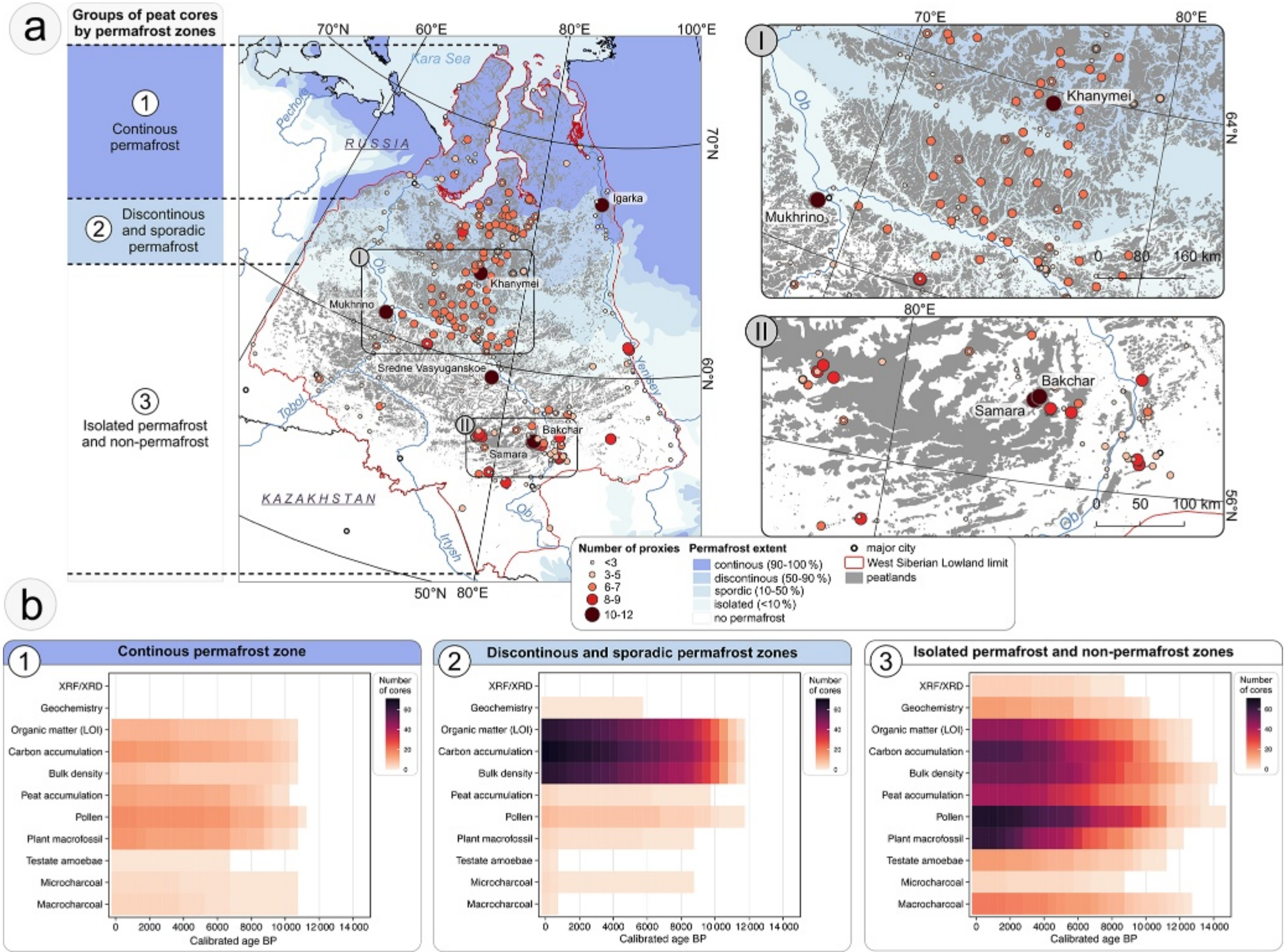

Figure 8. Palaeoecological proxies used in peat cores in the Western Siberian Peat Core Database: **(a)** spatial distribution of peat cores categorized by the number of proxies analysed, with names of peatlands (cores) with the greatest number of proxies, permafrost zones based on Brown et al. (2002), and peatland extent based on Sheng et al. (2004); **(b)** heatmaps of the temporal coverage of individual proxies within three groups of cores distinguished by permafrost zone: (1) the continuous permafrost zone, (2) the discontinuous and sporadic permafrost zones, and (3) the isolated permafrost and non-permafrost zones. Colour intensity reflects the number of cores contributing data within 500-year intervals. Abbreviations: XRF – X-ray fluorescence; XRD – X-ray diffraction. Heatmaps were prepared only based on cores with established chronologies.

sights into past environmental and climatic conditions; however, they are costly and require specialized isotope facilities (McClymont et al., 2010). Such data are scattered across WSL and are typically collected from cores analysed in extensive studies that integrate multiple other proxies (Fig. 7e) (Feurdean et al., 2019; Startsev et al., 2022).

Biological proxies

The group of palaeoecological proxies that has been the least frequently applied in WSL peat cores are biological proxies (Fig. 6b). They rely on the identification of remains of organisms preserved in peat and are therefore highly dependent on preservation conditions. Additionally, they are usually time-consuming and require specialist expertise. The most frequently used biological proxy, applied in 21.4 % of all cores, is plant macrofossils (referred to as "botanical composition" in older publications), which reflect local peatland vegetation and are essential for reconstructing peatland development and hydrology (Birks and Birks, 2000). However, the level of analytical detail varies between studies. In some cores, particularly in older works, the data are limited to reporting dominant *Sphagnum* species or other major plant groups, often at a low sampling resolution of 10 or 25 cm. In contrast, more recent studies tend to use higher-resolution sampling and more detailed identifications, frequently including subfossil vegetative fragments and carpological remains (e.g. Halaś et al., 2025; Novenko et al., 2022). Peat cores with plant macrofossil data are spread across WSL, with a higher concentration on Vasyugan Plain and in the area near Tomsk (Fig. B1h). Pollen is an excellent proxy for reconstructing past regional vegetation and landscape-scale ecological changes (Mander and Punyasena, 2018). Owing to its long-established use in palaeoecological studies, it was introduced very early in WSL research. To date, 16.1 % of all cores in the database contain pollen data. These cores cover the majority of WSL, with their highest frequency occurring in areas where core density is greatest (Fig. 7c). Non-pollen palynomorphs (NPPs) are additional microfossils that can be identified during standard palynological analysis (Shumilovskikh et al., 2021). Because Quaternary palynologists historically did not focus on these other palynomorphs, their identification is challenging, and their systematic documentation only began in the late 1970s, their use in WSL cores has remained limited. Although the scientific community has increasingly recognized the potential of this proxy to reflect local ecological conditions and it is now being applied at more sites (e.g. Feurdean et al., 2022; Halaś et al., 2025), only 1.1 % of all cores currently include NPP data, and these come from only a few locations in the WSL (Fig. B1m). Peatlands are also valuable archives of past fire activity, with charcoal commonly used as a proxy for this purpose. Depending on the intended spatial scale of fire reconstruction, different charcoal size fractions are analysed: macrocharcoal for local fires and microcharcoal for regional fire activity (Conedera et al., 2009). Both types are present in the WSL, although at low frequency. Macrocharcoal has been used more often, occurring in 4.0 % of all cores, whereas microcharcoal appears in only 1.5 %. There is no clear spatial pattern in their use; instead, they are found sporadically in isolated cores across the study area (Fig. B1j, l). A lack of fire-history research in WSL (and in Russia more broadly) was also noted by Pupysheva and Blyakharchuk (2023). They emphasized that fire proxies are relatively new to this region and highlighted the importance of expanding fire-history studies across this territory. Hydrology is one of the most important environmental variables controlling the condition of peatland (Rydin et al., 2013), and testate amoebae are a well-established proxy for reconstructing past hydrology of these ecosystems (Charman, 2001). Although their widespread use in palaeoecological research began roughly 40 years ago (Mitchell, 2025), their application in WSL peat cores remains very limited, appearing in only about 2.6 % of all studied cores. Testate amoebae have been used primarily in non-permafrost peatlands in the southern part of the WSL, while in other permafrost zones they have been applied only sporadically (Fig. 7d). Less frequently used biological proxies include arthropods, molluscs, oribatid mites, diatoms, and zoogenic remains, each recorded in less than 0.3 % of cores. Although these proxies can offer valuable insights into local environmental conditions, their preservation in peat is generally poor, and they are more characteristic of lake sediment studies. As a result, they are rarely applied in peatland research. This pattern is also evident in WSL, where their use in peat cores is limited to only a few isolated cases (Fig. B1n–r).

Overall, the WSPC database demonstrates a strong focus on fundamental physical and chemical proxies, particularly basal depth, carbon accumulation, and organic matter content, reflecting the importance of these variables in peatland palaeoecology. Biological proxies are applied more selectively, often depending on the research question, while more specialized proxies such as geochemistry, stable isotopes, or FTIR are rarely used. This distribution highlights both the breadth of multi-proxy approaches in WSL peatlands and the gaps in underrepresented proxy types, particularly in biological and specialized chemical analyses.

4.2.4 Age structure of peat cores and temporal coverage of proxies

The WSPC database includes three types of peat cores: (1) full-length sequences that extend from the basal mineral substrate to the sampling date and thus capture the complete peat accumulation history; (2) upper-only sequences that begin at the modern peat surface but do not reach the basal layer, typically resulting from targeted sampling strategies such as upper-core ecological reconstructions or from logistical constraints, particularly in permafrost regions; and (3) cores that may or may not reach the basal mineral substrate but are distinguished by the absence of the youngest peat layer due to climate-driven cessation of peat accumulation or degradation of previously accumulated peat, a pattern most commonly observed in polygonal peatlands in the northern part of the region. The temporal distribution of peat core ages, summarised in 300-year intervals, shows a highly uneven pattern, revealing several distinct phases across the time span up to ∼ 16 000 cal. yr BP (Fig. 9b). Since the majority of cores in the WSCP database were published after 1950 and type-3 cores are relatively rare, we assumed for this analysis that each peat core represents continuous data from 1950 to the deepest dated layer.

Peat cores covering only the near-modern period (0–2000 cal. yr BP) are quite rare in the database, usually less than 5 cores per 300-year interval (Fig. 9b). There is an increase in the number of cores that cover longer periods of the Late Holocene up to 4000 cal. yr BP, with 6–12 cores per interval. Cores covering the Middle Holocene (∼ 4000–8000 cal. yr BP) form the second most frequent group, averaging 10 cores per interval. The highest representation is observed for cores spanning ∼ 8000–11 000 cal. yr BP, with nearly half of all chronologically established cores reaching this period. Beyond ∼ 11 500 cal. yr BP, the number of cores declines sharply, with only individual cores reaching into the Late Glacial. The oldest peat core in the WSPC database dates to 15 623 cal. yr BP (core WSL_246) and is located near the Yenisey River within a present-day non-permafrost region (Fig. 9a). Peat cores older than 11 500 cal. yr BP are exclusively situated south of 62° N, where current ground

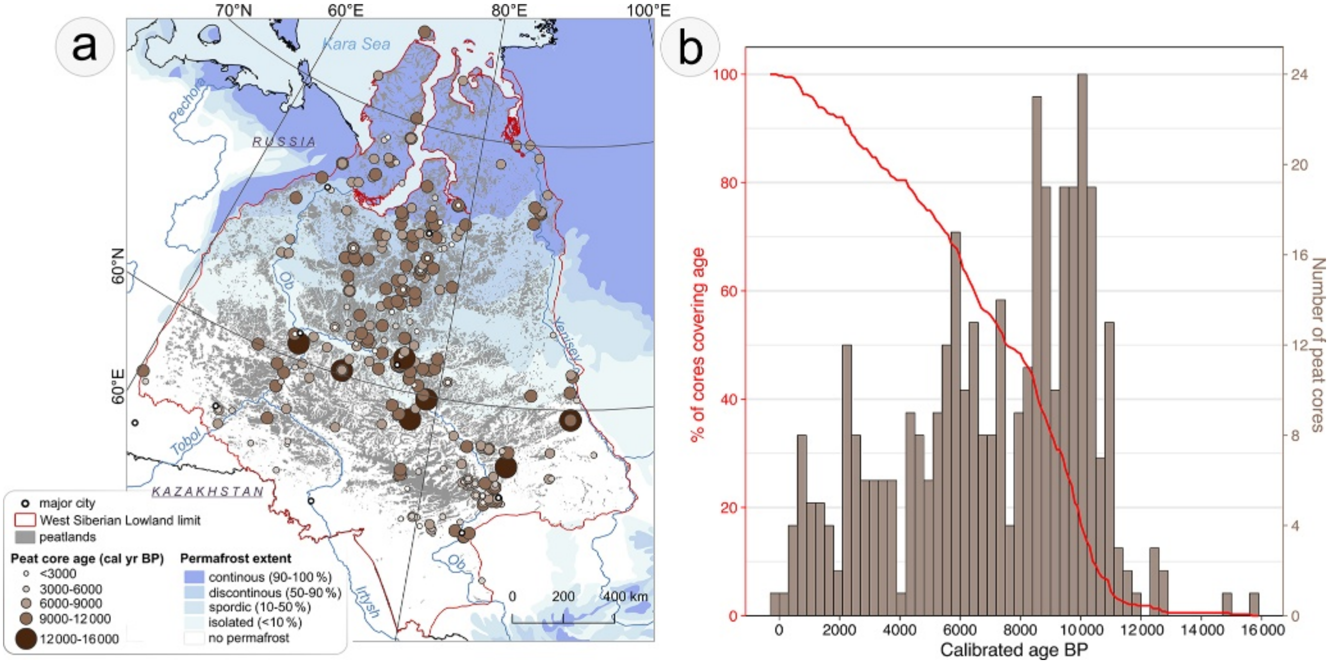

Figure 9. Age distribution of peat cores in the Western Siberian Peat Core Database (WSPC): **(a)** spatial distribution of peat cores with calibrated ages (cal. yr BP) of basal or dated bottom levels across Western Siberian Lowland; **(b)** histogram of the number of peat cores within 300-year age intervals, representing the temporal coverage and length of palaeoecological records in the database, and percentage of peat cores in the WSPC database covering age. Map and plot created only based on cores with established chronologies.

conditions correspond to non-permafrost or isolated permafrost zones, and all of these oldest records are located within 100 km of major river channels. The lack of records from this period is consistent with limited peatland development in WSL during the Late Glacial, when conditions were generally unfavourable for peat accumulation (Alexandrov et al., 2016; Velichko et al., 2011). In terms of coverage, ∼ 80 % of cores extend over the last 4000 cal. yr BP, ∼ 50 % reach 8000 cal. yr BP, and only ∼ 5 % cover 11 000 cal. yr BP.

Because the database includes both basal-depth and upper-only cores, these data cannot be interpreted as direct records of peatland initiation and serve as a basis for analysis spatial peatland development in WSL. Instead, it reflects the age extent of available peat profiles. Despite this limitation, the broad temporal pattern – many cores spanning the early Holocene and very few extending into the Late Glacial – broadly aligns with regional peatland development phases described for this region (Kremenetski et al., 2003).

Temporal coverage of selected proxies varies across permafrost zones, reflecting differences in peat core density, maximum peat age in each zone, and the overall frequency of proxy application (Fig. 8b). The longest peat records occur in isolated and non-permafrost zones, where the majority of studied proxies have been applied, and where most of them provide the greatest temporal coverage, with some extending to almost 15 000 cal. yr BP. In other permafrost zones less proxies have been used, in sporadic and discontinuous permafrost zones proxies' coverage span up to 11 500 cal. yr BP, whereas in continuous permafrost zone, maximum temporal coverage reaches ∼ 11 000 cal. yr BP. Temporal coverage of proxies also depends on the number of cores available for each time interval, which directly affects the completeness and spatial representativeness of the data. When only a few cores provide information for a given variable, such as peat accumulation, the insights are limited and largely local, whereas larger numbers of cores allow for more comprehensive and regionally representative interpretations.

Isolated and non-permafrost zones

The peat cores from isolated and non-permafrost zone provide the earliest and most continuous proxy coverage of all three regions, with several proxies extend into the Late Glacial, providing broader and more detailed insights into the regional peatland history (Fig. 8b). Pollen data for this region are present from ∼ 15 000 cal. yr BP, making it the oldest palaeoecological proxy across all regions and providing a continuous record of vegetation composition and broader regional ecological transitions from the Late Glacial through the Holocene. Although the earliest period is represented by only a few sites, the number of cores grows rapidly after 11 000 cal. yr BP, reaching more than 60 cores in the recent period. Thus, this region offers the highest resolution, most spatially extensive vegetation reconstructions from peatlands in WSL. Peat-property proxies, including organic matter and bulk density, as well as peat and carbon accumulation extend to ∼ 14 000 and 12 000 cal. yr BP, earlier than in any other region. Their steady increase to dozens of cores through the Holocene offers robust reconstruction of substrate evolution, decomposition dynamics, carbon accumulation rates, and peat accumulation phases. Plant macrofossils data are available until ∼ 12 000 cal. yr BP and reach over 60 cores in the Late Holocene, enabling high-resolution reconstructions of local plant assemblages, peatland microtopography, and fen-bog transitions. Hydrological reconstructions through testate amoebae extend to ∼ 11 000 cal. yr BP and increase to 14 cores, supporting long-term and spatially extensive water-table reconstructions. Geochemical and XRF/XRD records are present from ∼ 10 000–8500 cal. yr BP, capturing changes in mineral influx, ash content, and geochemical environment. These datasets are largely only available in this part of WSL; although representation increases through time, they still allow only spatially restricted interpretations. Fire proxies vary in temporal coverage. Macrocharcoal is recorded from ∼ 12 500 cal. yr BP, with moderate representation after 8500 cal. yr BP, providing the deepest temporal perspective on local fire history across WSL. Microcharcoal, which can inform on regional fire dynamics, is traceable to ∼ 8500 cal. yr BP but remains very sparse.

Sporadic and discontinuous permafrost zones

The temporal coverage in the discontinuous and sporadic permafrost zones differs markedly from the previous region. Here, a few proxies dominate, providing long-term data across the Holocene, while others are absent or offer temporally and spatially restricted information (Fig. 8b). Organic matter, carbon accumulation, and bulk density data are available until ∼ 11 500 cal. yr BP, and their representation increases sharply through the Early Holocene, remaining exceptionally high (> 60 cores) throughout the Mid- and Late Holocene. This suggests that this zone provides the strongest quantitative foundation for Holocene carbon-accumulation reconstructions among all permafrost regions. In contrast, peat accumulation data extend only to ∼ 9500 cal. yr BP and are available from a very limited number of cores. While these data add a quantitative dimension to vegetation productivity, low representation restricts their use to localized reconstructions rather than regional-scale trends. Pollen data, similar to bulk density, are present from ∼ 11 500 cal. yr BP but remain sparse until the Mid-Holocene. Only from ∼ 7000 cal. yr BP onward does pollen coverage expand to 7–9 cores per interval, allowing spatially broader vegetation reconstructions. Plant macrofossils and microcharcoal data extend to ∼ 8500 cal. yr BP but remain rare, providing long-term yet localized records of plant communities, peatland-surface conditions, and regional fire history. Geochemical information obtained from traditional geochemical analyses is limited to a single site but extends back to ∼ 6000 cal. yr BP, whereas XRF/XRD data are unavailable for peatlands located in these permafrost zones. Hydrological records through testate amoebae are largely absent, appearing only within the last 500 years, which restricts water-table reconstructions to the very recent past. A similar pattern is observed in macrocharcoal data; information on local fire activity, in contrast to the southern region of WSL, is almost entirely absent for peatlands in this region.

Continuous permafrost zone

Proxy data in the continuous permafrost zone are available up to ∼ 11 000 cal. yr BP, with pollen providing the longest and most continuous environmental record (Fig. 8b). Most other proxies are present until ∼ 10 500–10 000 cal. yr BP, and in all cases, representation peaks around 6500 cal. yr BP, though it remains relatively low compared to the other regions. These datasets allow reconstruction of peatland vegetation changes, substrate development, and peat and carbon accumulation dynamics across almost the entire Holocene; however, spatial coverage is limited due to the low number of cores. Hydrological information from testate-amoebae extends to ∼ 7000 cal. yr BP but is available from only a single site, making water table reconstructions largely site-specific. Fire proxies (micro- and macrocharcoal) are present through the Holocene but remain sparse, restricting fire history interpretations to localized events and preventing robust regional-scale reconstructions. Geochemical information, derived from traditional analyses or XRF/XRD, is absent for peatlands in the continuous permafrost zone.

In summary, there is a clear regional variation in the temporal coverage of selected proxies across different permafrost zones. The longest and most continuous records are found in isolated and non-permafrost zones, reflecting both the early initiation of peatlands in this region and the relatively easy accessibility for research due to the absence or spare presence of permafrost. In discontinuous and sporadic permafrost zones, only a few proxies provide long-term, spatially extensive coverage, primarily for basic peat and carbon properties, while other biological and geochemical proxies remain sparse. In continuous permafrost zones, many proxies extend into the early Holocene, but the low number of cores limits spatial representativeness, meaning that long-term reconstructions of ecological dynamics are largely site-specific.

5 Challenges and future directions in paleoenvironmental research in the Western Siberian Lowland

Fieldwork in WSL peatlands is associated with persistent and interrelated logistical, environmental, and political constraints, which together contribute to the underrepresentation of some areas in paleoenvironmental research. First, environmental conditions complicate fieldwork. In northern areas, permafrost dictates when and how sampling can occur. Winter freeze improves travel across bog surfaces but makes coring extremely difficult due to frozen sediments. In summer, the thawed active layer allows proper coring, yet saturated, unstable ground often makes sites inaccessible. This narrow and seasonally contradictory operational window limits the number of reachable localities. This also contributes to limited accessibility, many parts of WSL lacks roads or rail connections, and many sites can only be reached by navigable waterways, helicopter or specialized off-road vehicles. This greatly increases costs and restricts the spatial extent of sampling, leaving remote peatlands poorly studied. Additional logistical and political constraints, including permit requirements, transport coordination, and recent geopolitical restrictions further reduce access to certain regions (Schuur et al., 2024; Witze, 2022; López-Blanco et al., 2024). As a result, some parts of WSL, particularly remote and permafrost-affected zones, remain underrepresented in palaeoecological research simply because they are exceptionally difficult to reach and sample (Fig. 10a). Moreover, even regions that appear relatively well studied, such as the Great Vasyugan Mire, are often sampled unevenly, with research concentrated mainly along accessible margins and transport corridors, while large central areas remain poorly investigated. This issue is particularly important in the WSL, where peatlands form extensive and internally heterogeneous landscape-scale complexes rather than isolated systems. Consequently, individual peat cores cannot always be considered representative of entire peatland regions, especially for locally sensitive proxies such as testate amoebae, whereas broader-scale proxies such as pollen may reflect more regional environmental patterns.

These limitations are especially critical given the global climatic importance of WSL peatlands. The WSL stores one of the largest peat carbon pools on Earth (Hugelius et al., 2020; Kremenetski et al., 2003; Sheng et al., 2004) and acts both as a long-term carbon sink and a major methane source (Kirpotin et al., 2009; MacDonald et al., 2006; Smith et al., 2004), while ongoing climate change drives complex, regionally variable shifts in ecosystem functioning (Halaś et al., 2025; Zhang et al., 2022). In the context of global soil carbon and peatland assessments (Scharlemann et al., 2014), reducing spatial and methodological gaps in this region is therefore essential for both understanding local processes and improving global C–CH_4 budgets.

Looking ahead, the patterns revealed by the WSPC database suggest clear priorities. Continuous and sporadic permafrost zones, especially beyond major river corridors and well-studied complexes such as the Great Vasyugan Mire, should be key targets for new coring campaigns (Fig. 10a). In addition, some areas that appear well covered in terms of core numbers are represented mainly by low-resolution, single-proxy records based on older methods; where detailed reconstructions of hydrology, fire regimes or carbon dynamics are needed, such sites should be revisited or re-analysed using modern, high-resolution multi-proxy approaches. Future work would benefit from wider use of underrepresented biological proxies (e.g. testate amoebae, macro- and microcharcoal, non-pollen palynomorphs) and advanced geochemical and isotopic analyses, particularly in permafrost-affected peatlands (Fig. 10b).

At the same time, overcoming logistical and political barriers will require new collaboration and field strategies, including closer partnerships with regional institutions and local communities, greater use of remote sensing and existing infrastructure to pre-select coring sites, and flexible multi-site expeditions using lighter, easily deployable equipment. Aligning such practical solutions with the spatial and methodological gaps highlighted by the WSPC database will allow future research in WSL to move beyond opportunistic sampling towards systematically planned, hypothesis-driven studies that better capture the diversity and dynamics of WSL peatlands.

6 Database limitations

- *Incomplete coverage of literature sources* – the database is based on a literature review of available repositories, which may be missing some publications. The authors acknowledge that not all studies presenting peat core data from the region were identified or accessible.

- *Limited access to Russian-language literature published before 1990* – most pre-1990 Russian-language publications were not available in open-access repositories. As a result, some original sources could not be obtained, limiting the ability to gather comprehensive information on peat cores and proxy usage. Consequently, certain proxies may have been applied earlier or more frequently than indicated by this database.

- *Uncertainty related to incomplete reporting in key studies* – some works provided aggregated descriptions of coring efforts without reporting exact locations of individual cores. For example, Lapshina and Zarov (2023) described 355 sampling cores along hypsometric profiles, yet precise coordinates were not provided, allowing only 76 cores to be included in this database. It remains possible that many of these cores overlap with records included in other compilations (e.g., Hugelius et al., 2020), but this could not be verified.

- *Ambiguity in reporting complete basal peat sequences* – in most cases the oldest core from a study site represents a basal core; however, some publications did not clearly specify whether a core reached the mineral substrate. This ambiguity may introduce minor uncertainty into the interpretation of basal depths included in the database.

- *Existence of unpublished data* – some peat cores are known to exist (e.g., from reports, institutional archives,

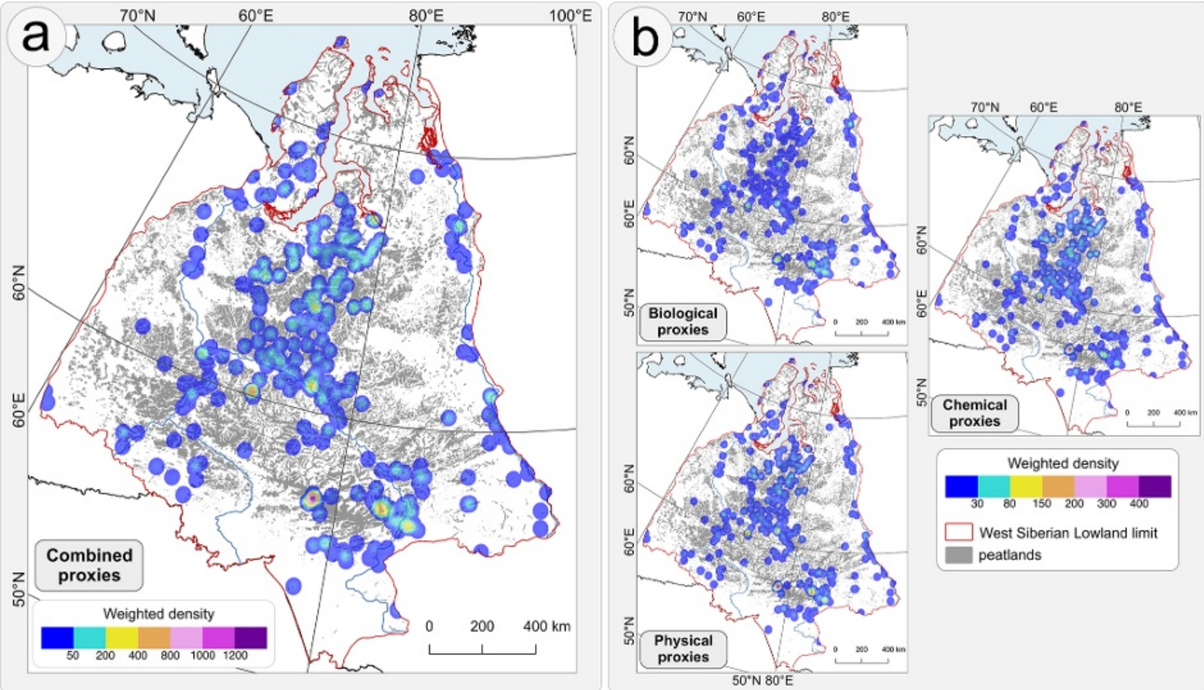

Figure 10. Spatial representation of peatland areas in Western Siberian Lowland sampled by peat cores and their relative contribution of information: **(a)** heatmap of combined scores of all proxy types, and **(b)** heatmaps of proxy group scores (biological, chemical, and physical). Heatmaps were generated using Kernel Density Estimation, with a 30 km radius, assuming each core represents the surrounding of 30 km, and weighted by the combined or group-specific scores to depict relative data density. Peat core scoring was based on both chronology and proxies.

or personal communications), but lack published stratigraphic or proxy data. These could not be incorporated into the database.

- *Variable spatial precision of reported core locations* – many older or regionally published studies provide only approximate locations (e.g., mire name or nearest settlement) rather than precise coordinates. As a result, included cores differ in coring location accuracy.

- *Dependence on secondary sources for inaccessible studies* – when original publications, particularly older Russian-language works, were unavailable, information was obtained from secondary citations in later papers. This reliance on indirect sources may introduce errors. For example, Liss and Berezina (1981) published stratigraphic diagrams with several dated levels within single core, but in later studies these levels were misinterpreted as separate basal cores. Such discrepancies highlight the risk of propagating mistakes when direct access to original materials is not possible.

- *Potential duplication or omission of cores* – some cores appear repeatedly across multiple publications, yet lack of precise metadata sometimes prevented determining whether two references referred to the same core. This introduces a small risk of either under- or over-counting cores.

7 Data availability

The data are available on the Zenodo platform at the following link: https://doi.org/10.5281/zenodo.20323517 (Halaś and Słowiński, 2026). We plan to expand this database in the future by providing a submission form that will allow researchers to contribute additional peat cores, either from new studies or from existing collections not yet included in the database.

8 Conclusions

The Western Siberian Peat Core Database (WSPC) provides a harmonized and georeferenced dataset of peat cores that greatly advances the capacity for regional analyses of Holocene environmental change in the Western Siberian Lowland (WSL). The literature review demonstrates a clear progression in WSL peatland research, from early single-proxy and low-resolution studies to modern multi-proxy approaches with higher chronological and analytical precision. Increasing attention to peatland hydrology, fire history, and carbon accumulation reflects both methodological developments and a growing recognition of the crucial ecological and climatic importance of WSL peatlands. The WSPC database integrates metadata from 654 georeferenced peat cores or cross-sections reported in 156 publications (1953–2025), documenting application of 26 palaeoecological proxies across biological, physical, chemical, and chronological categories. Spatial analyses reveal a concentration of sampling along major rivers (Ob, Yenisey, Irtysh, Tobol) and in the Great Vasyugan Mire, reflecting both the extent of peatlands and relative accessibility. Most cores originate from non-permafrost and discontinuous permafrost zones, whereas continuous permafrost regions remain poorly sampled. Temporal coverage varies substantially: ~ 80 % of cores span the last 4000 years, ~ 50 % extend to 8000 years, and only a limited number reach the Late Glacial ($\sim 15\,600$ cal. yr BP), with the longest and most continuous records found in non-permafrost and isolated permafrost zones. Overall, the dataset shows a strong dominance of fundamental physical and chemical proxies, particularly basal depth, carbon accumulation, and organic matter content, which underscores their central role in peatland palaeoecology. Biological proxies such as plant macrofossils, pollen, and testate amoebae are applied more selectively and largely depend on specific research goals, while specialized chemical proxies (e.g., traditional geochemical analysis, FTIR, XRF, stable isotopes) remain infrequently used. This distribution highlights both the breadth of existing multiproxy approaches and the clear gaps in the application of biological and advanced geochemical methods. Collectively, this database provides an essential foundation for large-scale reconstructions of Holocene peatland development, hydrology, fire regimes, and carbon dynamics, while clearly identifying spatial and proxy-specific gaps. Several limitations must be acknowledged, including incomplete access to older Russian-language literature, inconsistent reporting of complete basal peat sequences, variable spatial precision of core locations, reliance on secondary sources, and the existence of unpublished or inaccessible core data. These factors introduce minor uncertainties and may lead to under- or overrepresentation of some cores or proxies. Despite these constraints, the WSPC database constitutes a valuable and robust resource for regional and pan-WSL palaeoenvironmental research. At the same time, it highlights key spatial, temporal, and methodological gaps and provides clear guidance for future research priorities, particularly regarding the limited coverage of northern regions, the uneven application of different proxies, and the logistical challenges associated with fieldwork in the WSL peatlands.

Appendix A: Additional methodological information

Table A1. Proxies used in palaeoecological peatland studies in Western Siberia Lowland (WSL) included in the Western Siberian Peat Cores Database (WSPC).

Proxy type	Proxy	Information provided/interpretation	Examples of studies in the WSPC database
Biological[1]	Pollen	Pollen and spores provide information on past vegetation composition, allowing reconstruction of historical vegetation dynamics and the climatic conditions (Mander and Punyasena, 2018).	Blyakharchuk (2003); Novenko et al. (2023); Peteet et al. (1998)
	Non-pollen palynomorphs (NPPs)	NPP assemblages reflect local ecological conditions, including hydrology, fire, erosion, and grazing activities, providing complementary information to pollen for reconstructing past environments (Shumilovskikh et al., 2021; Van Geel, 2001).	Feurdean et al. (2022); Halaś et al. (2025)
	Plant macrofossils	Provide information on local vegetation and flora with high taxonomic precision, allowing reconstruction of site-scale vegetation dynamics, paleoclimatic conditions (Birks and Birks, 2000).	Preis (2015); Tarasov et al. (1998); Tikhonravova et al. (2023)
	Testate amoebae (TA)	Mainly used for reconstruction of past changes in peatland hydrology and as a proxy for hydroclimate (Charman, 2001; Mitchell and Payne, 2018).	Halaś et al. (2025); Kurina et al. (2020); Willis et al. (2015)
	Oribatid mites	Good bioindicators of microhabitat and moisture conditions in peatlands (Seniczak et al., 2022).	Kurina et al. (2017, 2023)
	Molluscs	Useful for reconstruction of water chemistry, hydrology and paleoclimate, like precipitation and temperature (Horsák, 2011).	Kurina et al. (2017, 2023)
	Arthropods	Arthropods serve as bioindicators, used to assess biodiversity, restoration success, habitat alteration, and potential impacts of climate change (Batzer et al., 2016).	Panova et al. (2010)
	Diatoms	Diatoms are mostly used in minerotrophic peatlands, indicate past water level, chemical conditions or human disturbances (Carballeira and Pontevedra-Pombal, 2020).	Paradossky et al. (2019)
	Microcharcoal	Provide information on past fire history, based on the size of charcoal particles the distance to the source can be determined. Microcharcoal is used to recontract regional fire history, while macrocharcoal is used for local-scale fire reconstructions (Conedera et al., 2009).	Halaś et al. (2025); Lamentowicz et al. (2015); Shefer et al. (2024)
	Macrocharcoal		Feurdean et al. (2019); Novenko et al. (2023); Ryabogina et al. (2024)
Physical	Bulk density	Provide information on peat compaction, peat accumulation, decomposition and carbon content (Chambers and Charman, 2004).	Preis et al. (2024); Smith et al. (2012)
	Moisture content	Moisture controls decomposition, microbial activity and nutrient mobility (Rydin et al., 2006).	Preis et al. (2024); Tikhonravova et al. (2023)
	Degree of decomposition/Peat humification	Is a measure of peat decomposition, useful as proxy to reconstruct past hydrological and climatic conditions (Biester et al., 2014).	Syso and Peregon (2009); Tsyganov et al. (2021); Turunen et al. (2001)
	Peat accumulation	Gives information about past climate variability, peatland development and productivity (Swindles et al., 2025).	Borren et al. (2004); Malyasova et al. (1991)
	Basal depth	Basal depth provides information on peatland initiation, development and functioning, it is also essential for carbon accumulation calculation and in climate change models (Parry et al., 2014).	Kremenetski et al. (2003); MacDonald et al. (2006); Smith et al. (2004)

Table A1. Continued.

Proxy type	Proxy	Information provided/interpretation	Examples of studies in the WSPC database
Chemical	Ash content	Informs about mineral input, dust or pollution deposition, erosion, or fire signal (Tolonen, 1984).	Kurina et al. (2023); Veretennikova et al. (2021)
	pH	Paleo pH provides information about trophic status, carbon/methane cycling and can be used as an indirect proxy for paleoclimate (Schaaff et al., 2024).	Stepanova and Volkova (2017); Syso and Peregon (2009)
	Organic matter (LOI)	It helps to identify non-organic input and reconstruct land-use history (Chambers and Charman, 2004).	Lapshina and Zarov (2023); Minayeva et al. (2006); Peteet et al. (1998)
	Carbon accumulation	Provides information about carbon sequestration over time, indicates past changes in peatland productivity, decomposition and indirectly climate conditions (Charman et al., 2015).	Sheng et al. (2004); Turunen et al. (2001); Yu et al. (2009)
	Stable isotopes ($\delta^{13}C$, $\delta^{15}N$, δD, $\delta^{18}O$)	Stable isotopes combined with other analysis are valuable tools to reconstruct past temperature, humidity, and water table conditions (McClymont et al., 2010).	Feurdean et al. (2019); Novenko et al. (2024); Startsev et al. (2022)
	Geochemistry[2]	To determine chemical composition of peat, natural and anthropogenic fluxes of metals, secondary sources of mineral matter e.g. sea spray, fires or industrial emissions (Shotyk, 1988).	Fiałkiewicz-Koziełet al. (2016); Veretennikova et al. (2021)
	X-ray fluorescence (XRF)/X-ray diffraction (XRD)	XRF determines elemental composition of the sediment, interpretation depends on the elements/element ratios used, e.g. used to infer anthropogenic impact, hydrological shifts or dust input. Measurements can be of uncertain reliability (Longman et al., 2019). XRD identifies crystalline minerals in a sample, allowing direct, non-destructive mineral characterization, though amorphous or poorly crystalline materials may not be detected (Sjöström et al., 2019).	Feurdean et al. (2022); Leonova et al. (2022); Shvartseva et al. (2024)
	FTIR (Fourier transform infrared spectroscopy)	FTIR spectra can indicate peat decomposition, organic matter quality, peat mineral matter and assessment of peatland restoration success (Artz et al., 2008; Martínez Cortizas et al., 2021).	Kurina et al. (2023)
Chronological	Dating (e.g., ^{14}C, ^{210}Pb, ^{137}Cs)	Used to determine peat components age, for age–depth model calculations, accumulation rate and sedimentation chronology (Chambers and Charman, 2004).	Borisova et al. (2011); Glebov et al. (2002); Kremenetski et al. (2003)

[1] Among the biological proxies, a category termed "zoogenic remains" was also distinguished, which was used in the context of the study by Paradossky et al. (2019). In that study, the authors identified general groups of zoogenic remains rather than specific taxa. [2] General group of analysis applied on peat core excluding stable isotopes, XRF and FTIR.

Table A2. Results of calibration of uncalibrated radiocarbon ages (yr BP) for peat cores in Western Siberian Peat Cores Database (WSPC) with reference to the source of original (uncalibrated) ages.

No.	Core ID	^{14}C age (yr BP)	$\pm 1\sigma$ (yr)	Calibrated age range (cal. yr BP)	Median calibrated age (cal. yr BP)	Reference
1	WS_6	8710	105	9539–10 127	9676	MacDonald et al. (2006)
2	WS_8	4578	72	4992–5465	5310	Leonova et al. (2021); Preis et al. (2024)
3	WS_15	5611	54	6304–6519	6398	Leonova et al. (2021); Preis et al. (2024)
4	WS_67	5260	60	5921–6207	5997	Lapshina and Zarov (2023)
5	WS_68	1780	70	1534–1846	1644	Lapshina and Zarov (2023)
6	WS_71	5260	160	5666–6355	5997	Blyakharchuk (2003)
7	WS_134	8450	60	9308–9532	9479	Blyakharchuk (2003)
8	WS_158	4310	90	4601–5253	4856	Preis (2024)
9	WS_171	9780	210	10 588–11 912	11 207	Khotinsky (1984)
10	WS_221	9000	100	9753–10 395	10 196	MacDonald et al. (2006)
11	WS_228	8400	80	9149–9525	9454	Liss and Berezina (1981)
12	WS_251	10 600	80	12 236–12 723	12 627	Khotinsky (1984)
13	WS_549	4840	110	5329–5860	5587	Vasil'chuk et al. (2001)
14	WS_567	7420	110	8019–8406	8280	Vasil'chuk et al. (2001)
16	WS_584	8670	100	9504–10 100	9553	Punning et al. (1974)
15	WS_585	7960	100	8559–9083	8930	Punning et al. (1974)
17	WS_589	6550	170	7054–7729	7429	MacDonald et al. (2006)
18	WS_590	7640	220	8028–9008	8414	MacDonald et al. (2006)
19	WS_591	7730	220	8089–9151	8524	MacDonald et al. (2006)
20	WS_592	7800	170	8269–9083	8591	MacDonald et al. (2006)
21	WS_593	7820	200	8233–9224	8595	MacDonald et al. (2006)
22	WS_594	8000	50	8656–9000	8820	MacDonald et al. (2006)
23	WS_595	8000	200	8436–9399	8820	MacDonald et al. (2006)
24	WS_596	8180	40	9022–9274	9106	MacDonald et al. (2006)
25	WS_597	8180	230	8538–9584	9106	MacDonald et al. (2006)
26	WS_598	8400	240	8706–10 069	9454	MacDonald et al. (2006)
27	WS_645	8790	170	9512–10 235	9774	Vasil'chuk et al. (2001)

Table A3. Proxy groups and individual proxy weights used in the scoring framework.

Proxy group	Proxy	Weight
Biological	Pollen	2.0
	Non-pollen palynomorphs (NPPs)	1.2
	Plant macrofossils	1.5
	Testate amoebae	2.5
	Microcharcoal	1.5
	Macrocharcoal	1.5
	Oribatid mites	0.5
	Molluscs	0.5
	Diatoms	1.0
	Arthropods	0.2
	Zoogenic remains	0.2
Physical	Bulk density	2.0
	Moisture content	0.5
	Degree of decomposition	1.0
	Peat humification	1.0
	Peat accumulation	2.0
	Basal depth	1.0
Chemical	Ash content	1.5
	pH	1.0
	Organic matter (LOI)	2.0
	Carbon accumulation	2.5
	Stable isotopes	2.5
	Geochemistry	2.0
	XRF/XRD	2.0
	FTIR	2.0

Table A4. Components of scoring framework for peat cores in WSPC database.

Component	Description	Scaling	Weight
Chronology (chron)	Presence of an independent age model	Binary: 1 = present, 0 = absent	1
Record length (record)	Total temporal coverage of the core	Scaled 0.05–1.0: $<$ 200 years = 0.05 200–500 years = 0.2 500–2000 years = 0.4 2000–5000 years = 0.6 5000–10 000 years = 0.8 $>$ 10 000 years = 1.0	1
Proxy count (count)	Number of proxy available	Linearly rescaled 0–1 (1–12 proxies)	1
Proxy group scores (proxies)	Weighted sum of proxies within each group	According to Table A3	4
All proxies combined (proxies)	Weighted sum of all proxies across groups	According to Table A3	5

Combined Score = $S_{\text{chron}} \times W_{\text{chron}} + S_{\text{record}} \times W_{\text{record}} + S_{\text{count}} \times W_{\text{count}} + \sum_{S\ \text{proxies}} \times W_{\text{proxies}}$, where: S – score, W – weight

Appendix B: Spatial distribution of palaeoecological proxies in the WSPC database

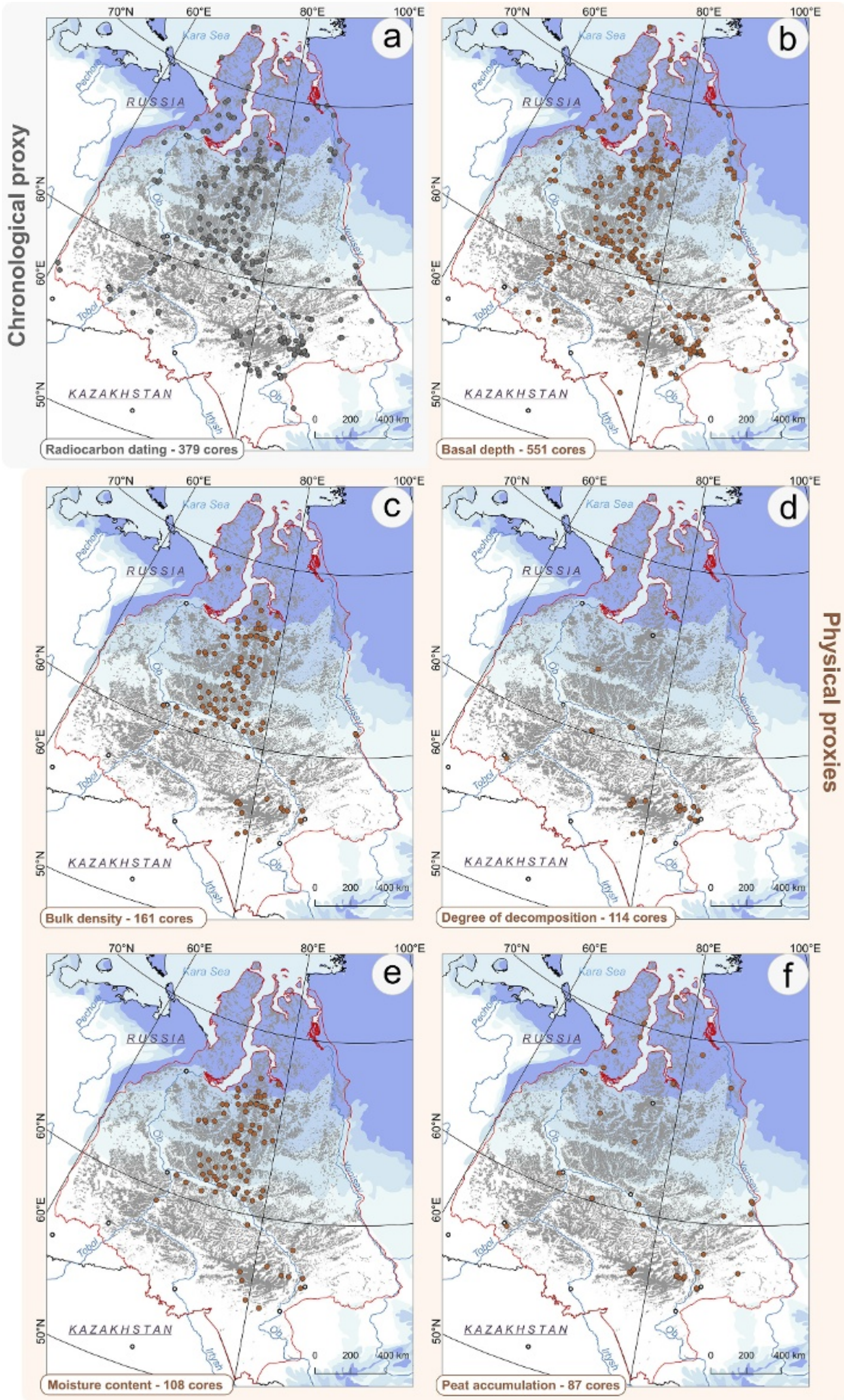

Figure B1.

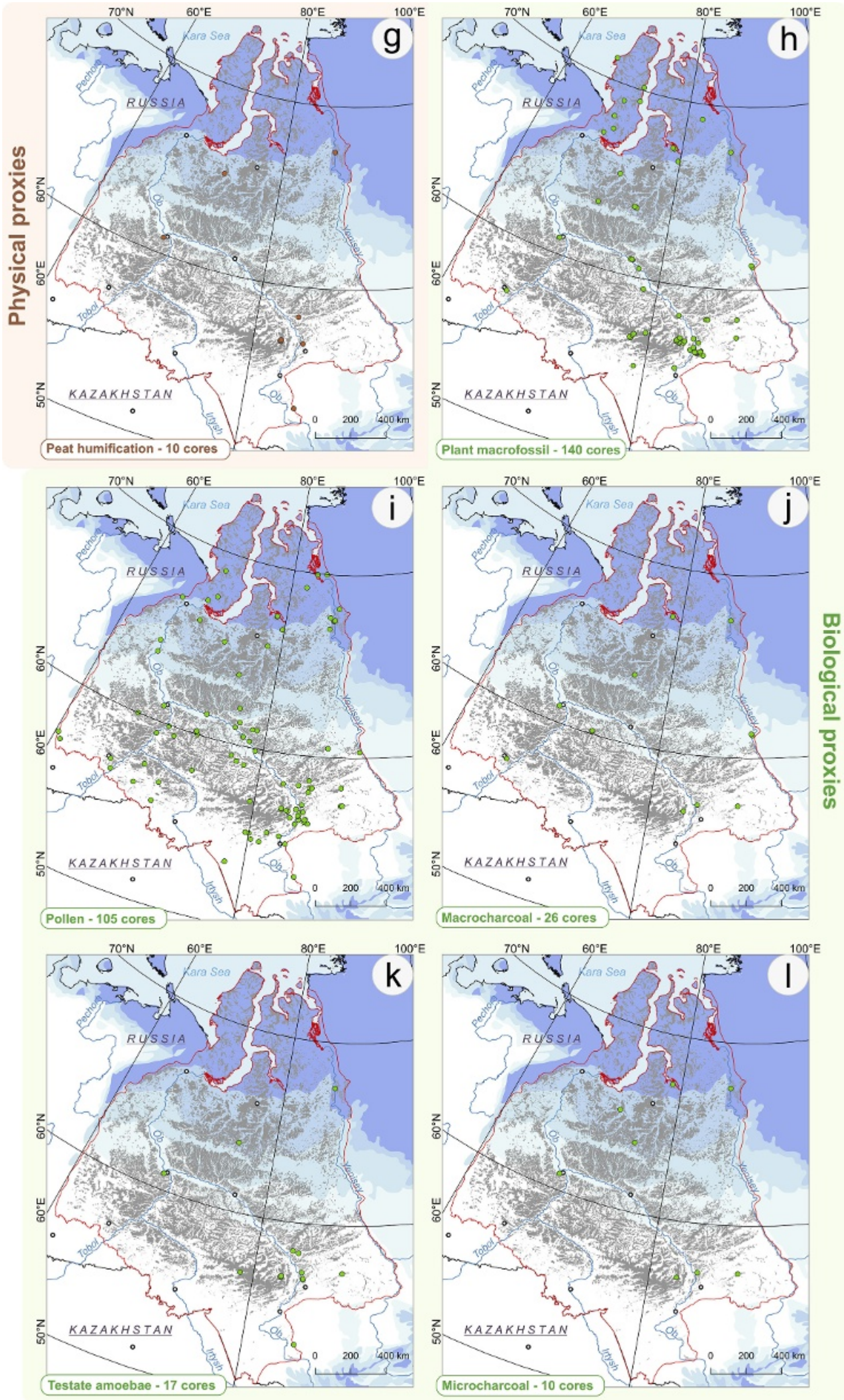
Physical proxies
Biological proxies
g
h
i
j
k
l
Kara Sea
RUSSIA
KAZAKHSTAN
Peat humification - 10 cores
Plant macrofossil - 140 cores
Pollen - 105 cores
Macrocharcoal - 26 cores
Testate amoebae - 17 cores
Microcharcoal - 10 cores

Figure B1.

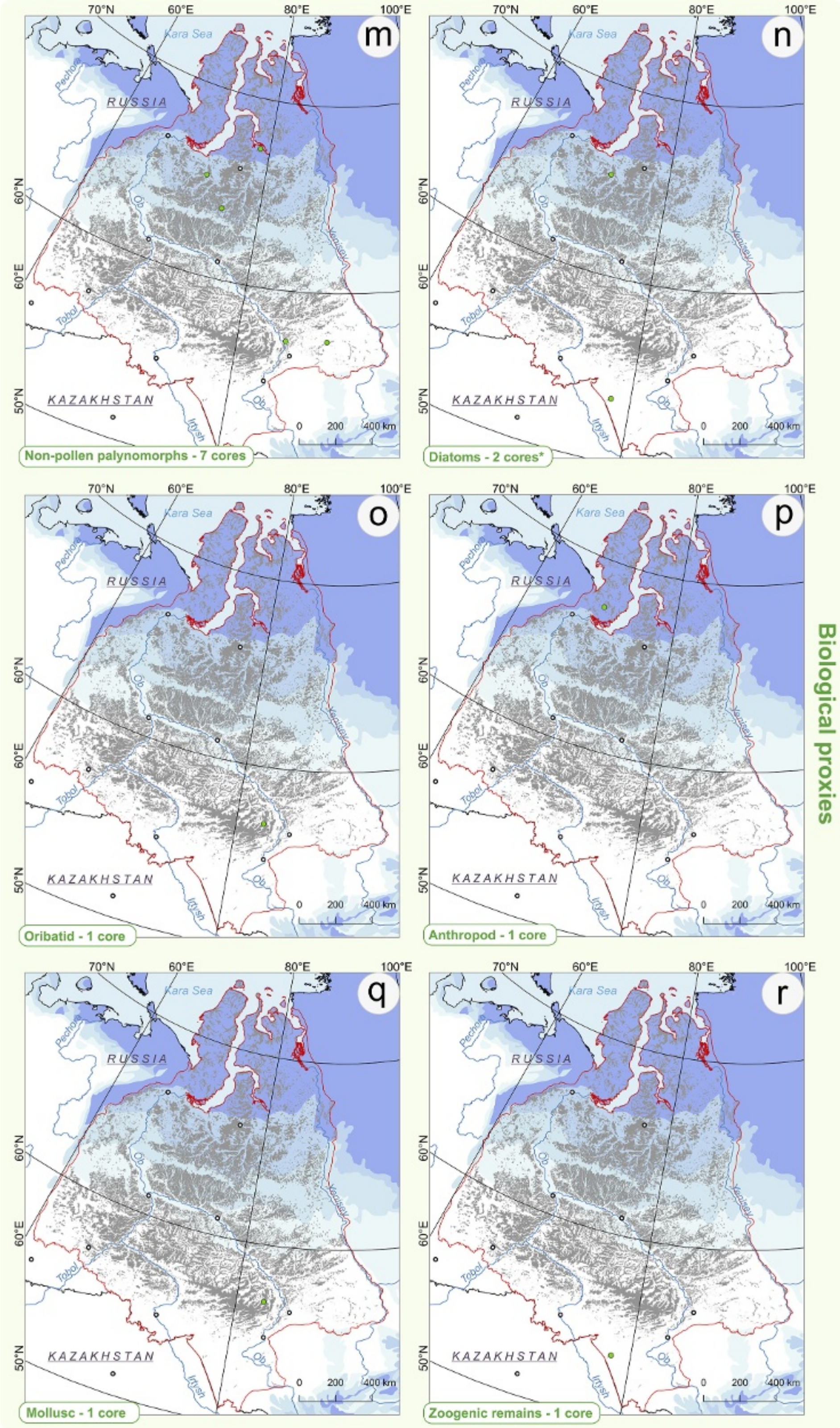
m
n
o
p
q
r
Kara Sea
RUSSIA
KAZAKHSTAN
Pechora
Ob
Tobol
Irtysh
Yenisey
70°N
60°E
80°E
100°E
60°N
50°N
0 200 400 km
Non-pollen palynomorphs - 7 cores
Diatoms - 2 cores*
Oribatid - 1 core
Anthropod - 1 core
Mollusc - 1 core
Zoogenic remains - 1 core
Biological proxies

Figure B1.

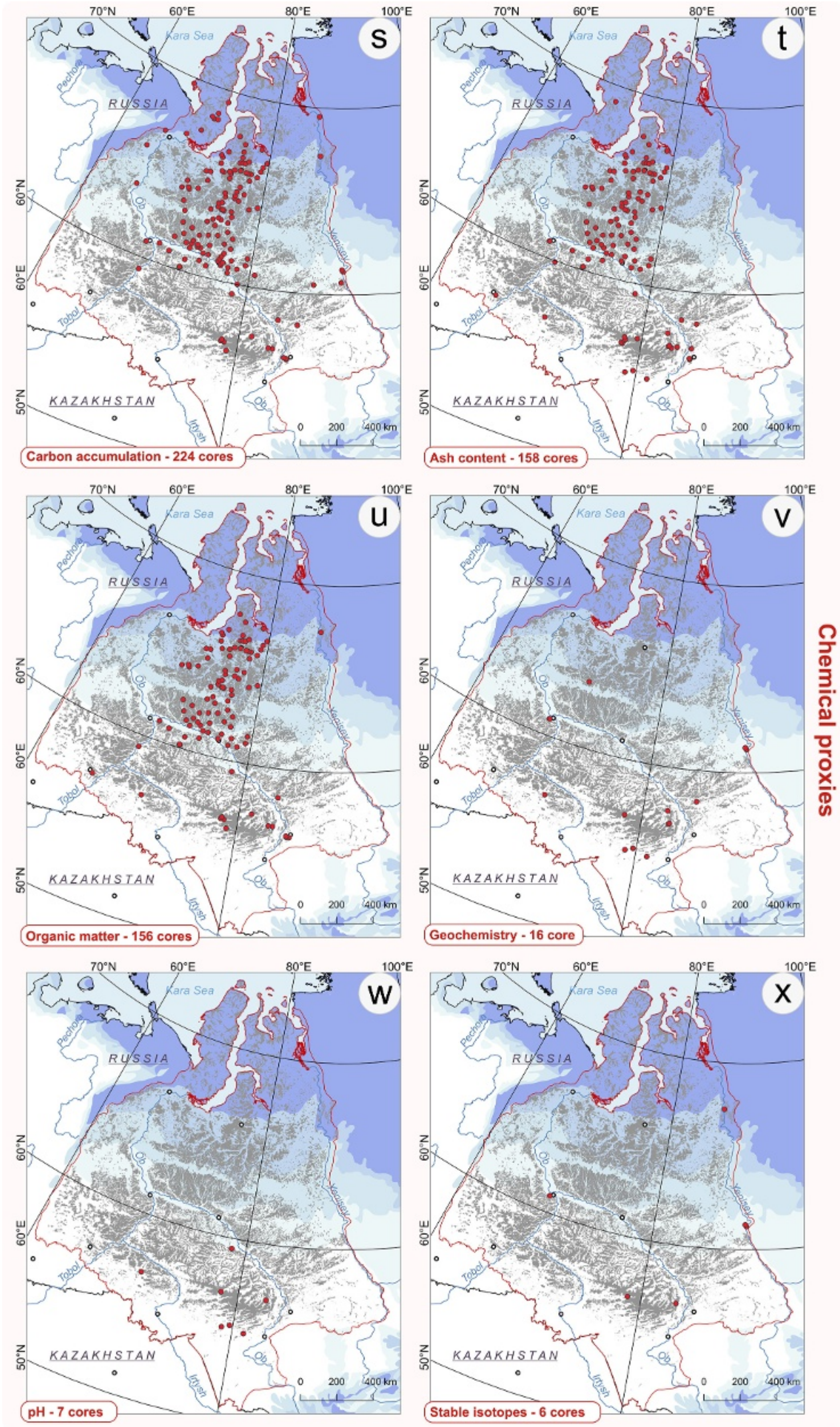
s
t
u
v
w
x
Kara Sea
RUSSIA
KAZAKHSTAN
Pechora
Ob
Tobol
Irtysh
Yenisey
70°N
60°N
50°N
60°E
80°E
100°E
0 200 400 km
Carbon accumulation - 224 cores
Ash content - 158 cores
Organic matter - 156 cores
Geochemistry - 16 core
pH - 7 cores
Stable isotopes - 6 cores
Chemical proxies

Figure B1.

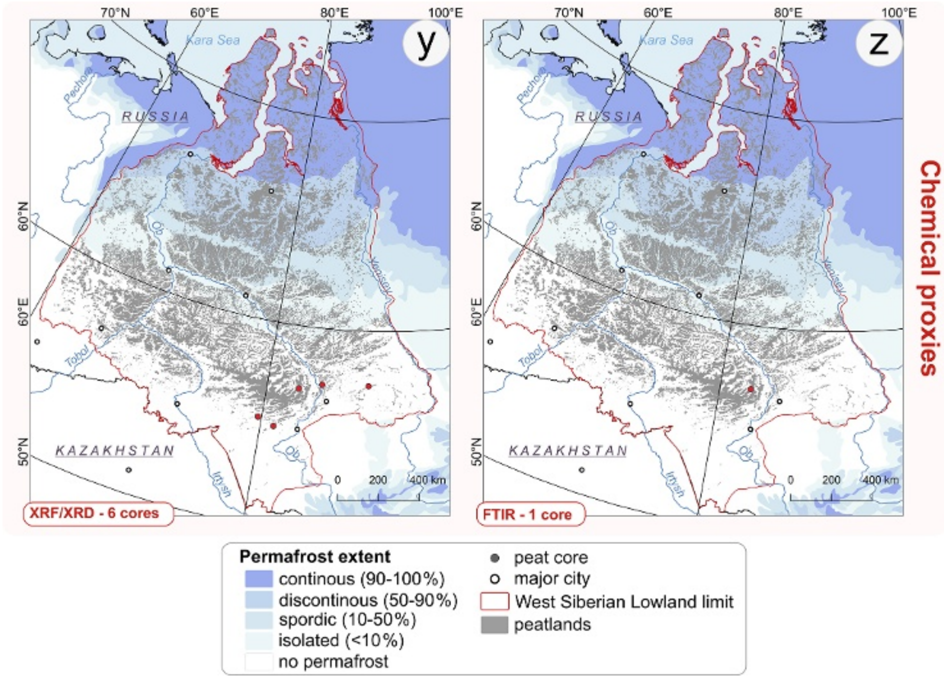

Figure B1. Spatial distribution of peat cores included in the Western Siberian Peat Core Database with records of proxies: **(a)** radiocarbon dating, **(b)** basal depth, **(c)** bulk density, **(d)** degree of decomposition, **(e)** moisture content, **(f)** peat accumulation, **(g)** peat humification, **(h)** plant macrofossils, **(i)** pollen, **(j)** macrocharcoal, **(k)** testate amoebae, **(l)** microcharcoal, **(m)** non-pollen palynomorphs, **(n)** diatoms, **(o)** oribatid, **(p)** arthropod peat humification, **(q)** mollusc, **(r)** zoogenic remains, **(s)** carbon accumulation, **(t)** ash content, **(u)** organic matter, **(v)** geochemistry, **(w)** pH, **(x)** stable isotopes, **(y)** XRF (X-ray fluorescence)/XRD (X-ray diffraction), **(z)** FTIR (Fourier transform infrared spectroscopy). * In one core (located in the north), diatoms were applied only on the lake section of the core below the peat.

Author contributions. AH designed the research, conducted the literature review, compiled the database, wrote the original draft of the manuscript and led the revision process, including preparing the responses to the reviewers' comments and implementing the manuscript and database corrections. MS contributed to the research design, supervised the project, revised the manuscript, contributed to the writing, and participated in responding to the reviewers' comments and manuscript corrections.

Competing interests. The contact author has declared that neither of the authors has any competing interests.

Disclaimer. Publisher's note: Copernicus Publications remains neutral with regard to jurisdictional claims made in the text, published maps, institutional affiliations, or any other geographical representation in this paper. The authors bear the ultimate responsibility for providing appropriate place names. Views expressed in the text are those of the authors and do not necessarily reflect the views of the publisher.

Acknowledgements. We would like to sincerely thank the reviewers of this manuscript, Sebastian Wetterich and the anonymous Reviewer #1, for their valuable comments and constructive suggestions. The manuscript and database were substantially improved as a result of their feedback.

Financial support. The research has been supported by the National Science Centre in Poland (grant no. 2019/35/O/ST10/02903).

Review statement. This paper was edited by Birgit Heim and reviewed by Sebastian Wetterich and one anonymous referee.

References

Alexandrov, G. A., Brovkin, V. A., and Kleinen, T.: The influence of climate on peatland extent in Western Siberia since the Last Glacial Maximum, Sci. Rep., 6, 24784, https://doi.org/10.1038/srep24784, 2016.

Artz, R. R. E., Chapman, S. J., Jean Robertson, A. H., Potts, J. M., Laggoun-Défarge, F., Gogo, S., Comont, L., Disnar, J.-R., and Francez, A.-J.: FTIR spectroscopy can be used as a screening tool for organic matter quality in regenerating cutover peatlands, Soil Biol. Biochem., 40, 515–527, https://doi.org/10.1016/j.soilbio.2007.09.019, 2008.

Barber, K. E.: Peatlands as scientific archives of past biodiversity, Biodivers. Conserv., 2, 474–489, https://doi.org/10.1007/BF00056743, 1993.

Baryshnikov, M. K.: Carex-Hypnum Bogs of the West Vasuganye, Moscow, 37 pp., 1929.

Batzer, D., Wu, H., Wheeler, T., and Eggert, S.: Peatland Invertebrates, in: Invertebrates in Freshwater Wetlands: An International Perspective on their Ecology, edited by: Batzer, D. and Boix, D., Springer International Publishing, Cham, 219–250, https://doi.org/10.1007/978-3-319-24978-0_7, 2016.

Beck, H. E., Zimmermann, N. E., McVicar, T. R., Vergopolan, N., Berg, A., and Wood, E. F.: Present and future Köppen-Geiger climate classification maps at 1-km resolution, Sci. Data, 5, 180214, https://doi.org/10.1038/sdata.2018.214, 2018.

Biester, H., Knorr, K.-H., Schellekens, J., Basler, A., and Hermanns, Y.-M.: Comparison of different methods to determine the degree of peat decomposition in peat bogs, Biogeosciences, 11, 2691–2707, https://doi.org/10.5194/bg-11-2691-2014, 2014.

Birks, H. H. and Birks, H. J. B.: Future Uses of Pollen Analysis Must Include Plant Macrofossils, J. Biogeogr., 27, 31–35, 2000.

Blyakharchuk, T.: Four new pollen sections tracing the Holocene vegetational development of the southern part of the West Siberan Lowland, Holocene, 13, 715–731, https://doi.org/10.1191/0959683603hl658rp, 2003.

Blyakharchuk, T. A., Kurina, I. V., and Pologova, N. N.: Pozdnegolotsenovaya dinamika rastitel'nogo pokrova i uvlazhnennosti klimata yugo-vostochnogo sektora Zapadno-Sibirskoy ravniny po dannym palinologicheskogo i rizopodnogo issledovaniy torfyanykh otlozheniy [Late Holocene dynamics of vegetation cover and climate humidity in the southeastern sector of the West Siberian Plain based on palynological and rhizopod studies of peat deposits], Bull. Tomsk State Univ. Biol., 164–189, https://doi.org/10.17223/19988591/45/9, 2019.

Borisova, O. K., Novenko, E. Y., Zelikson, E. M., and Kremenetski, K. V.: Lateglacial and Holocene vegetational and climatic changes in the southern taiga zone of West Siberia according to pollen records from Zhukovskoye peat mire, Quat. Int., 237, 65–73, https://doi.org/10.1016/j.quaint.2011.01.015, 2011.

Borren, W., Bleuten, W., and Lapshina, E. D.: Holocene peat and carbon accumulation rates in the southern taiga of western Siberia, Quat. Res., 61, 42–51, https://doi.org/10.1016/j.yqres.2003.09.002, 2004.

Botch, M. S. and Masing, V. V.: Mire ecosystems in the USSR, in: Ecosystems of the World, vol. 4A, Mires: Swamp, Bog, Fen and Moor, edited by: Gore, A. J. P., Elsevier Science, New York, 95–152, ISBN 0444420037, 1983.

Botch, M. S., Kobak, K. I., Vinson, T. S., and Kolchugina, T. P.: Carbon pools and accumulation in peatlands of the former Soviet Union, Glob. Biogeochem. Cycles, 9, 37–46, https://doi.org/10.1029/94GB03156, 1995.

Bronzov, A. Y.: Verkhovye bolota Narymskogo kraya (bassein reki Vasiugan) [Bogs of the Narymski region (watershed of the Vasiugan River)], Proc. Peat Inst., 3, 1–100, 1930.

Brown, J., Ferrians, O., Heginbottom, J. A., and Melnikov, E.: Circum-Arctic Map of Permafrost and Ground-Ice Conditions (2), National Snow and Ice Data Center [data set], https://doi.org/10.7265/SKBG-KF16, 2002.

Carballeira, R. and Pontevedra-Pombal, X.: Diatoms in Paleoenvironmental Studies of Peatlands, Quaternary, 3, 10, https://doi.org/10.3390/quat3020010, 2020.

Chambers, F. M. and Charman, D. J.: Holocene environmental change: contributions from the peatland archive, The Holocene, 14, 1–6, https://doi.org/10.1191/0959683604hl684ed, 2004.

Charman, D.: Biostratigraphic and palaeoenvironmental applications of testate amoebae, Quaternary Sci. Rev., 20, 1753–1764, https://doi.org/10.1016/S0277-3791(01)00036-1, 2001.

Charman, D. J., Amesbury, M. J., Hinchliffe, W., Hughes, P. D. M., Mallon, G., Blake, W. H., Daley, T. J., Gallego-Sala, A. V., and Mauquoy, D.: Drivers of Holocene peatland carbon accumulation across a climate gradient in northeastern North America, Quaternary Sci. Rev., 121, 110–119, https://doi.org/10.1016/j.quascirev.2015.05.012, 2015.

Conedera, M., Tinner, W., Neff, C., Meurer, M., Dickens, A. F., and Krebs, P.: Reconstructing past fire regimes: methods, applications, and relevance to fire management and conservation, Quaternary Sci. Rev., 28, 555–576, https://doi.org/10.1016/j.quascirev.2008.11.005, 2009.

Dranitsyn, D. A.: Secondary podzols and the shift in the podzol zone in the northern part of the Ob'-Irtysh watershed, Proc. Dokuchaev Soil Comm., 2, 33–93, 1914.

Duchkov, A. D.: Characteristics of permafrost in Siberia, in: Advances in the Geological Storage of Carbon Dioxide, 81–91, https://doi.org/10.1007/1-4020-4471-2_08, 2006.

Efremov, S. P. and Efremova, T. T.: Present stocks of peat and organic carbon in bog ecosystems of west Siberia, in: Carbon Storage and Atmospheric Exchange by West Siberian Peatlands, Utrecht Univ., Utrecht, Netherlands, 73–78, 2001.

Feurdean, A., Gałka, M., Florescu, G., Diaconu, A.-C., Tanţău, I., Kirpotin, S., and Hutchinson, S. M.: 2000 years of variability in hydroclimate and carbon accumulation in western Siberia and the relationship with large-scale atmospheric circulation: A multi-proxy peat record, Quaternary Sci. Rev., 226, 105948, https://doi.org/10.1016/j.quascirev.2019.105948, 2019.

Feurdean, A., Diaconu, A.-C., Pfeiffer, M., Gałka, M., Hutchinson, S. M., Butiseaca, G., Gorina, N., Tonkov, S., Niamir, A., Tantau, I., Zhang, H., and Kirpotin, S.: Holocene wildfire regimes in western Siberia: interaction between peatland moisture conditions and the composition of plant functional types, Clim. Past, 18, 1255–1274, https://doi.org/10.5194/cp-18-1255-2022, 2022.

Fiałkiewicz-Kozieł, B., Smieja-Król, B., Frontasyeva, M., Słowiński, M., Marcisz, K., Lapshina, E., Gilbert, D., Buttler, A., Jassey, V. E. J., Kaliszan, K., Laggoun-Défarge, F., Kołaczek, P., and Lamentowicz, M.: Anthropogenic- and natural sources of dust in peatland during the Anthropocene, Sci. Rep., 6, 38731, https://doi.org/10.1038/srep38731, 2016.

Glavtorffond RSFSR: Torfianye mestorozhdenia Zapadnoi Sibiri [Peat Deposits in Western Siberia], Glavtorffond RSFSR, Moscow, 1956.

Glebov, F. Z., Toleyko, L. S., Starikov, E. V., and Zhidovlenko, V. A.: Palinologicheskaya kharakteristika i datirovanie po 14C torfyanika v Aleksandrovskom rayone Tomskoy oblasti (srednetaezhnaya podzona) [Palynology and 14C dating of a peat bog from the Aleksandrovsk district of Tomskregion (middle taiga sub-belt)], in: Tipy bolot SSSR i printsipy ikh klassifikatsii [Types of the USSR Bogs and Principles of their Classification], Nauka, Leningrad, 194–199, 1974.

Glebov, F. Z., Karpenko, L. V., and Dashkovskaya, I. S.: Climatic Changes, Successions of Peatlands and Zonal Vegetation, and Peat Accumulation Dynamics in the Holocene (the West-Siberia Peat Profile "Vodorasdel"), Clim. Change, 55, 175–181, https://doi.org/10.1023/A:1020216922975, 2002.

Gordiagin, A. Y.: Data to know about soils and vegetation of West Siberia, Proc. Nat. Soc. Kazan Univ., 34, 222, 1901.

Gorodkov, B. N.: Permafrost in the Northern Area, Leningrad, 109 pp., 1932.

Govorukhin, V. S.: Vegetation of the summer pasture area of reindeer, Zemlevedenie, 35, 68–92, 1933.

Greifswald Mire Centre: Global Peatland Map 2.0. Underlying dataset of the UNEP Global Peatland Assessment – The State of the World's Peatlands: Evidence for action toward the conservation, restoration, and sustainable management of peatlands, Global Peatlands Initiative, https://nextcloud.uni-greifswald.de/public.php/dav/files/s7Ln5QKxdQG5aaA/?accept=zip (last access: 3 June 2026), 2022.

Halaś, A. and Słowiński, M.: Western Siberian Peat Core Database (WSPC), Zenodo [data set], https://doi.org/10.5281/zenodo.20323517, 2026.

Halaś, A., Lamentowicz, M., Obremska, M., Łuców, D., and Słowiński, M.: Peatland development reconstruction and complex biological responses to permafrost thawing in Western Siberia, Biogeosciences, 22, 4797–4822, https://doi.org/10.5194/bg-22-4797-2025, 2025.

Haslett, J. and Parnell, A. C.: A simple monotone process with application to radiocarbon-dated depth chronologies, J. R. Stat. Soc. Ser. C Appl. Stat., 57, 399–418, 2008.

Horsák, M.: Mollusc assemblages in palaeoecological reconstructions: an investigation of their predictive power using transfer function models, Boreas, 40, 459–467, https://doi.org/10.1111/j.1502-3885.2010.00195.x, 2011.

Hugelius, G., Loisel, J., Chadburn, S., Jackson, R. B., Jones, M., MacDonald, G., Marushchak, M., Olefeldt, D., Packalen, M., Siewert, M. B., Treat, C., Turetsky, M., Voigt, C., and Yu, Z.: Large stocks of peatland carbon and nitrogen are vulnerable to permafrost thaw, P. Natl. Acad. Sci. USA, 117, 20438–20446, https://doi.org/10.1073/pnas.1916387117, 2020.

Ivanov, K. E. and Novikov, S. M.: Bolota Zapadnoi Sibiri, ikh stroenie i gidrologicheskiy rezhim [Bogs of West Siberia, their structure and hydrology], Gidrometeoizdat, Leningrad, 447 pp., 1976.

Khotinsky, N. A.: Holocene vegetation history, in: Late Quaternary Environments of the Soviet Union, ISBN 978-0-8166-1250-5, 1984.

Kirpotin, S. N., Berezin, A., Bazanov, V., Polishchuk, Y., Vorobiov, S., Mironycheva-Tokoreva, N., Kosykh, N., Volkova, I., Dupre, B., Pokrovsky, O., Kouraev, A., Zakharova, E., Shirokova, L., Mognard, N., Biancamaria, S., Viers, J., and Kolmakova, M.: Western Siberia wetlands as indicator and regulator of climate change on the global scale, Int. J. Environ. Stud., 66, 409–421, https://doi.org/10.1080/00207230902753056, 2009.

Kremenetski, K. V., Velichko, A. A., Borisova, O. K., MacDonald, G. M., Smith, L. C., Frey, K. E., and Orlova, L. A.: Peatlands of the Western Siberian lowlands: current knowledge on zonation, carbon content and Late Quaternary history, Quaternary Sci. Rev., 22, 703–723, https://doi.org/10.1016/S0277-3791(02)00196-8, 2003.

Kurakova, A. A.: Landscape-Hydrological Zoning of the Flat Areas of Western Siberia and Its Application in the Analysis of River Bank Erosion, Geogr. Nat. Resour., 45, 397–409, https://doi.org/10.1134/S1875372824700720, 2024.

Kurina, I. V., Veretennikova, E. E., Salisch, L. V., Egorova, M. L., Dolgin, V. N., Udaloi, A. V., and Golovatskaya, E. A.: Primenenie zooindikatorov dlya rekonstruktsii usloviy prirodnoy sredy golotsena v torfyanoy zalezhi nizinnogo bolota [The use of zoo-indicators for the reconstruction of paleoenvironments in the Holocene in the peat deposits of an eutrophic peatland], Zool. Zhurnal, 96, 973–986, https://doi.org/10.7868/S0044513417080086, 2017.

Kurina, I. V., Li, H., and Barashkov, D. R.: Use of testate amoebae to infer paleohydrology during fen and fen-bog transition stages of ombrotrophic mire development, J. Paleolimnol., 63, 147–158, https://doi.org/10.1007/s10933-019-00107-y, 2020.

Kurina, I. V., Veretennikova, E. E., Il'ina, A. A., Egorova, M. L., Salisch, L. V., Dolgin, V. N., Udaloi, A. V., Golovatskaya, E. A., Dyukarev, E. A., and Smirnov, S. V.: Multi-proxy climate and environmental records from a Holocene eutrophic mire, southern taiga subzone, West Siberia, Boreas, 52, 223–239, https://doi.org/10.1111/bor.12604, 2023.

Lamentowicz, M., Słowiński, M., Marcisz, K., Zielińska, M., Kaliszan, K., Lapshina, E., Gilbert, D., Buttler, A., Fiałkiewicz-Kozieł, B., Jassey, V. E. J., Laggoun-Defarge, F., and Kołaczek, P.: Hydrological dynamics and fire history of the last 1300 years in western Siberia reconstructed from a high-resolution, ombrotrophic peat archive, Quat. Res., 84, 312–325, https://doi.org/10.1016/j.yqres.2015.09.002, 2015.

Lapshina, E. D. and Zarov, E. A.: Stratigraphy of peat deposits and mire development in the southernpart of the forest zone of Western Siberia in Holocene., Environ. Dyn. Glob. Clim. Change, 14, 70–101, https://doi.org/10.18822/edgcc568688, 2023.

Leonova, G. À., Maltsev, À. Å., Preis, Y. I., and Miroshnichenko, L. V.: Biogeochemistry of holocene peatlands in the baraba forest-steppe (southern West Siberia), Appl. Geochem., 124, 104811, https://doi.org/10.1016/j.apgeochem.2020.104811, 2021.

Leonova, G. A., Maltsev, A. E., Preis, Y. I., Miroshnichenko, L. V., Shavekin, A. S., and Rubanov, M. V.: Biogeochemical Features of Holocene Sediments in Oligotrophic Bogs of the Baraba Forest Steppe, Geochem. Int., 60, 183–202, https://doi.org/10.1134/S0016702922020069, 2022.

Levkovskaya, G. M., Kind, N. V., Zavelsky, F. C., and Forova, V. S.: Absolute age of peat bogs of the Igarka City region and the division of the West Siberia Holocene, Bull. Comm. Quat. Stud., 37, 94–101, 1970.

Liss, O. L. and Berezina, N.: Bolotnye sistemy Zapadnoy Sibiri [Bogs of the West Siberian Lowland], Moscow University publishing, Moscow, 206 pp., ISBN 5-8125-0150-5, 1981.

Liss, O. L. and Kulikova, G. G.: About the regional classification of bogs in Tomsk region, Vestn. Mosk. Univ., 4, 87–91, 1967.

Loisel, J., Yu, Z., Beilman, D. W., Camill, P., Alm, J., Amesbury, M. J., Anderson, D., Andersson, S., Bochicchio, C., Barber, K., Belyea, L. R., Bunbury, J., Chambers, F. M., Charman, D. J., De Vleeschouwer, F., Fiałkiewicz-Kozieł, B., Finkelstein, S. A., Gałka, M., Garneau, M., Hammarlund, D., Hinchcliffe, W., Holmquist, J., Hughes, P., Jones, M. C., Klein, E. S., Kokfelt, U., Korhola, A., Kuhry, P., Lamarre, A., Lamentowicz, M., Large, D., Lavoie, M., MacDonald, G., Magnan, G., Mäkilä, M., Mallon, G., Mathijssen, P., Mauquoy, D., McCarroll, J., Moore, T. R., Nichols, J., O'Reilly, B., Oksanen, P., Packalen, M., Peteet, D., Richard, P. J., Robinson, S., Ronkainen, T., Rundgren, M., Sannel, A. B. K., Tarnocai, C., Thom, T., Tuittila, E.-S., Turetsky, M., Väliranta, M., van der Linden, M., van Geel, B., van Bellen, S., Vitt, D., Zhao, Y., and Zhou, W.: A database and synthesis of northern peatland soil properties and Holocene carbon and nitrogen accumulation, The Holocene, 24, 1028–1042, https://doi.org/10.1177/0959683614538073, 2014.

Longman, J., Veres, D., and Wennrich, V.: Utilisation of XRF core scanning on peat and other highly organic sediments, Quatern. Int., 514, 85–96, https://doi.org/10.1016/j.quaint.2018.10.015, 2019.

López-Blanco, E., Topp-Jørgensen, E., Christensen, T. R., Rasch, M., Skov, H., Arndal, M. F., Bret-Harte, M. S., Callaghan, T. V., and Schmidt, N. M.: Towards an increasingly biased view on Arctic change, Nat. Clim. Change, 14, 152–155, https://doi.org/10.1038/s41558-023-01903-1, 2024.

L'vov, Y. A.: Metodicheskie materialy k tipologii i klassifikatsii bolot Tomskoy oblasti [Methodical materials for the typology and classification of the Tomsk Province mires], in: Tipy bolot SSSR i printsipy ikh klassifikatsii [Types of the USSR Bogs and Principles of their Classification], Nauka, Leningrad, 188–194, 1974.

MacDonald, G. M., Beilman, D. W., Kremenetski, K. V., Sheng, Y., Smith, L. C., and Velichko, A. A.: Rapid Early Development of Circumarctic Peatlands and Atmospheric CH4 and CO2 Variations, Science, 314, 285–288, https://doi.org/10.1126/science.1131722, 2006.

Malyasova, E. S., Novikov, S. M., and Usova, L. I.: Dynamics of peat accumulation and the formation of palsa mires in the Western Siberia, Bot. Zhurnal, 9, 1227–1238, 1991.

Mander, L. and Punyasena, S. W.: Fossil Pollen and Spores in Paleoecology, in: Methods in Paleoecology: Reconstructing Cenozoic Terrestrial Environments and Ecological Communities, edited by: Croft, D. A., Su, D. F., and Simpson, S. W., Springer International Publishing, Cham, 215–234, https://doi.org/10.1007/978-3-319-94265-0_11, 2018.

Map of West Siberian wetlands: Karta bolot Zapadnoi Sibiri, Moscow: Main Administration of Geodesy and Cartography, 1970.

Map of West Siberian wetlands: Karta bolot Zapadnoi Sibiri, Omsk, 1996.

Martínez Cortizas, A., López-Merino, L., Silva-Sánchez, N., Sjöström, J. K., and Kylander, M. E.: Investigating the Mineral Composition of Peat by Combining FTIR-ATR and Multivariate Analysis, Minerals, 11, 1084, https://doi.org/10.3390/min11101084, 2021.

McClymont, E. L., Pendall, E., and Nichols, J.: Stable isotopes and organic geochemistry in peat: Tools to investigate past hydrology, temperature and biogeochemistry, PAGES News, 18, 15–18, https://doi.org/10.22498/pages.18.1.15, 2010.

Minayeva, T., Bleuten, W., Sirin, A., and Lapshina, E. D.: Eurasian Mires of the Southern Taiga Belt: Modern Features and Response to Holocene Palaeoclimate, in: Wetlands and Natural Resource Management, edited by: Verhoeven, J. T. A., Beltman, B., Bobbink, R., and Whigham, D. F., Springer, Berlin, Heidelberg, 315–341, https://doi.org/10.1007/978-3-540-33187-2_14, 2006.

Mitchell, E. A. D.: A brief history of testate amoebae research and introducing the International Society for Testate Amoeba Research (ISTAR), Acta Protozool., 2024, 1–14, 2025.

Mitchell, E. A. D. and Payne, R.: Testate Amoeba Analysis, in: The Encyclopedia of Archaeological Sciences, 1–4, https://doi.org/10.1002/9781119188230.saseas0576, 2018.

Neustadt, M. I.: On absolute age of peat bogs of Western Siberia., Rev. Roum. Biol. Ser. Bot., 12, 181–186, 1967.

Neustadt, M. I.: The world natural phenomenon – Bogs of the West Siberian Lowland, Izv. Akad. Nauk SSSR, 21–34, 1971.

Neustadt, M. I.: Holocene peatland development, in: Late Quaternary Environments of the Soviet Union, University of Minnesota Press, Minneapolis, 201–206, ISBN 0-8166-1250-1, 1984.

Novenko, E., Rudenko, O., Mazei, N., Kupriyanov, D., Andreev, R., Shatunov, A., Kusilman, M., Prokushkin, A., and Olchev, A.: Effects of Climate Change and Fire on the Middle and Late Holocene Forest History in Yenisei Siberia, Forests, 14, 2321, https://doi.org/10.3390/f14122321, 2023.

Novenko, E. Y., Mazei, N. G., Kupriyanov, D., Shatunov, A. E., Andreev, R. A., Makarova, E. A., Borodina, K. A., Rudenko, O., Prokushkin, A. S., and Volkova, E. M.: Izmeneniya rastitel'nosti Prieniseyskoy Sibiri v poslednie 4700 let: novye paleoekologicheskie dannye iz rayona Igarki (Krasnoyarskiy kray) [Vegetation changes in Yenisei Siberia over the last 4700 years: new palaeoecological data from Igarka area; Krasnoyarsk Region], Geomorfologiya, 53, 5–6, https://doi.org/10.31857/S0435428122030129, 2022.

Novenko, E. Y., Prokushkin, A. S., Mazei, N. G., Zazovskaya, E. P., Kupriyanov, D. A., Shatunov, A. E., Andreev, R. A., Makarova, E. A., Kusilman, M. V., Serikov, S. I., Xiuyuan, G., Babeshko, K. V., Tsyganov, A. N., and Mazei, Y. A.: The mid- and late Holocene palsa palaeoecology and hydroclimatic changes in Yenisei Siberia revealed by a high-resolution peat archive, Quat. Int., 682, 8–21, https://doi.org/10.1016/j.quaint.2024.01.013, 2024.

Olson, D. M., Dinerstein, E., Wikramanayake, E. D., Burgess, N. D., Powell, G. V. N., Underwood, E. C., D'amico, J. A., Itoua, I., Strand, H. E., Morrison, J. C., Loucks, C. J., Allnutt, T. F., Ricketts, T. H., Kura, Y., Lamoreux, J. F., Wettengel, W. W., Hedao, P., and Kassem, K. R.: Terrestrial Ecoregions of the World: A New Map of Life on Earth: A new global map of terrestrial ecoregions provides an innovative tool for conserving biodiversity, Bioscience, 51, 933–938, https://doi.org/10.1017/S0033822200033695, 2001.

Olsson, I. U.: Radiocarbon Dating History: Early Days, Questions, and Problems Met, Radiocarbon, 51, 1–43, https://doi.org/10.1017/S0033822200033695, 2009.

Panova, N. K., Trofimova, S. S., Antipina, T. G., Zinoviev, E. V., Gilev, A. V., and Erokhin, N. G.: Holocene dynamics of vegetation and ecological conditions in the southern Yamal Peninsula according to the results of comprehensive analysis of a relict peat bog deposit, Russ. J. Ecol., 41, 20–27, https://doi.org/10.1134/S1067413610010042, 2010.

Paradossky, V. L., Pechatnova, Y. V., and Solomonova, M. Y.: The natural transformations of the Northern Kulunda in the second half of the Holocene based on studying the microbiomorphic profile of swampy phytocenosis, Ukr. J. Ecol., 9, 406–411, 2019.

Parry, L. E., West, L. J., Holden, J., and Chapman, P. J.: Evaluating approaches for estimating peat depth, J. Geophys. Res.-Biogeo., 119, 567–576, https://doi.org/10.1002/2013JG002411, 2014.

Peteet, D., Andreev, A., Bardeen, W., and Mistretta, F.: Long-term Arctic peatland dynamics, vegetation and climate history of the Pur-Taz region, Western Siberia, Boreas, 27, 115–126, https://doi.org/10.1111/j.1502-3885.1998.tb00872.x, 1998.

Polishchuk, Y. M., Bogdanov, A. N., Polishchuk, V. Y., Manasypov, R. M., Shirokova, L. S., Kirpotin, S. N., and Pokrovsky, O. S.: Size Distribution, Surface Coverage, Water, Carbon, and Metal Storage of Thermokarst Lakes in the Permafrost Zone of the Western Siberia Lowland, Water, 9, 228, https://doi.org/10.3390/w9030228, 2017.

Preis, Y.: Indicators of paleocryogenic processes that disrupt the patterns of peatland autogenic development in the zone of seasonal freezing of rocks of Western Siberia, Limnol. Freshw. Biol., 562–567, https://doi.org/10.31951/2658-3518-2024-A-4-562, 2024.

Preis, Y., Maltsev, A., and Leonova, G.: Assessment of Holocene climate influence on hydrothermal regime of paleoecotopes within Ryams of the Baraba forest-steppe (southern Western Siberia), Limnol. Freshw. Biol., 580–587, https://doi.org/10.31951/2658-3518-2024-A-4-580, 2024.

Preis, Y. I.: Detal'naya rekonstruktsiya funktsional'nogo sostoyaniya bolota kak otklik na izmeneniya kontinental'nogo klimata golotsena (srednyaya tayga Zapadnoy Sibiri) [Detailed reconstruction of bog functional state as a response to continental climate changes in Holocene (the middle taiga of Western Siberia)], News Tomsk Polytech. Univ. Eng. Georesources, 326, 90–102, 2015.

Punning, J. M., Kakum, T., and Rajamäe, R.: Tallinn Radiocarbon Dates II, Radiocarbon, 16, 388–394, https://doi.org/10.1017/S0033822200059683, 1974.

Pupysheva, M. A. and Blyakharchuk, T. A.: Fires and their Significance in the Earth's Post-Glacial Period: a Review of Methods, Achievements, Groundwork, Contemp. Probl. Ecol., 16, 303–315, https://doi.org/10.1134/S1995425523030095, 2023.

QGIS Development Team: QGIS Geographic Information System, Zenodo, https://doi.org/10.5281/zenodo.6139224, 2025.

R Core Team: R: A Language and Environment for Statistical Computing, R Foundation for Statistical Computing, Vienna, Austria, https://www.R-project.org/ (last access: 3 June 2026), 2022.

Reimer, P. J., Austin, W. E. N., Bard, E., Bayliss, A., Blackwell, P. G., Ramsey, C. B., Butzin, M., Cheng, H., Edwards, R. L., Friedrich, M., Grootes, P. M., Guilderson, T. P., Hajdas, I., Heaton, T. J., Hogg, A. G., Hughen, K. A., Kromer, B., Manning, S. W., Muscheler, R., Palmer, J. G., Pearson, C., Plicht, J. V. D., Reimer, R. W., Richards, D. A., Scott, E. M., Southon, J. R., Turney, C. S. M., Wacker, L., Adolphi, F., Büntgen, U., Capano, M., Fahrni, S. M., Fogtmann-Schulz, A., Friedrich, R., Köhler, P., Kudsk, S., Miyake, F., Olsen, J., Reinig, F., Sakamoto, M., Sookdeo, A., and Talamo, S.: The IntCal20 Northern Hemisphere Radiocarbon Age Calibration Curve (0–55 cal kBP), Radiocarbon, 62, 725–757, https://doi.org/10.1017/RDC.2020.41, 2020.

Rudmin, M., Ruban, A., Savichev, O., Mazurov, A., Dauletova, A., and Savinova, O.: Authigenic and Detrital Minerals in Peat Environment of Vasyugan Swamp, Western Siberia, Minerals, 8, 500, https://doi.org/10.3390/min8110500, 2018.

Ryabogina, N. E., Nesterova, M. I., Utaygulova, R. R., and Trubitsyna, E. D.: Forest fires in southwest Western Siberia: the impact of climate and economic transitions over 9000 years, J. Quaternary Sci., 39, 432–442, https://doi.org/10.1002/jqs.3593, 2024.

Rydin, H., Gunnarsson, U., and Sundberg, S.: The Role of Sphagnum in Peatland Development and Persistence, in: Boreal Peatland Ecosystems, edited by: Wieder, R. K. and Vitt, D. H., Springer, Berlin, Heidelberg, 47–65, https://doi.org/10.1007/978-3-540-31913-9_4, 2006.

Rydin, H., Jeglum, J. K., and Bennett, K. D.: The Biology of Peatlands, OUP Oxford, 397 pp., ISBN 978-0-19-960299-5, 2013.

Schaaff, V., Grossi, V., Makou, M., Garcin, Y., Deschamps, P., Sebag, D., Ngounou Ngatcha, B., and Ménot, G.: Constraints on hopanes and brGDGTs as pH proxies in peat, Geochim. Cosmochim. Acta, 373, 342–354, https://doi.org/10.1016/j.gca.2024.03.034, 2024.

Scharlemann, J. P., Tanner, E. V., Hiederer, R., and Kapos, V.: Global soil carbon: understanding and managing the largest terrestrial carbon pool, Carbon Manag., 5, 81–91, https://doi.org/10.4155/cmt.13.77, 2014.

Schuur, E. A. G., Pallandt, M., and Göckede, M.: Russian collaboration loss risks permafrost carbon emissions network, Nat. Clim. Change, 14, 410–411, https://doi.org/10.1038/s41558-024-02001-6, 2024.

Seniczak, A., Seniczak, S., Iturrondobeitia, J. C., Gwiazdowicz, D. J., Waldon-Rudzionek, B., Flatberg, K. I., and Bolger, T.: Mites (Oribatida and Mesostigmata) and vegetation as complementary bioindicators in peatlands, Sci. Total Environ., 851, 158335, https://doi.org/10.1016/j.scitotenv.2022.158335, 2022.

Shefer, N. V., Loiko, S. V., Kriñkov, I. V., and Lim, A. G.: The most comprehensive history of fire activity in the Pur-Taz interfluve over the last 11,000 years (Western Siberia, Russia), Acta Biol. Sib., 10, 1755–1777, https://doi.org/10.5281/zenodo.14525710, 2024.

Sheng, Y.: West Siberian Lowland Peatland GIS Data Collection, Arctic Data Center [data set], https://doi.org/10.5065/D65T3HM5, 2016.

Sheng, Y., Smith, L. C., MacDonald, G. M., Kremenetski, K. V., Frey, K. E., Velichko, A. A., Lee, M., Beilman, D. W., and Dubinin, P.: A high-resolution GIS-based inventory of the west Siberian peat carbon pool, Global Biogeochem. Cy., 18, https://doi.org/10.1029/2003GB002190, 2004.

Shotyk, W.: Review of the inorganic geochemistry of peats and peatland waters, Earth-Sci. Rev., 25, 95–176, https://doi.org/10.1016/0012-8252(88)90067-0, 1988.

Shumilovskikh, L., O'Keefe, J. M. K., and Marret, F.: An overview of the taxonomic groups of non-pollen palynomorphs, Geol. Soc. Lond. Spec. Publ., 511, 13–61, https://doi.org/10.1144/SP511-2020-65, 2021.

Shvartseva, O., Gaskova, O., Yurtaev, A., Boguslavsky, A., Kolpakova, M., and Mashkova, D.: Water–Rock–Organic Matter Interactions in Wetland Ecosystem: Hydrogeochemical Investigation and Computer Modeling, Water, 16, 428, https://doi.org/10.3390/w16030428, 2024.

Sjöström, J. K., Bindler, R., Granberg, T., and Kylander, M. E.: Procedure for Organic Matter Removal from Peat Samples for XRD Mineral Analysis, Wetlands, 39, 473–481, https://doi.org/10.1007/s13157-018-1093-7, 2019.

Smith, L. C., MacDonald, G., Frey, K. E., Velichko, A. A., Kremenetski, K., Borisova, O. K., Dubinin, P., and Forster, R. R.: U.S.-Russia venture probes Siberian peatlands' sensitivity to climate, Eos Trans. Am. Geophys. Union, https://doi.org/10.1029/00EO00357, 2000.

Smith, L. C., MacDonald, G. M., Velichko, A. A., Beilman, D. W., Borisova, O. K., Frey, K. E., Kremenetski, K. V., and Sheng, Y.: Siberian Peatlands a Net Carbon Sink and Global Methane Source Since the Early Holocene, Science, 303, 353–356, https://doi.org/10.1126/science.1090553, 2004.

Smith, L. C., Beilman, David. W., Kremenetski, K. V., Sheng, Y., MacDonald, G. M., Lammers, R. B., Shiklomanov, A. I., and Lapshina, E. D.: Influence of permafrost on water storage in West Siberian peatlands revealed from a new database of soil properties, Permafrost Periglac., 23, 69–79, https://doi.org/10.1002/ppp.735, 2012.

Solomeshch, A. I.: The West Siberian Lowland, in: The World's Largest Wetlands: Ecology and Conservation, edited by: Fraser, L. H. and Keddy, P. A., Cambridge University Press, Cambridge, 11–62, https://doi.org/10.1017/CBO9780511542091.003, 2005.

Startsev, V., Gorbach, N., Mazur, A., Prokushkin, A., Karpenko, L., and Dymov, A.: Macrocharcoal Signals in Histosols Reveal Wildfire History of Vast Western Siberian Forest-Peatland Complexes, Plants, 11, 3478, https://doi.org/10.3390/plants11243478, 2022.

Stepanova, V. A. and Volkova, I. I.: Osobennosti genezisa Nikolaevskogo ryama v lesostepi Zapadnoy Sibiri [Genesis features of the Nikolaevka ryam in the forest-steppe of Western Siberia], Tomsk State Univ. J. Biol., 202–223, https://doi.org/10.17223/19988591/40/12, 2017.

Swindles, G. T., Mullan, D. J., Brannigan, N. T., Fewster, R. E., Sim, T. G., Gallego-Sala, A., Blaauw, M., Lamentowicz, M., Jassey, V. E. J., Marcisz, K., Green, S. M., Roland, T. P., Loisel, J., Amesbury, M. J., Blundell, A., Chambers, F. M., Charman, D. J., Evans, C. R. C., Feurdean, A., Galloway, J. M., Gałka, M., Karofeld, E., Keaveney, E. M., Korhola, A., Lamentowicz, Ł., Langdon, P., Mauquoy, D., McKeown, M. M., Mitchell, E. A. D., Plunkett, G., Roe, H. M., Turner, T. E., Sillasoo, Ü., Väliranta, M., van der Linden, M., and Warner, B.: Climate and water-table levels regulate peat accumulation rates across Europe, PLOS One, 20, e0327422, https://doi.org/10.1371/journal.pone.0327422, 2025.

Syso, A. I. and Peregon, A. M.: The features of peat-accumulation process at the southern slope of the Great Vasyugan Bog, Contemp. Probl. Ecol., 2, 124–127, https://doi.org/10.1134/S1995425509020064, 2009.

Tarasov, P. E., Webb III, T., Andreev, A. A., Afanas'eva, N. B., Berezina, N. A., Bezusko, L. G., Blyakharchuk, T. A., Bolikhovskaya, N. S., Cheddadi, R., Chernavskaya, M. M., Chernova, G. M., Dorofeyuk, N. I., Dirksen, V. G., Elina, G. A., Filimonova, L. V., Glebov, F. Z., Guiot, J., Gunova, V. S., Harrison, S. P., Jolly, D., Khomutova, V. I., Kvavadze, E. V., Osipova, I. M., Panova, N. K., Prentice, I. C., Saarse, L., Sevastyanov, D. V., Volkova, V. S., and Zernitskaya, V. P.: Present-day and mid-Holocene biomes reconstructed from pollen and plant macrofossil data from the former Soviet Union and Mongolia, J. Biogeogr., 25, 1029–1053, https://doi.org/10.1046/j.1365-2699.1998.00236.x, 1998.

Tikhonravova, Y., Kuznetsova, A., Slagoda, E., and Koroleva, E.: Holocene permafrost peatland evolution in drained lake basins on the Pur-Taz Interfluve, North-Western Siberia, Quatern. Int., 669, 32–42, https://doi.org/10.1016/j.quaint.2023.07.005, 2023.

Tiuremnov, S. N.: Torfyanye mestorozhdeniya [Peat Deposits], Nedra, Moscow, 487 pp., 1976.

Tolonen, K.: Interpretation of changes in the ash content of ombrotrophic peat layers, Bull. Geol. Soc. Finl., 56, 207–219, https://doi.org/10.17741/bgsf/56.1-2.013, 1984.

Treat, C. C., Jones, M. C., Camill, P., Gallego-Sala, A., Garneau, M., Harden, J. W., Hugelius, G., Klein, E. S., Kokfelt, U., Kuhry, P., Loisel, J., Mathijssen, P. J. H., O'Donnell, J. A., Oksanen, P. O., Ronkainen, T. M., Sannel, A. B. K., Talbot, J., Tarnocai, C., and Väliranta, M.: Effects of permafrost aggradation on peat properties as determined from a pan-Arctic synthesis of plant macrofossils, J. Geophys. Res.-Biogeo., 121, 78–94, https://doi.org/10.1002/2015JG003061, 2016.

Trofimova, I. E. and Balybina, A. S.: Classification of climates and climatic regionalization of the West-Siberian plain, Geogr. Nat. Resour., 35, 114–122, https://doi.org/10.1134/S1875372814020024, 2014.

Tsyganov, A. N., Zarov, E. A., Mazei, Y. A., Kulkov, M. G., Babeshko, K. V., Yushkovets, S. Y., Payne, R. J., Ratcliffe, J. L., Fatyunina, Y. A., Zazovskaya, E. P., and Lapshina, E. D.: Key periods of peatland development and environmental changes in the middle taiga zone of Western Siberia during the Holocene, Ambio, 50, 1896–1909, https://doi.org/10.1007/s13280-021-01545-7, 2021.

Turunen, J., Tahvanainen, T., Tolonen, K., and Pitkänen, A.: Carbon accumulation in West Siberian Mires, Russia Sphagnum peatland distribution in North America and Eurasia during the past 21,000 years, Global Biogeochem. Cy., 15, 285–296, https://doi.org/10.1029/2000GB001312, 2001.

UNEP: The State of the World's Peatlands: Evidence for action toward the conservation, restoration, and sustainable management of peatlands, Global Peatlands Initiative, United Nations Environment Programme, Nairobi, ISBN 978-92-807-3991-6, 2022.

Vaganov, E. A., Vedrova, E. F., Verkhovets, S. V., Efremov, S. P., Efremova, T. T., Kruglov, V. B., Onuchin, A. A., Sukhinin, A. I., and Shibistova, O. B.: Forests and swamps of Siberia in the global carbon cycle, Sib. Ecol. J., 4, 631–649, 2005.

Van Geel, B.: Non-Pollen Palynomorphs, in: Tracking Environmental Change Using Lake Sediments: Terrestrial, Algal, and Siliceous Indicators, edited by: Smol, J. P., Birks, H. J. B., Last, W. M., Bradley, R. S., and Alverson, K., Springer Netherlands, Dordrecht, 99–119, https://doi.org/10.1007/0-306-47668-1_6, 2001.

Vasil'chuk, Y. K., Jungner, H., and Vasil'chuk, A. C.: 14C Dating of Peat and δ18O-δd in Ground Ice From Northwest Siberia, Radiocarbon, 43, 527–540, https://doi.org/10.1017/S0033822200041187, 2001.

Velichko, A. A., Timireva, S. N., Kremenetski, K. V., MacDonald, G. M., and Smith, L. C.: West Siberian

Plain as a late glacial desert, Quatern. Int., 237, 45–53, https://doi.org/10.1016/j.quaint.2011.01.013, 2011.

Veretennikova, E. E., Kuryina, I. V., Dyukarev, E. A., Golovatskaya, E. A., and Smirnov, S. V.: Geochemical Features of Peat Deposits at Oligotrophic Bogs in the Southern Taiga Subzone of West Siberia, Geochem. Int., 59, 618–631, https://doi.org/10.1134/S0016702921050098, 2021.

Volkov, V. S., Gurtovaya, Y., Firsov, L. V., Panychev, V. A., and Orlova, L. A.: Stroenie, vozrast i istoriya formirovaniya golotsenovogo torfyanika u s. Gorno-Slinkina na Irtyshe [Structure, age and history of development of the Holocene peat-bog near Gorno-Slinkino village on the Irtysh River], in: Pleistotsen Sibiri i smezhnykh oblastei, Nauka, Moscow, 34–39, 1973.

Wickham, H.: ggplot2: Elegant Graphics for Data Analysis, Springer-Verlag New York, ISBN 978-3-319-24277-4, 2016.

Wickham, H., François, R., Henry, L., Müller, K., Vaughan, D., Software, P., and PBC: dplyr: A Grammar of Data Manipulation, https://doi.org/10.32614/CRAN.package.dplyr, 2023.

Willis, K. S., Beilman, D., Booth, R. K., Amesbury, M., Holmquist, J., and MacDonald, G.: Peatland paleohydrology in the southern West Siberian Lowlands: Comparison of multiple testate amoeba transfer functions, sites, and Sphagnum δ13C values, The Holocene, 25, 1425–1436, https://doi.org/10.1177/0959683615585833, 2015.

Witze, A.: Russia's war in Ukraine forces Arctic climate projects to pivot, Nature, 607, 432–432, https://doi.org/10.1038/d41586-022-01868-9, 2022.

Xu, J., Morris, P. J., Liu, J., and Holden, J.: PEATMAP: Refining estimates of global peatland distribution based on a meta-analysis, CATENA, 160, 134–140, https://doi.org/10.1016/j.catena.2017.09.010, 2018.

Yu, Z., Beilman, D. W., and Jones, M. C.: Sensitivity of Northern Peatland Carbon Dynamics to Holocene Climate Change, in: Carbon Cycling in Northern Peatlands, American Geophysical Union (AGU), 55–69, https://doi.org/10.1029/2008GM000822, 2009.

Zhang, H., Väliranta, M., Swindles, G. T., Aquino-López, M. A., Mullan, D., Tan, N., Amesbury, M., Babeshko, K. V., Bao, K., Bobrov, A., Chernyshov, V., Davies, M. A., Diaconu, A.-C., Feurdean, A., Finkelstein, S. A., Garneau, M., Guo, Z., Jones, M. C., Kay, M., Klein, E. S., Lamentowicz, M., Magnan, G., Marcisz, K., Mazei, N., Mazei, Y., Payne, R., Pelletier, N., Piilo, S. R., Pratte, S., Roland, T., Saldaev, D., Shotyk, W., Sim, T. G., Sloan, T. J., Słowiński, M., Talbot, J., Taylor, L., Tsyganov, A. N., Wetterich, S., Xing, W., and Zhao, Y.: Recent climate change has driven divergent hydrological shifts in high-latitude peatlands, Nat. Commun., 13, 4959, https://doi.org/10.1038/s41467-022-32711-4, 2022.

Zhilinsky, I. I.: Ocherk gidrotekhnicheskikh rabot v rayone Sibirskoi zheleznoi dorogi po obvodneniyu pereselencheskikh uchastkov v Ishimskoi stepi i osusheniyu bolot v Barabe. 1895–1904 gg [Description of hydrotechnical works in the area of the Siberian railroad to insure water supply for settlements in the Ishim steppe and to drain bogs in the Baraba forest-steppe (1895–1904)], Saint-Petersburg, 829 pp., 1907.

Deklaracje współautorów

Instytut Geografii i Przestrzennego Zagospodarowania im. Stanisława Leszczyckiego
Polska Akademia Nauk

Warszawa, 28.04.2026

Mgr Agnieszka Halaś
Zakład Dynamiki Krajobrazów Minionych
Instytut Geografii i Przestrzennego Zagospodarowania im. Stanisława Leszczyckiego
Polska Akademia Nauk
ul. Twarda 51/55
00-818 Warszawa
aj.halas@twarda.pan.pl

Oświadczenie o wkładzie autorskim w artykule naukowym

Oświadczam, że mój wkład w artykule:

> **Halaś, A.**, Lamentowicz, M., Łuców, D., and Słowiński, M.: Developing a new testate amoeba hydrological transfer function for permafrost peatlands of NW Siberia, Quaternary Science Reviews, 308, 108067, https://doi.org/10.1016/j.quascirev.2023.108067, 2023.

wynosił **50%** i był następujący:

- laboratoryjna obróbka prób powierzchniowych oraz rdzenia torfowego,
- wykonanie analizy współczesnych i subfosylnych ameb skorupkowych,
- współtworzenie hydrologicznej funkcji transferu w oparciu o analizę współczesnych zbiorowisk ameb skorupkowych,
- wykonanie rekonstrukcji poziomu wody w oparciu o analizę ameb skorupkowych,
- przeprowadzenie analizy gęstości objętościowej w torfie,
- przygotowanie koncepcji manuskryptu,
- synteza oraz interpretacja danych,
- przeprowadzenie analiz statystycznych,
- przygotowanie wszystkich rycin i map znajdujących się w manuskrypcie oraz materiale uzupełniającym,
- przygotowanie pierwszej wersji manuskryptu,
- przygotowanie odpowiedzi na uwagi recenzentów,
- autor korespondencyjny.

Agnieszka Halaś

Poznań, 28.04.2026

Prof. dr hab. Mariusz Lamentowicz
Pracownia Ekologii Zmian Klimatu
Instytut Geoekologii i Geoinformacji
Wydział Nauk Geograficznych i Geologicznych
Uniwersytet im. Adama Mickiewicza w Poznaniu
Ul. Bogumiła Krygowskiego 10
61-680 Poznań
mariusz.lamentowicz@uam.edu.pl

Oświadczenie o wkładzie autorskim w artykule naukowym

Oświadczam, że mój wkład w artykule:

> Halaś, A., **Lamentowicz, M**., Łuców, D., and Słowiński, M.: Developing a new testate amoeba hydrological transfer function for permafrost peatlands of NW Siberia, Quaternary Science Reviews, 308, 108067, https://doi.org/10.1016/j.quascirev.2023.108067, 2023.

wynosił **20%** i był następujący:

- udział w pracach terenowych związanych z pozyskaniem prób powierzchniowych i rdzenia torfowego,
- wsparcie merytoryczne analizy ameb skorupkowych,
- współtworzenie hydrologicznej funkcji transferu w oparciu o analizę współczesnych zbiorowisk ameb skorupkowych,
- przygotowanie koncepcji manuskryptu,
- interpretacja danych,
- komentowanie i edytowanie manuskryptu.

Mariusz
Lamentowicz

Uniwersytet Gdański

Związek Uczelni Fahrenheita

Katedra Geomorfologii i Geologii Czwartorzędu
Wydział Oceanografii i Geografii

29.04.2026r. Gdańsk

Oświadczenie o wkładzie autorskim w artykule naukowym

Oświadczam, że mój wkład w artykule:

> Halaś, A., Lamentowicz, M., Łuców, D., and Słowiński, M.: Developing a new testate amoeba hydrological transfer function for permafrost peatlands of NW Siberia, Quaternary Science Reviews, 308, 108067, https://doi.org/10.1016/j.quascirev.2023.108067, 2023.

wynosił **10%** i był następujący:

- udział w pracach terenowych związanych z pozyskaniem prób powierzchniowych i rdzenia torfowego,
- udział w laboratoryjnej obróbce prób powierzchniowych,
- wsparcie merytoryczne analizy ameb skorupkowych,
- interpretacja danych,
- komentowanie i edytowanie manuskryptu.

Z poważaniem,
dr Dominika Łuców

D Łuców

Katedra Geomorfologii i Geologii Czwartorzędu
tel. (58) 523 65 41
e-mail: dominika.lucow@ug.edu.pl
ul. prof. Marii Janion 3
80-309 Gdańsk
www.ug.edu.pl

Instytut Geografii i Przestrzennego Zagospodarowania im. Stanisława Leszczyckiego
Polska Akademia Nauk

Warszawa, 28.04.2026

Prof. dr hab. Michał Słowiński
Zakład Dynamiki Krajobrazów Minionych
Instytut Geografii i Przestrzennego Zagospodarowania im. Stanisława Leszczyckiego
Polska Akademia Nauk
ul. Twarda 51/55
00-818 Warszawa
michal.slowinski@geopan.torun.pl

Oświadczenie o wkładzie autorskim w artykule naukowym

Oświadczam, że mój wkład w artykule:

> Halaś, A., Lamentowicz, M., Łuców, D., and **Słowiński, M.:** Developing a new testate amoeba hydrological transfer function for permafrost peatlands of NW Siberia, Quaternary Science Reviews, 308, 108067, https://doi.org/10.1016/j.quascirev.2023.108067, 2023.

wynosił **20%** i był następujący:

- pozyskanie finansowania (Narodowe Centrum Nauki, PRELUDIUM BIS1, nr 2019/35/O/ST10/02903),
- udział w pracach terenowych związanych z pozyskaniem prób powierzchniowych i rdzenia torfowego,
- wykonanie analizy makroskopowych szczątków roślin w próbach powierzchniowych,
- przygotowanie koncepcji manuskryptu,
- interpretacja danych,
- komentowanie i edytowanie manuskryptu.

Warszawa, 28.04.2026

Mgr Agnieszka Halaś
Zakład Dynamiki Krajobrazów Minionych
Instytut Geografii i Przestrzennego Zagospodarowania im. Stanisława Leszczyckiego
Polska Akademia Nauk
ul. Twarda 51/55
00-818 Warszawa
aj.halas@twarda.pan.pl

Oświadczenie o wkładzie autorskim w artykule naukowym

Oświadczam, że mój wkład w artykule:

> **Halaś, A.,** Lamentowicz, M., Obremska, M., Łuców, D., and Słowiński, M.: Peatland development reconstruction and complex biological responses to permafrost thawing in Western Siberia, Biogeosciences, 22, 4797–4822, https://doi.org/10.5194/bg-22-4797-2025, 2025.

wynosił **50%** i był następujący:

- laboratoryjna obróbka rdzeni torfowych,
- współtworzenie modeli wiek-głębokość,
- wykonanie analizy subfosylnych ameb skorupkowych,
- wykonanie analizy makroskopowych fragmentów węgli drzewnych,
- wykonanie rekonstrukcji poziomu wody i pH w oparciu o analizę ameb skorupkowych,
- przeprowadzenie analizy gęstości objętościowej, obliczenie tempa akumulacji torfu i tempa akumulacji węgla w torfie,
- przygotowanie koncepcji manuskryptu,
- synteza oraz interpretacja danych paleoekologicznych,
- przygotowanie wszystkich rycin i map znajdujących się w manuskrypcie oraz materiale uzupełniającym,
- przygotowanie pierwszej wersji manuskryptu,
- przygotowanie odpowiedzi na uwagi recenzentów,
- autor korespondencyjny.

Agnieszka Halaś

Poznań, 28.04.2026

Prof. dr hab. Mariusz Lamentowicz
Pracownia Ekologii Zmian Klimatu
Instytut Geoekologii i Geoinformacji
Wydział Nauk Geograficznych i Geologicznych
Uniwersytet im. Adama Mickiewicza w Poznaniu
Ul. Bogumiła Krygowskiego 10
61-680 Poznań
mariusz.lamentowicz@uam.edu.pl

Oświadczenie o wkładzie autorskim w artykule naukowym

Oświadczam, że mój wkład w artykule:

> Halaś, A., **Lamentowicz, M.**, Obremska, M., Łuców, D., and Słowiński, M.: Peatland development reconstruction and complex biological responses to permafrost thawing in Western Siberia, Biogeosciences, 22, 4797–4822, https://doi.org/10.5194/bg-22-4797-2025, 2025.

wynosił **15%** i był następujący:

- udział w pracach terenowych związanych z pozyskaniem rdzeni torfowych,
- wsparcie merytoryczne analizy ameb skorupkowych,
- przygotowanie koncepcji manuskryptu,
- interpretacja danych paleoekologicznych,
- komentowanie i edytowanie manuskryptu.

Mariusz
Lamentowicz

Warszawa, 28.04.2026

Dr Milena Obremska
Instytut Nauk Geologicznych
Polska Akademia Nauk
ul. Twarda 51/55
00-818 Warszawa
mobremska@twarda.pan.pl

Oświadczenie o wkładzie autorskim w artykule naukowym

Oświadczam, że mój wkład w artykule:

> Halaś, A., Lamentowicz, M., **Obremska, M.,** Łuców, D., and Słowiński, M.: Peatland development reconstruction and complex biological responses to permafrost thawing in Western Siberia, Biogeosciences, 22, 4797–4822, https://doi.org/10.5194/bg-22-4797-2025, 2025.

wynosił **15%** i był następujący:

- wykonanie analizy palinologicznej,
- wykonanie analizy mikroskopowych fragmentów węgli drzewnych,
- interpretacja danych paleoekologicznych,
- komentowanie i edytowanie manuskryptu.

Uniwersytet Gdański | Związek Uczelni Fahrenheita

Katedra Geomorfologii i Geologii Czwartorzędu
Wydział Oceanografii i Geografii

29.04.2026r. Gdańsk

Oświadczenie o wkładzie autorskim w artykule naukowym

Oświadczam, że mój wkład w artykule:

> Halaś, A., Lamentowicz, M., Obremska, M., Łuców, D., and Słowiński, M.: Peatland development reconstruction and complex biological responses to permafrost thawing in Western Siberia, Biogeosciences, 22, 4797–4822, https://doi.org/10.5194/bg-22-4797-2025, 2025.

wynosił **5%** i był następujący:

- udział w pracach terenowych związanych z pozyskaniem rdzeni torfowych,
- wsparcie merytoryczne analizy ameb skorupkowych,
- interpretacja danych paleoekologicznych,
- komentowanie i edytowanie manuskryptu.

Z poważaniem,
dr Dominika Łuców

D. Łuców

Katedra Geomorfologii i Geologii Czwartorzędu
tel. (58) 523 65 41
e-mail: dominika.lucow@ug.edu.pl
ul. prof. Marii Janion 3
80-309 Gdańsk
www.ug.edu.pl

Instytut Geografii i Przestrzennego Zagospodarowania im. Stanisława Leszczyckiego
Polska Akademia Nauk

Warszawa, 28.04.2026

Prof. dr hab. Michał Słowiński
Zakład Dynamiki Krajobrazów Minionych
Instytut Geografii i Przestrzennego Zagospodarowania im. Stanisława Leszczyckiego
Polska Akademia Nauk
ul. Twarda 51/55
00-818 Warszawa
michal.slowinski@geopan.torun.pl

Oświadczenie o wkładzie autorskim w artykule naukowym

Oświadczam, że mój wkład w artykule:

> Halaś, A., Lamentowicz, M., Obremska, M., Łuców, D., and **Słowiński, M.**: Peatland development reconstruction and complex biological responses to permafrost thawing in Western Siberia, Biogeosciences, 22, 4797–4822, https://doi.org/10.5194/bg-22-4797-2025, 2025.

wynosił **15%** i był następujący:

- pozyskanie finansowania (Narodowe Centrum Nauki, PRELUDIUM BIS1, nr 2019/35/O/ST10/02903),
- udział w pracach terenowych związanych z pozyskaniem rdzeni torfowych,
- wybór makroskopowych szczątków roślin do datowania C^{14},
- współtworzenie modeli wiek-głębokość,
- wykonanie analizy makroskopowych szczątków roślin,
- wsparcie merytoryczne analizy makroskopowych węgli drzewnych,
- przygotowanie koncepcji manuskryptu,
- interpretacja danych paleoekologicznych,
- komentowanie i edytowanie manuskryptu.

Michał Słowiński

Instytut Geografii i Przestrzennego Zagospodarowania im. Stanisława Leszczyckiego
Polska Akademia Nauk

Warszawa, 5.06.2026

Mgr Agnieszka Halaś
Zakład Dynamiki Krajobrazów Minionych
Instytut Geografii i Przestrzennego Zagospodarowania im. Stanisława Leszczyckiego
Polska Akademia Nauk
ul. Twarda 51/55
00-818 Warszawa
aj.halas@twarda.pan.pl

Oświadczenie o wkładzie autorskim w artykule naukowym

Oświadczam, że mój wkład w artykule:

> **Halaś, A.** and Słowiński, M.: Peat core research in the Western Siberian Lowland: applications of palaeoecological proxies, regions studied, and future prospects, Earth System Science Data, 18, 3853–3888, https://doi.org/10.5194/essd-18-3853-2026, 2026.

wynosił **90%** i był następujący:

- opracowanie koncepcji manuskryptu,
- wykonanie przeglądu literatury,
- zebranie danych oraz utworzenie i opracowanie bazy danych,
- przeprowadzenie analiz statystycznych i przestrzennych,
- synteza oraz interpretacja danych,
- przygotowanie wszystkich rycin oraz map znajdujących się w manuskrypcie,
- przygotowanie pierwszej wersji manuskryptu,
- przygotowanie odpowiedzi na uwagi recenzentów,
- autor korespondencyjny.

Signature Not Verified

Dokument podpisany przez
Agnieszka Halaś
Data: 2026.06.10 12:58:36
CEST

Instytut Geografii i Przestrzennego Zagospodarowania im. Stanisława Leszczyckiego
Polska Akademia Nauk

Warszawa, 5.06.2026

Prof. dr hab. Michał Słowiński
Zakład Dynamiki Krajobrazów Minionych
Instytut Geografii i Przestrzennego Zagospodarowania im. Stanisława Leszczyckiego
Polska Akademia Nauk
ul. Twarda 51/55
00-818 Warszawa
michal.slowinski@geopan.torun.pl

Oświadczenie o wkładzie autorskim w artykule naukowym

Oświadczam, że mój wkład w artykule:

> Halaś, A. and **Słowiński, M.**: Peat core research in the Western Siberian Lowland: applications of palaeoecological proxies, regions studied, and future prospects, Earth System Science Data, 18, 3853–3888, https://doi.org/10.5194/essd-18-3853-2026, 2026.

wynosił **10%** i był następujący:

- pozyskanie finansowania (Narodowe Centrum Nauki, PRELUDIUM BIS1, nr 2019/35/O/ST10/02903),
- opracowanie koncepcji manuskryptu,
- udział w interpretacji wyników,
- komentowanie i edytowanie manuskryptu.

MICHAŁ SŁOWIŃSKI

Dokument podpisany przez Michał Słowiński; IGiPZ PAN
Data: 2026.06.09 21:19:51 CEST